Functional MRI: Basics and Beyond

Peter A. Bandettini, Ph.D

bandettini@nih.gov

Unit on Functional Imaging Methods
Laboratory of Brain and Cognition
&
Functional MRI Core Facility

DEPARTMENT OF HEALTH & HUMAN SERVICES · USA

NIMH
National Institute
of Mental Health

NATIONAL INSTITUTES OF HEALTH

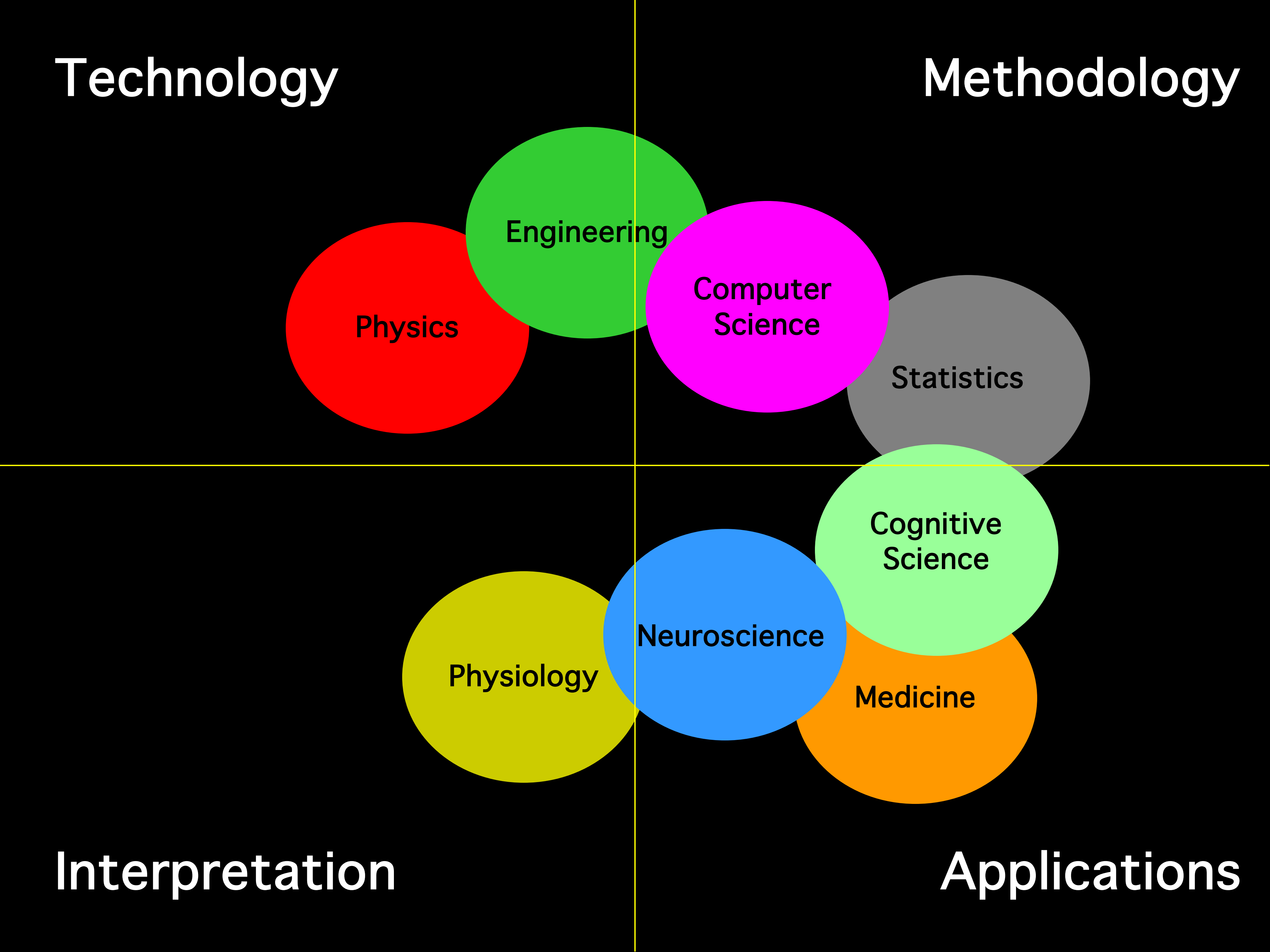
Technology
Methodology
Engineering
Physics
Computer Science
Statistics
Cognitive Science
Neuroscience
Physiology
Medicine
Interpretation
Applications

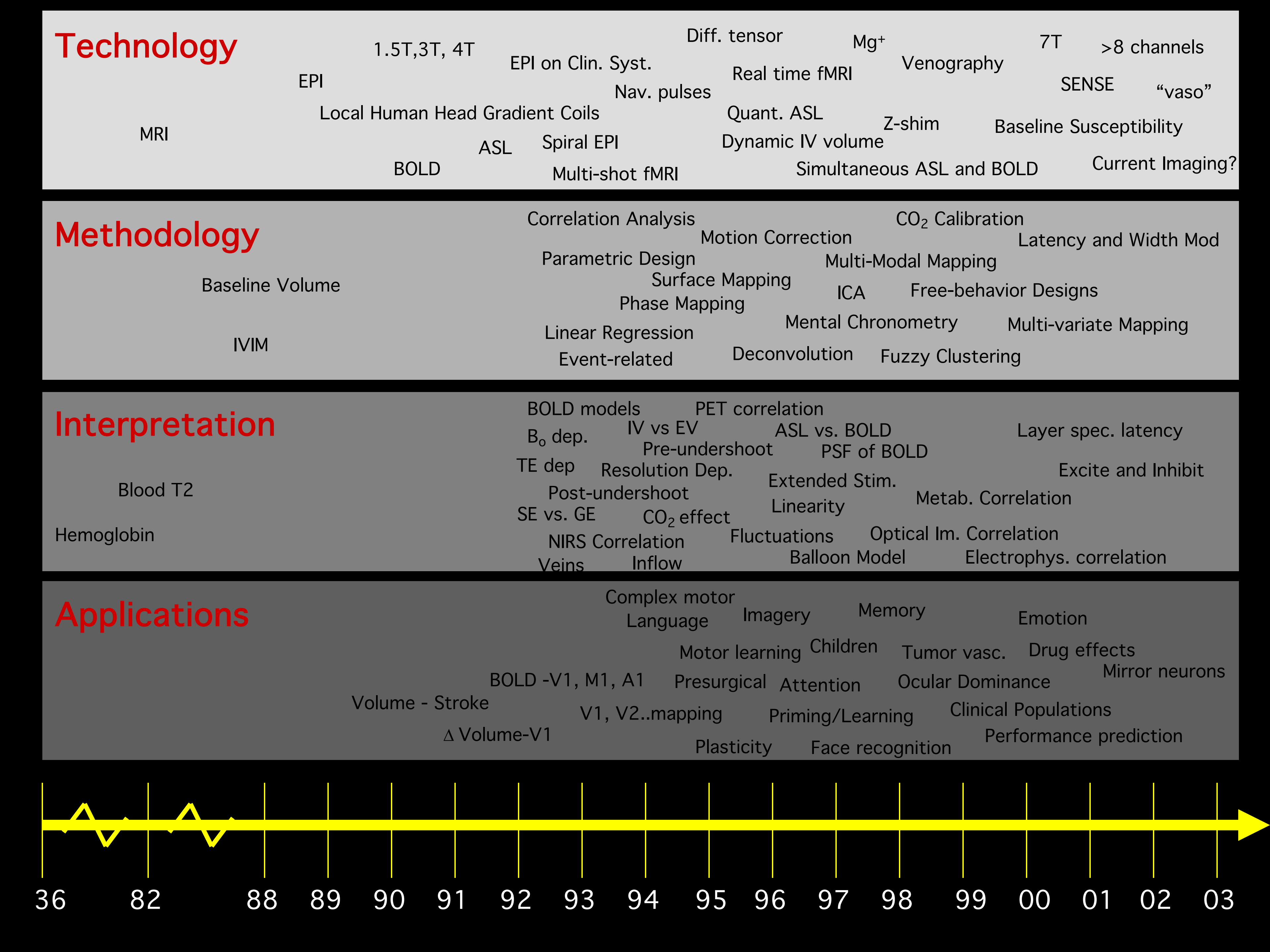

Technology
MRI
EPI
1.5T,3T, 4T
Local Human Head Gradient Coils
BOLD
ASL
EPI on Clin. Syst.
Spiral EPI
Multi-shot fMRI
Nav. pulses
Diff. tensor
Real time fMRI
Quant. ASL
Dynamic IV volume
Simultaneous ASL and BOLD
Mg+
Z-shim
Venography
7T
SENSE
Baseline Susceptibility
>8 channels
"vaso"
Current Imaging?
Methodology
Baseline Volume
IVIM
Correlation Analysis
Parametric Design
Linear Regression
Event-related
Surface Mapping
Phase Mapping
Motion Correction
Deconvolution
Mental Chronometry
ICA
Multi-Modal Mapping
CO2 Calibration
Free-behavior Designs
Fuzzy Clustering
Latency and Width Mod
Multi-variate Mapping
Interpretation
Blood T2
Hemoglobin
BOLD models
Bo dep.
TE dep
SE vs. GE
Post-undershoot
NIRS Correlation
Veins
IV vs EV
Pre-undershoot
Resolution Dep.
CO2 effect
Inflow
PET correlation
ASL vs. BOLD
PSF of BOLD
Extended Stim.
Linearity
Fluctuations
Balloon Model
Optical Im. Correlation
Metab. Correlation
Electrophys. correlation
Layer spec. latency
Excite and Inhibit
Applications
Volume - Stroke
Δ Volume-V1
BOLD -V1, M1, A1
V1, V2..mapping
Complex motor
Language
Motor learning
Presurgical
Plasticity
Imagery
Children
Attention
Priming/Learning
Face recognition
Memory
Tumor vasc.
Ocular Dominance
Clinical Populations
Performance prediction
Emotion
Drug effects
Mirror neurons
36
82
88
89
90
91
92
93
94
95
96
97
98
99
00
01
02
03

FMRI Basics and Beyond

- Information Content
- Sensitivity
- Resolution
- Image quality
- Paradigm Design and Processing

FMRI Basics and Beyond

- Information Content
- Sensitivity
- Resolution
- Image quality
- Paradigm Design and Processing

Contrast in Functional MRI

- Blood Volume (invasive)
  – Contrast agent injection and time series collection of T2* or T2 - weighted images.
- BOLD
  – Time series collection of T2* or T2 - weighted images.
- Perfusion
  – T1 weighting
  – Arterial spin labeling
- $CMRO_2$
  – BOLD and Perfusion w/

  Normalization to global perfusion change with global stress.
- Blood Volume (noninvasive)
  – Time series collection with IV signal removed.

Blood Volume Imaging

Susceptibility Contrast agent bolus injection and time series collection of T2* or T2 - weighted images

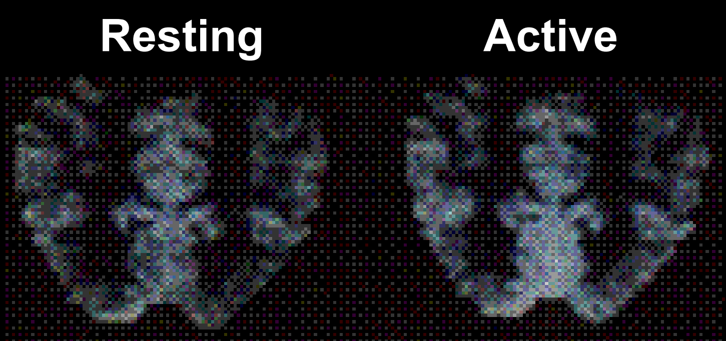

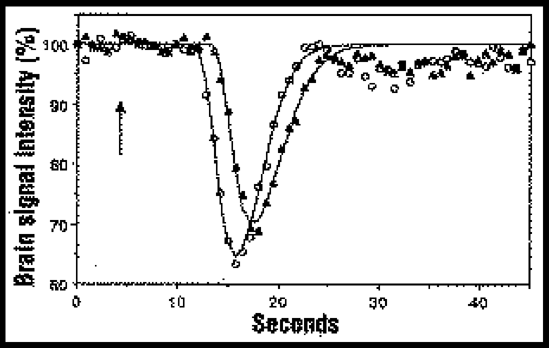

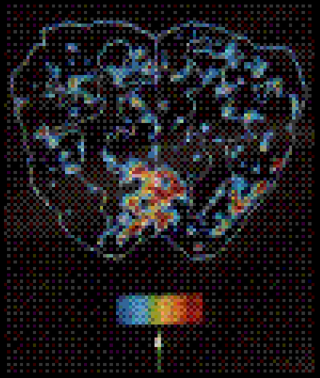

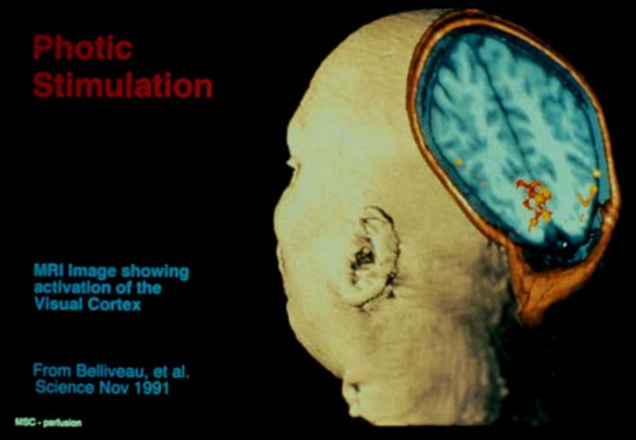

Susceptibility Contrast

Susceptibility-Induced Field Distortion in the Vicinity of a Microvessel $\perp$ to B_O.

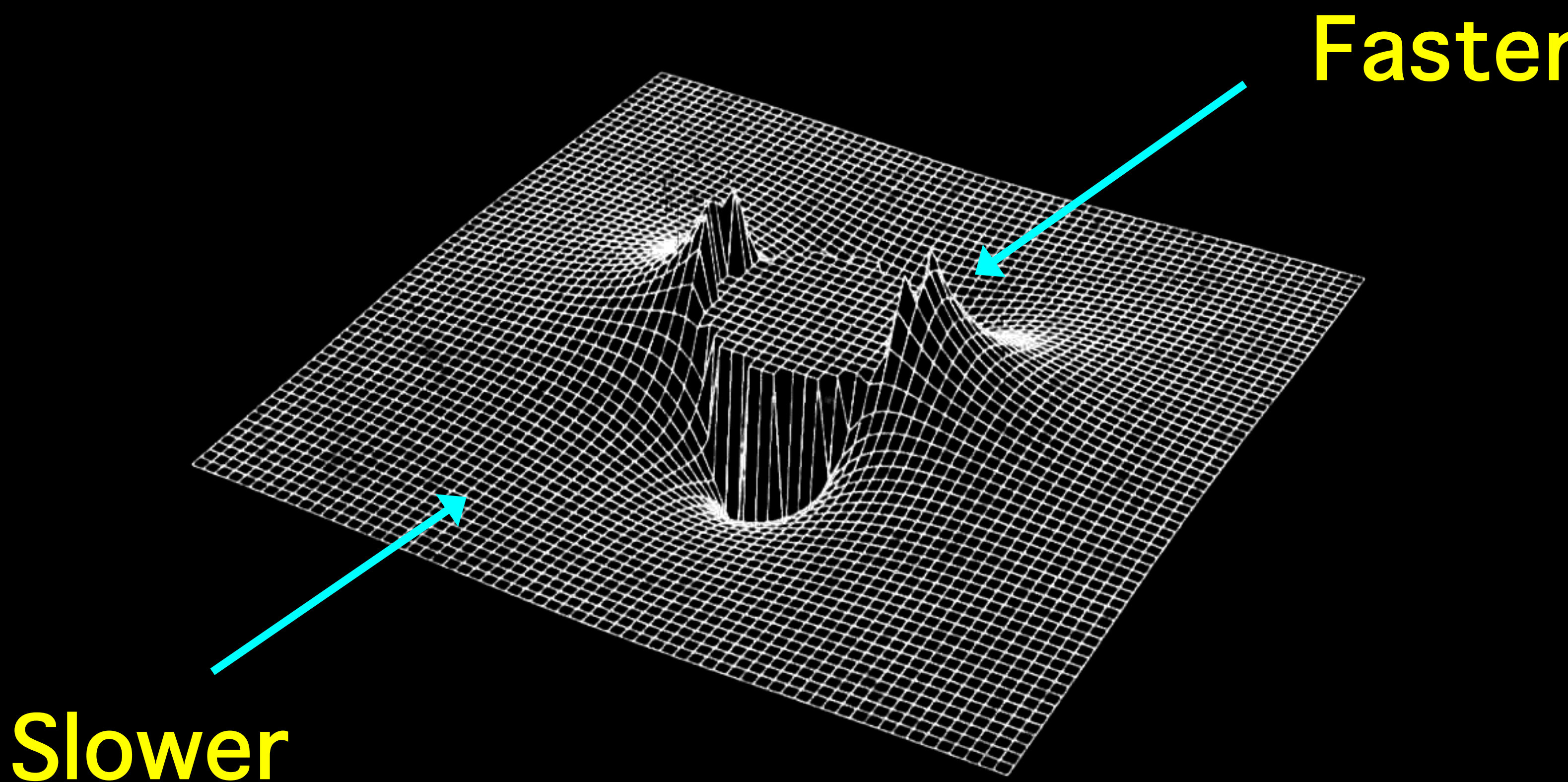

L. Pauling, C. D. Coryell, (1936) “The magnetic properties and structure of hemoglobin, oxyhemoglobin, and carbonmonoxyhemoglobin.” Proc.Natl. Acad. Sci. USA 22, 210-216.

Thulborn, K. R., J. C. Waterton, et al. (1982).“Oxygenation dependence of the transverse relaxation time of water protons in whole blood at high field.” Biochim. Biophys. Acta. 714: 265-270.

S. Ogawa, T. M. Lee, A. R. Kay, D. W. Tank, (1990) “Brain magnetic resonance imaging with contrast dependent on blood oxygenation.” Proc. Natl. Acad. Sci. USA 87, 9868-9872.

R. Turner, D. LeBihan, C. T. W. Moonen, D. Despres, J. Frank, (1991). Echo-planar time course MRI of cat brain oxygenation changes. Magn. Reson. Med. 27, 159-166.

BOLD Contrast in the Detection of Neuronal Activity

Cerebral Tissue Activation

↓

Local Vasodilation

↓

Increase in Cerebral Blood Flow and Volume → **Oxygen Delivery Exceeds Metabolic Need**

↓

Increase in Capillary and Venous Blood Oxygenation

↓

Decrease in Deoxy-hemoglobin

Deoxy-hemoglobin: paramagnetic
Oxy-hemoglobin: diamagnetic

↓

Decrease in susceptibility-related intravoxel dephasing → **Increase in T2 and T2***

↓

Local Signal Increase in T2 and T2* - weighted sequences

Blood Oxygenation Imaging

•K. K. Kwong, et al, (1992) "Dynamic magnetic resonance imaging of human brain activity during primary sensory stimulation." Proc. Natl. Acad. Sci. USA. 89, 5675-5679.

•S. Ogawa, et al., (1992) "Intrinsic signal changes accompanying sensory stimulation: functional brain mapping with magnetic resonance imaging. Proc. Natl. Acad. Sci. USA." 89, 5951-5955.

•P. A. Bandettini, et al., (1992) "Time course EPI of human brain function during task activation." Magn. Reson. Med 25, 390-397.

•Blamire, A. M., et al. (1992). "Dynamic mapping of the human visual cortex by high-speed magnetic resonance imaging." Proc. Natl. Acad. Sci. USA 89: 11069-11073.

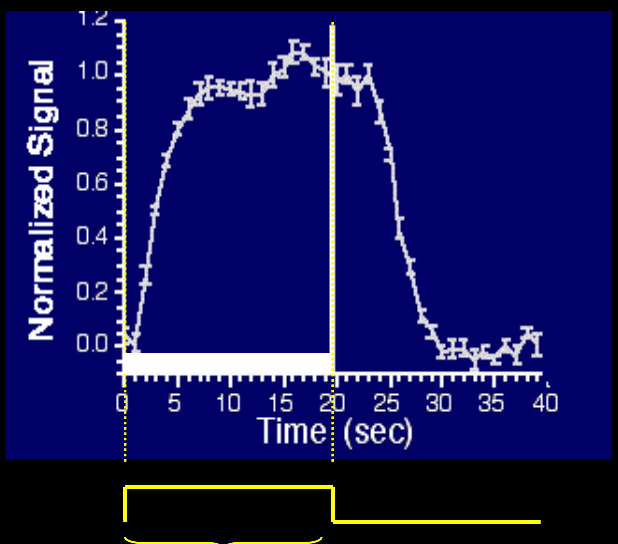

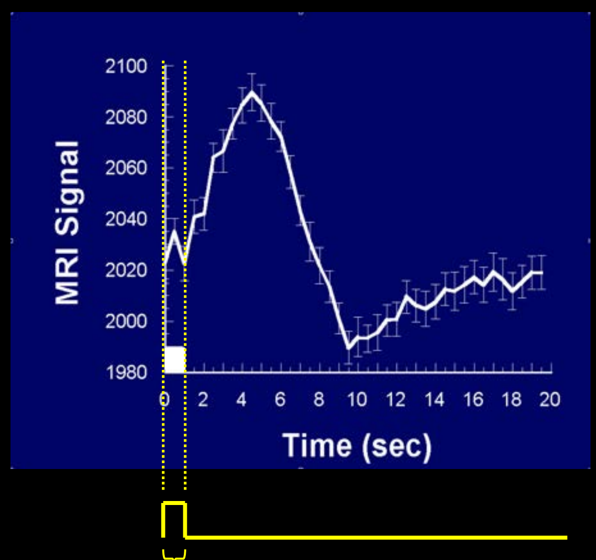

task

task

The vascular response

Factors influencing
[Deoxy-Hb] concentration

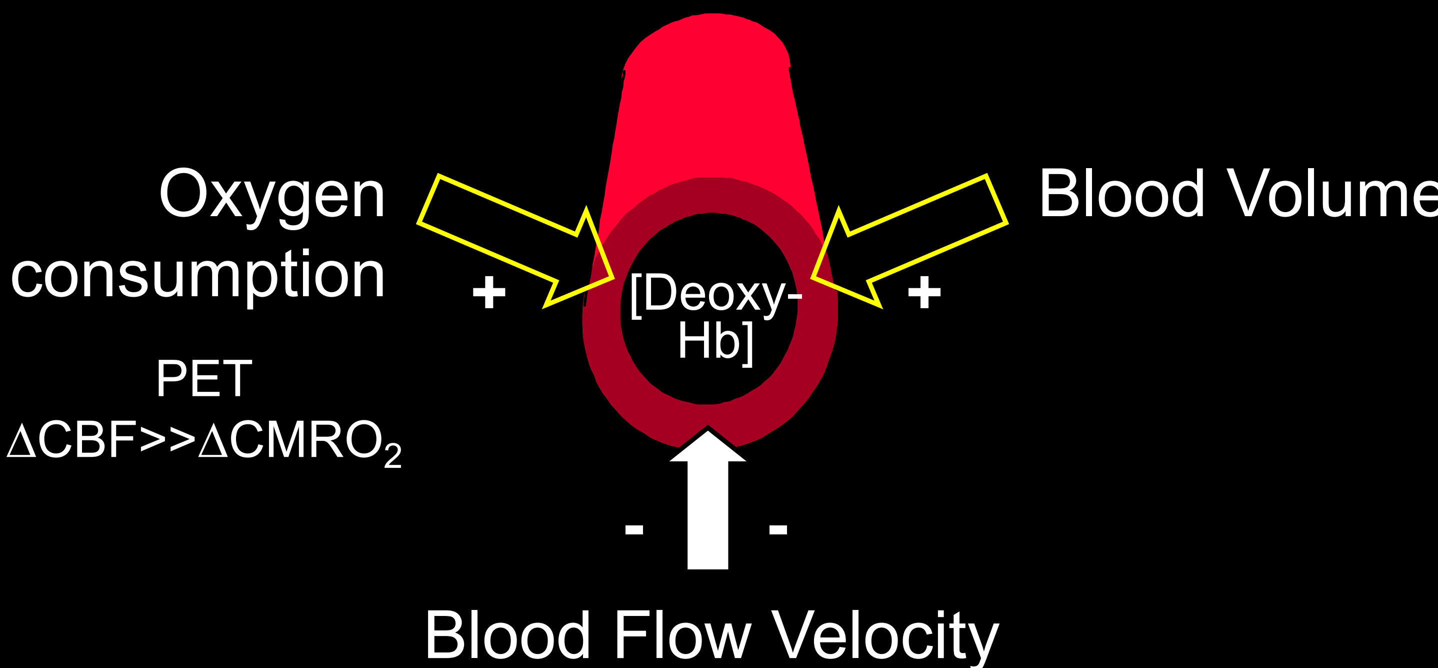

Courtesy of Arno Villringer

Time course of BOLD signal

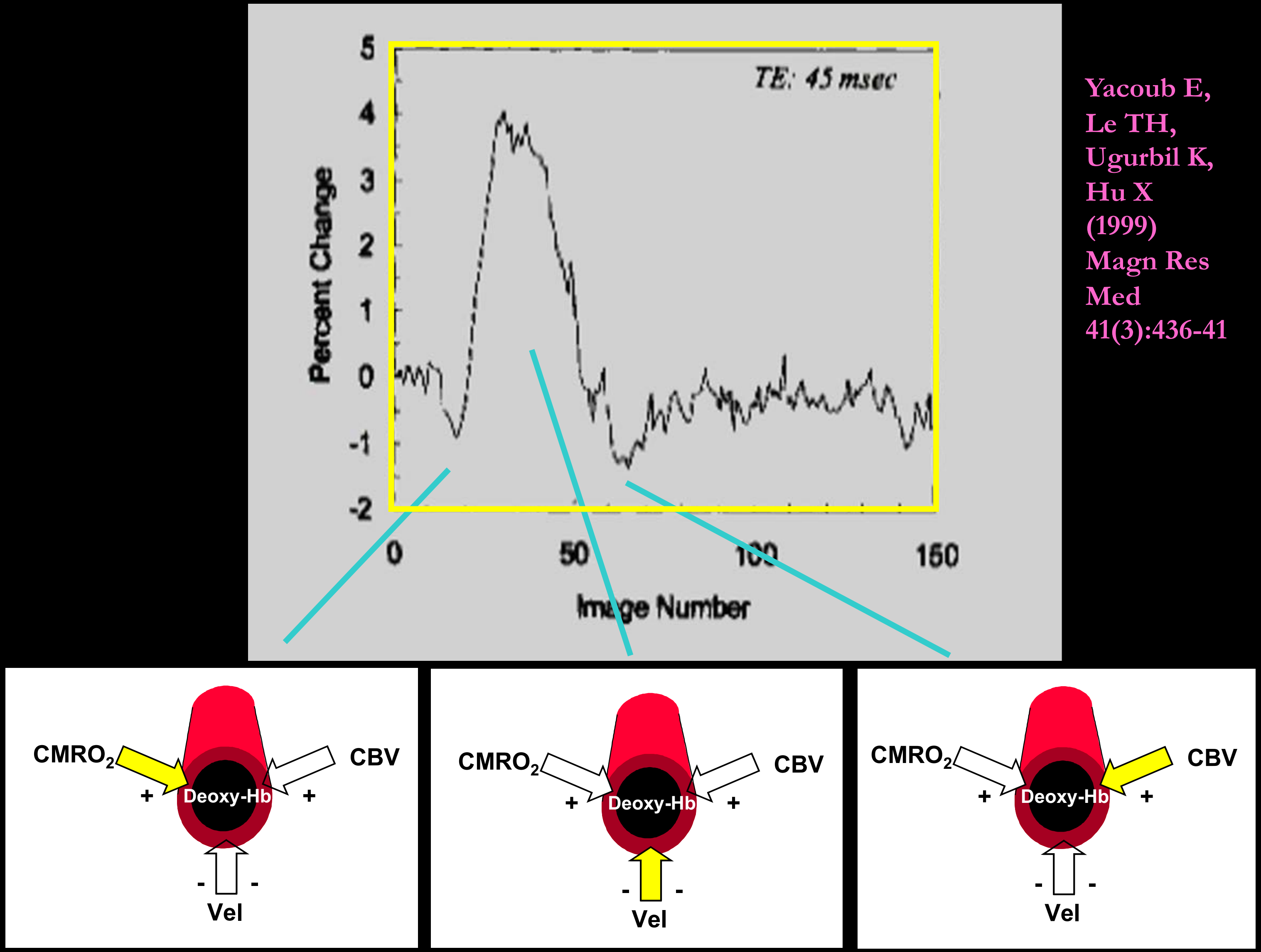

Yacoub E, Le TH, Ugurbil K, Hu X (1999) Magn Res Med 41(3):436-41

Courtesy of Arno Villringer

Blood Perfusion Imaging

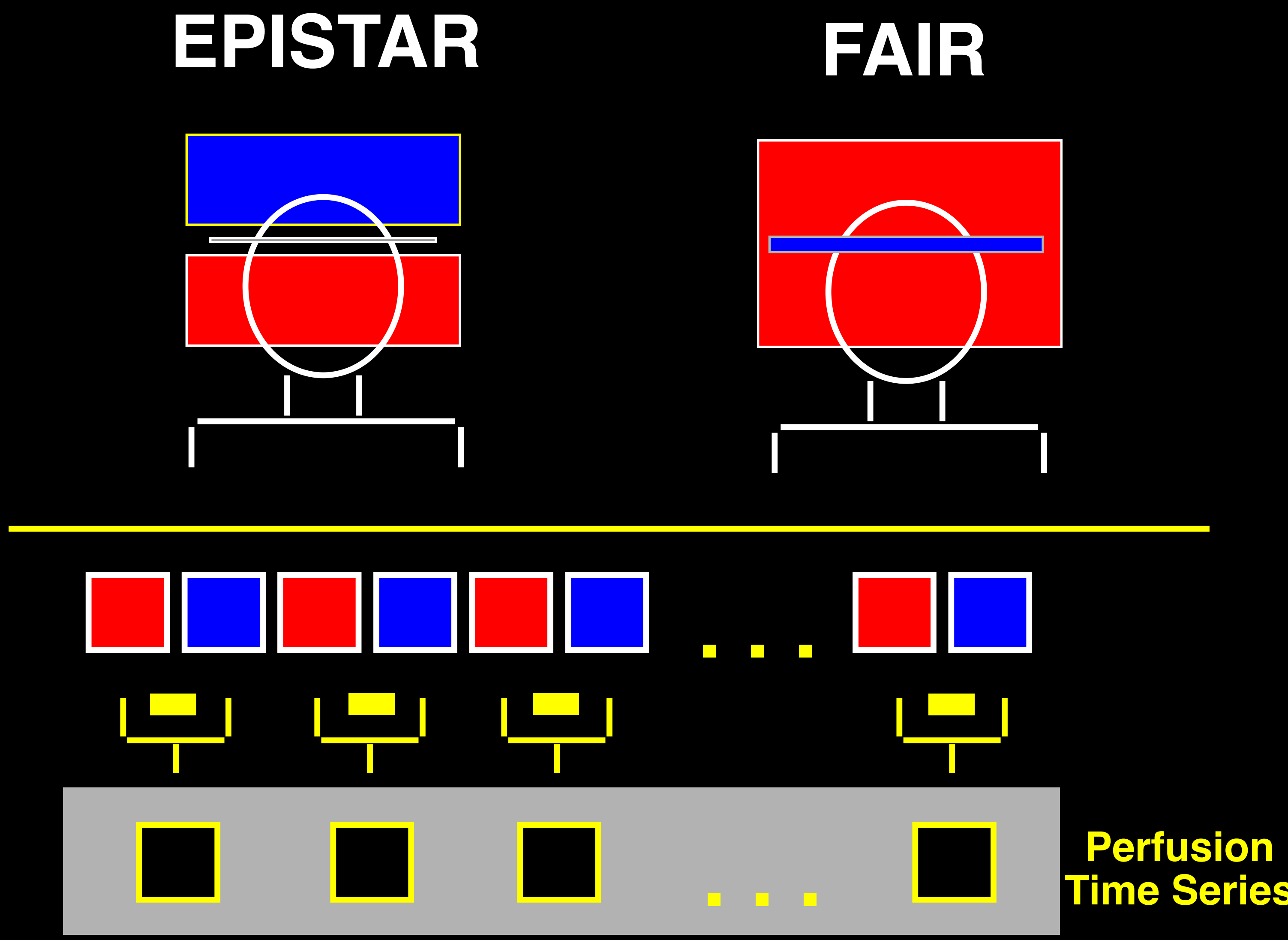

TI (ms) | FAIR | EPISTAR

200

400

600

800

1000

1200

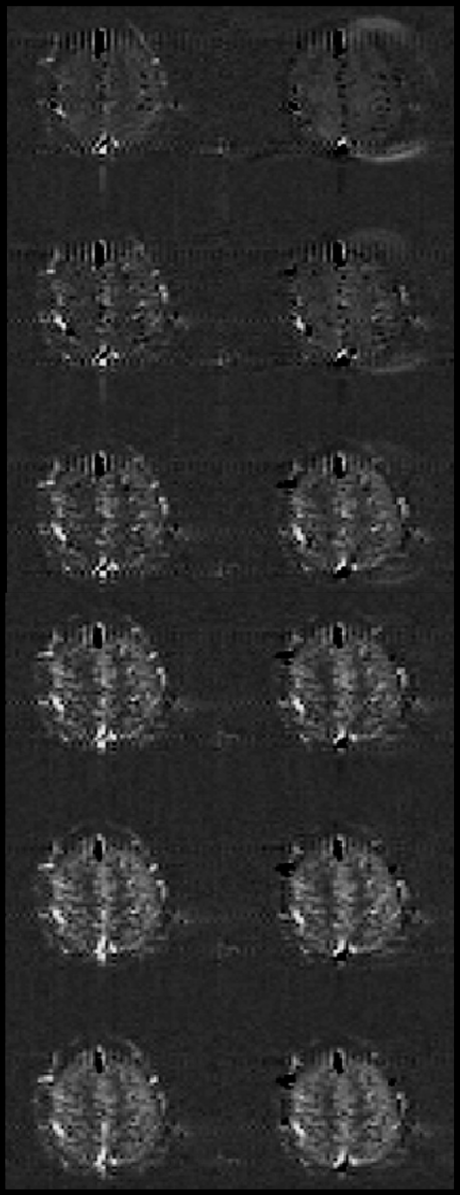

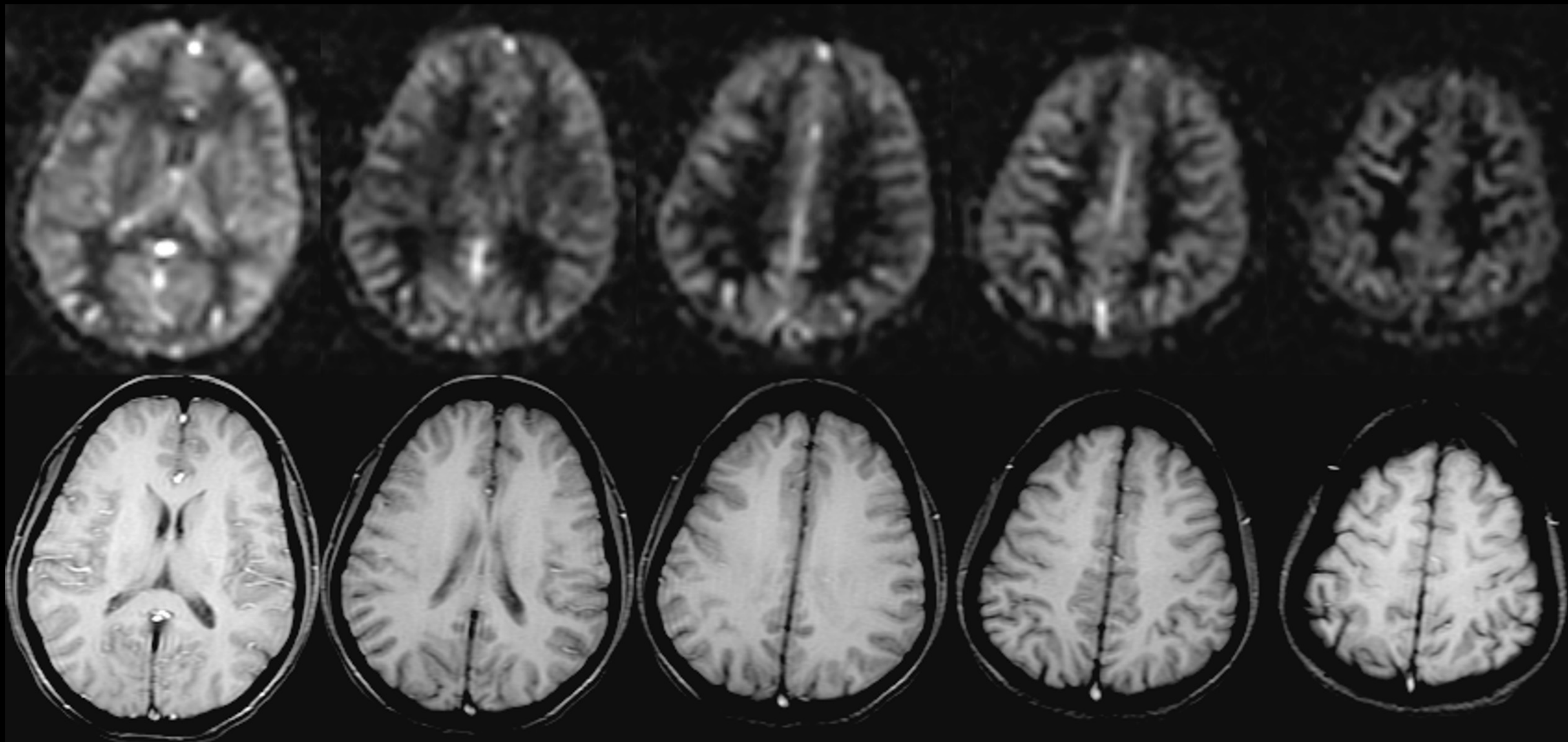

Williams, D. S., Detre, J. A., Leigh, J. S. & Koretsky, A. S. (1992) “Magnetic resonance imaging of perfusion using spin-inversion of arterial water.” Proc. Natl. Acad. Sci. USA 89, 212-216.

Edelman, R., Siewert, B. & Darby, D. (1994) “Qualitative mapping of cerebral blood flow and functional localization with echo planar MR imaging ans signal targeting with alternating radiofrequency (EPISTAR).” Radiology **192**, 1-8.

Kim, S.-G. (1995) “Quantification of relative cerebral blood flow change by flow-sensitive alternating inversion recovery (FAIR) technique: application to functional mapping.” Magn. Reson. Med. **34**, 293-301.

Kwong, K. K. et al. (1995) “MR perfusion studies with T1-weighted echo planar imaging.”Magn. Reson. Med. **34**, 878-887.

Comparison with Positron Emission Tomography

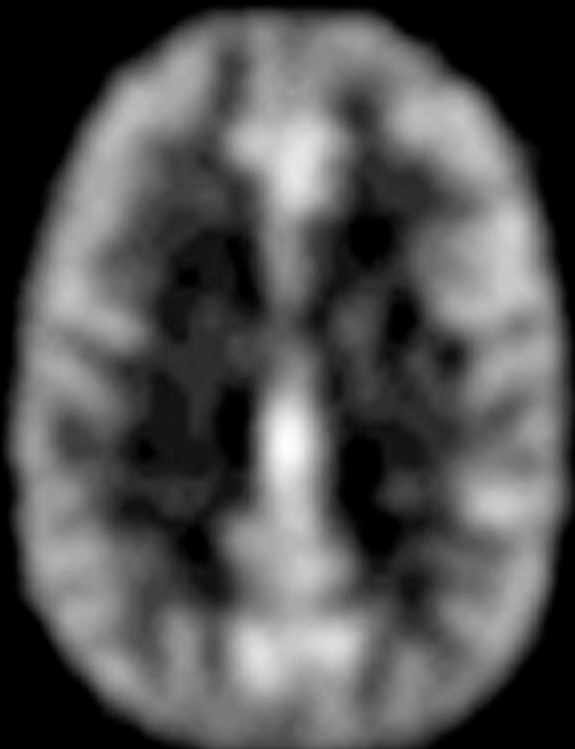

PET: $H_2{}^{15}O$

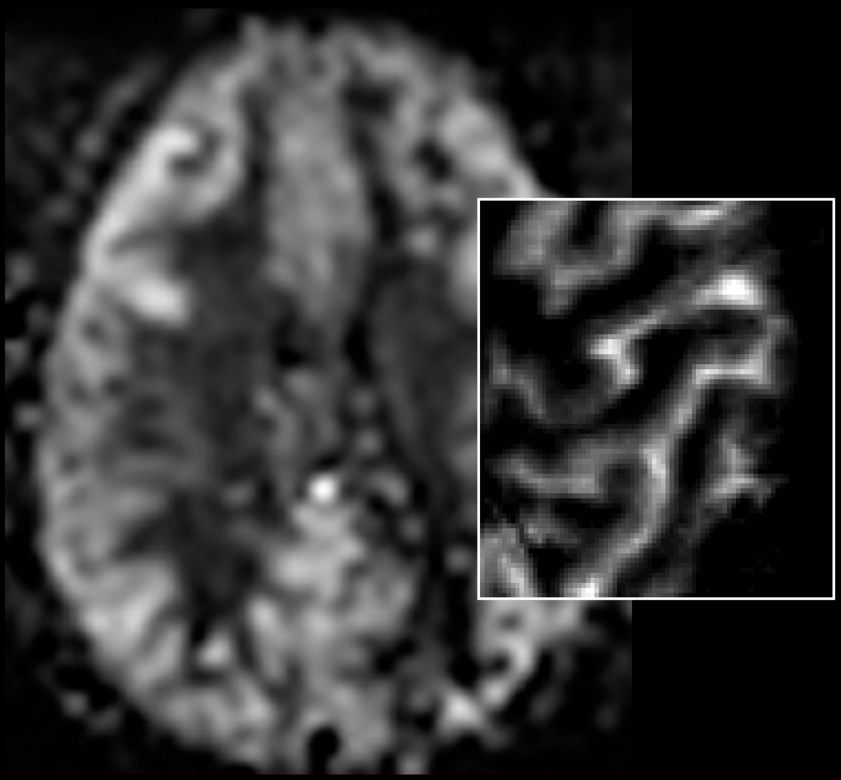

MRI: ASL

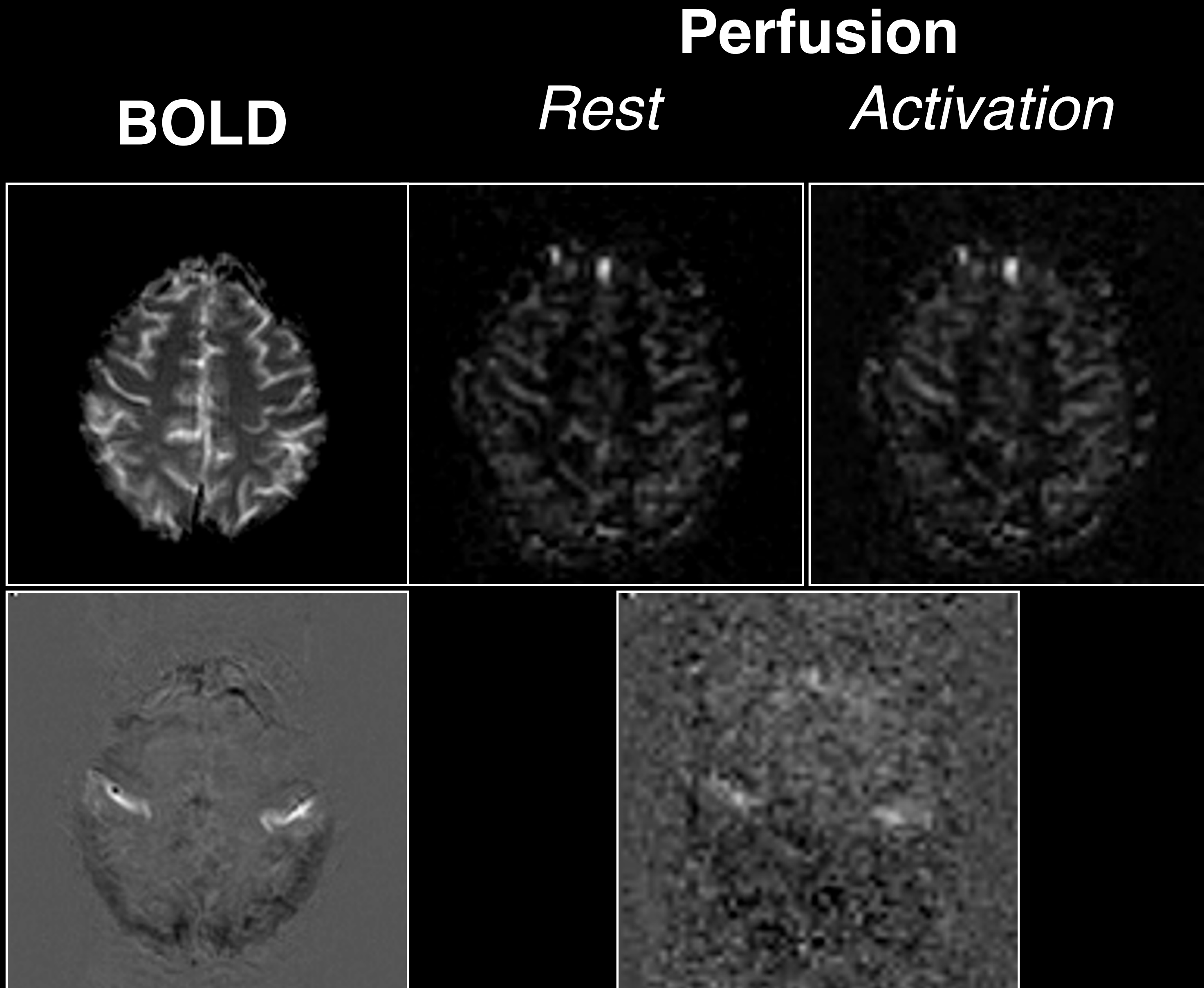

P. A. Bandettini, E. C. Wong, Magnetic resonance imaging of human brain function: principles, practicalities, and possibilities, *in* "Neurosurgery Clinics of North America: Functional Imaging" (M. Haglund, Ed.), p.345-371, W. B. Saunders Co., 1997.

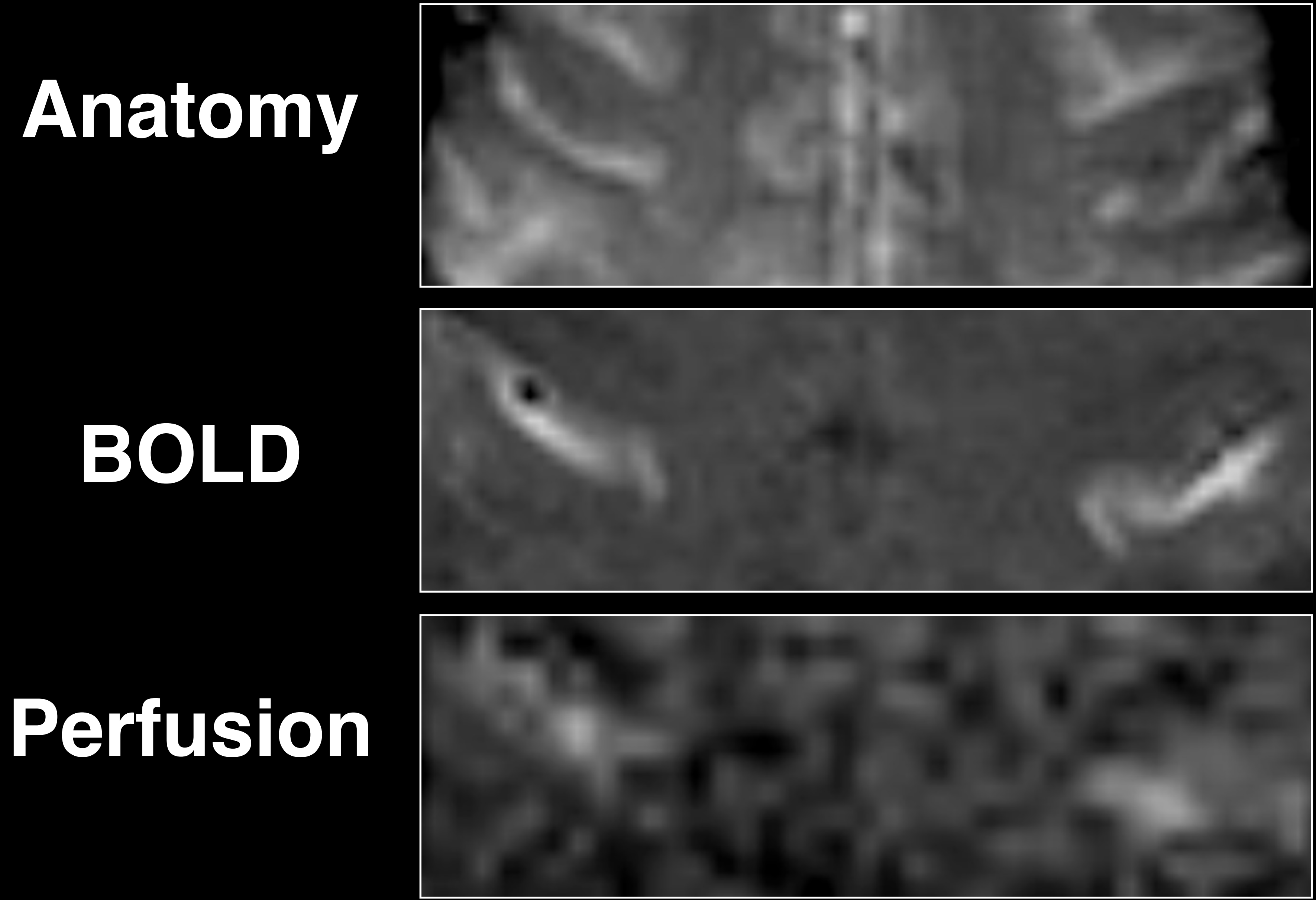

P. A. Bandettini, E. C. Wong, Magnetic resonance imaging of human brain function: principles, practicalities, and possibilities, *in* "Neurosurgery Clinics of North America: Functional Imaging" (M. Haglund, Ed.), p.345-371, W. B. Saunders Co., 1997.

T1 - weighted

Flow weighted

T2* weighted

BOLD weighted

T1 and T2* weighted

Flow and BOLD weighted

P. A. Bandettini, E. C. Wong, Echo - planar magnetic resonance imaging of human brain activation, *in* "Echo Planar Imaging: Theory, Technique, and Application" (F. Schmitt, M. Stehling, R. Turner, Eds.), p.493-530, Springer - Verlag, Berlin, 1997

	+	-
Volume	• unique information • baseline information • multislice trivial	• invasive • low C / N for func.
BOLD	• highest C / N • easy to implement • multislice trivial • non invasive • highest temp. res.	• complicated signal • no baseline info.
Perfusion	• unique information • control over ves. size • baseline information • non invasive	• multislice non trivial • lower temp. res. • low C / N

Hemodynamic Specificity

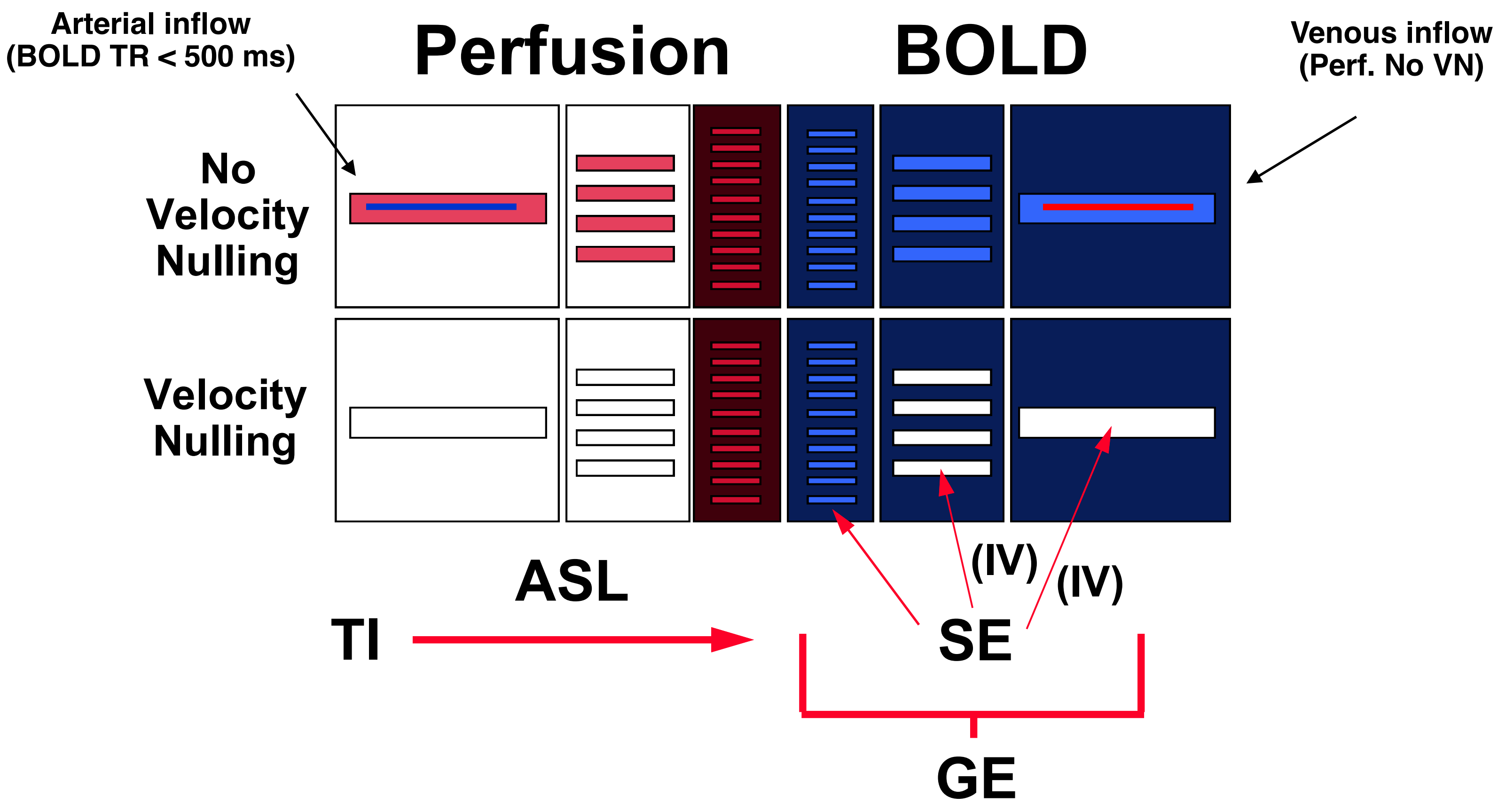

Mapping of $CMRO_2$

Activation:	Flow	$\Uparrow\Uparrow$
	$CMRO_2$	$\Uparrow$
	Blood Oxygenation	$\Uparrow$
CO_2 stress:	Flow	$\Uparrow\Uparrow$
	$CMRO_2$	$\Rightarrow$
	Blood Oxygenation	$\Uparrow\Uparrow$

Hemdodynamic Stress Calibration

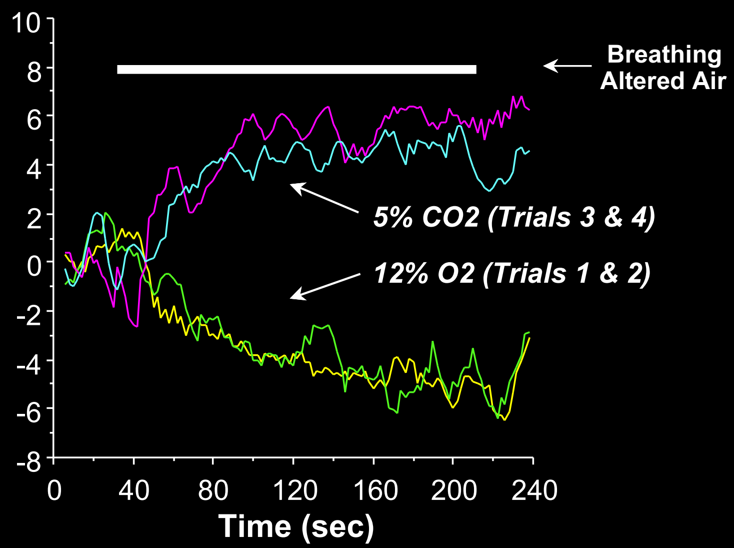

5% CO2

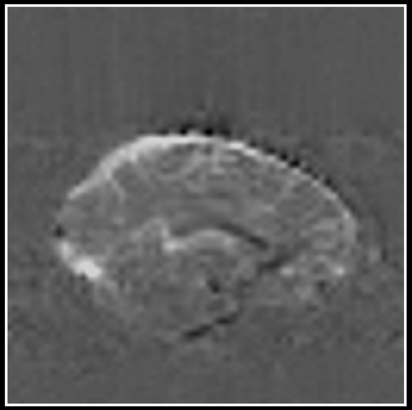

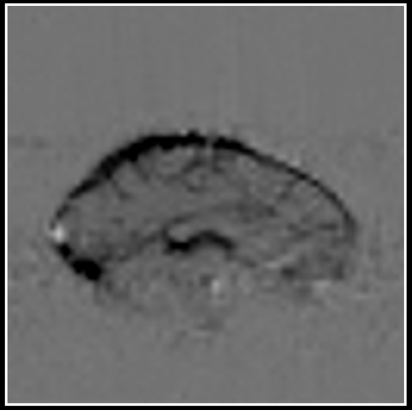

12% O2

P. A. Bandettini, E. C. Wong, A hypercapnia - based normalization method for improved spatial localization of human brain activation with fMRI. *NMR in Biomedicine* 10, 197-203 (1997).

Proc. Natl. Acad. Sci. USA
Vol. 96, pp. 9403–9408, August 1999
Neurobiology

Linear coupling between cerebral blood flow and oxygen consumption in activated human cortex

Richard D. Hoge*†, Jeff Atkinson*, Brad Gill*, Gérard R. Crelier*, Sean Marrett‡, and G. Bruce Pike*

*Room WB325, McConnell Brain Imaging Centre, Montreal Neurological Institute, Quebec, Canada H3A 2B4; and ‡Nuclear Magnetic Resonance Center, Massachusetts General Hospital, Building 149, 13th Street, Charlestown, MA 02129

CBF

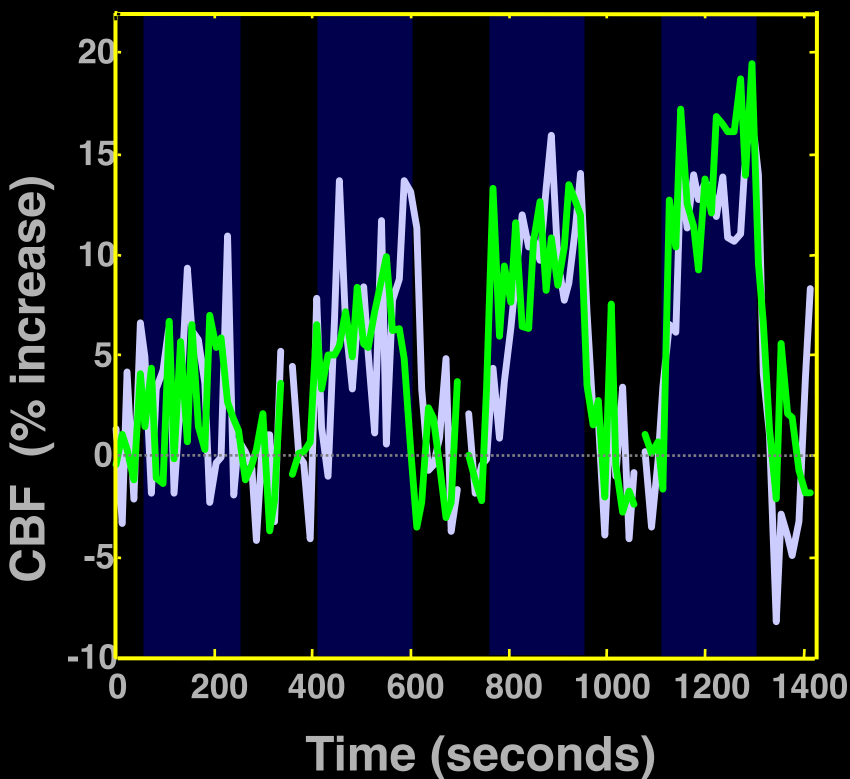

BOLD

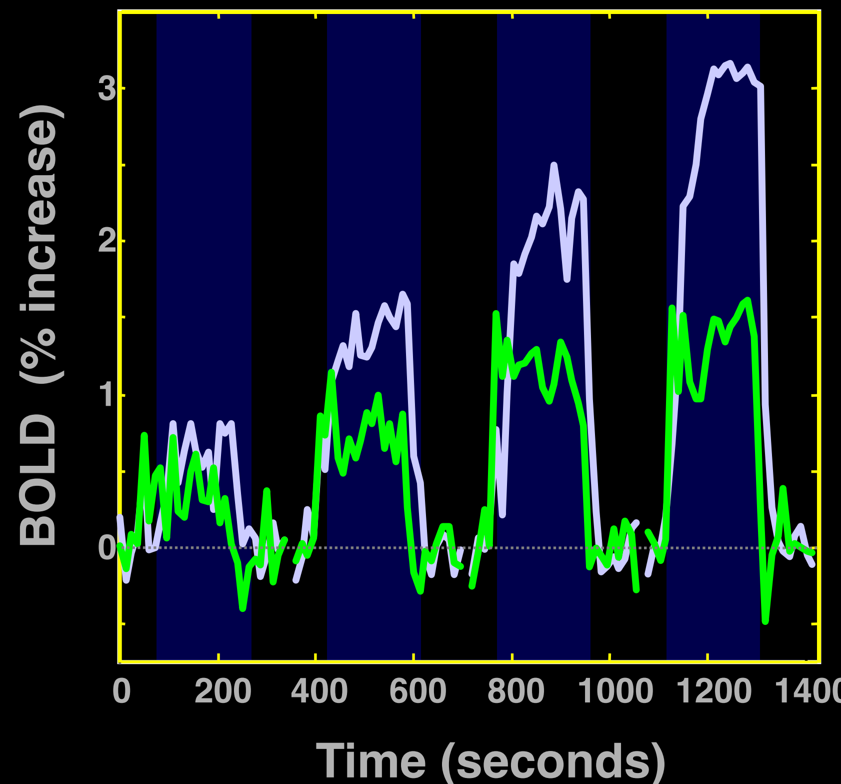

Simultaneous Perfusion and BOLD imaging during graded visual activation and hypercapnia

CBF-$CMRO_2$ coupling

Hoge, et al.

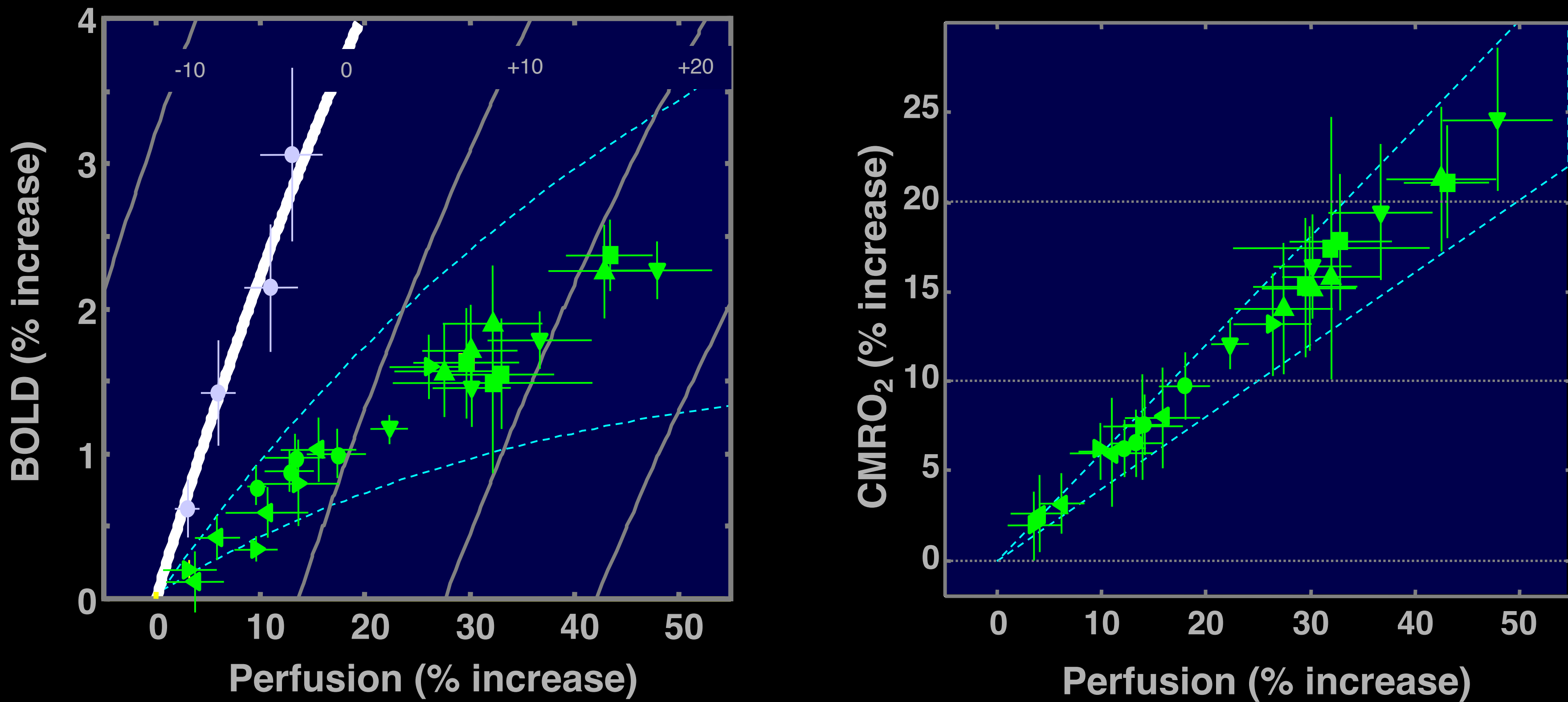

Characterizing Activation-induced $CMRO_2$ changes using calibration with hypercapnia

Hoge, et al.

Computed $CMRO_2$ Changes

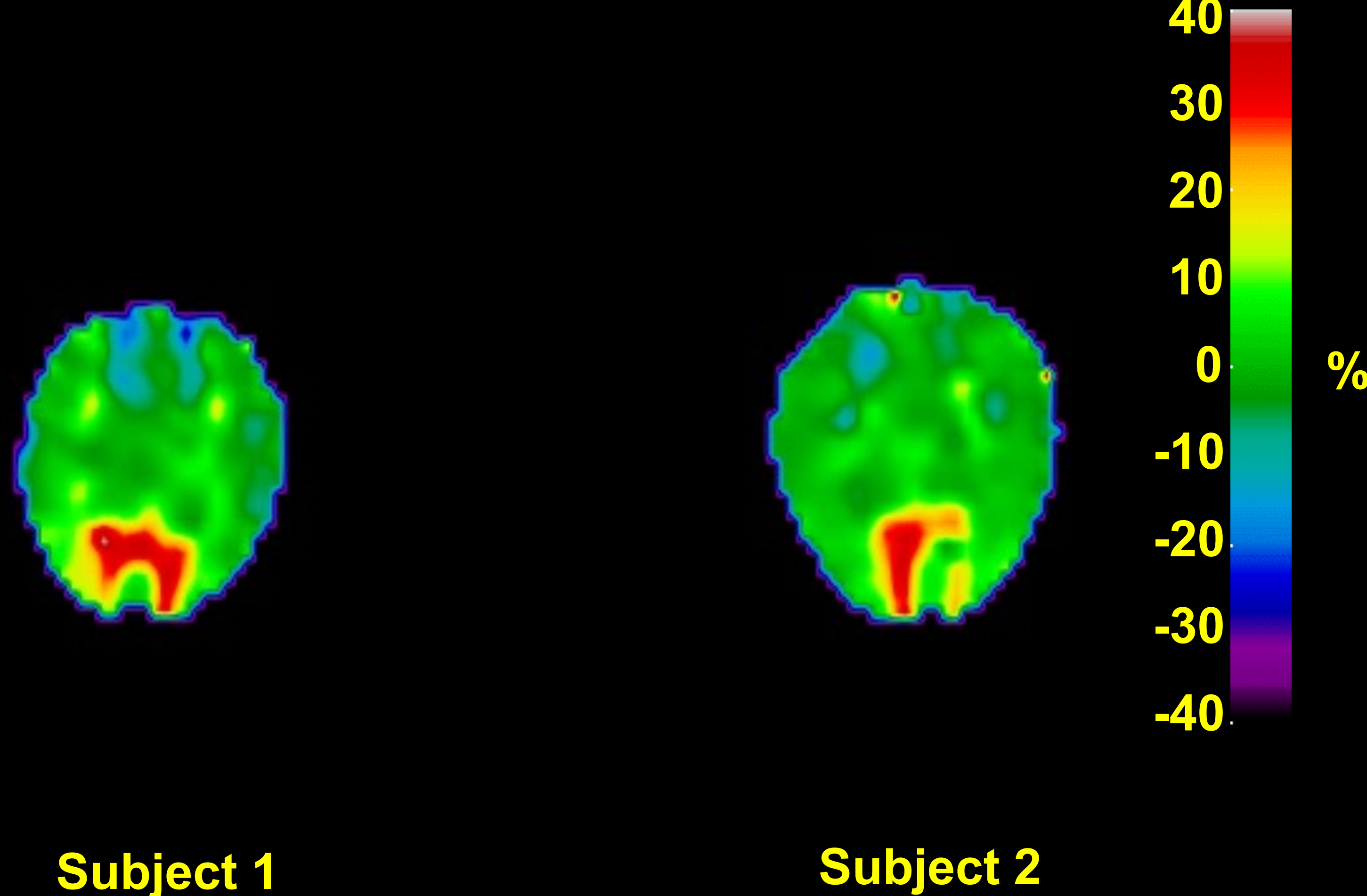

NMR IN BIOMEDICINE
NMR Biomed. 2001;**14**:441–447
DOI:10.1002/nbm.717

Quantitative measurements of cerebral metabolic rate of oxygen utilization using MRI: a volunteer study

Hongyu An,[1] Weili Lin,[2]* Azim Celik[3] and Yueh Z. Lee[2]

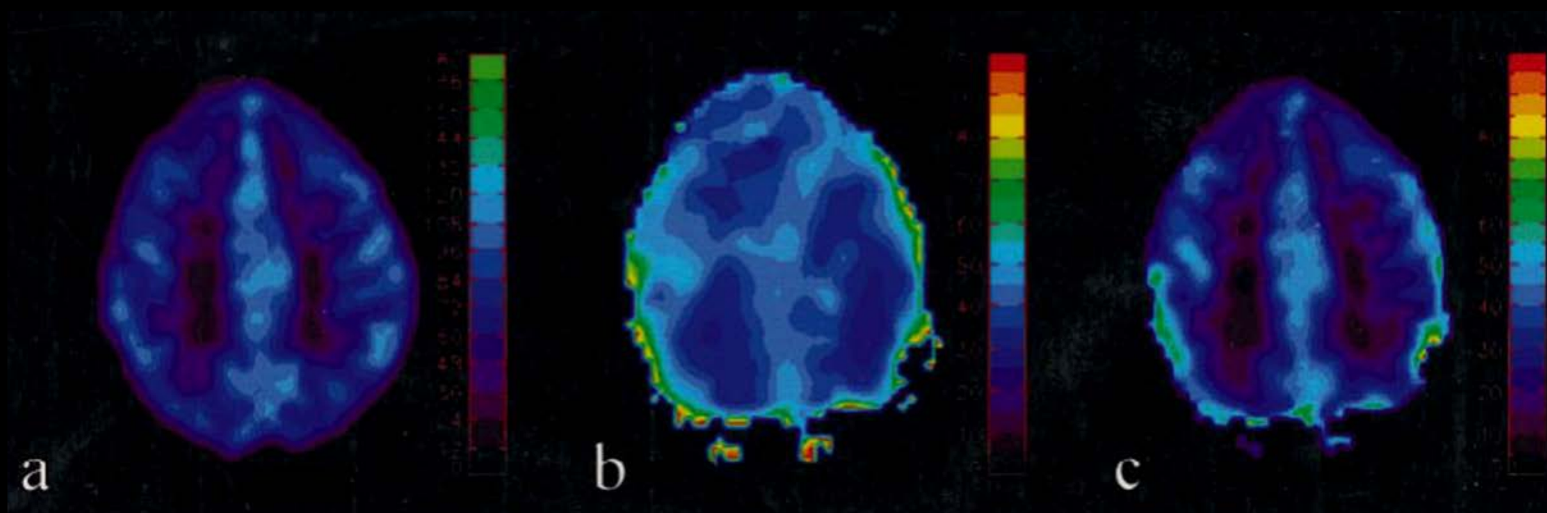

CBF OEF $CMRO_2$

Functional Magnetic Resonance Imaging Based on Changes in Vascular Space Occupancy

Hanzhang Lu,[1–3] Xavier Golay,[1,3] James J. Pekar,[1,3] and Peter C.M. van Zijl[1,3*]

MAGNET RESON MED 50 (2): 263-274 AUG 2003

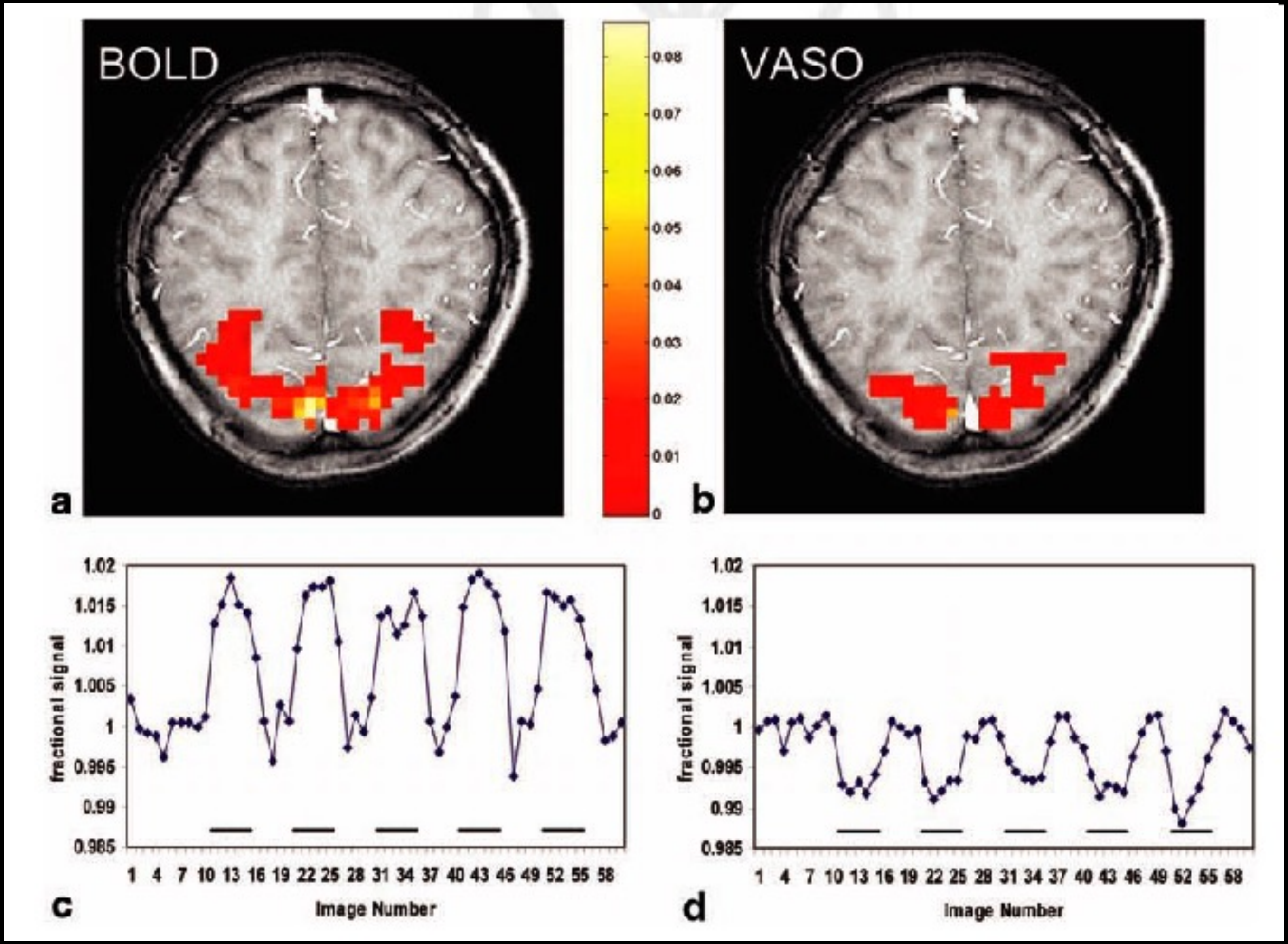

Neuronal Current Imaging?

•Neuronal activity is directly associated with ionic currents.

•These bio-currents induce **spatially distributed and transient** magnetic flux density changes and magnetic field gradients.

•In the context of MRI, these currents therefore alter **the magnetic phase** of surrounding water protons.

Derivation of B field generated in an MRI voxel by a current dipole

Single dendritic tree having a diameter d, and length L behaves like a conductor with conductivity σ. Resistance is R=V/I, where $R=4L/(\pi d^2 \sigma)$. From Biot-Savart:

$$B= \frac{\mu_0}{4\pi}\frac{Q}{r^2} = \frac{\mu_0}{16}\frac{d^2 \sigma V}{r^2}$$

by substituting $d = 4\mu m$, $\sigma \approx 0.25\ \Omega^{-1}\ m^{-1}$, V = 10mV and

r = 4cm (measurement distance when using MEG) the resulting value is: **$B \approx 0.002$ fT**

Because **B_{MEG}=100fT** (or more) is measured by MEG on the scalp, a large number of neurons, (0.002 fT x 50,000 = 100 fT), must coherently act to generate such field. These bundles of neurons produce, within a typical voxel, 1 mm x 1 mm x 1 mm, a field of order:

$$B_{MRI} = B_{MEG}\left(\frac{r_{MEG}}{r_{MRI}}\right)^2 = B_{MEG}\left(\frac{4\ cm}{0.1\ cm}\right)^2 = 1600\ B_{MEG}$$

$B_{MRI} \approx 0.2$nT

J. Bodurka, P. A. Bandettini. Toward direct mapping of neuronal activity: MRI detection of ultra weak transient magnetic field changes, Magn. Reson. Med. 47: 1052-1058, (2002).

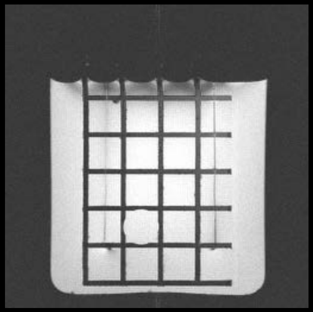

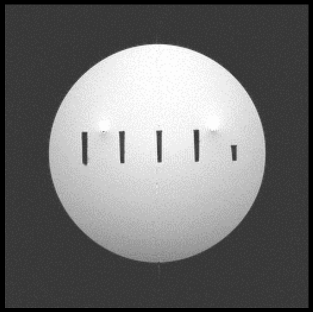

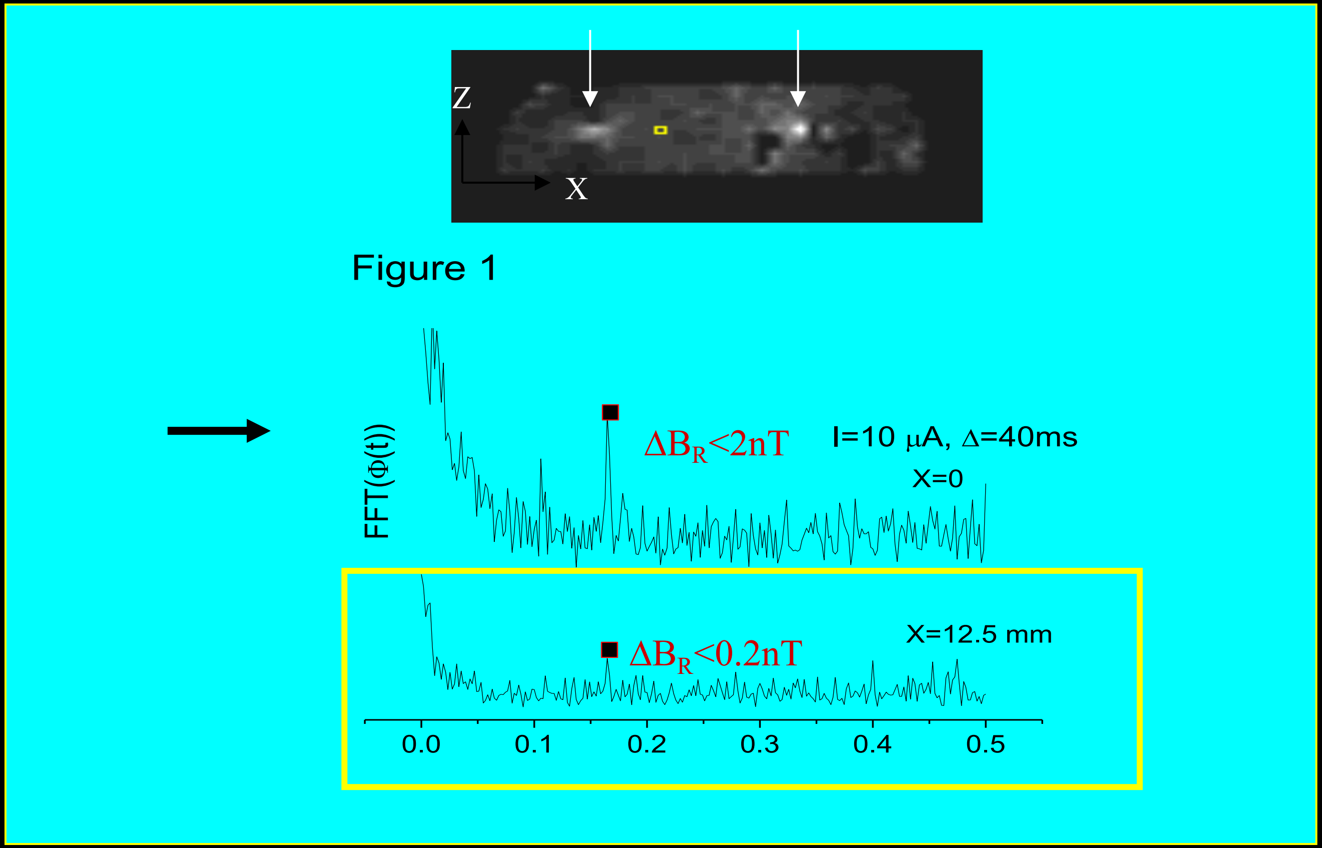

J. Bodurka, P. A. Bandettini. Toward direct mapping of neuronal activity: MRI detection of ultra weak transient magnetic field changes, Magn. Reson. Med. 47: 1052-1058, (2002).

In Vitro Results

Newborn rat brains have been found to exhibit spontaneous and synchronous firing at specific frequencies

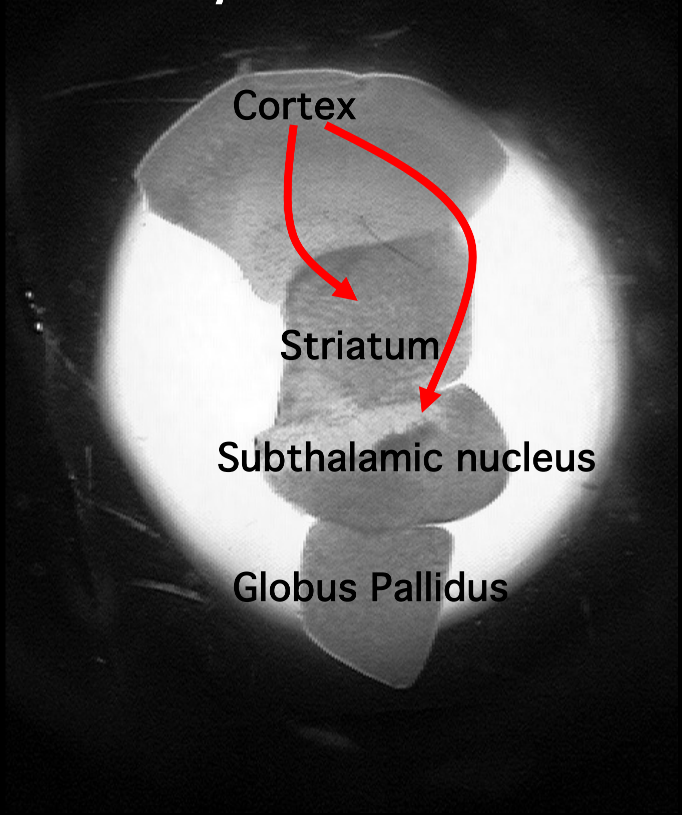

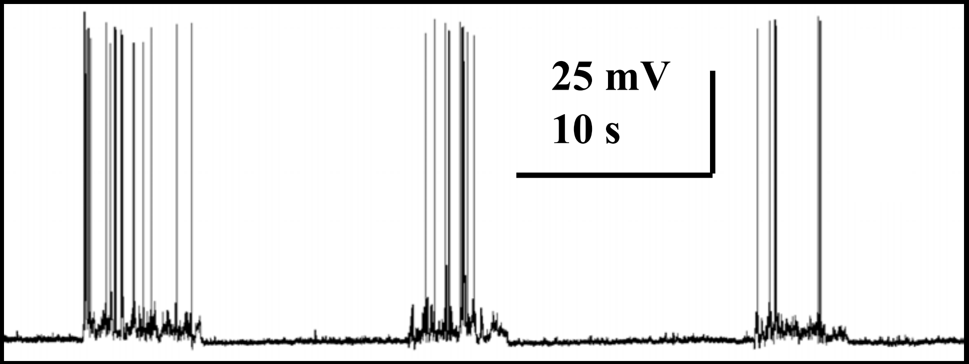

Plenz, D. and S.T. Kital. Nature, 1999. **400**: p. 677-682.

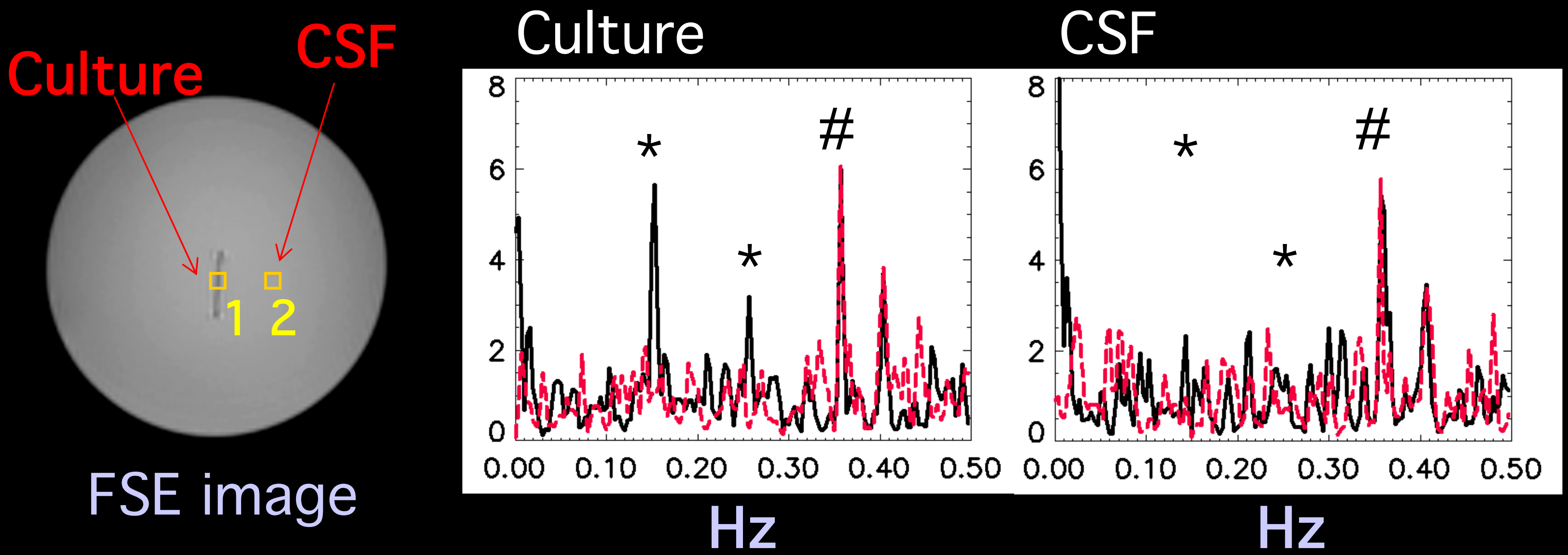

Active state: 10 min, Inactive state: 10 min after TTX admin.

*: activity

#: scanner pump frequency

Petridou et al.

Neuronal Activation

?

Hemodynamics

?

Measured Signal

?

Noise

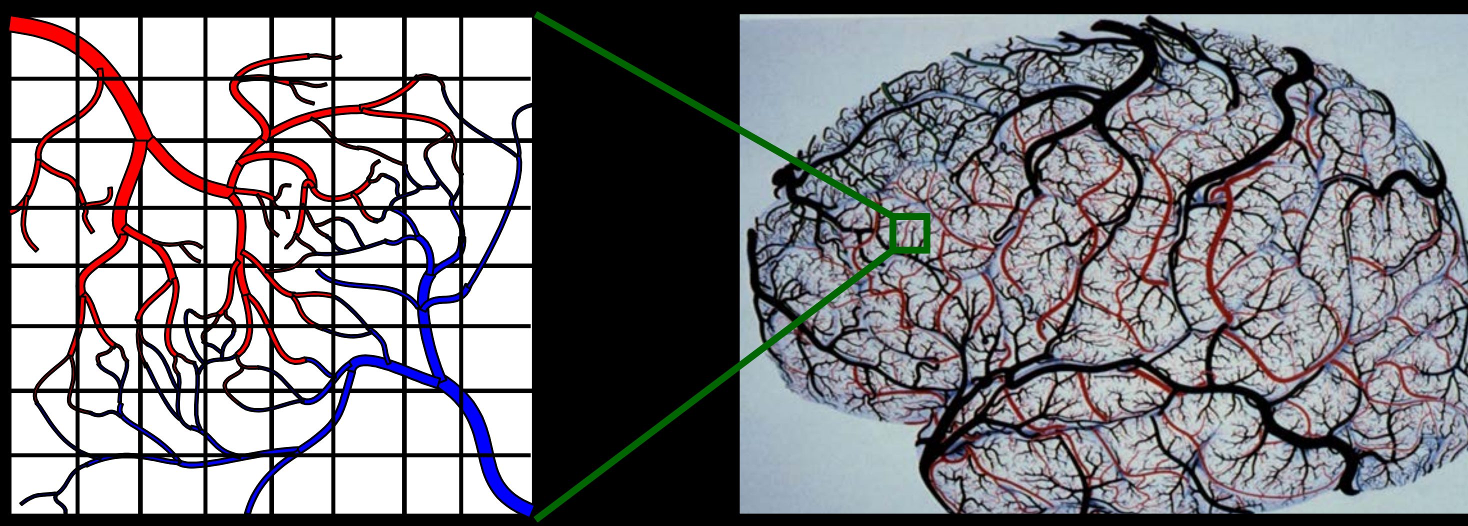

What we observe..

- Magnitude
- Location
- Parametric Dependence
- Latency

What we observe..

- Magnitude
- Location
- Parametric Dependence
- Latency

Basic Concepts of TE and Field Strength Dependence of BOLD

Baseline Signal

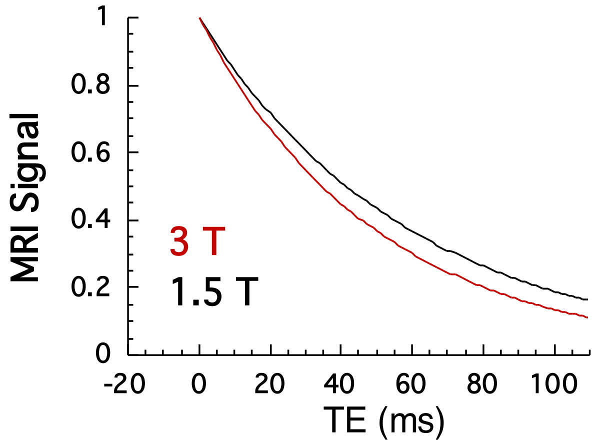

Percent Change

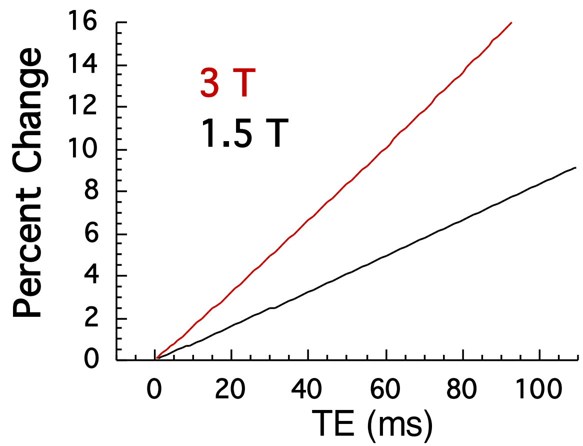

Functional Contrast

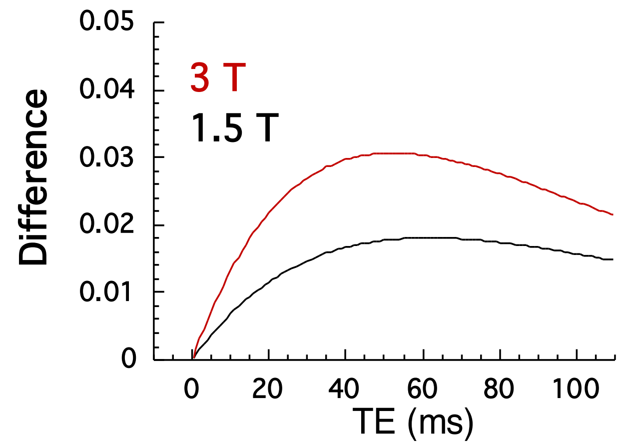

Magnetic Resonance in Medicine 45:595–604 (2001)

Neuroimaging at 1.5 T and 3.0 T: Comparison of Oxygenation-Sensitive Magnetic Resonance Imaging

Gunnar Krüger,* Andreas Kastrup, and Gary H. Glover

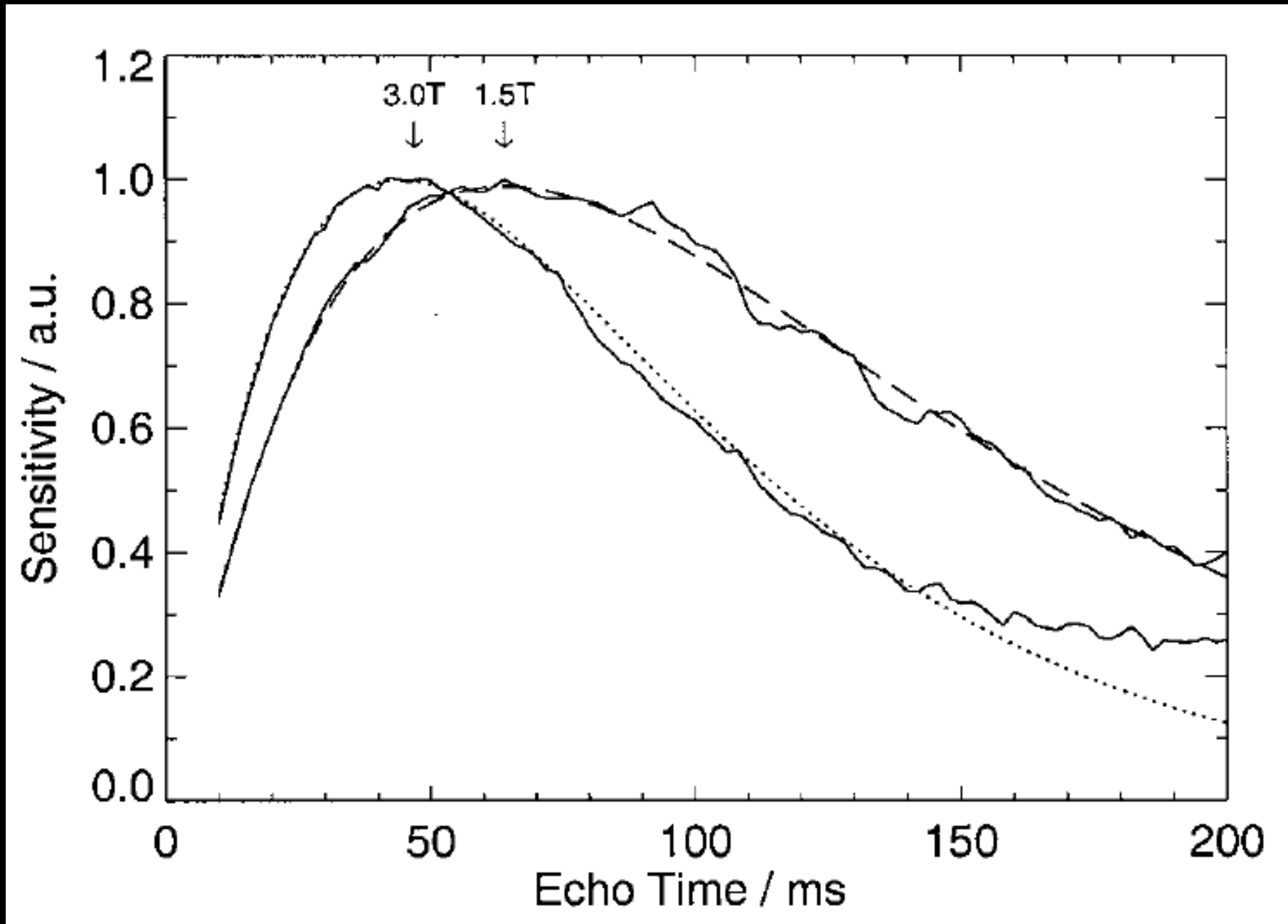

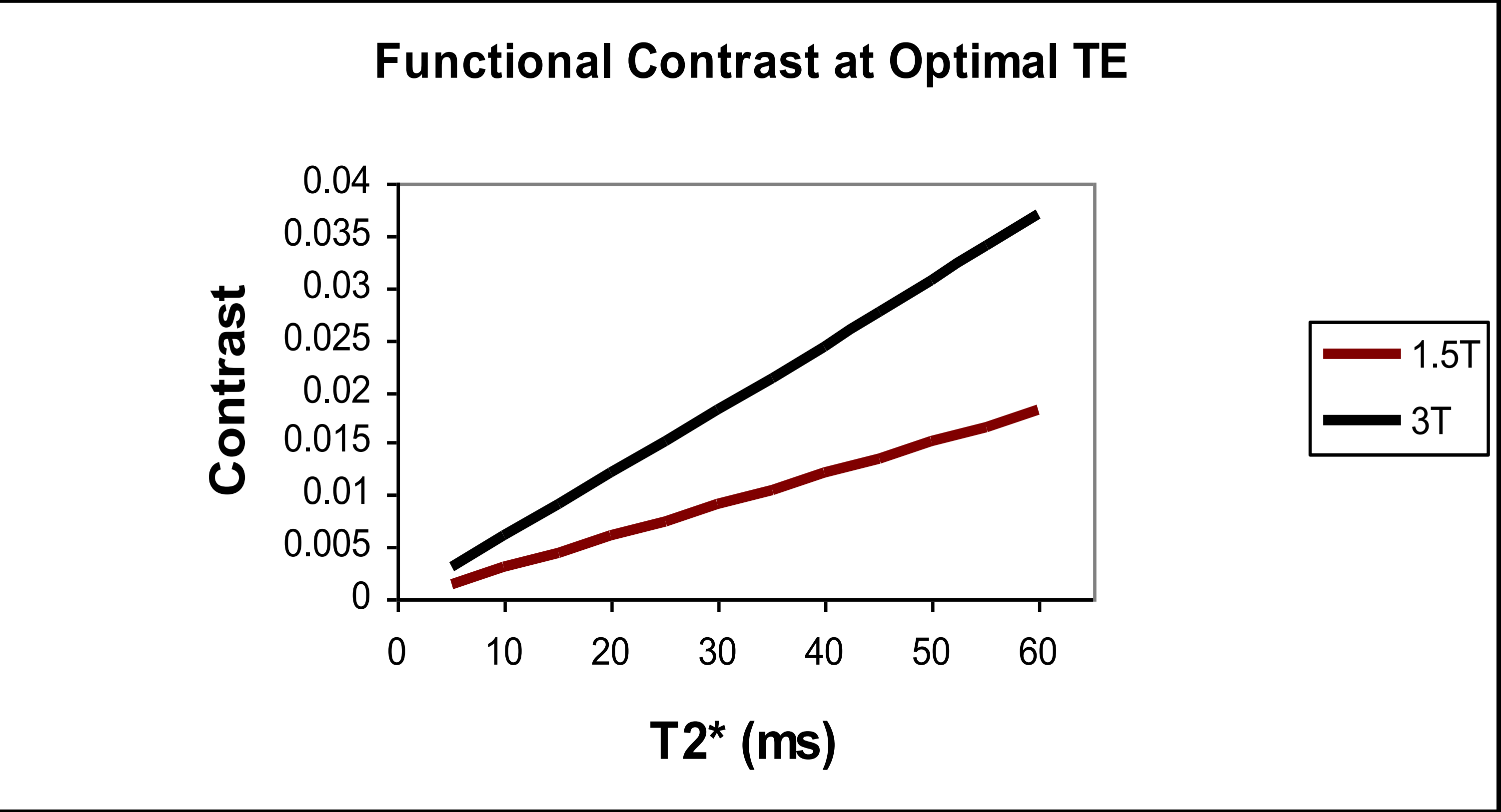
Functional Contrast at Optimal TE
Contrast
0.04
0.035
0.03
0.025
0.02
0.015
0.01
0.005
0
0
10
20
30
40
50
60
T2* (ms)
1.5T
3T

Magnetic Resonance in Medicine 45:595–604 (2001)

Neuroimaging at 1.5 T and 3.0 T: Comparison of Oxygenation-Sensitive Magnetic Resonance Imaging

Gunnar Krüger,* Andreas Kastrup, and Gary H. Glover

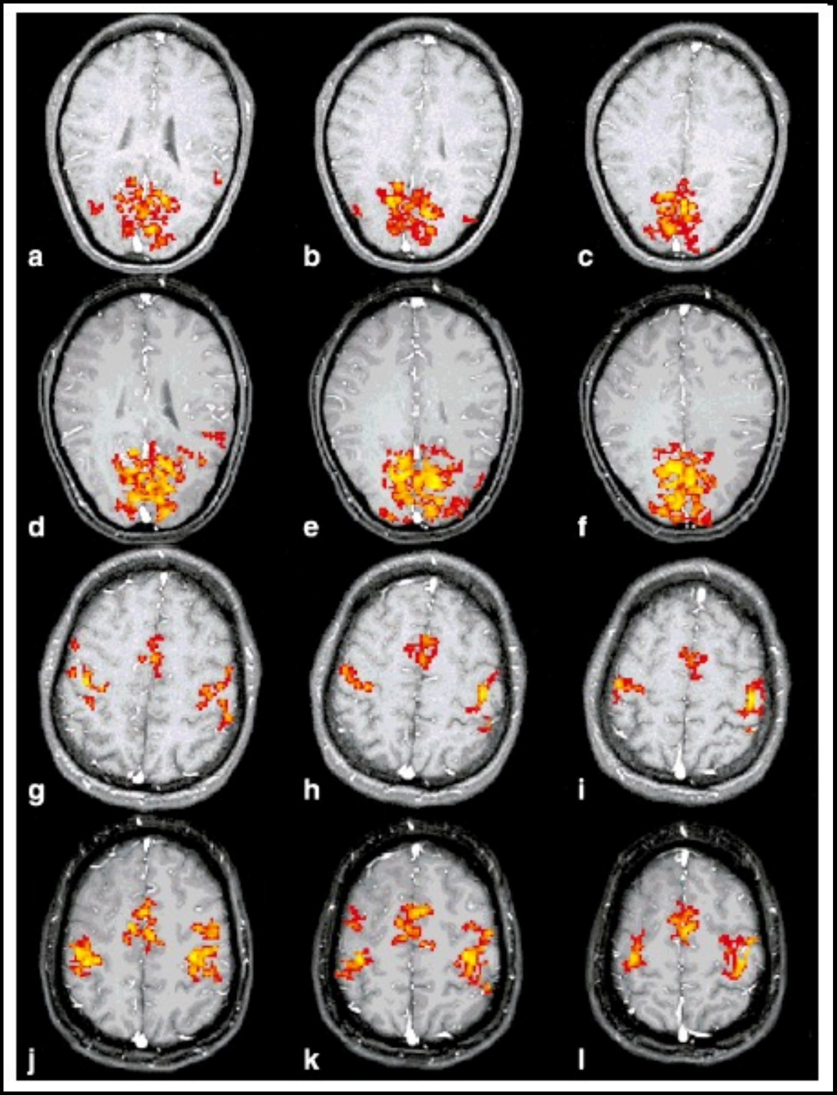

1.5

3.0

1.5

3.0

Gradient-Echo EPI

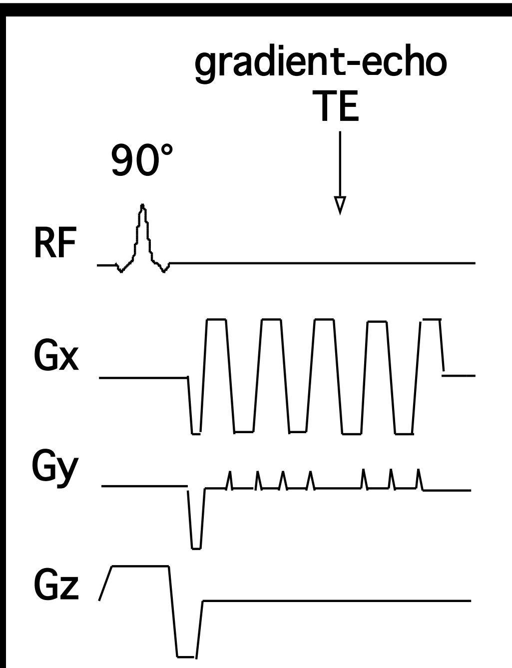

Spin-Echo EPI

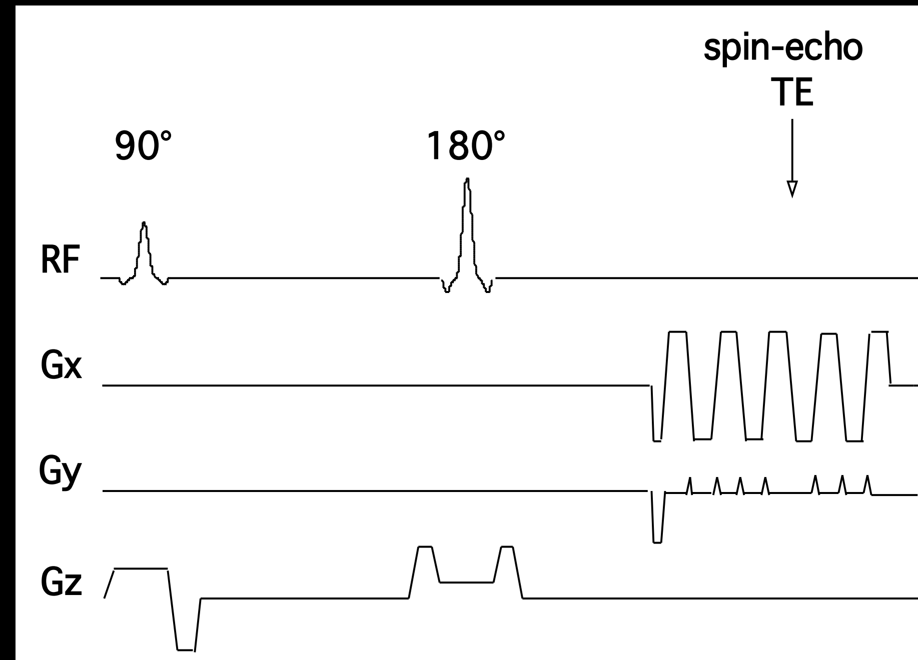

Contrast

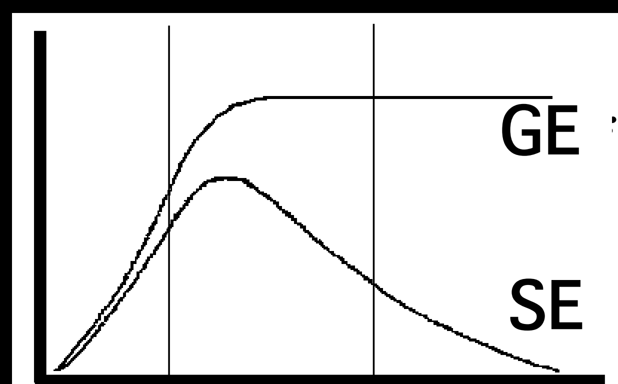

2.5 to 3 μm 3 to 15 μm 15 to ∞ μm

compartment size

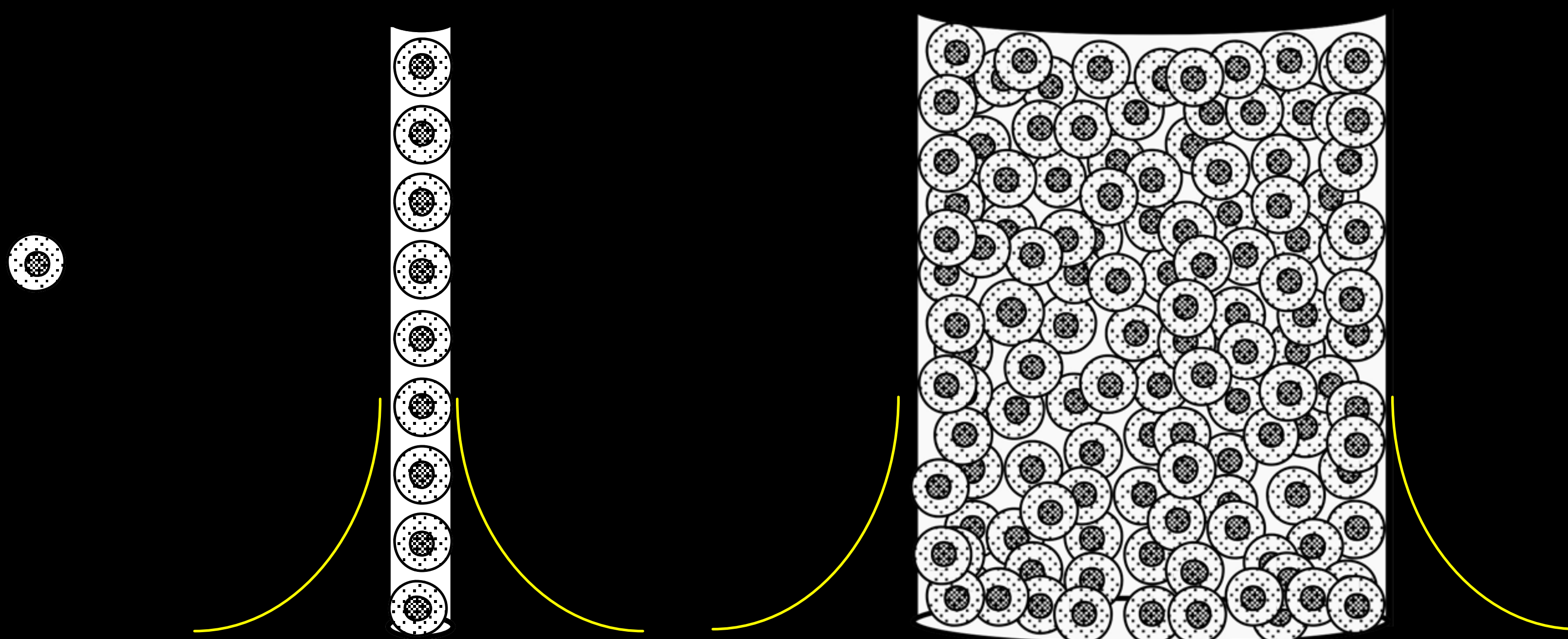

Bolus Injection of Gadolinium: Simultaneous GE and SE

GE
TE = 30 ms

SE
TE = 110 ms

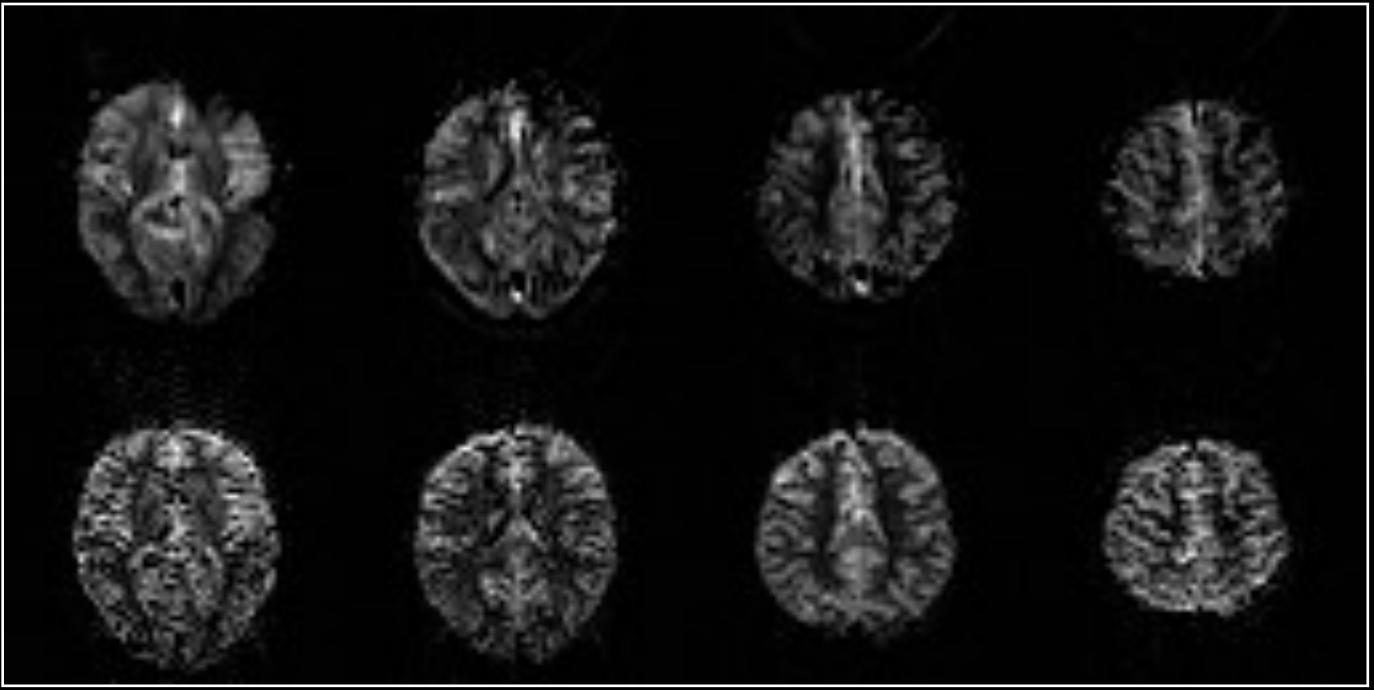

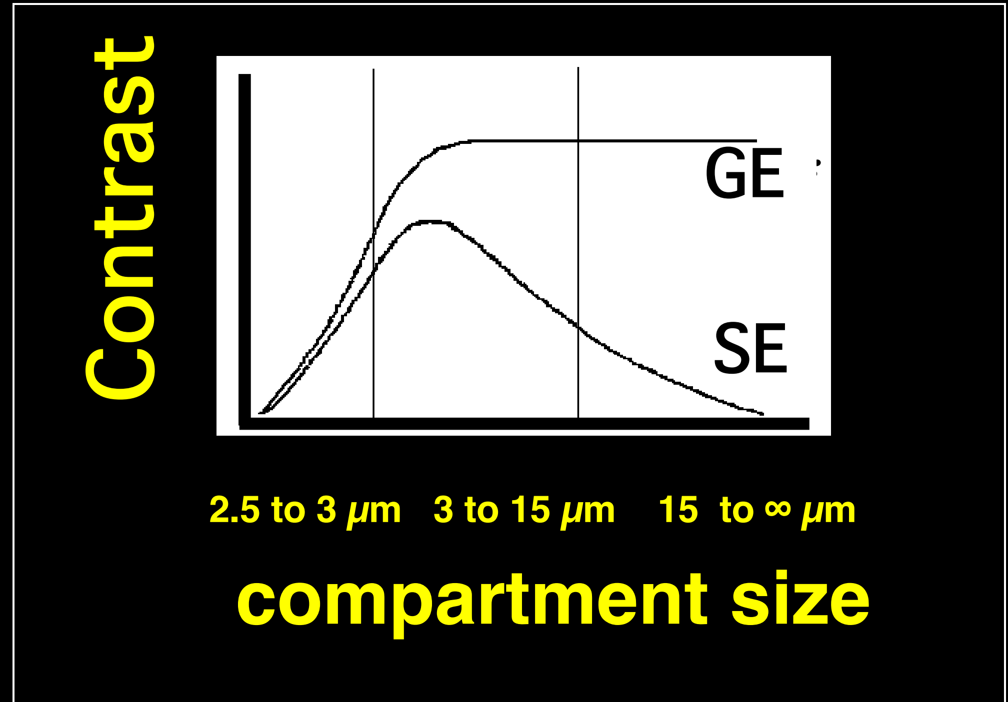

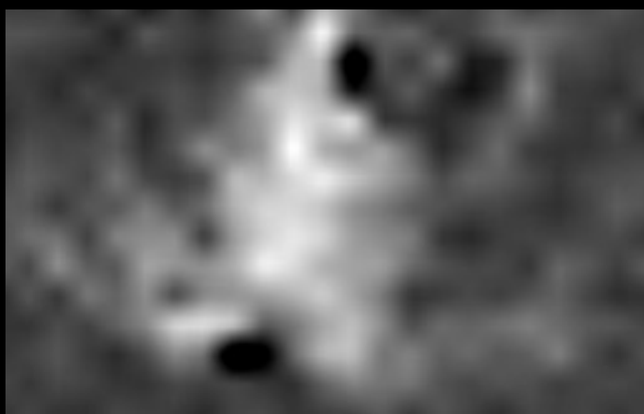

Gradient - Echo

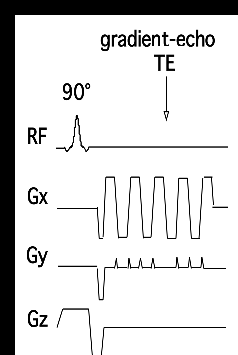

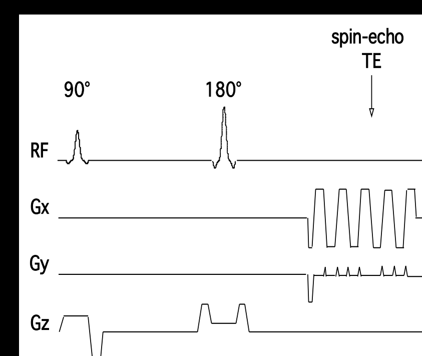

Spin - Echo

no diffusion weighting

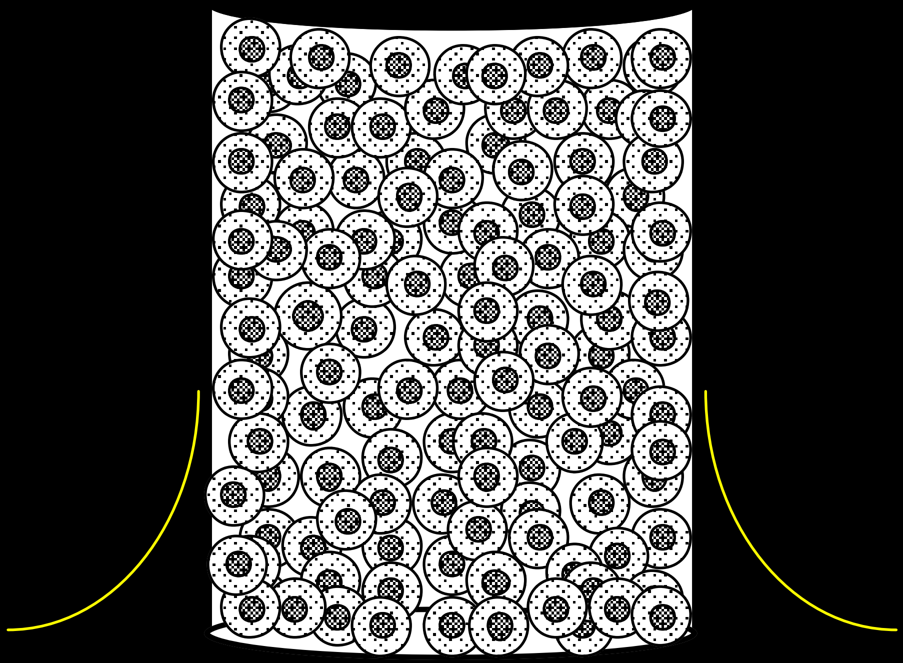

diffusion weighting

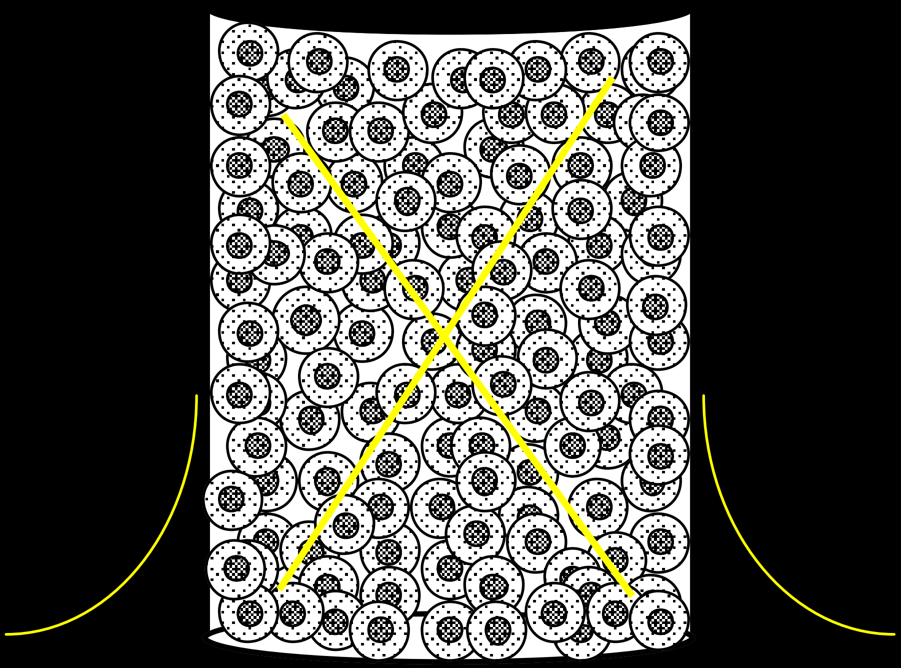

Summary of Diffusion-Weighted fMRI Data

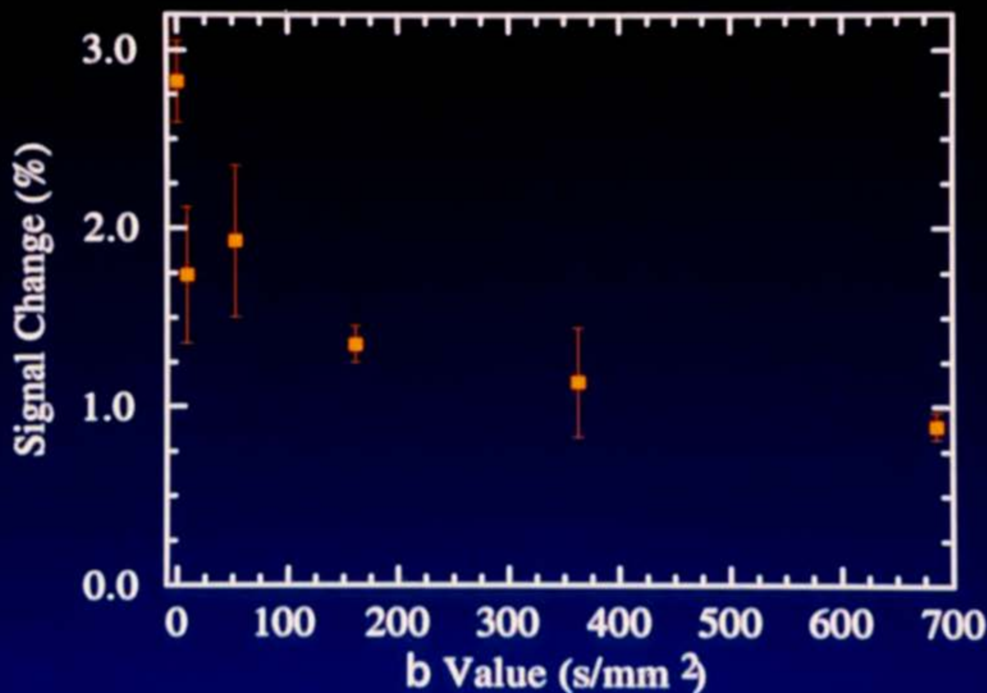

J. L. Boxerman, P. A. Bandettini, K. K. Kwong, J. R. Baker, T. L. Davis, B. R. Rosen, R. M. Weisskoff, The intravascular contribution to fMRI signal change: monte carlo modeling and diffusion - weighted studies in vivo. *Magn. Reson. Med.* 34, 4-10 (1995).

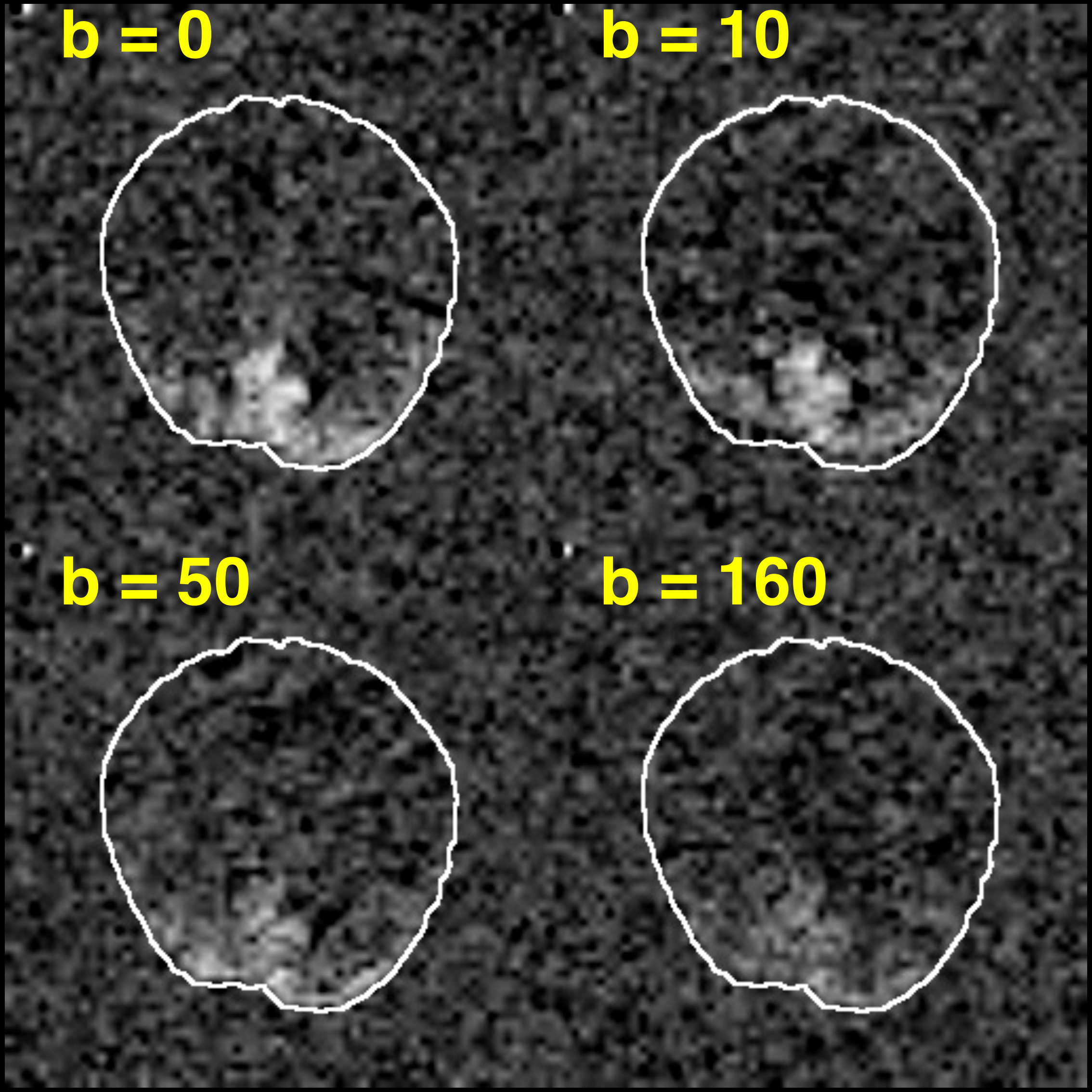

J. L. Boxerman, P. A. Bandettini, K. K. Kwong, J. R. Baker, T. L. Davis, B. R. Rosen, R. M. Weisskoff, The intravascular contribution to fMRI signal change: monte carlo modeling and diffusion - weighted studies in vivo. *Magn. Reson. Med.* 34, 4-10 (1995).

What we observe..

- Magnitude
- Location
- Parametric Dependence
- Latency

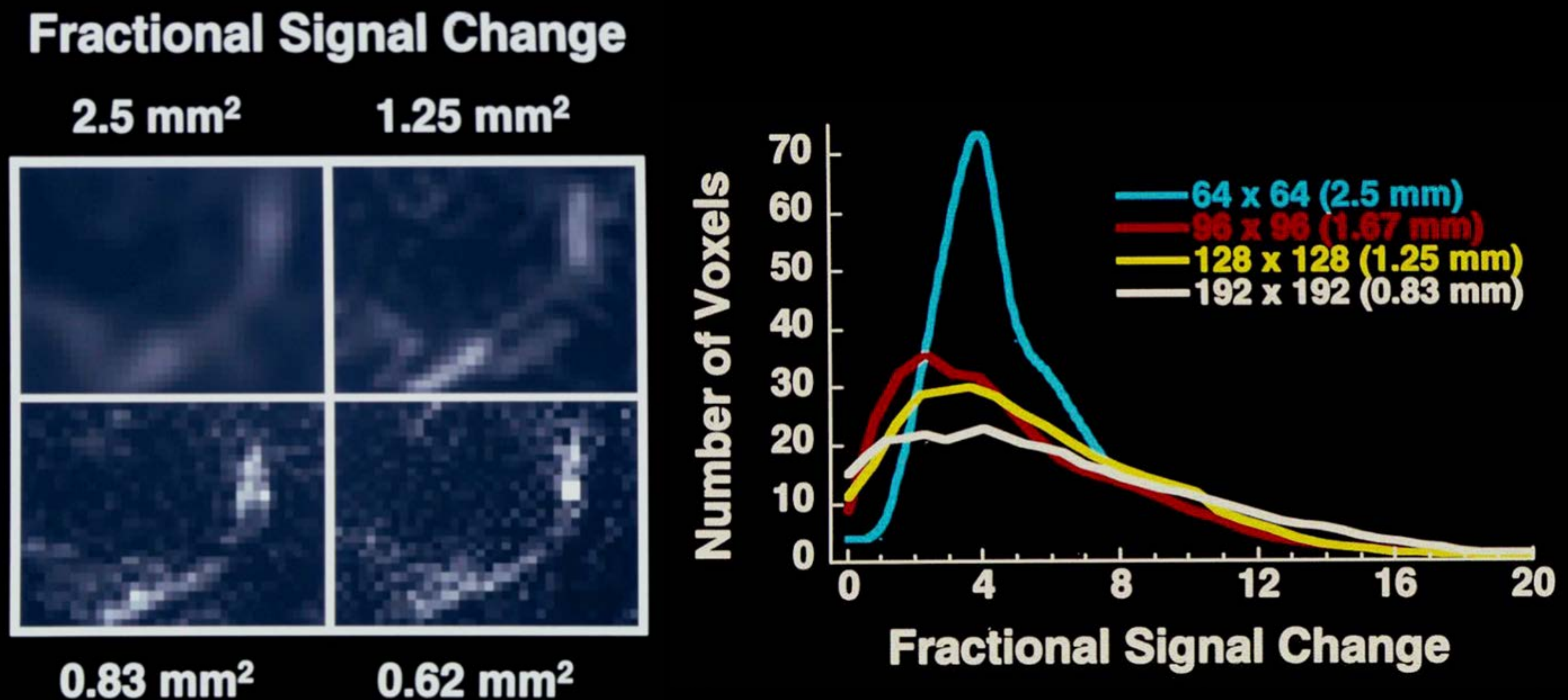

Jesmanowicz, P. A. Bandettini, J. S. Hyde, (1998) "Single shot half k-space high resolution EPI for fMRI at 3T." ***Magn. Reson. Med.*** **40, 754-762.**

Location

Anatomy

BOLD

Perfusion

Angiogram
Perfusion
BOLD

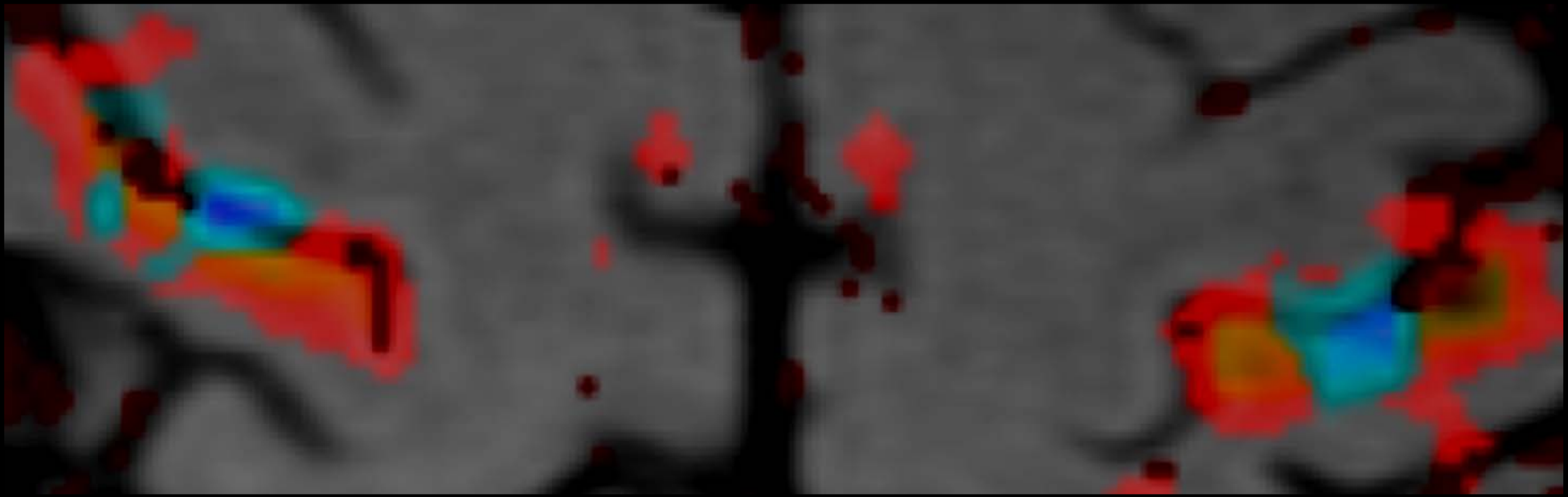

The spatial extent of the BOLD response

Ziad S. Saad,[a,b,*] Kristina M. Ropella,[b] Edgar A. DeYoe,[c] and Peter A. Bandettini[a]

[a] *Laboratory of Brain and Cognition, National Institute of Mental Health, NIH, Bethesda, MD 20892-1148, USA*
[b] *Department of Biomedical Engineering Marquette University, Milwaukee, WI 53233, USA*
[c] *Department of Cell Biology, Neurobiology and Anatomy, Medical College of Wisconsin, Milwaukee, WI 53226, USA*

Received 16 August 2002; revised 29 October 2002; accepted 21 November 2002

NeuroImage, **19:** 132-144, (2003).

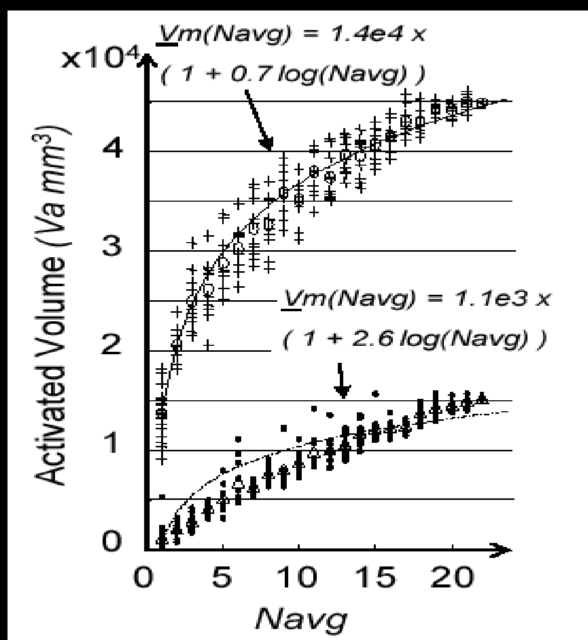

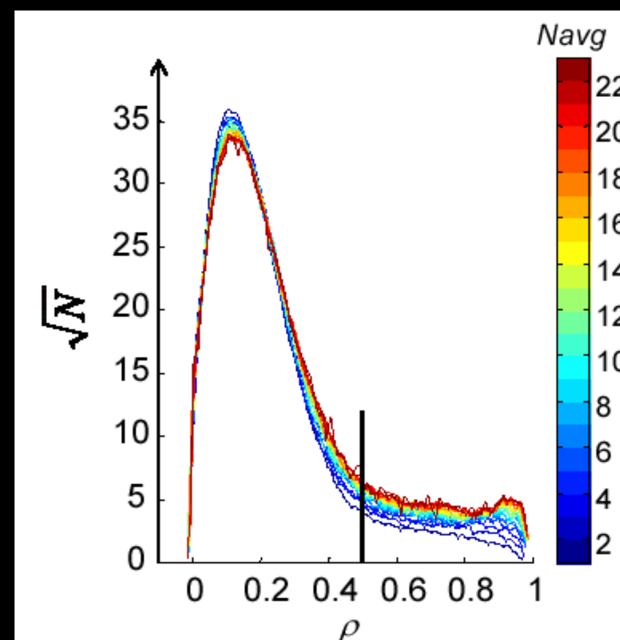

What we observe..

- Magnitude
- Location
- Parametric Dependence
- Latency

Motor Cortex

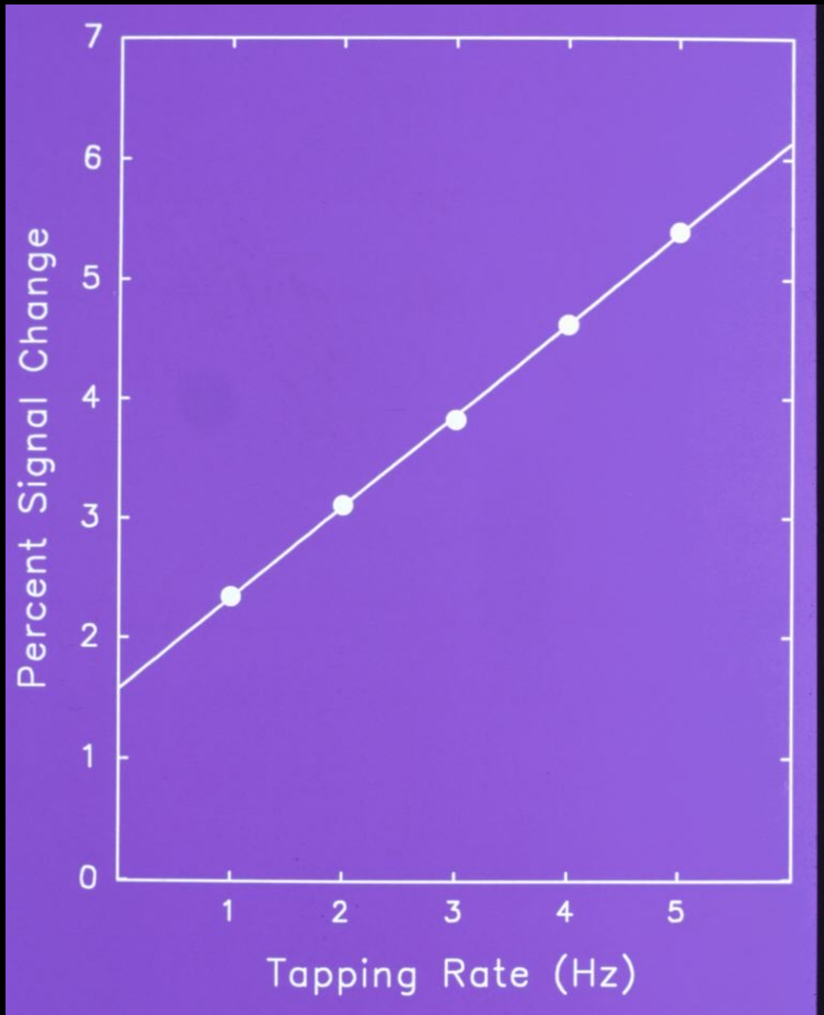

S. M. Rao et al, (1996) "Relationship between finger movement rate and functional magnetic resonance signal change in human primary motor cortex." *J. Cereb. Blood Flow and Met.* 16, 1250-1254.

Auditory Cortex

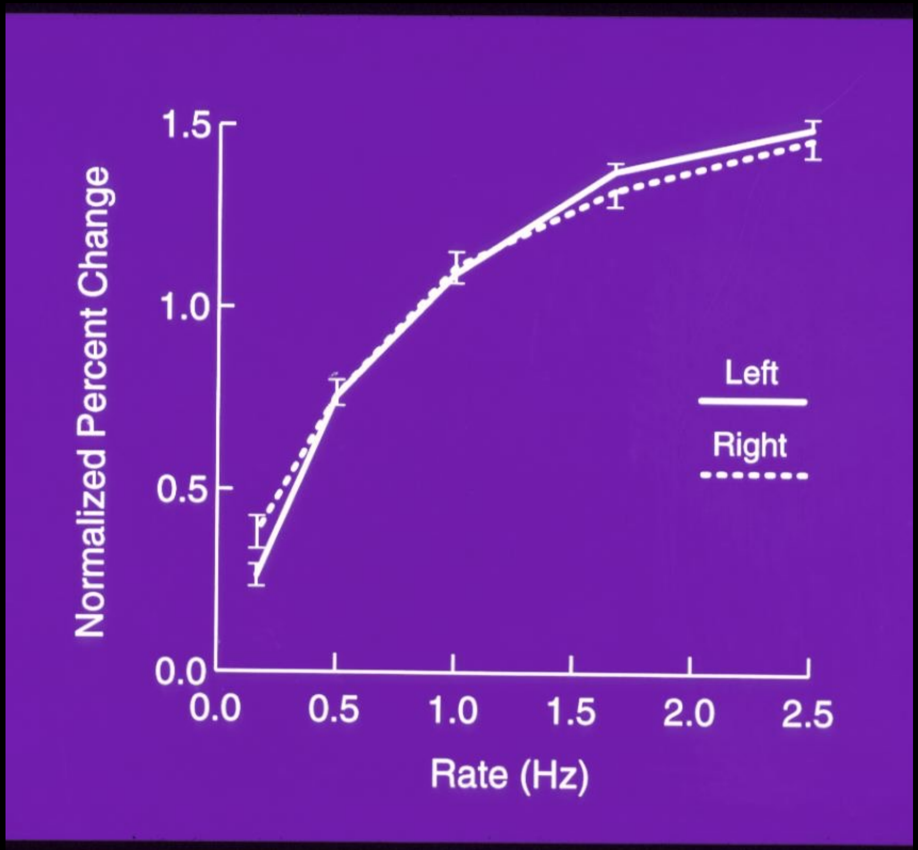

J. R. Binder, et al, (1994). "Effects of stimulus rate on signal response during functional magnetic resonance imaging of auditory cortex." *Cogn. Brain Res.* 2, 31-38

fMRI responses in human V1 are proportional to average firing rates in monkey V1

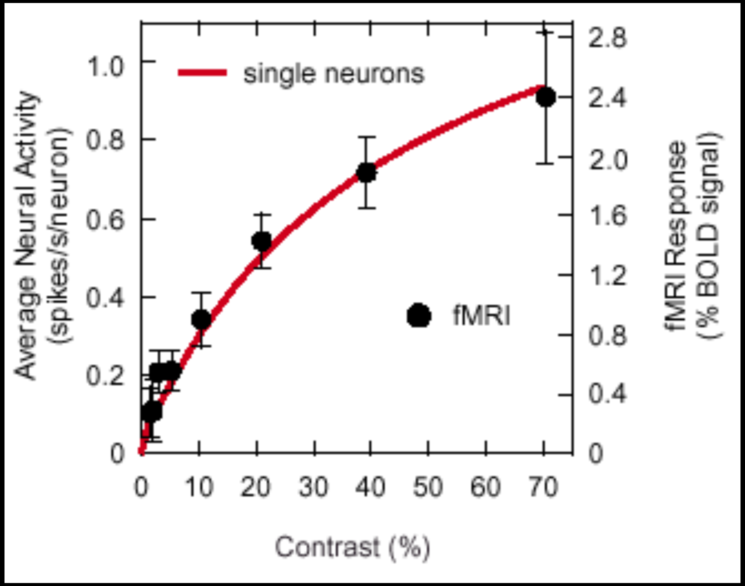

Heeger, D. J., Huk, A. C., Geisler, W. S., and Albrecht, D. G. 2000.Spikes versus BOLD: What does neuroimaging tell us about neuronal activity? *Nat. Neurosci.* **3:** 631–633.

0.4 spikes/sec -> 1% BOLD

Rees, G., Friston, K., and Koch, C. 2000. A direct quantitative relationship between the functional properties of human and macaque V5. *Nat. Neurosci.* **3:** 716–723.

9 spikes/sec -> 1% BOLD

Magnetic Resonance in Medicine 41:469–473 (1999)

Simultaneous Recording of Evoked Potentials and T_2^*-Weighted MR Images During Somatosensory Stimulation of Rat

Gerrit Brinker, Christian Bock, Elmar Busch, Henning Krep, Konstantin-Alexander Hossmann, and Mathias Hoehn-Berlage

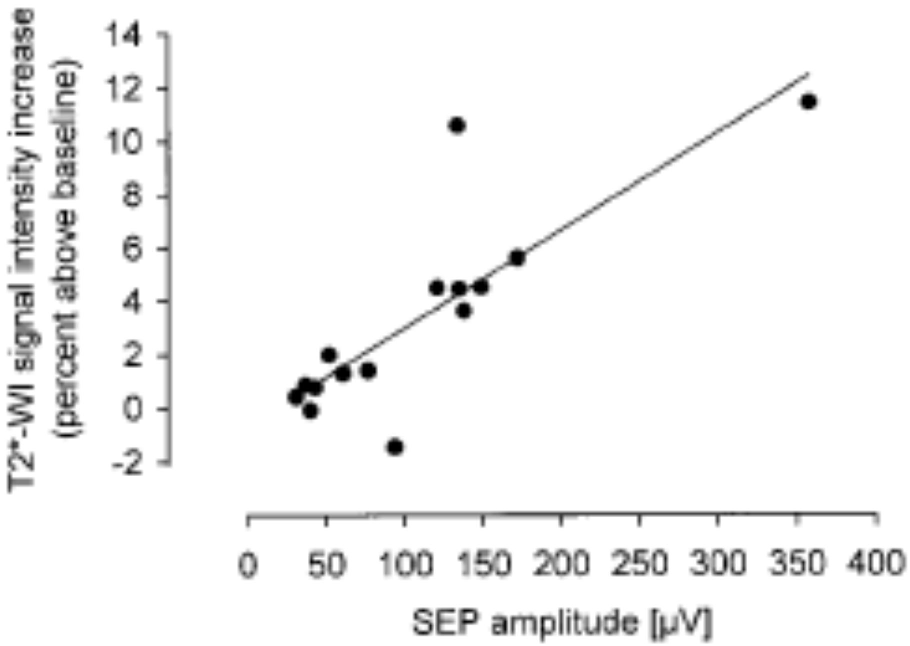

FIG. 3. Correlation of the increase of T_2^*-weighted imaging signal intensity with the peak-to-peak amplitude of the somatosensory evoked potential (SEP) during forepaw stimulation at increasing frequencies (data are from one individual animal; r = 0.82).

Negative BOLD effect

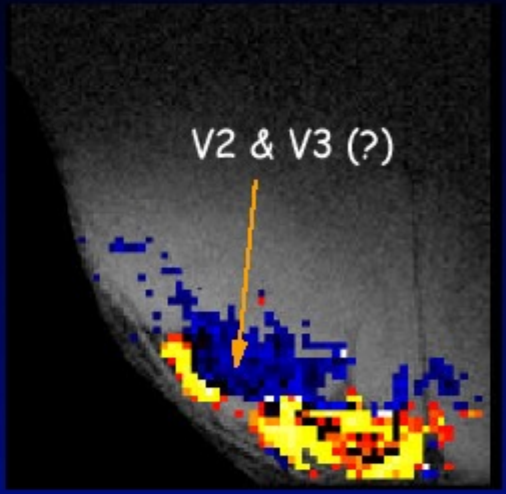

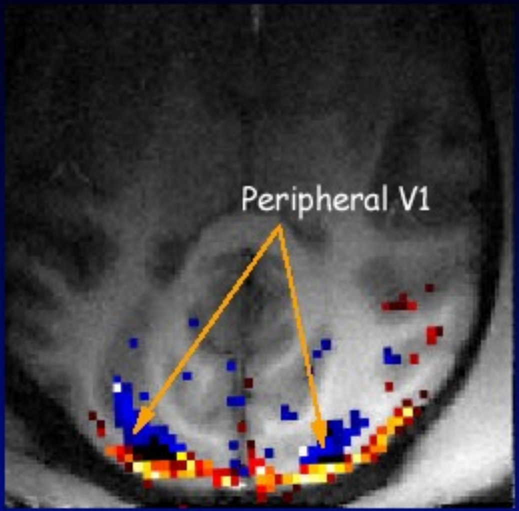

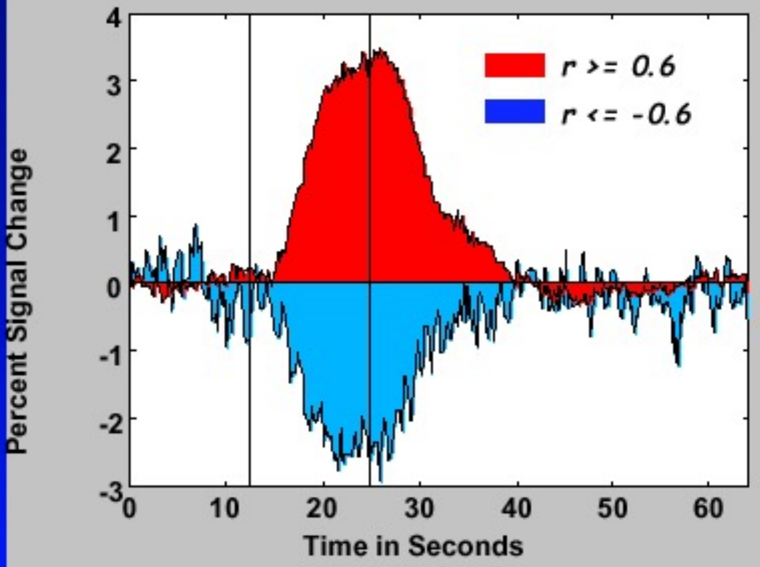

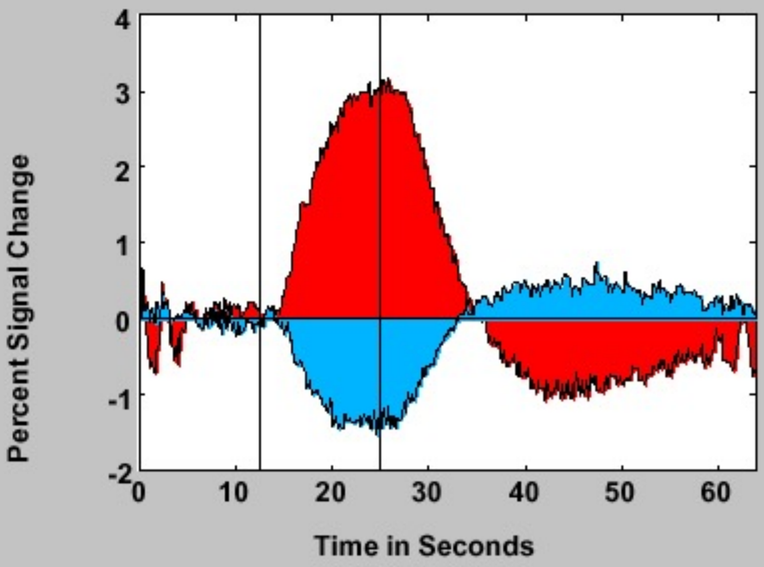

HBM 2003
Poster number: 308

The Negative BOLD Response in Monkey V1 Is Associated with Decreases in Neuronal Activity

Amir Shmuel*†, Mark Augath, Axel Oeltermann, Jon Pauls, Yusuke Murayama, Nikos K. Logothetis

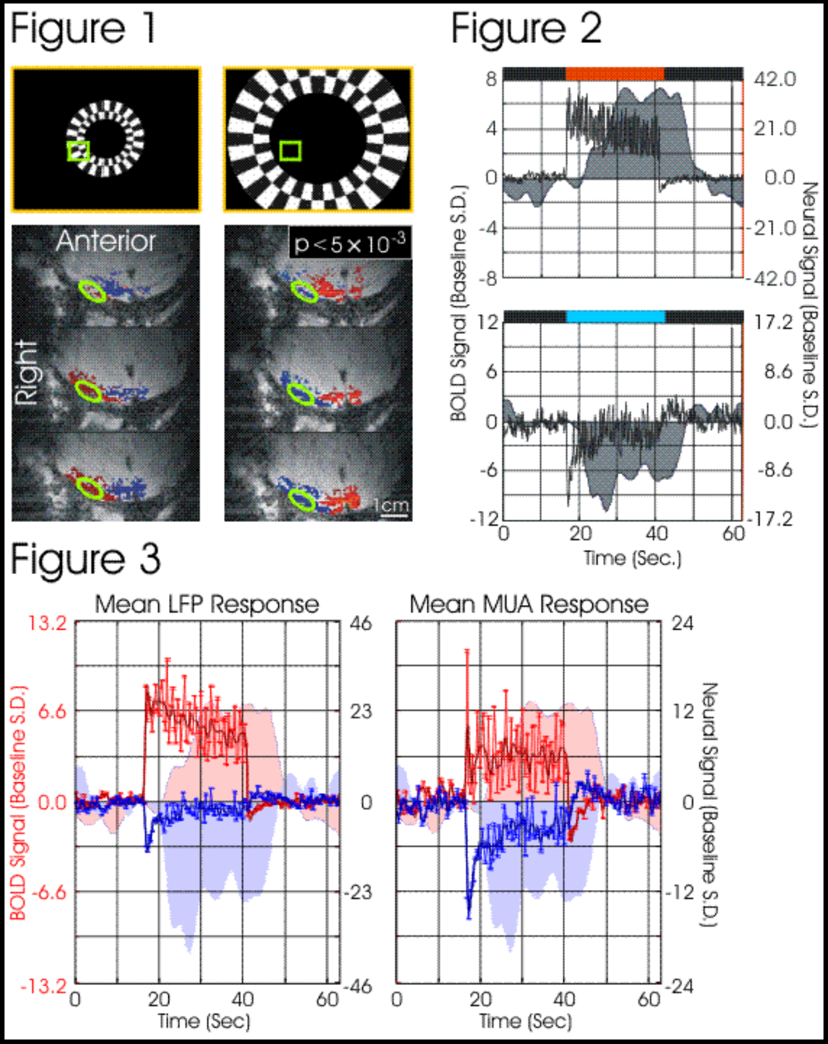

Logothetis et al. (2001) "Neurophysiological investigation of the basis of the fMRI signal" Nature, 412, 150-157

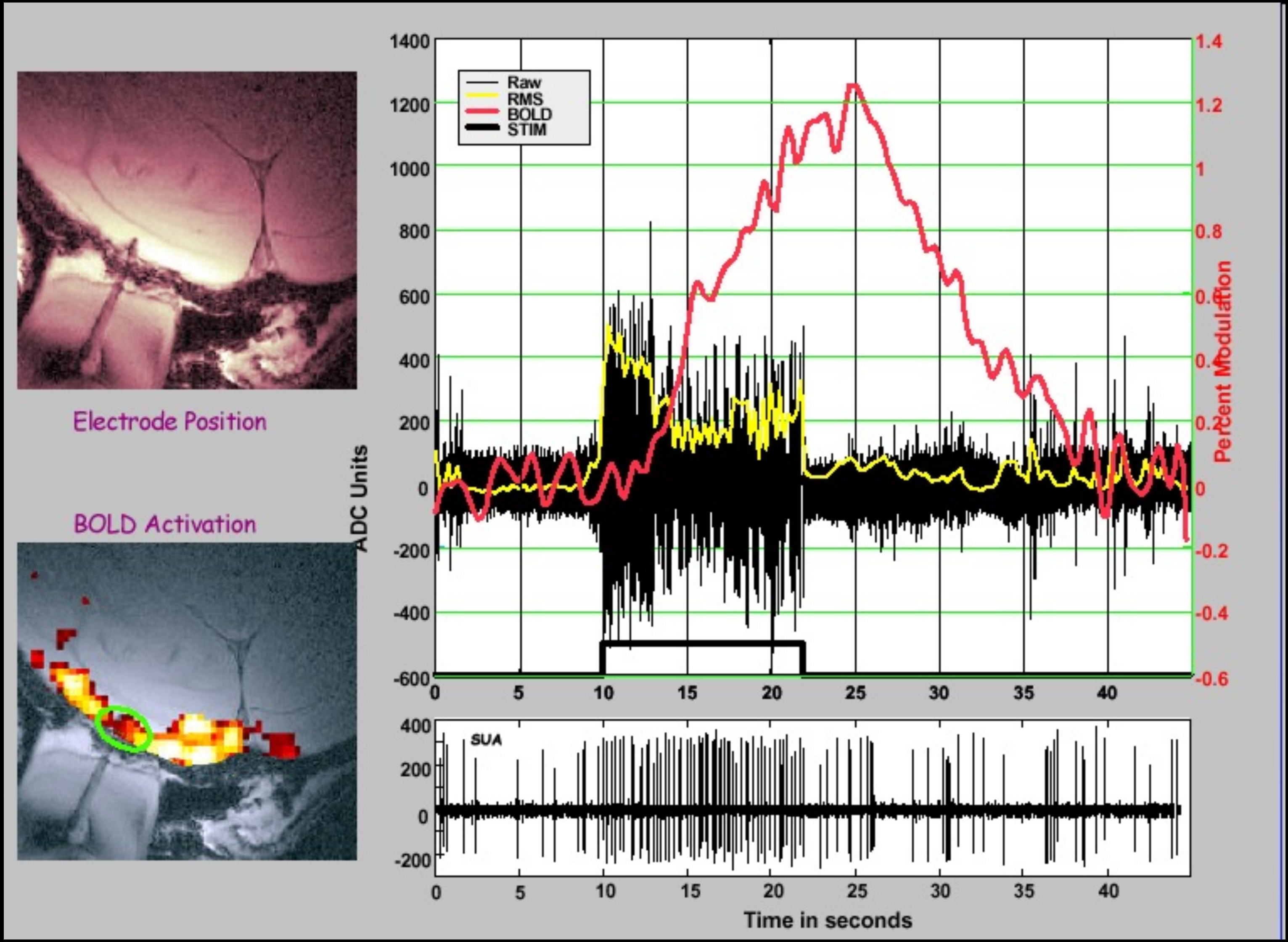

Logothetis et al. (2001) "Neurophysiological investigation of the basis of the fMRI signal" Nature, 412, 150-157

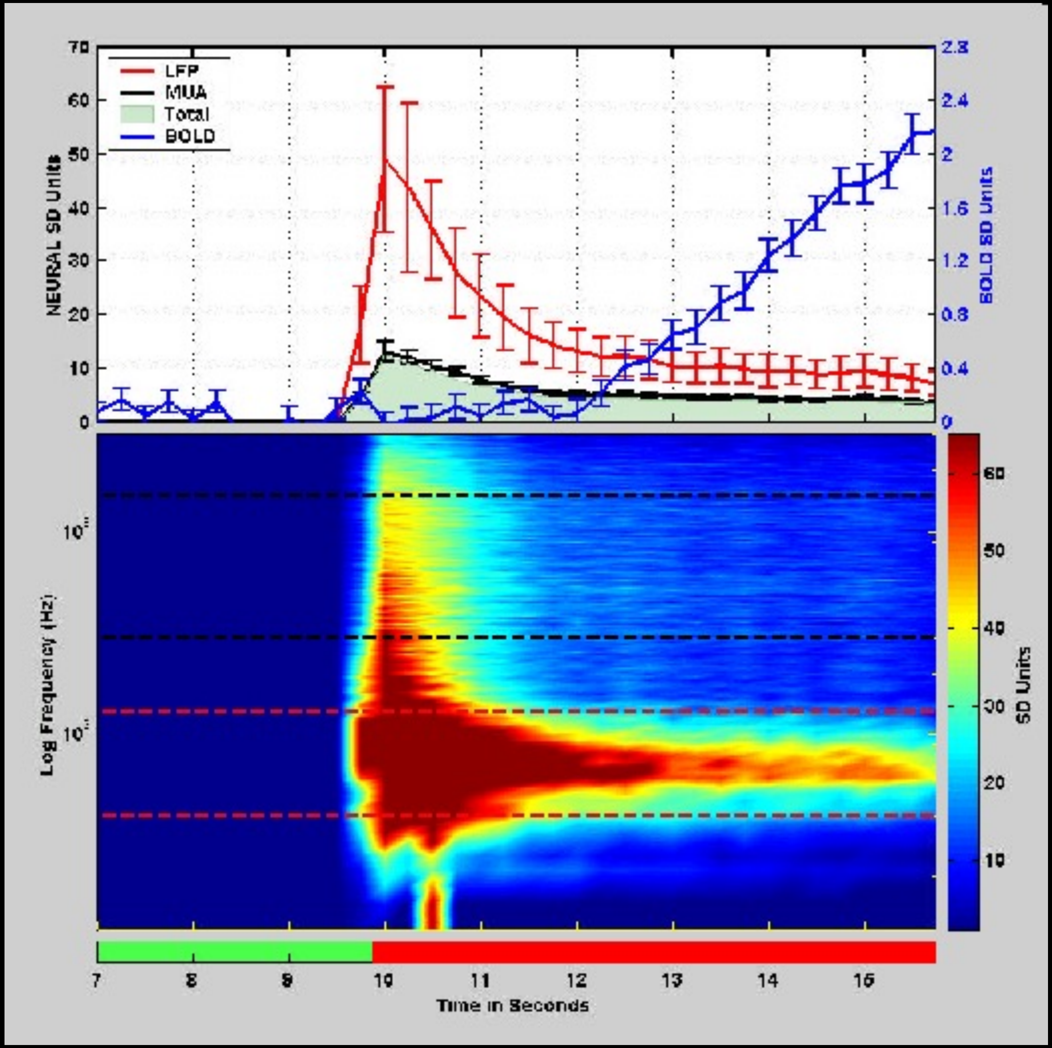

The Journal of Neuroscience, May 15, 2003 • 23(10):3963–3971 • 3963

The Underpinnings of the BOLD Functional Magnetic Resonance Imaging Signal

Nikos K. Logothetis
Max Planck Institute for Biological Cybernetics, 72076 Tuebingen, Germany

In summary, MUA mostly represents the spiking of neurons, with single-unit recordings mainly reporting on the activity of the projection neurons that form the exclusive output of a cortical area. LFPs, on the other hand, represent slow waveforms, including synaptic potentials, afterpotentials of somatodendritic spikes, and voltage-gated membrane oscillations, that reflect the input of a given cortical areas as well as its local intracortical processing, including the activity of excitatory and inhibitory interneurons.

Logothetis et al. (2001) "Neurophysiological investigation of the basis of the fMRI signal" Nature, 412, 150-157

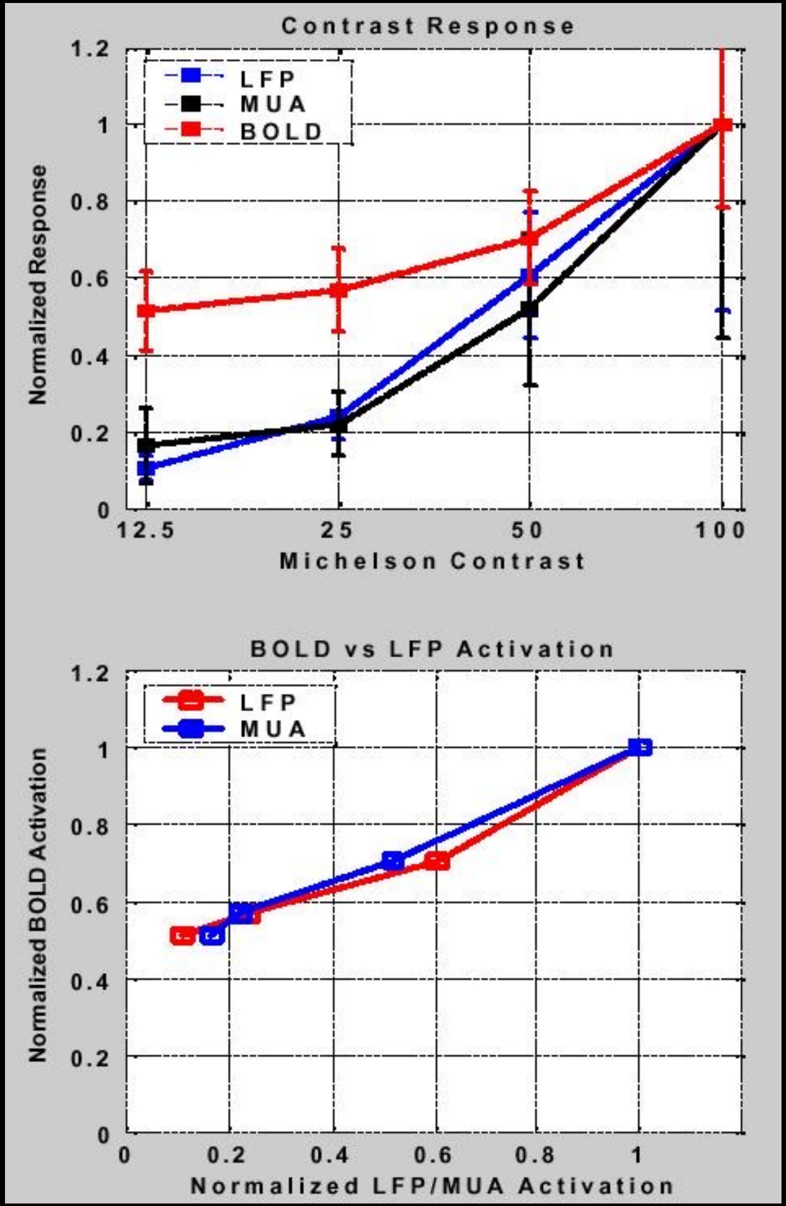

Evidence that inhibitory input produces increased blood flow

Journal of Physiology (1998), 512.2, pp.555–566

Modification of activity-dependent increases of cerebral blood flow by excitatory synaptic activity and spikes in rat cerebellar cortex

Claus Mathiesen *†, Kirsten Caesar *, Nuran Akgören * and Martin Lauritzen *‡

**Department of Medical Physiology, The Panum Institute, University of Copenhagen,* †*NeuroSearch A/S, Glostrup and* ‡*Department of Clinical Neurophysiology, Glostrup Hospital, Denmark*

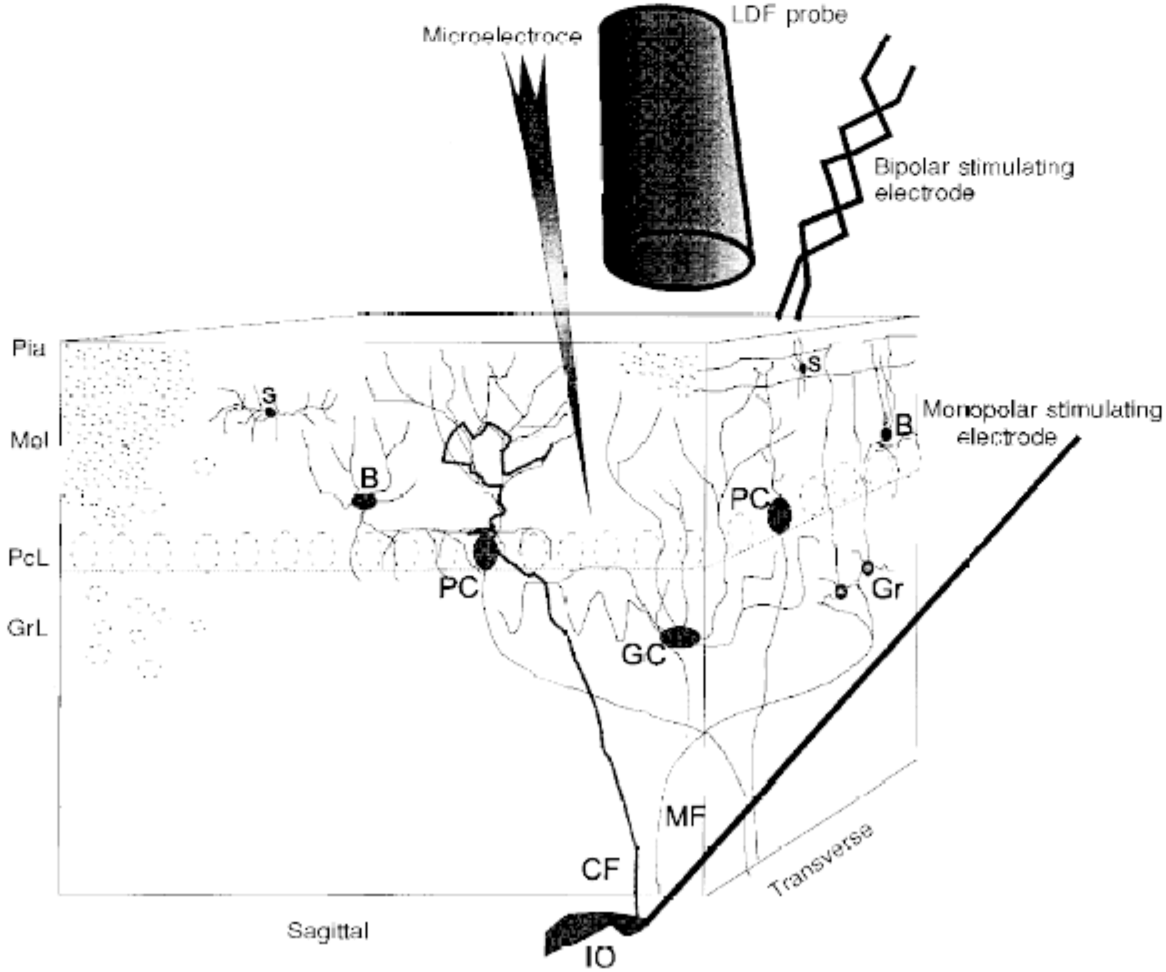

Figure 1. Schematic three-dimensional drawing of experimental set-up, including neurones of interest and position of laser Doppler probe, stimulating and recording electrodes

The positions of the three cerebellar layers, molecular (Mol, with a thickness of 400 μm), Purkinje cell (PcL, about 100 μm) and granular (GrL, 400–500 μm), are indicated. The molecular layer contains granule cell axons, called parallel fibres, the dendrites of Purkinje cells, stellate cells (S) and basket cells (B). The granule cell layer contains granule cells (Gr) and Golgi cells (GC). The superficial parallel fibres were stimulated by a bipolar stimulating electrode, while climbing fibres (CF) were stimulated by a monopolar electrode lowered into the caudal part of the inferior olive (IO). Field potentials and single unit spike activity were recorded with a glass microelectrode. CBF was recorded by a laser Doppler flowmetry (LDF) probe located 0·3–0·5 mm above the pial surface (Pia).

Divergence of spike rate and blood flow during parallel fiber stimulation

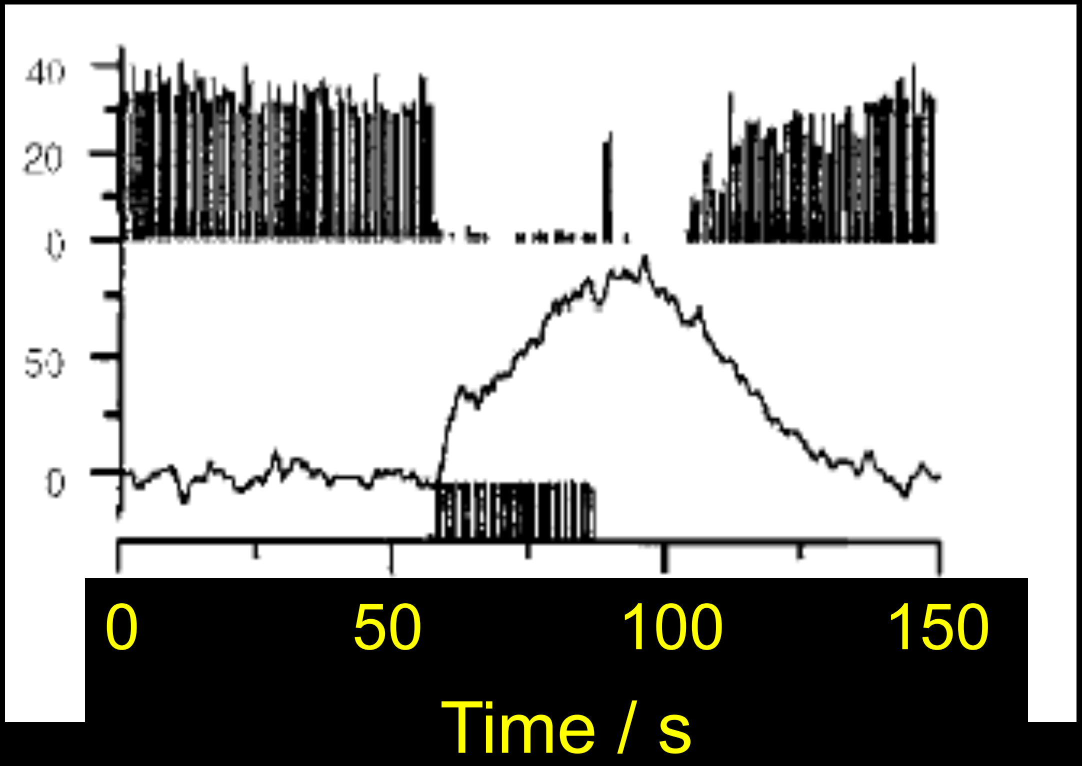

Mathiesen, Caesar, Akgören, Lauritzen (1998), J Physiol 512.2:555-566

NEUROIMAGE **6**, 270–278 (1997)
ARTICLE NO. NI970300

Characterizing the Relationship between BOLD Contrast and Regional Cerebral Blood Flow Measurements by Varying the Stimulus Presentation Rate

Geraint Rees, A. Howseman, O. Josephs, C. D. Frith, K. J. Friston, R. S. J. Frackowiak, and R. Turner
The Wellcome Department of Cognitive Neurology, Institute of Neurology, Queen Square, London WC1N 3BG, United Kingdom

Flow modulation is not necessarily the same as BOLD modulation

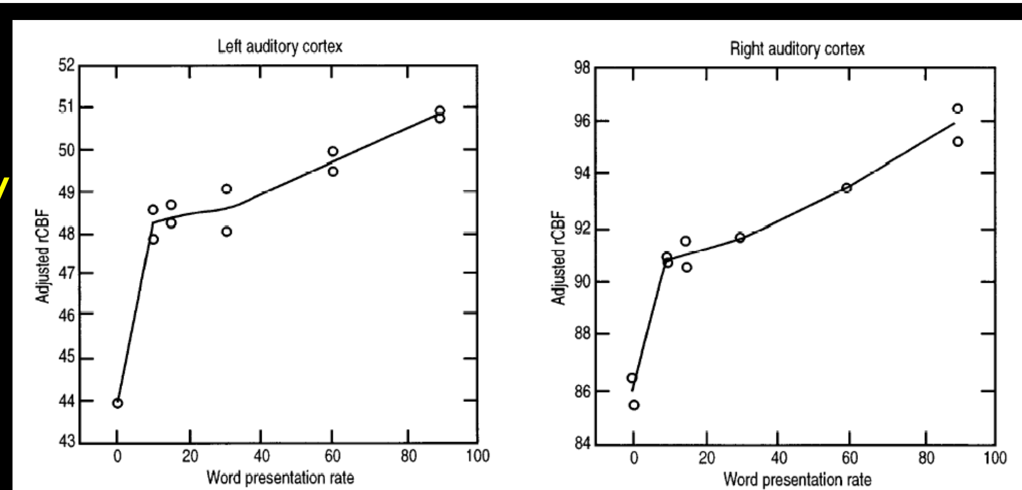

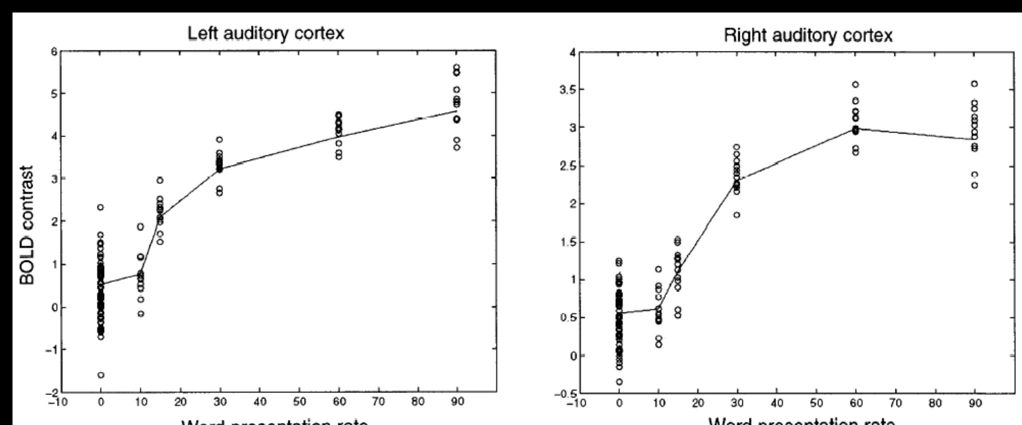

Negative BOLD in carotid artery disease

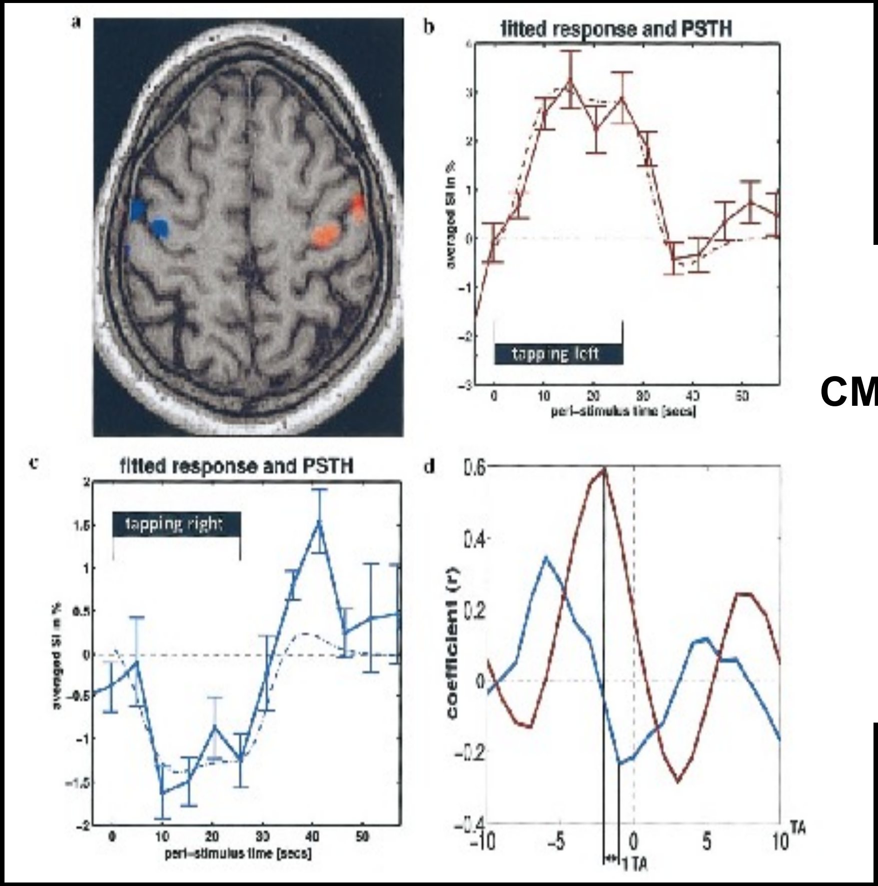

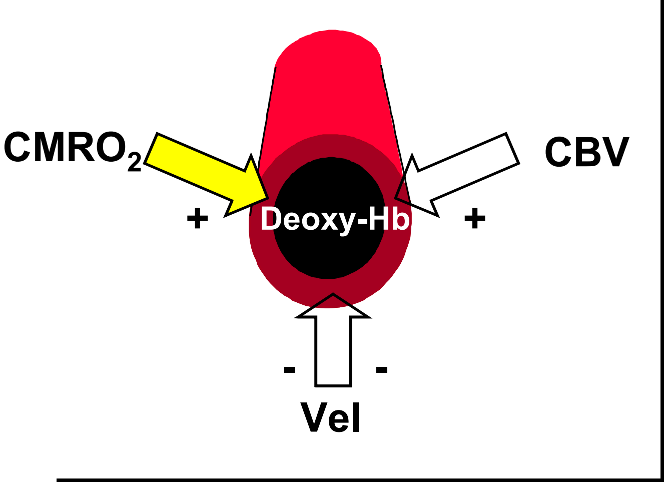

Röther et al. NeuroImage 2002

Courtesy of Arno Villringer

Increase in deoxy-Hb and oxy-Hb during focal seizure

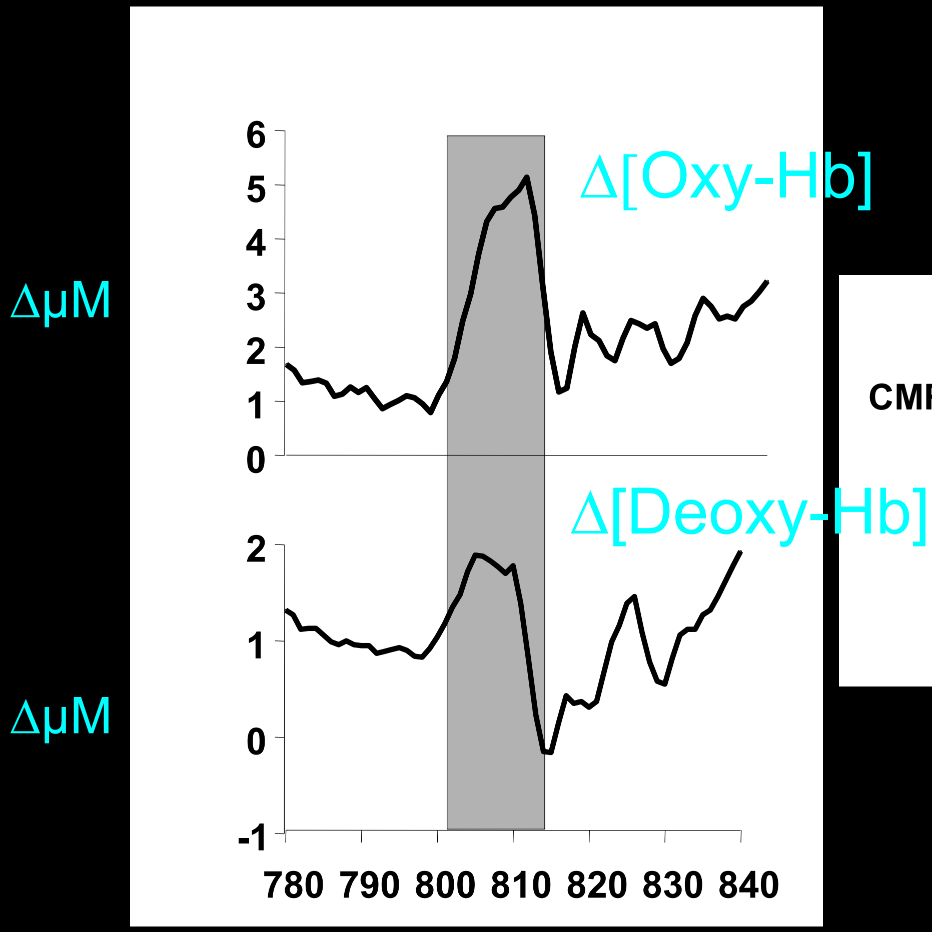

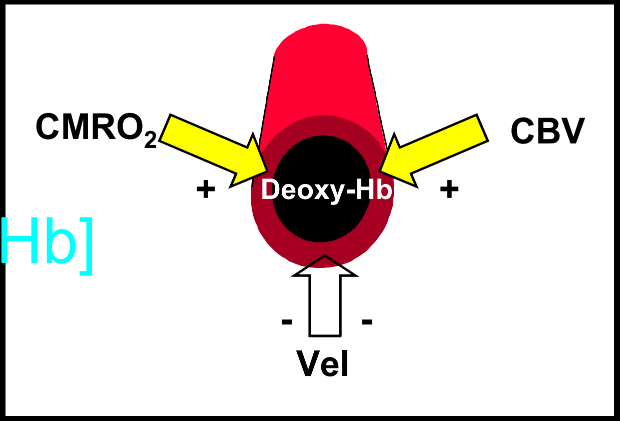

Courtesy of Arno Villringer

Altered neurovascular coupling: Pathology, drugs

Pathologic state / Drug	**Reference**
Carotid occlusion	Röther et al. 2002
Transient global ischemia	Schmitz et al. 1998
Penumbra of cerebral ischemia	Mies et al. 1993, Wolf et al. 1997
Subarachnoid hemorrhage	Dreier et al. 2000
Trauma	Richards et al. 2001
Epilepsy	Fink et al. 1996, Brühl et al. 1998, von Pannwitz et al. 2002
Alzheimer´s disease	Hock et al. 1996, Niwa et al. 2000
Theophylline	Ko et al. 1990, Dirnagl et al. 1994
Scopolamine	Tsukada et al. 1998

Courtesy of Arno Villringer

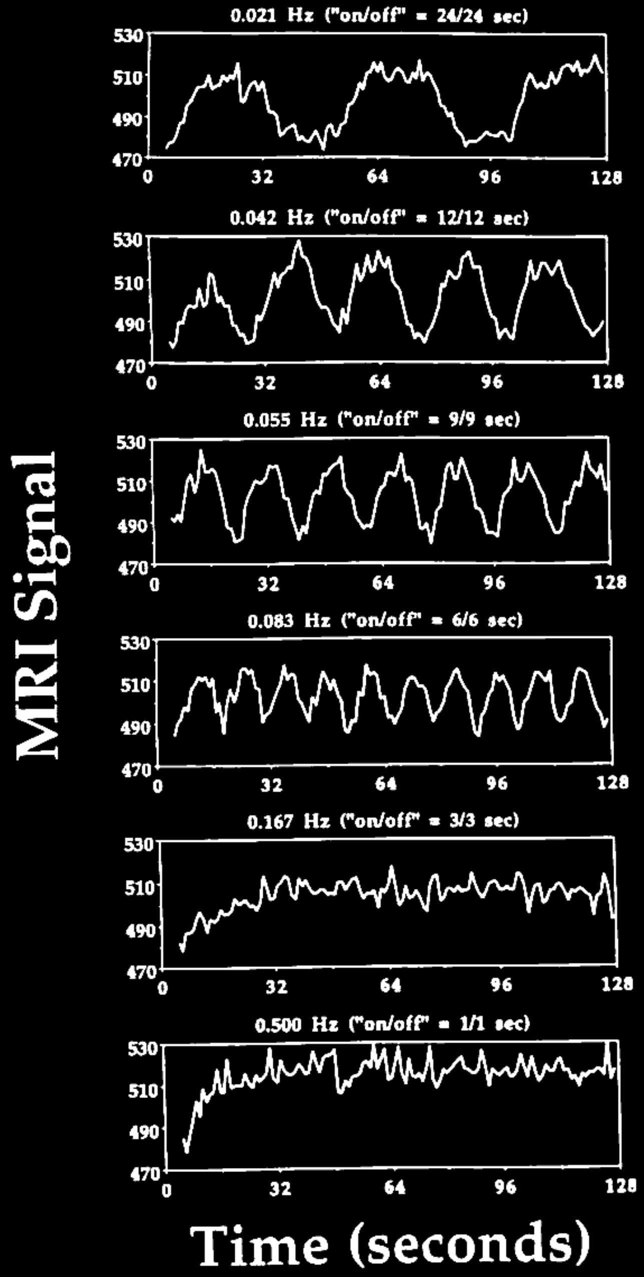

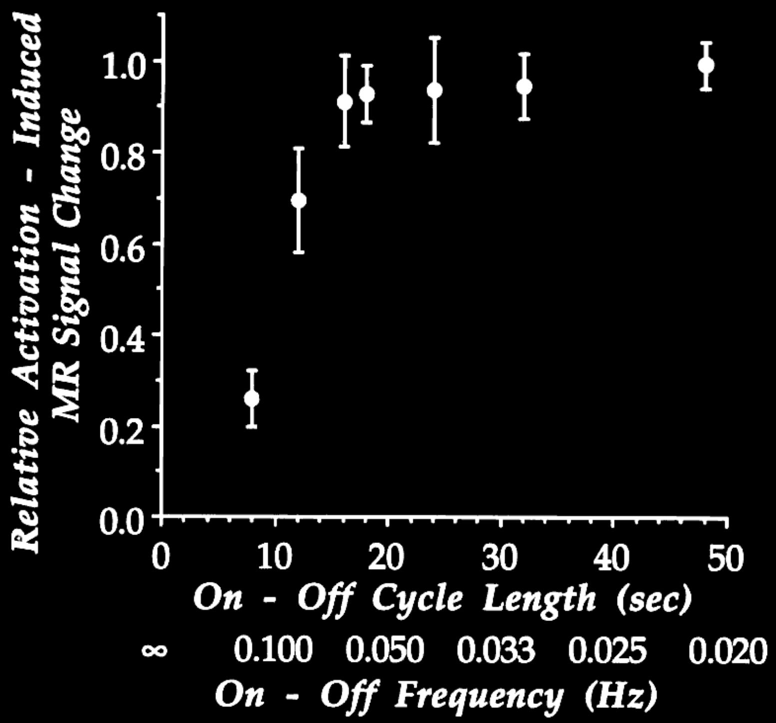

P. A. Bandettini, Functional MRI temporal resolution *in* "Functional MRI" (C. Moonen, and P. Bandettini., Eds.), p. 205-220, Springer - Verlag,. 1999.

BOLD

Flow

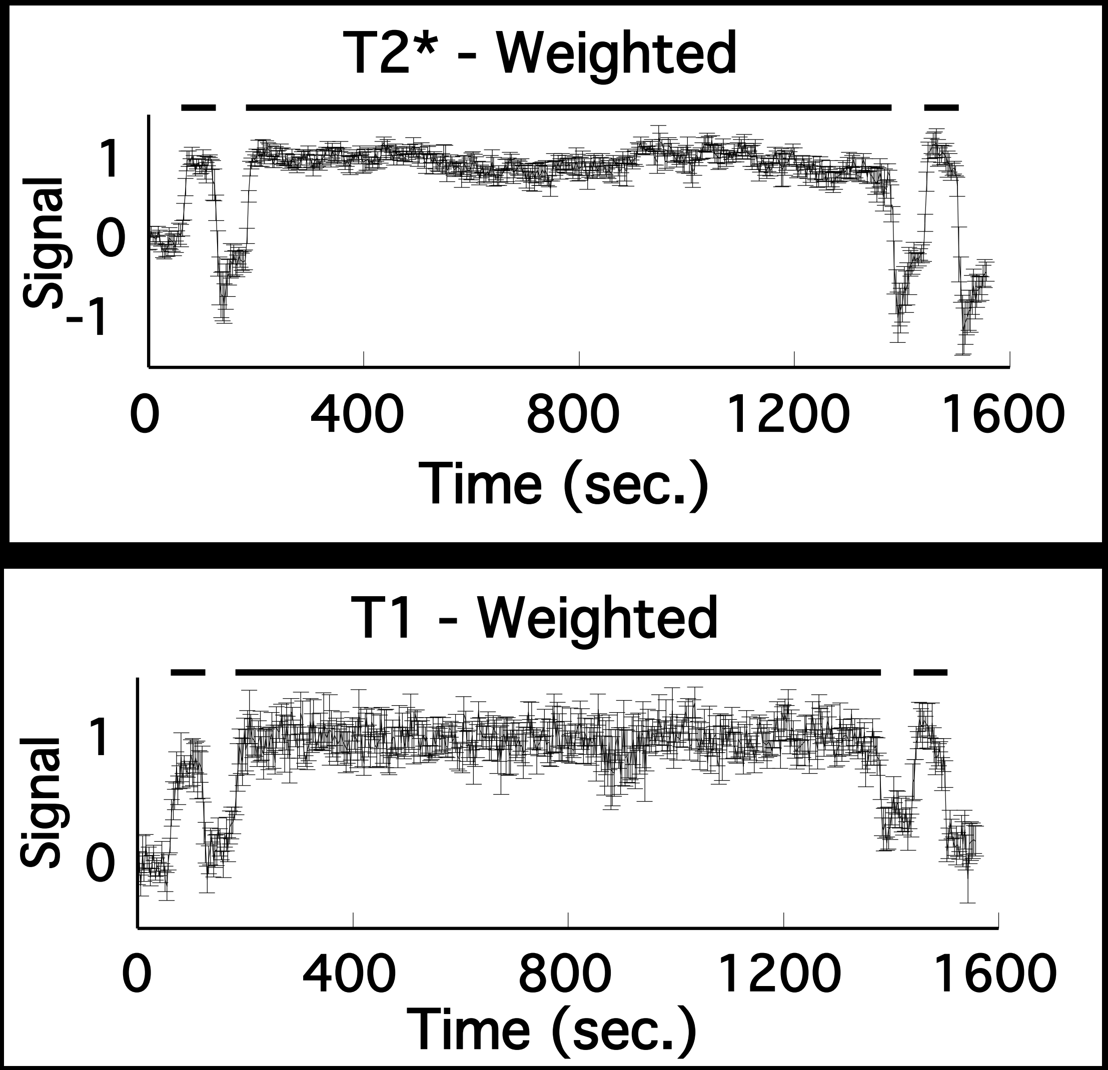

P. A. Bandettini, K. K. Kwong, T. L. Davis, R. B. H. Tootell, E. C. Wong, P. T. Fox, J. W. Belliveau, R. M. Weisskoff, B. R. Rosen, (1997). "Characterization of cerebral blood oxygenation and flow changes during prolonged brain activation." *Human Brain Mapping* 5, 93-109.

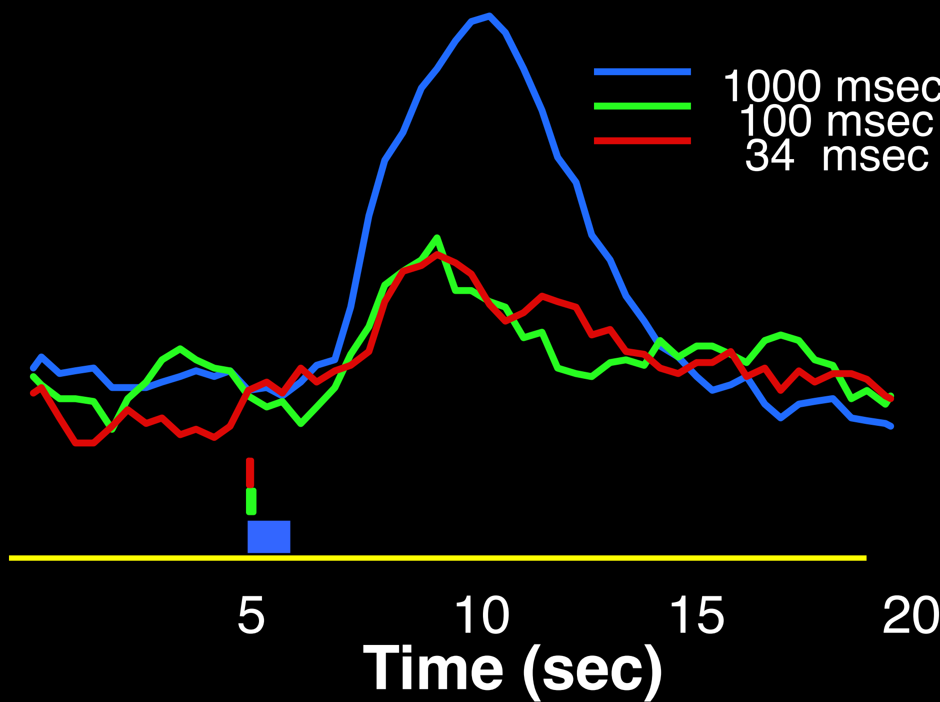

R. L. Savoy, et al., Pushing the temporal resolution of fMRI: studies of very brief visual stimuli, onset variability and asynchrony, and stimulus-correlated changes in noise [oral], 3'rd Proc. Soc. Magn. Reson., Nice, p. 450. (1995).

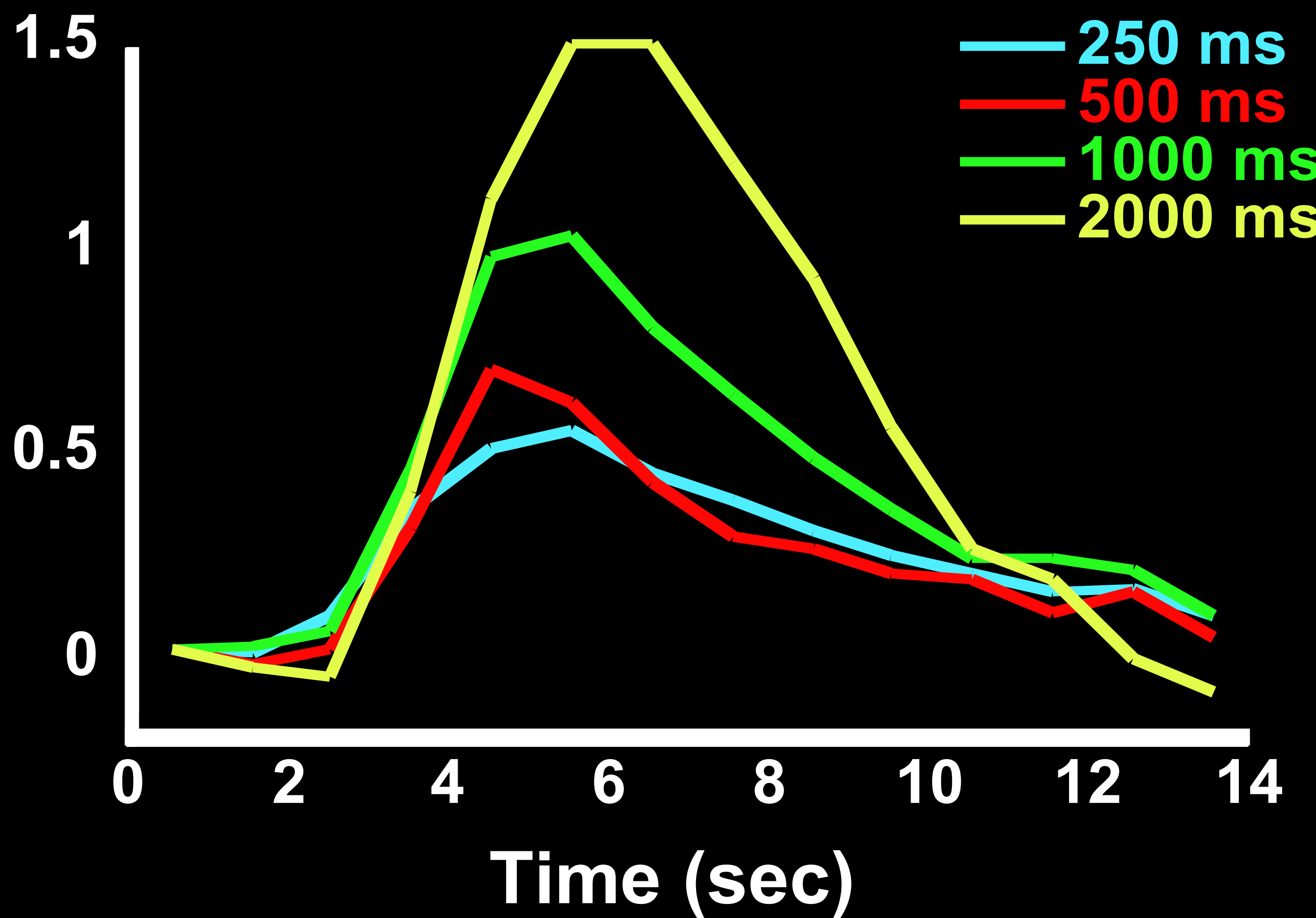
1.5
1
0.5
0
250 ms
500 ms
1000 ms
2000 ms
0
2
4
6
8
10
12
14
Time (sec)

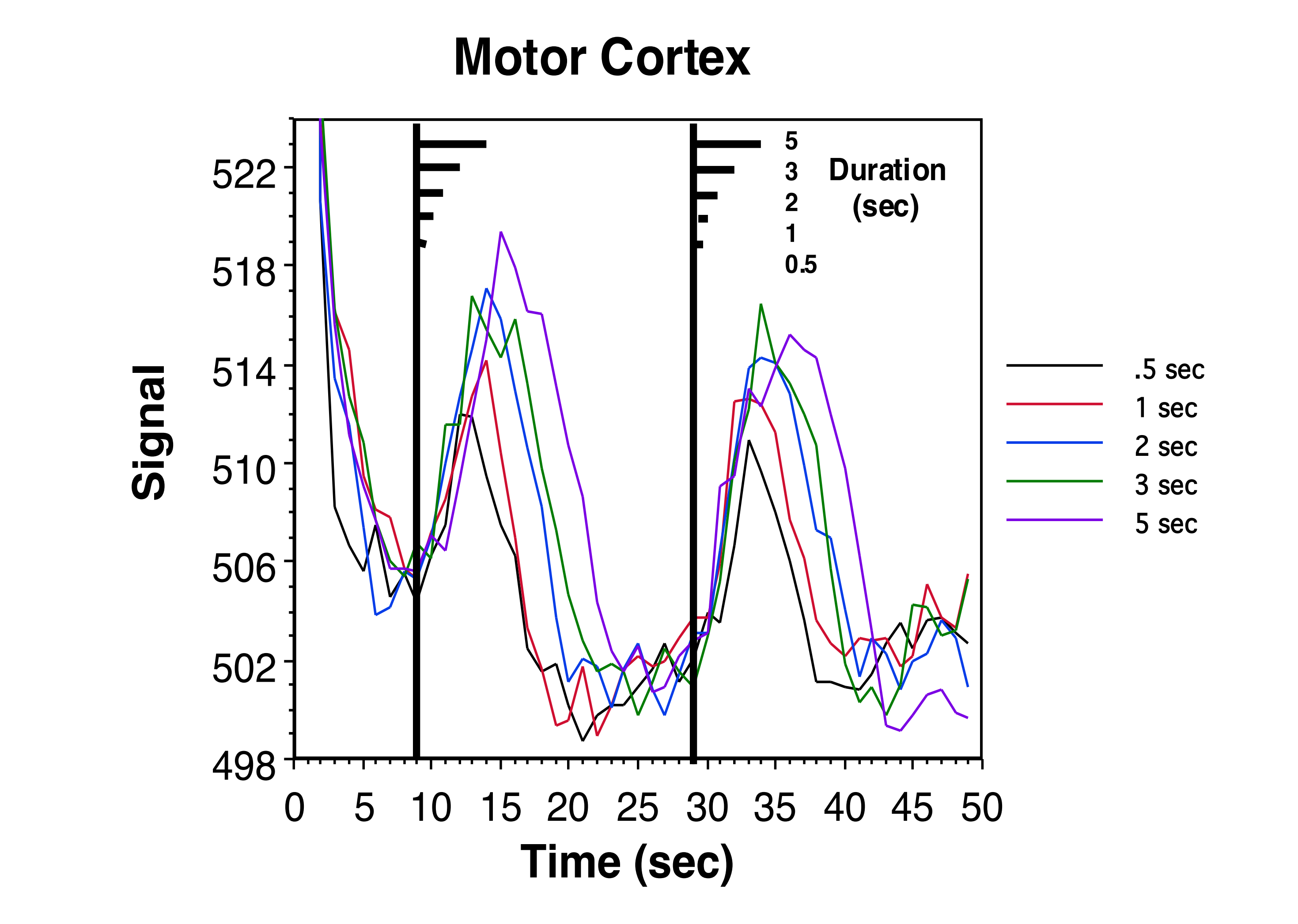

Bandettini, et al., The functional dynamics of blood oxygenation level contrast in the motor cortex, 12'th Proc. Soc. Magn. Reson. Med., New York, p. 1382. (1993).

Dynamic Nonlinearity Assessment

Different stimulus "ON" periods

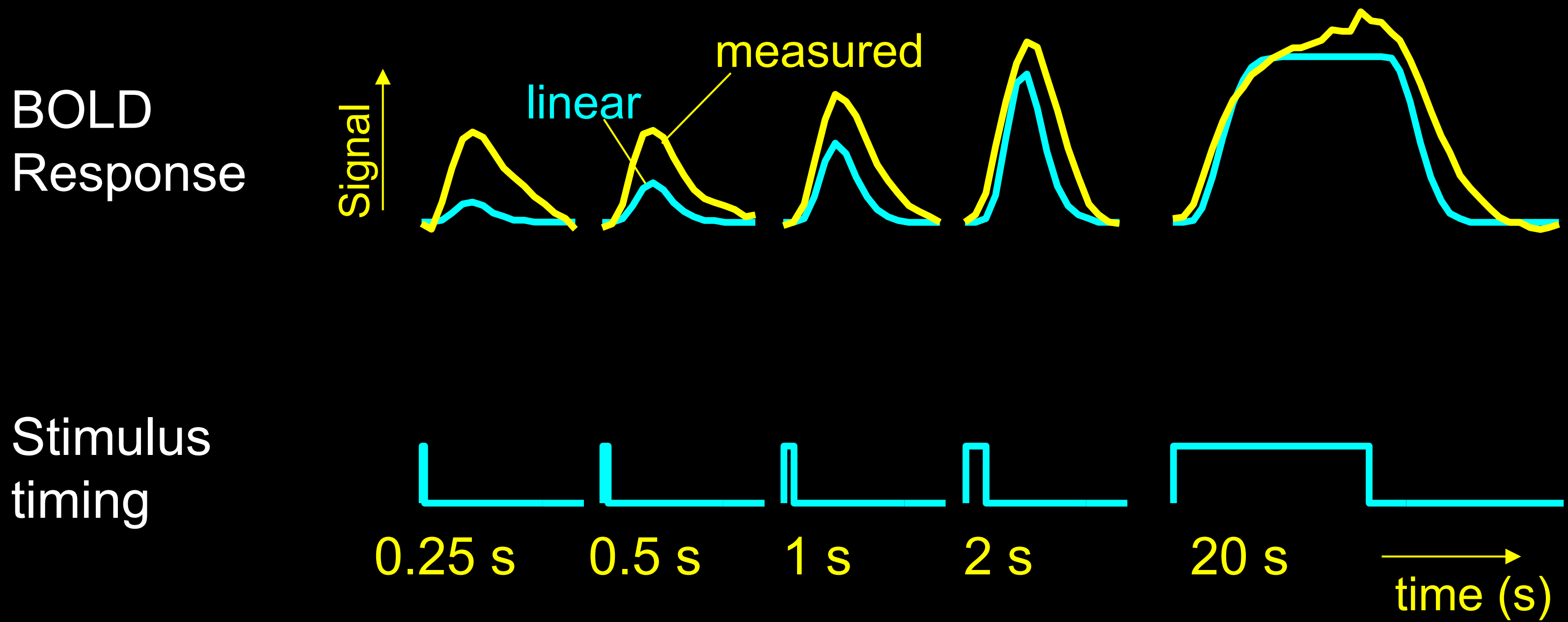

Brief stimuli produce larger responses than expected

R. M. Birn, Z. Saad, P. A. Bandettini, (2001) "Spatial heterogeneity of the nonlinear dynamics in the fMRI BOLD response." ***NeuroImage*****, 14: 817-826.**

Spatial Heterogeneity of BOLD Nonlinearity

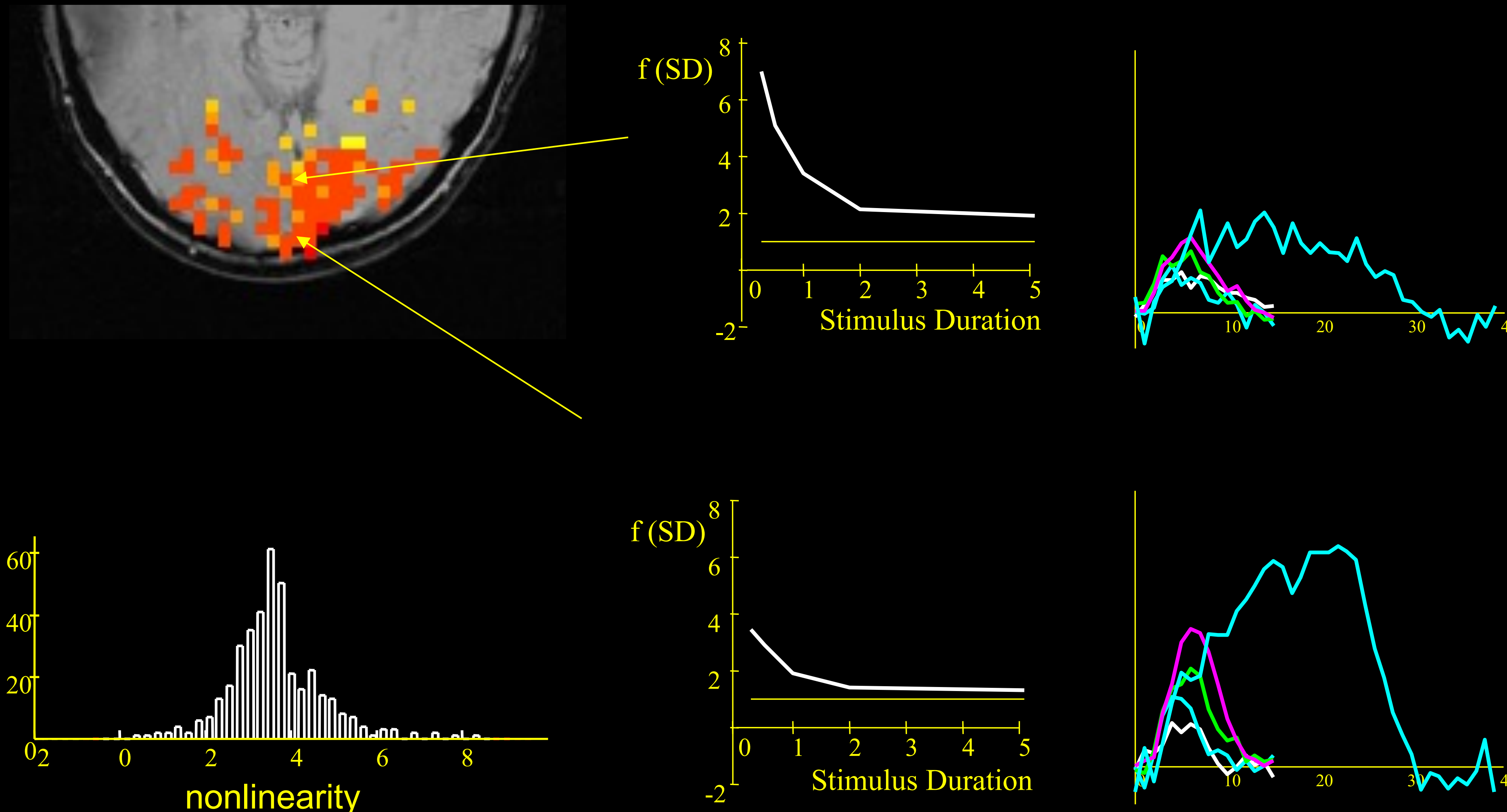

R. M. Birn, Z. Saad, P. A. Bandettini, (2001) "Spatial heterogeneity of the nonlinear dynamics in the fMRI BOLD response." ***NeuroImage*****, 14: 817-826.**

Results – visual task

Nonlinearity

Magnitude

Latency

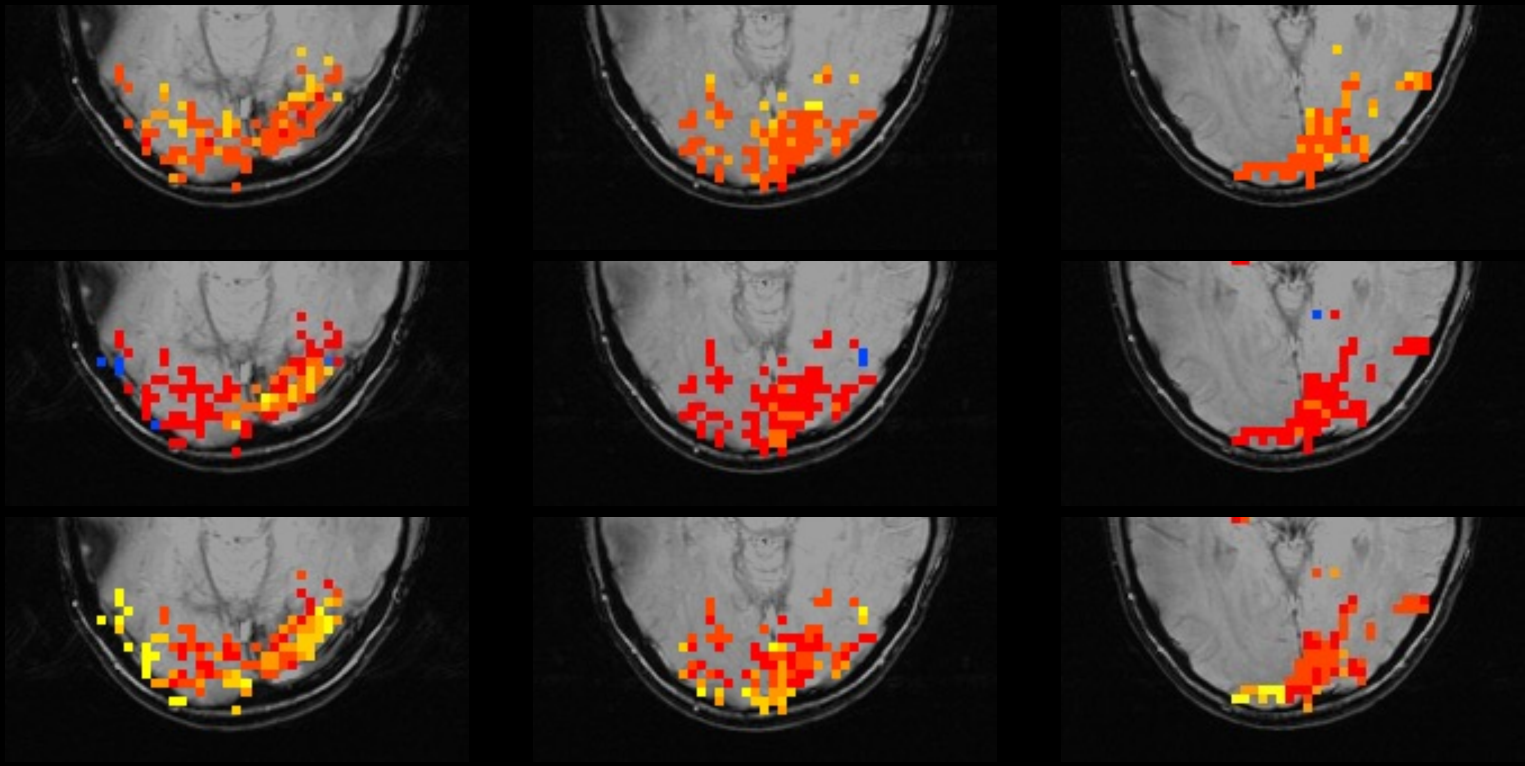

R. M. Birn, Z. Saad, P. A. Bandettini, (2001) “Spatial heterogeneity of the nonlinear dynamics in the fMRI BOLD response.” *NeuroImage*, 14: 817-826.

Results – motor task

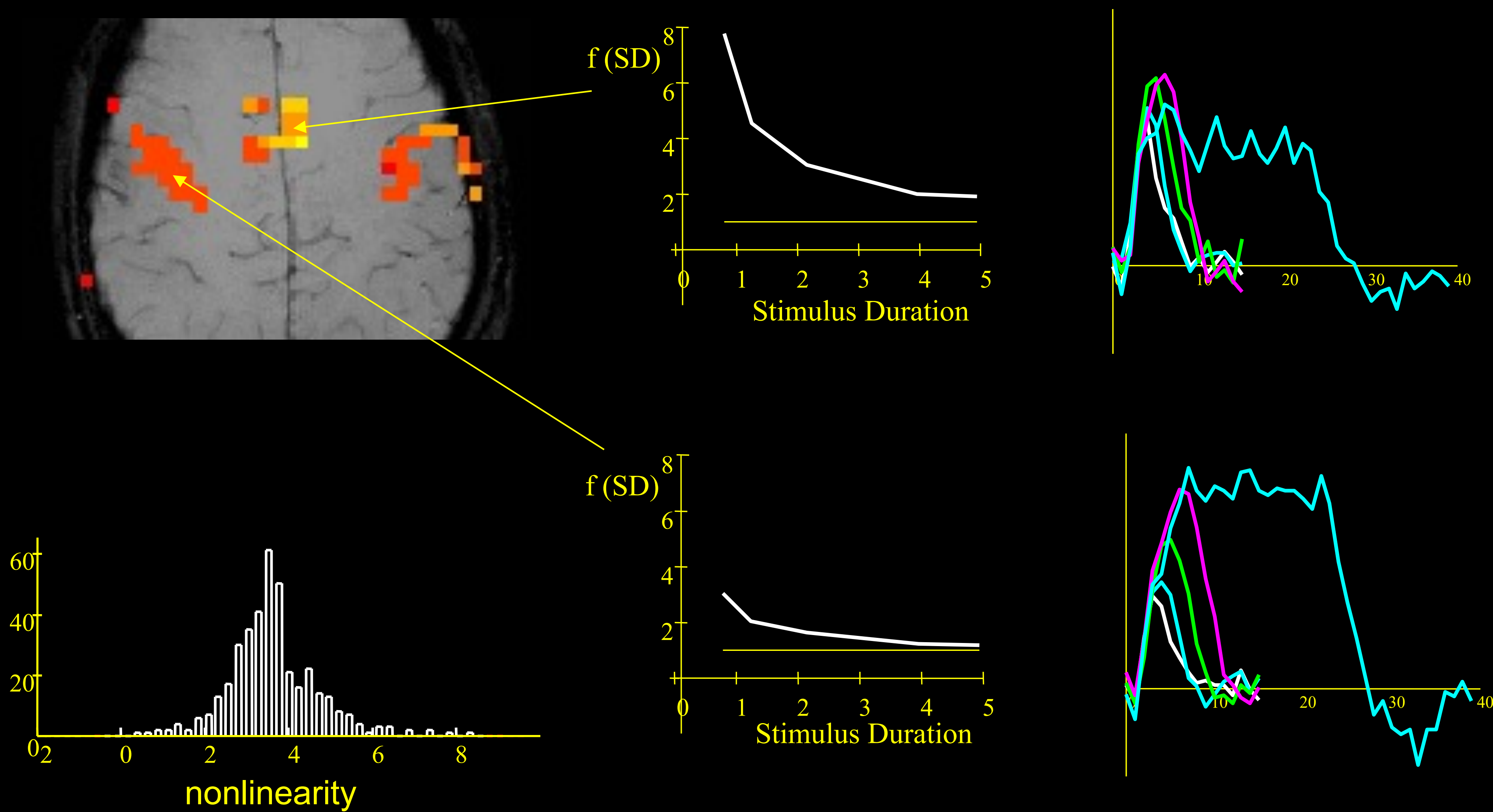

Results – motor task

Nonlinearity

Magnitude

Latency

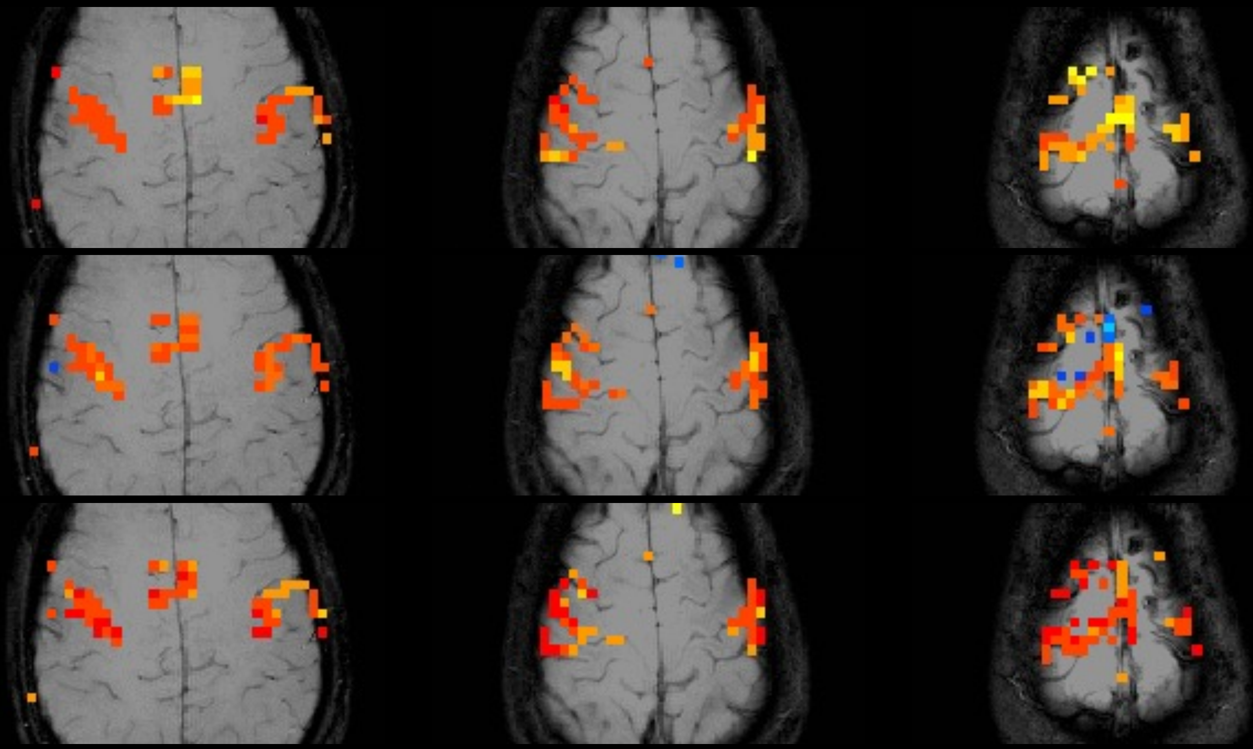

Reproducibility

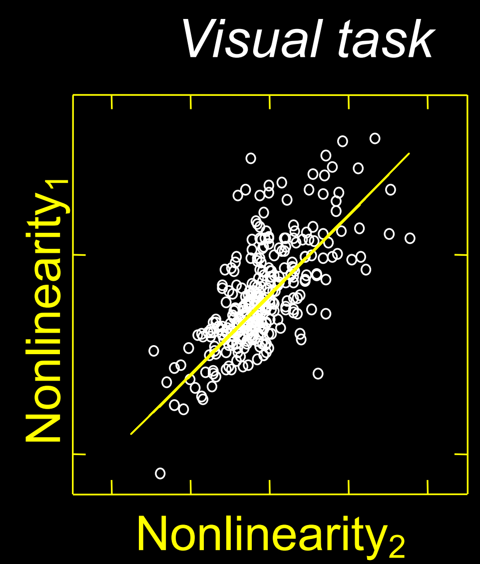

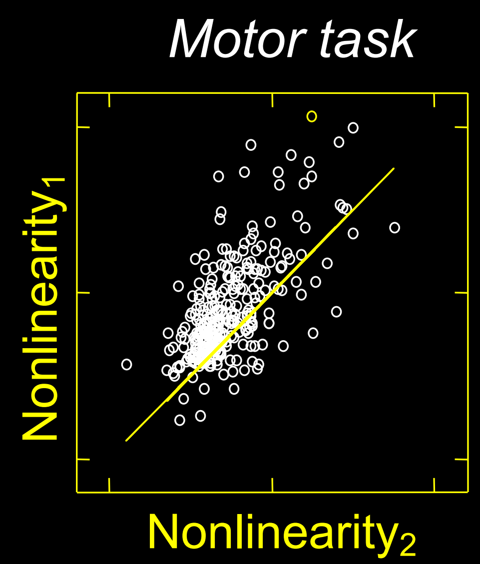

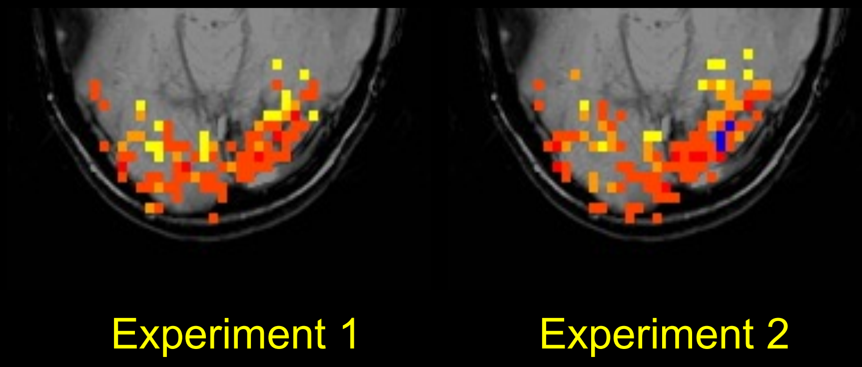

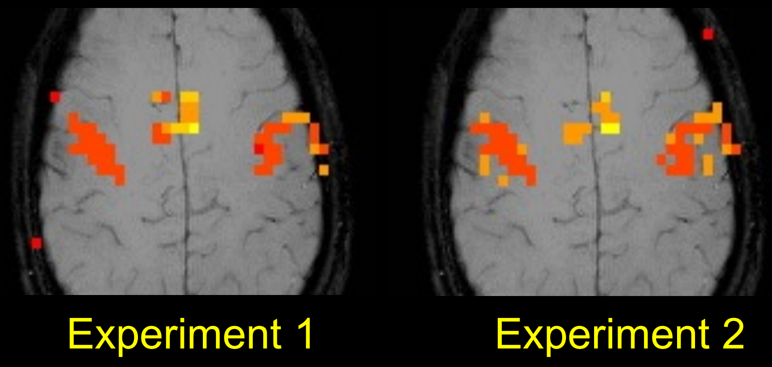

Sources of this Nonlinearity

- Neuronal

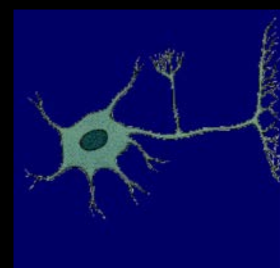

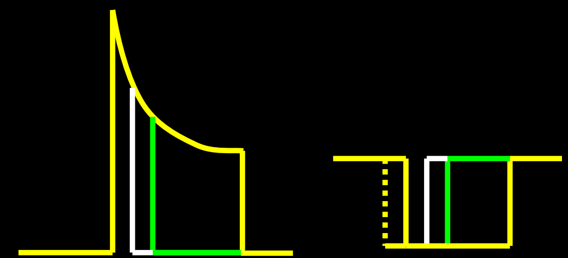

- Hemodynamic
  - Oxygen extraction
  - Blood volume dynamics

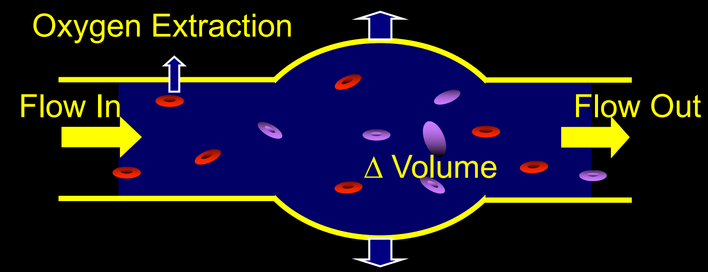

BOLD Correlation with Neuronal Activity

Logothetis et al. (2001) "Neurophysiological investigation of the basis of the fMRI signal" Nature, 412, 150-157.

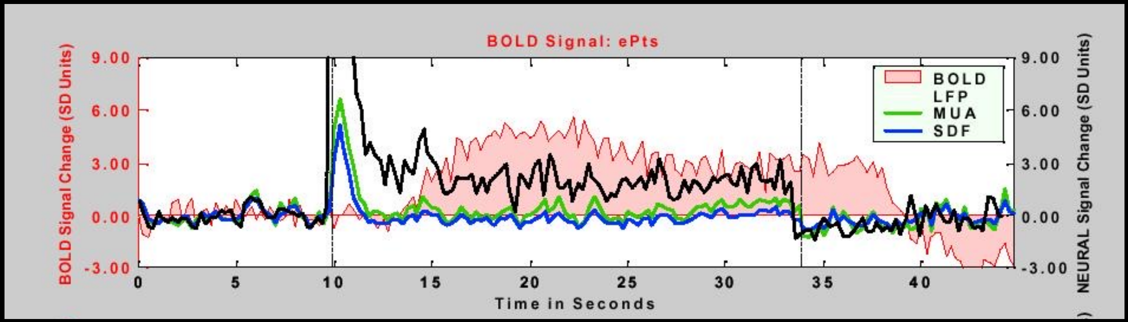

P. A. Bandettini and L. G. Ungerleider, (2001) "From neuron to BOLD: new connections." Nature Neuroscience, 4: 864-866.

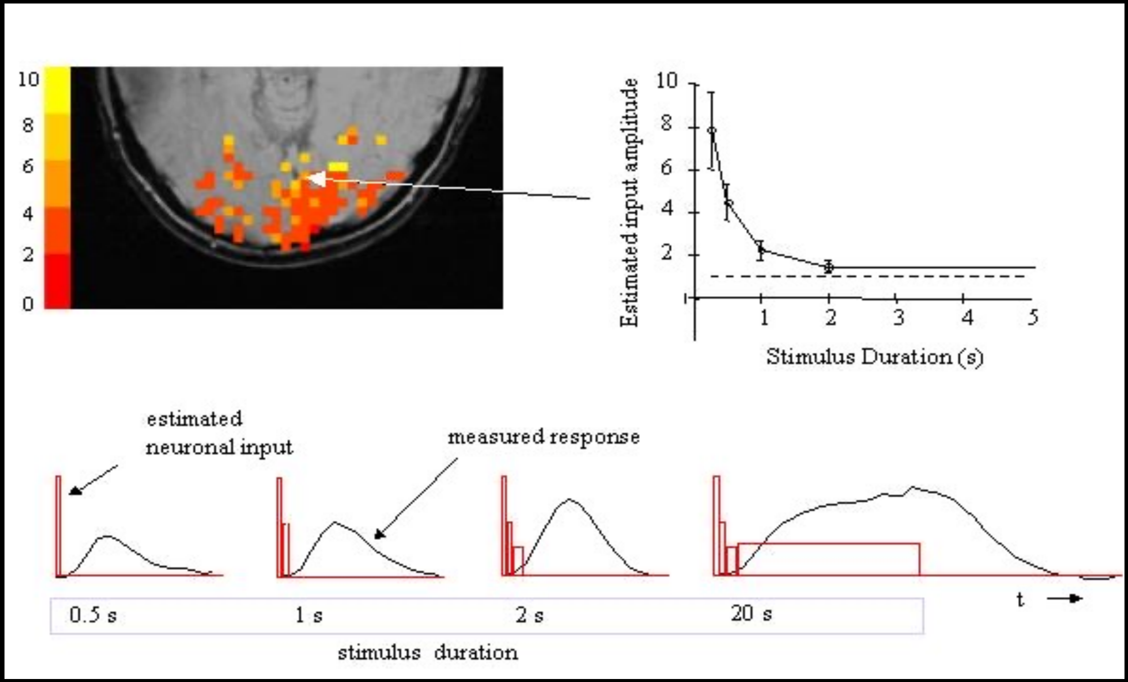

Stationary grating

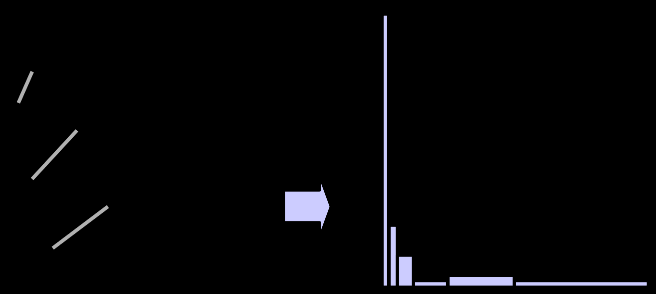

Contrast-reversing checkerboard

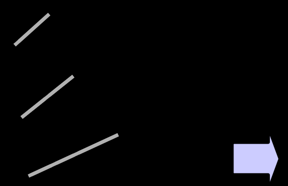

Different stimulus "ON" periods

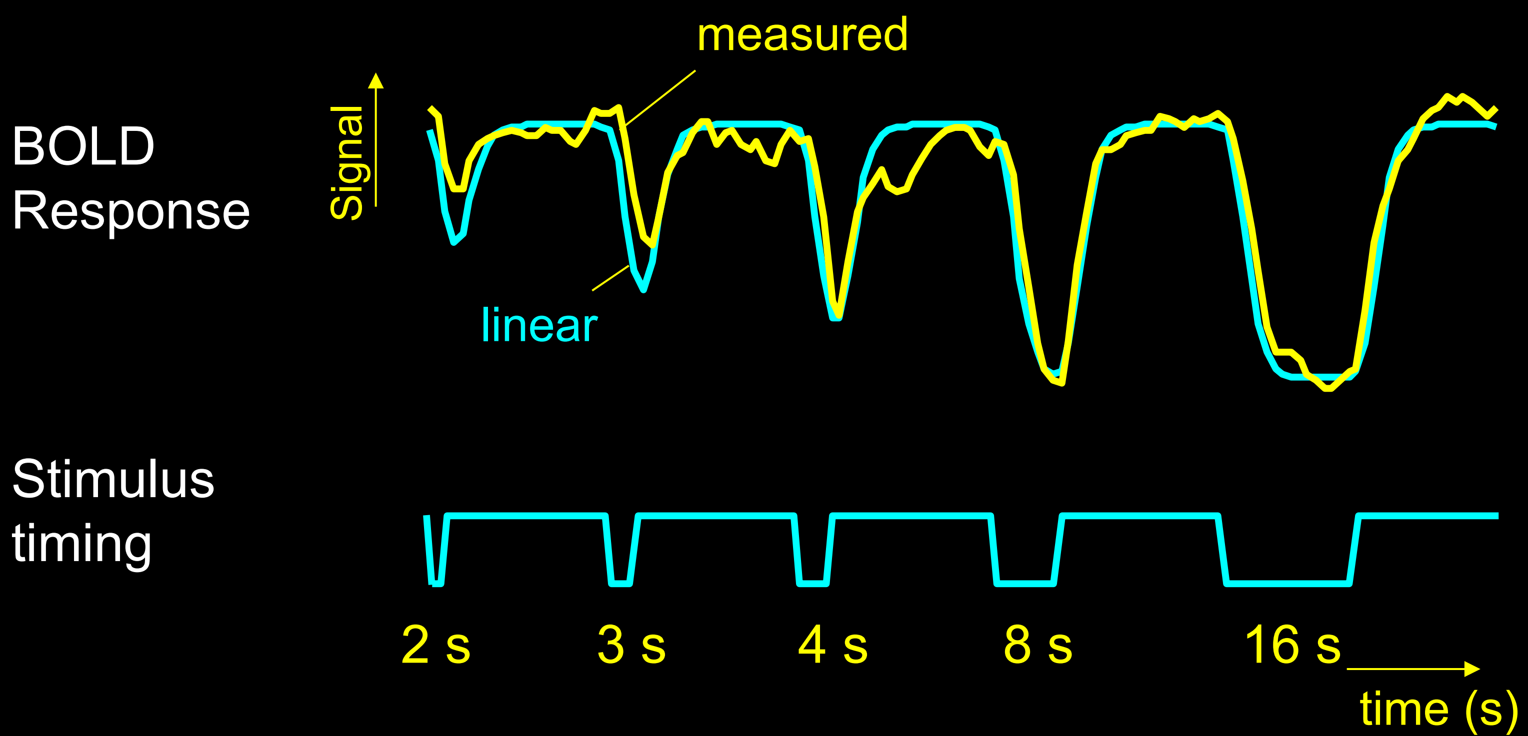

Brief stimulus OFF periods produce smaller decreases than expecte

What we observe..

- Magnitude
- Location
- Parametric Dependence
- Latency

Time Course Comparison Across Brain Regions

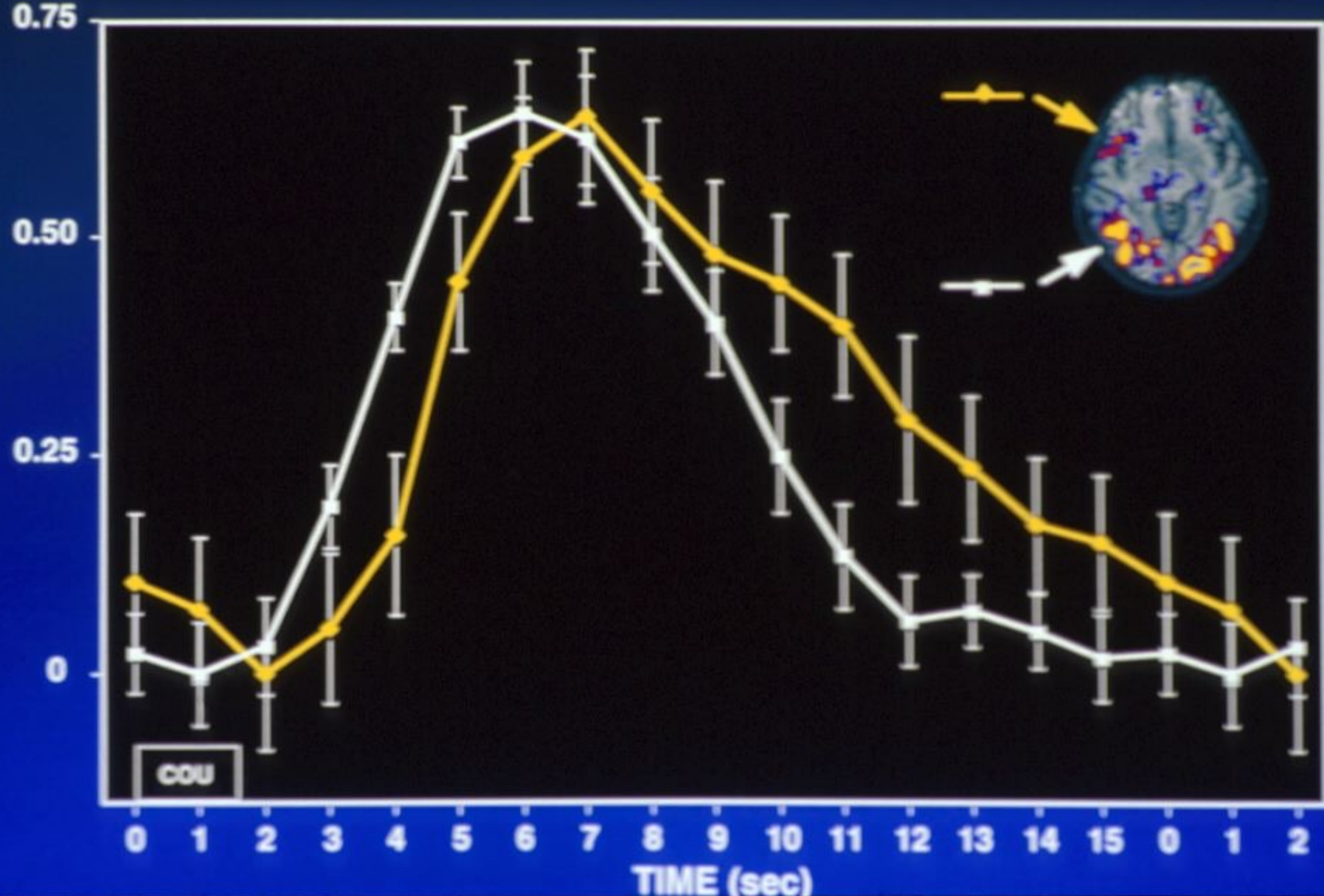

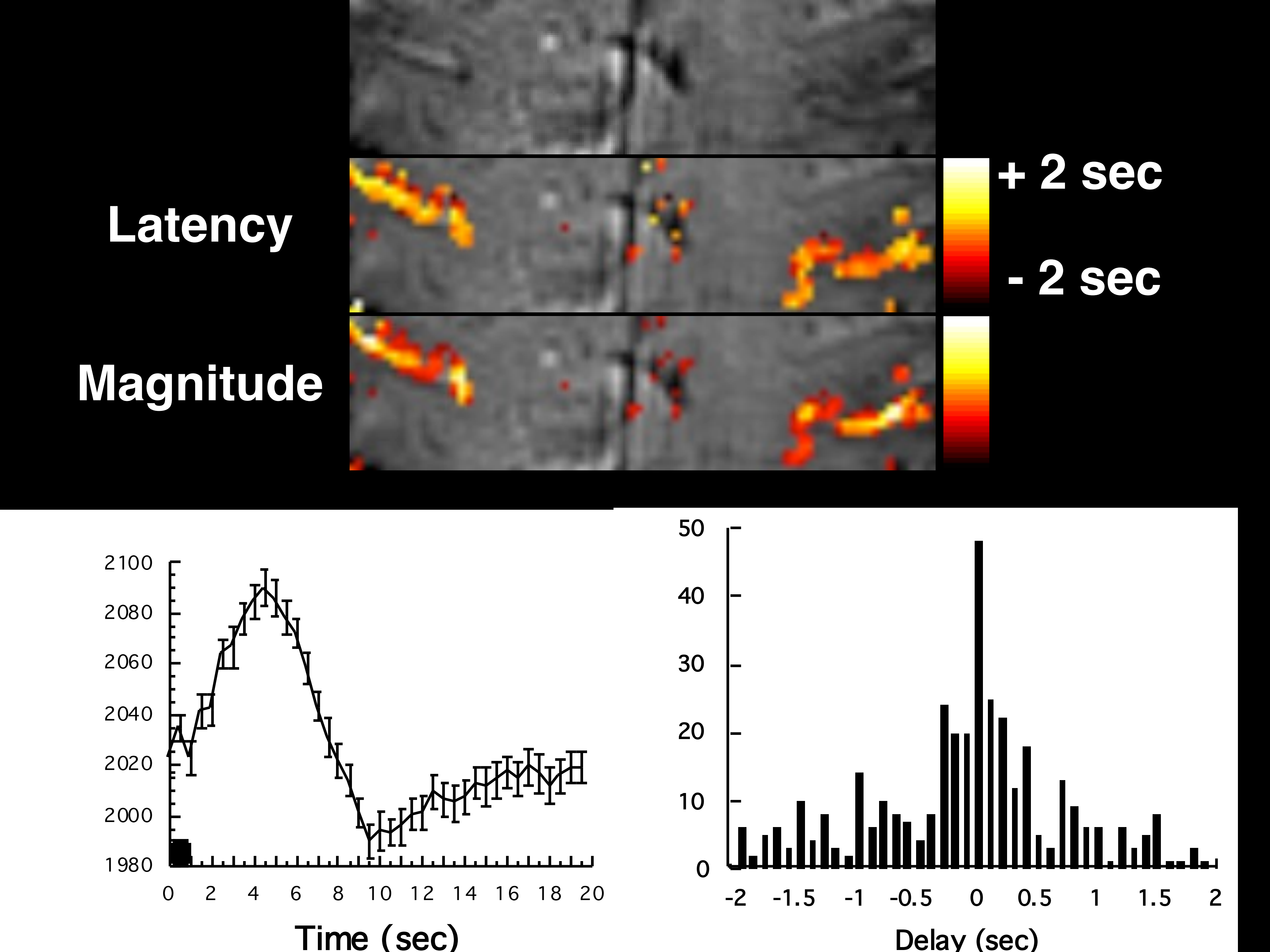

Latency
Magnitude
+ 2 sec
- 2 sec
2100
2080
2060
2040
2020
2000
1980
0 2 4 6 8 10 12 14 16 18 20
Time (sec)
50
40
30
20
10
0
-2 -1.5 -1 -0.5 0 0.5 1 1.5 2
Delay (sec)

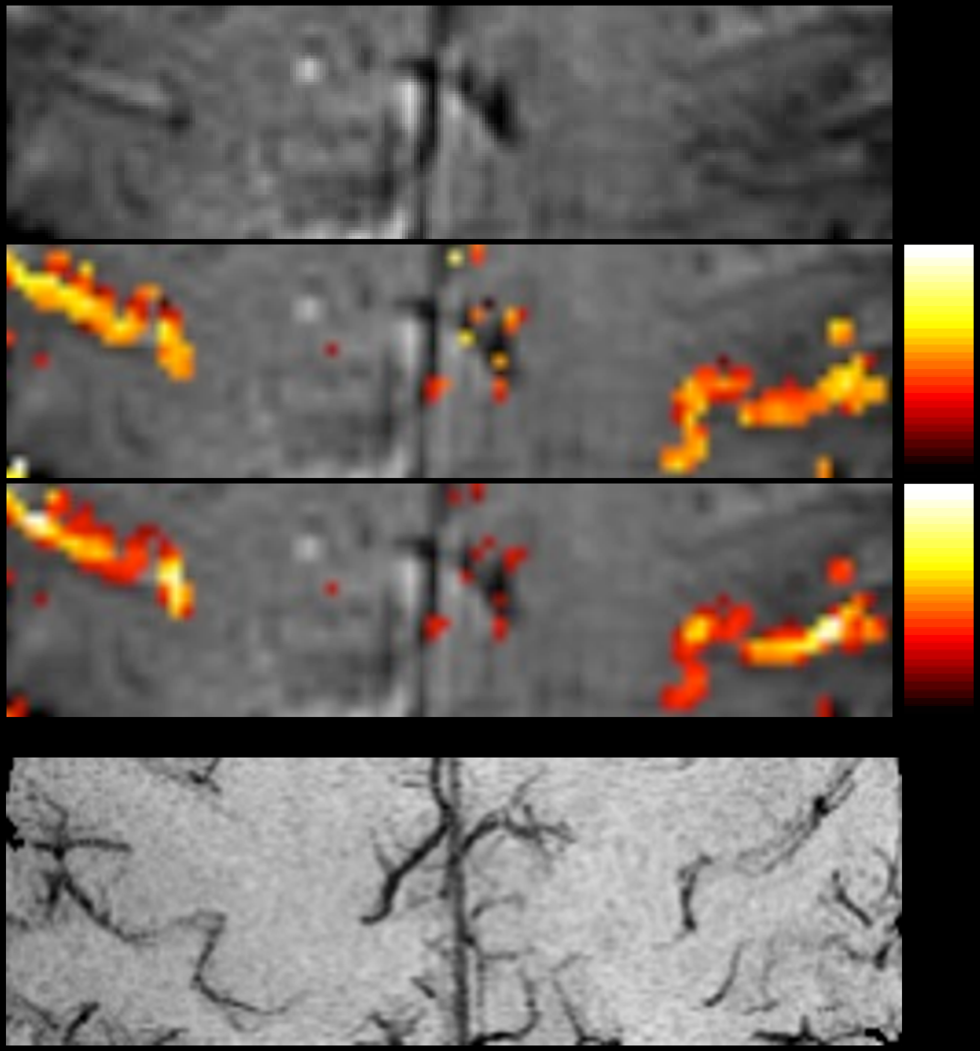

A tangent into venograms
(3 Tesla)

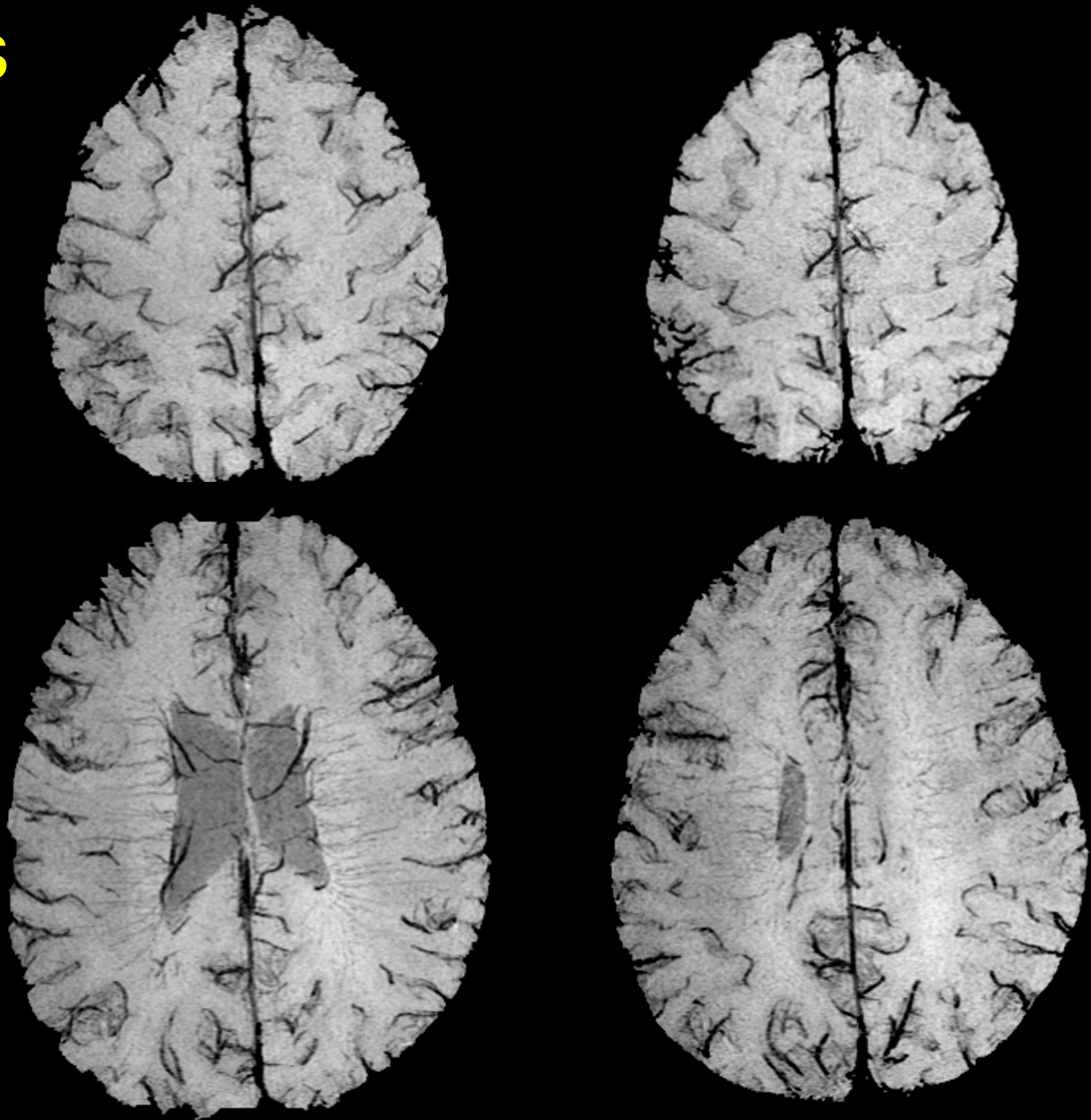

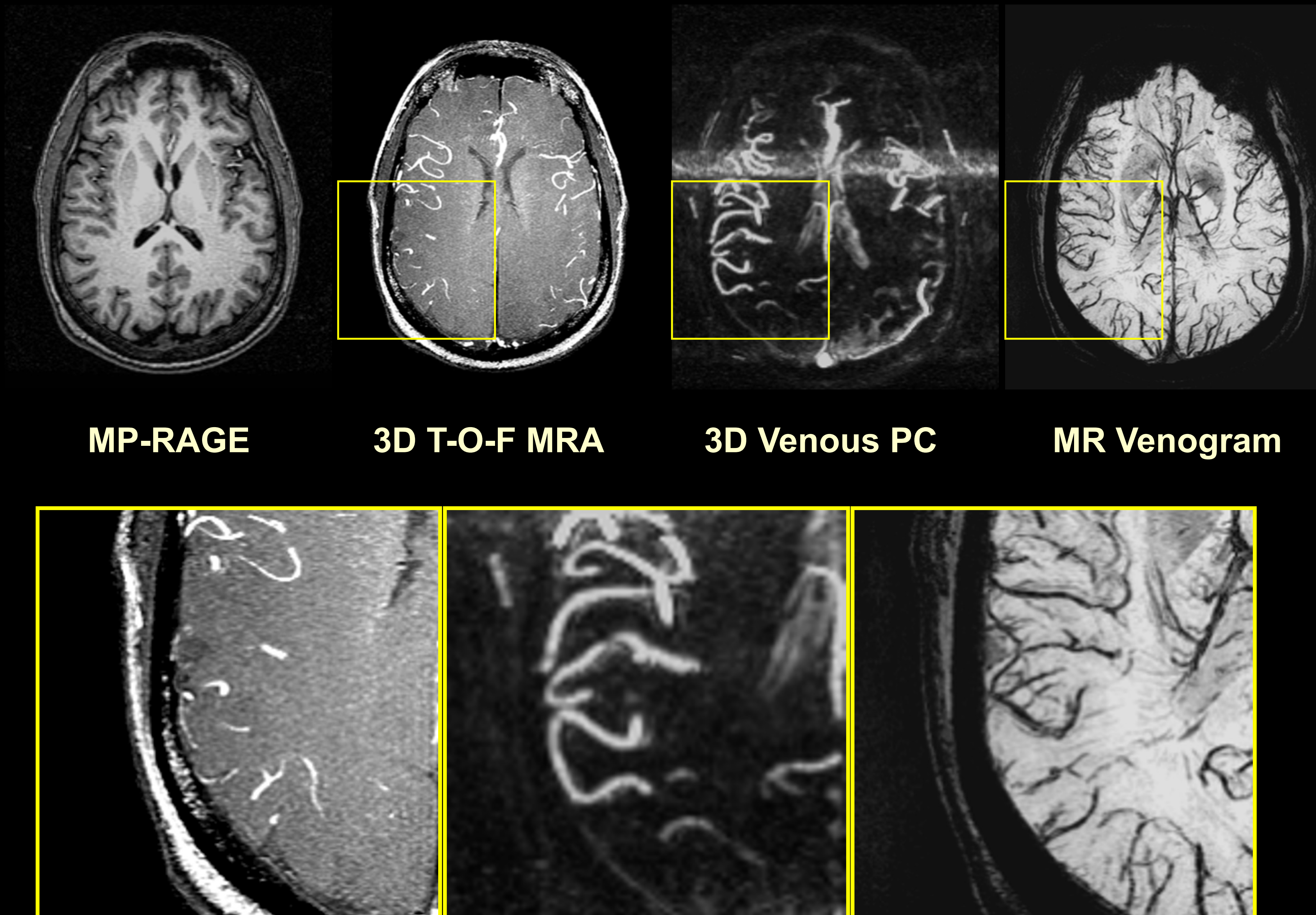
MP-RAGE
3D T-O-F MRA
3D Venous PC
MR Venogram

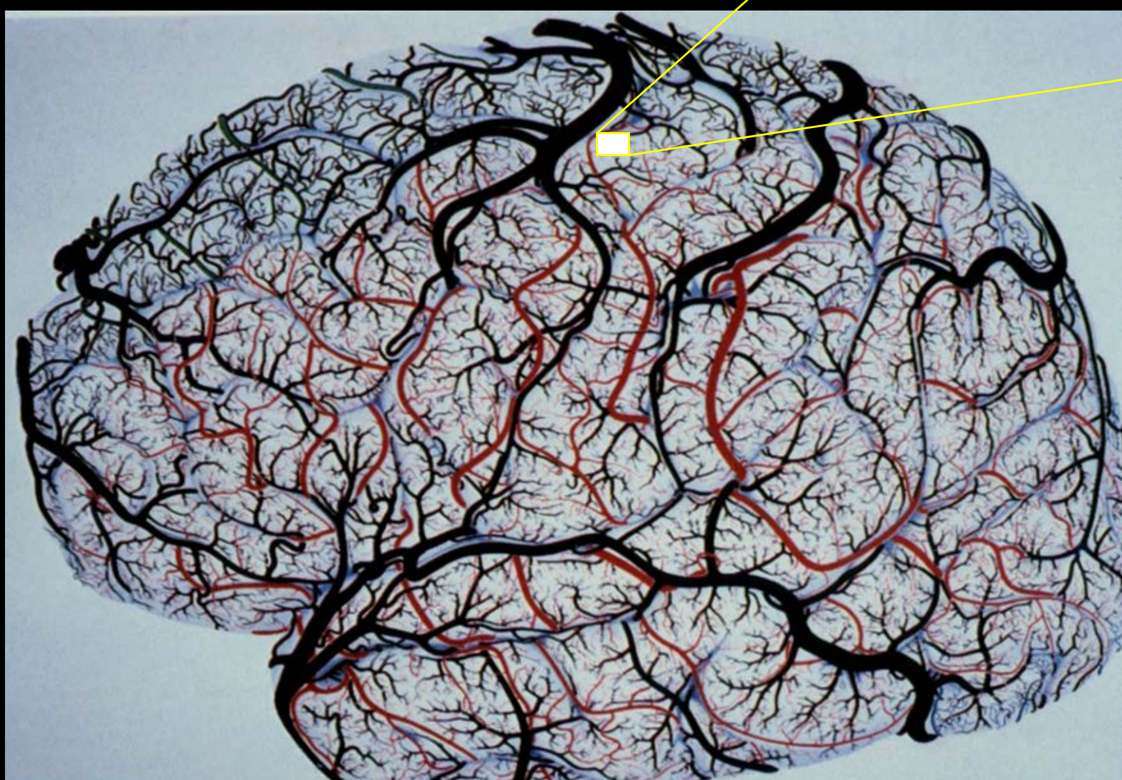

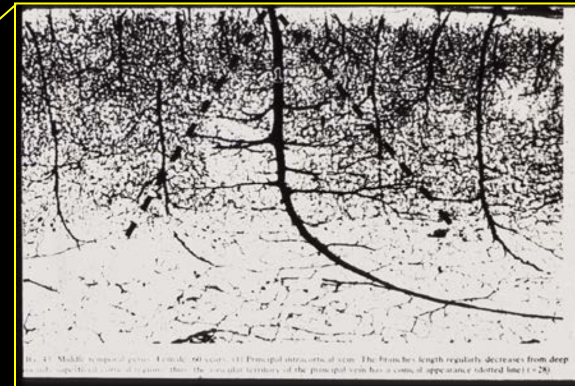
Middle temporal gyrus. Female, 60 years. (1) Principal intracortical vein. The branches length regularly decreases from deep
superficial cortical regions; thus the vascular territory of the principal vein has a conical appearance (dotted line) (×28)

Hemodynamic Latency and Variability Following Neuronal Activation

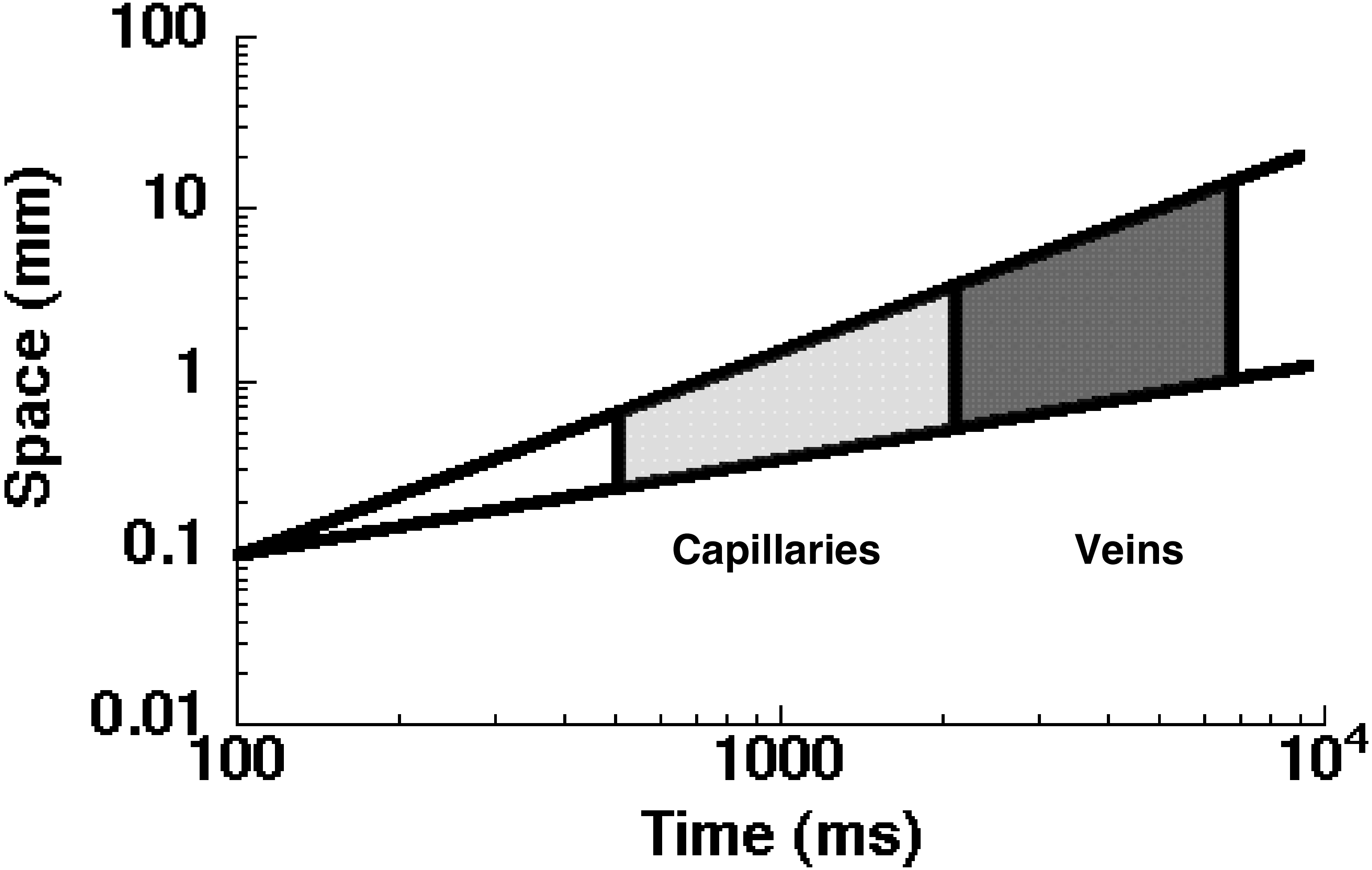

Regions of Interest Used for Hemi-Field Experiment

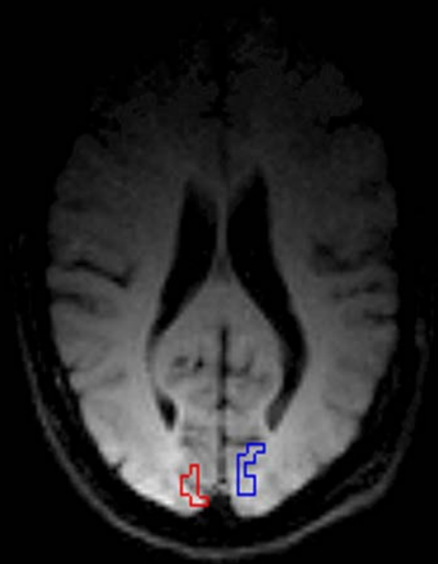

Right Hemisphere

Left Hemisphere

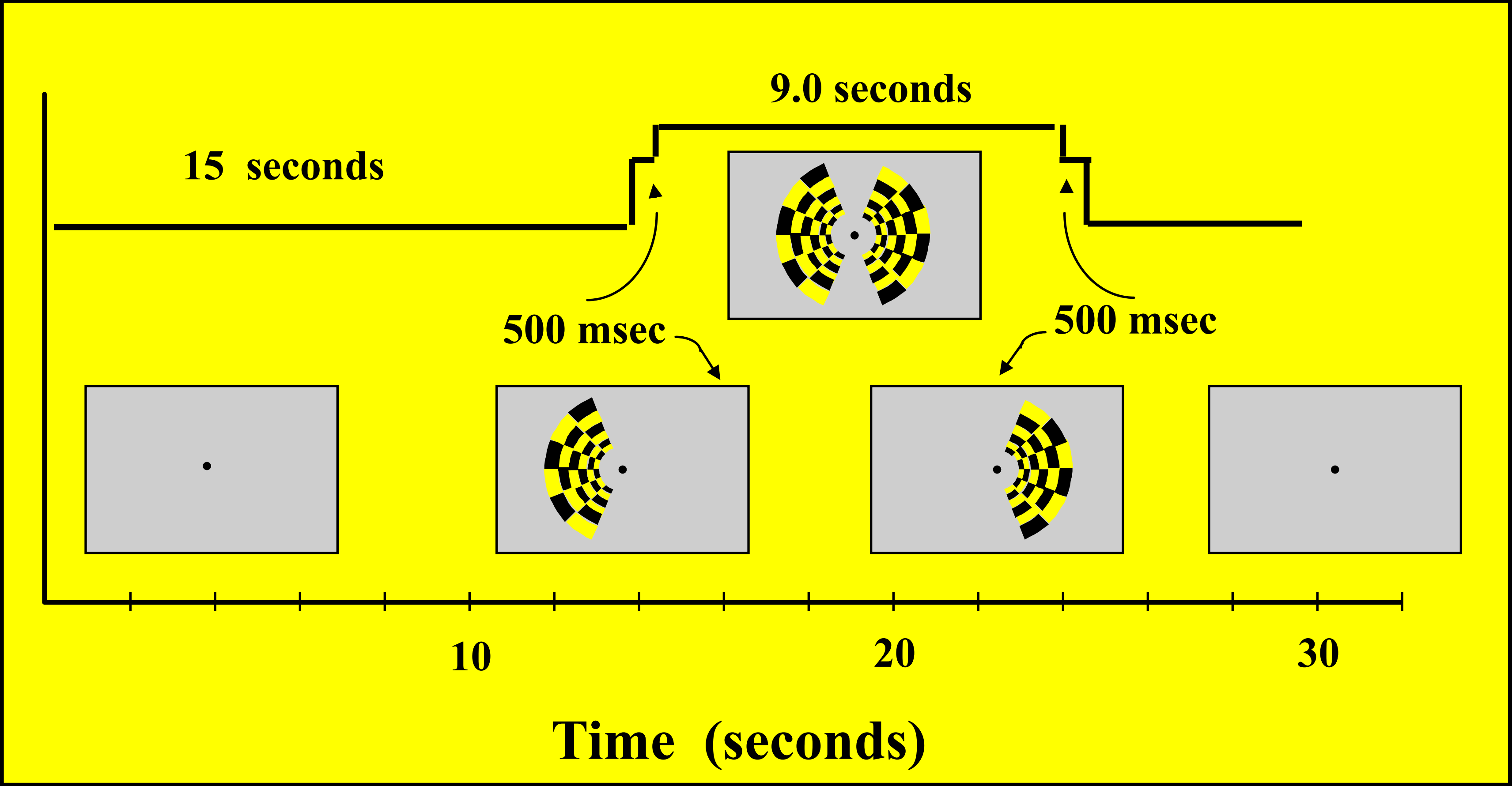

9.0 seconds
15 seconds
500 msec
500 msec
10
20
30
Time (seconds)

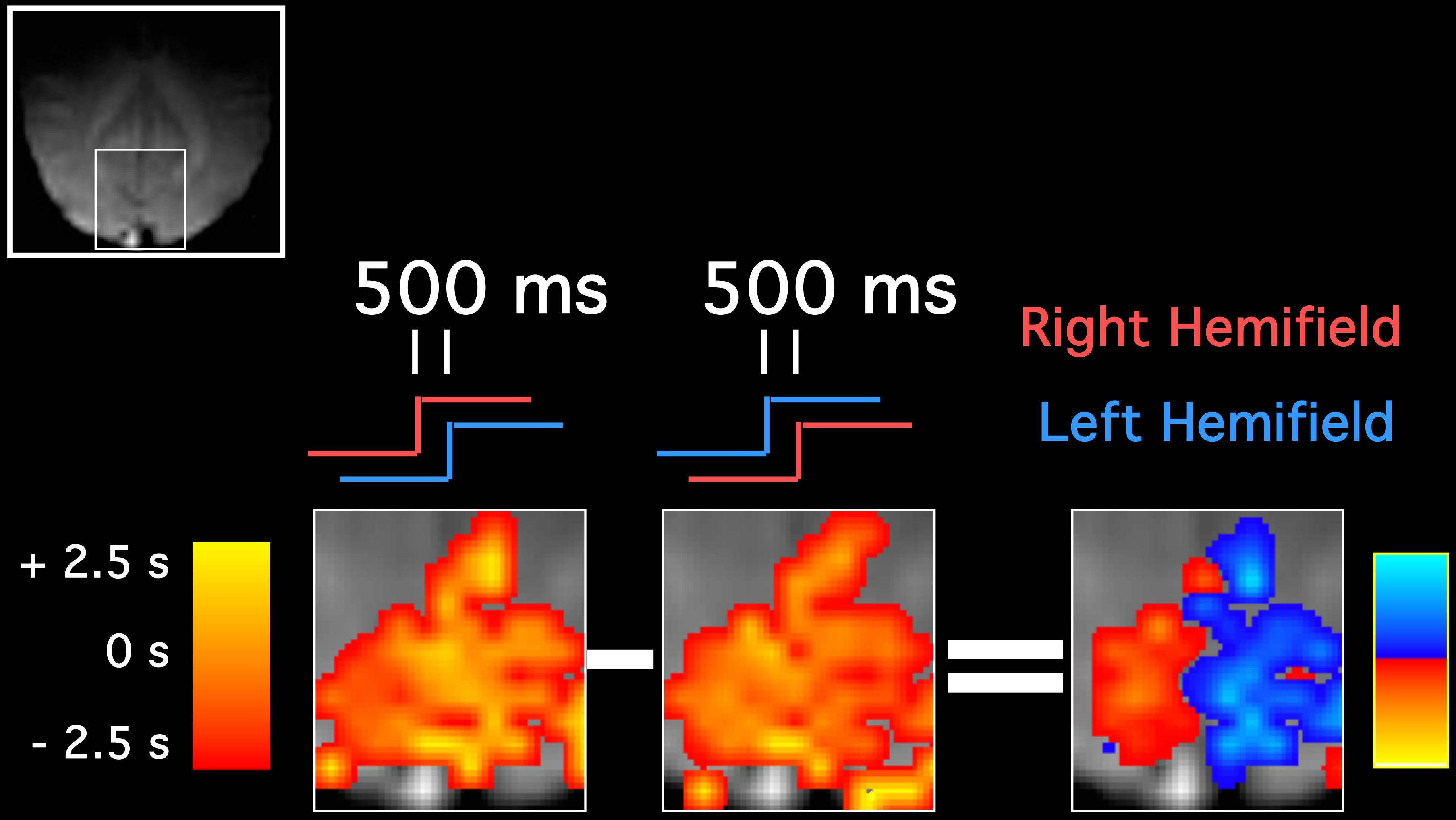

500 ms
500 ms
Right Hemifield
Left Hemifield
+ 2.5 s
0 s
- 2.5 s

Understanding neural system dynamics through task modulation and measurement of functional MRI amplitude, latency, and width

P. S. F. Bellgowan*†, Z. S. Saad‡, and P. A. Bandettini*

*Laboratory of Brain and Cognition and ‡Scientific and Statistical Computing Core, National Institute of Mental Health, Bethesda, MD 20892

Communicated by Leslie G. Ungerleider, National Institutes of Health, Bethesda, MD, December 19, 2002 (received for review October 31, 2002)

Proc. Nat'l. Acad. Sci. USA **100**, 1415-1419 (2003).

Lexical Delay

Rotational Delay

Rotational Delay	Words	Non-Words	Mean Reaction Time
0^0	smudge	dierts	823 ms
60^0	frolic	cuhlos	891 ms
120^0	slouch	gedmus	1446 ms
Mean Reaction Time	986 ms	1219 ms	

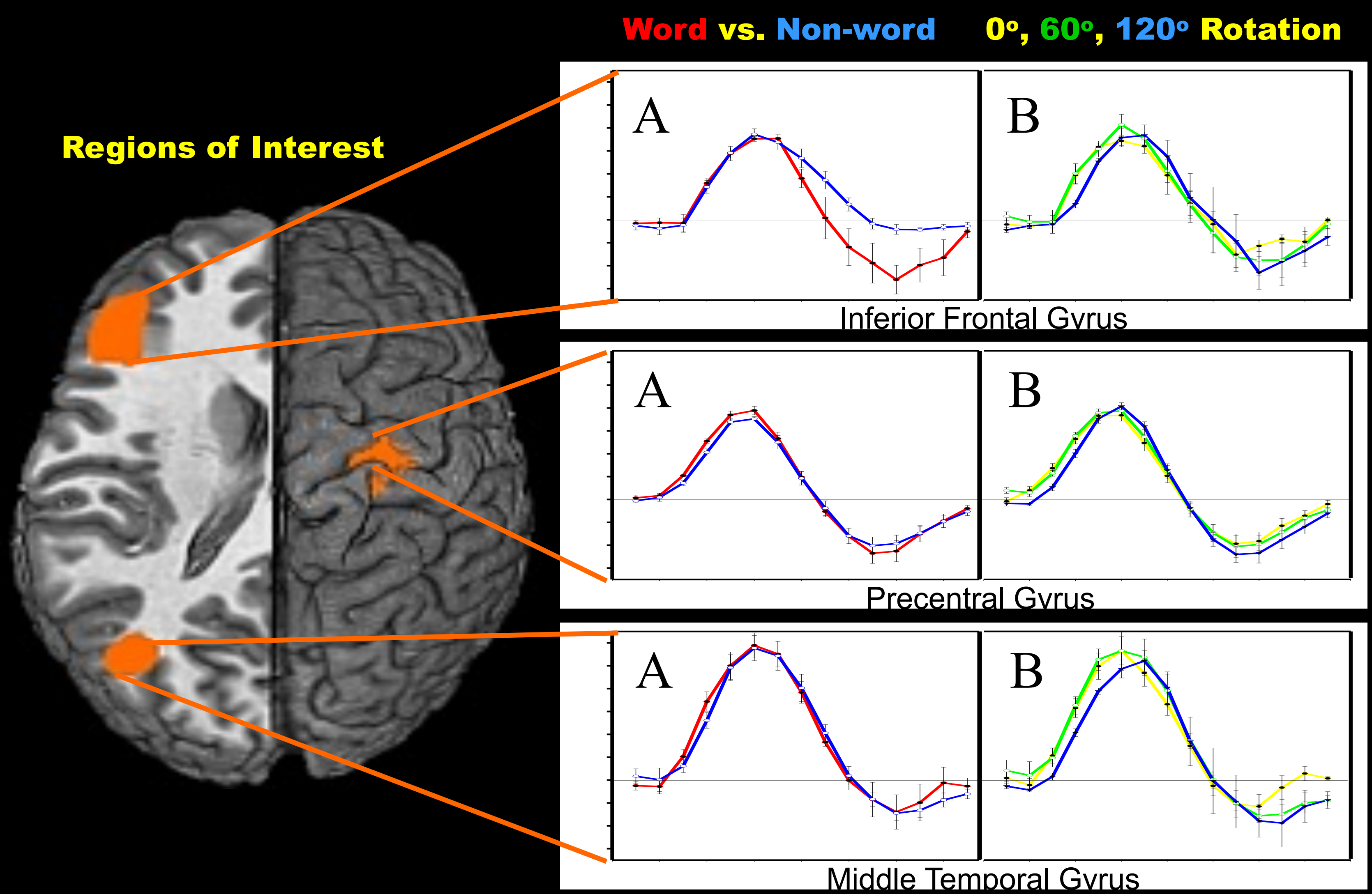

Word vs. Non-word
0°, 60°, 120° Rotation
Regions of Interest
A
B
Inferior Frontal Gyrus
A
B
Precentral Gyrus
A
B
Middle Temporal Gyrus

No calibration

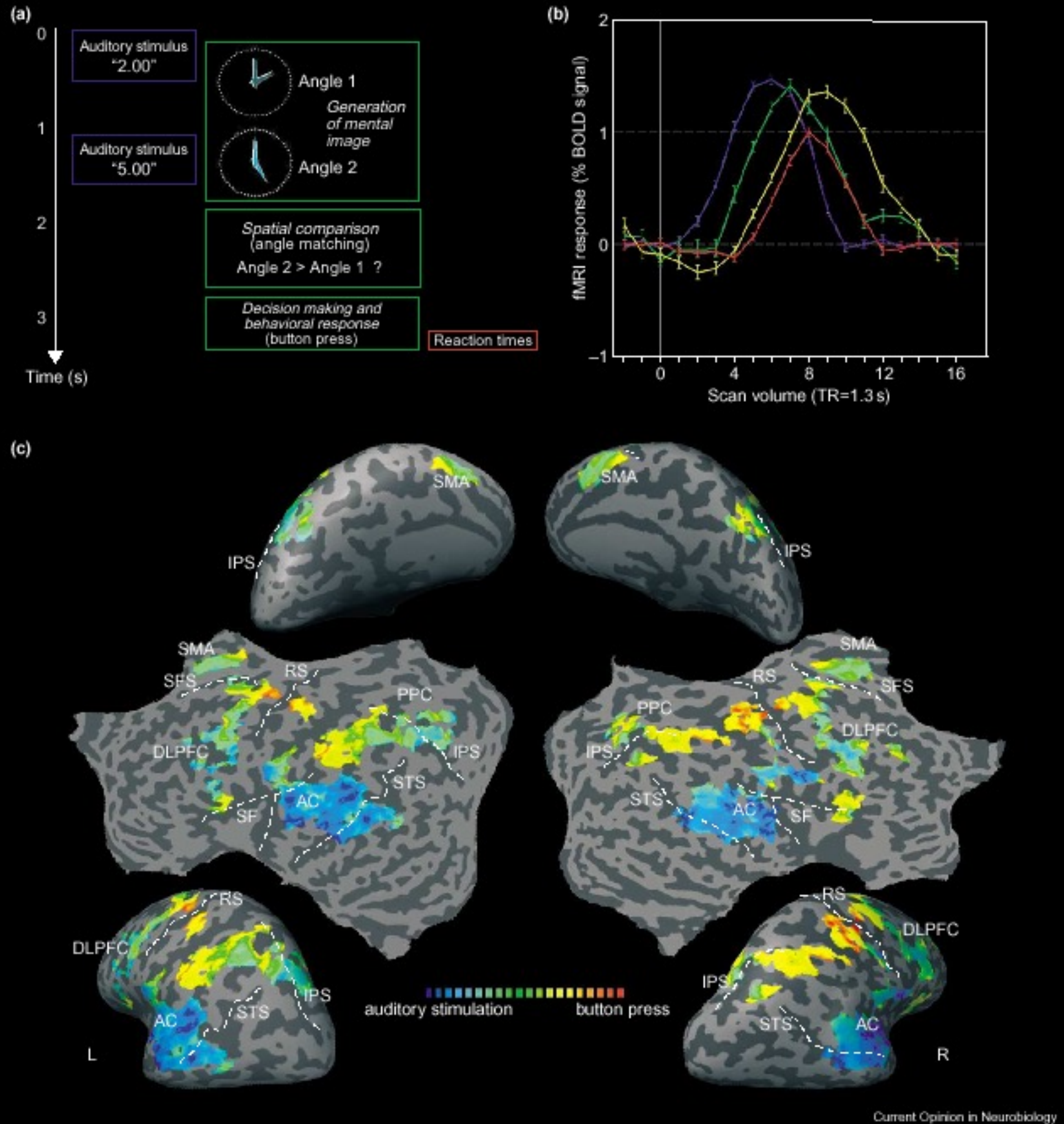

Formisano, E. and R. Goebel, *Tracking cognitive processes with functional MRI mental chronometry.* Current Opinion in Neurobiology, 2003. **13**: p. 174-181.

Laminar specificity of functional MRI onset times during somatosensory stimulation in rat

Afonso C. Silva* and Alan P. Koretsky

Laboratory of Functional and Molecular Imaging, National Institute of Neurological Disorders and Stroke, Bethesda, MD 20892

15182–15187 | PNAS | **November 12, 2002** | vol. 99 | no. 23

No calibration

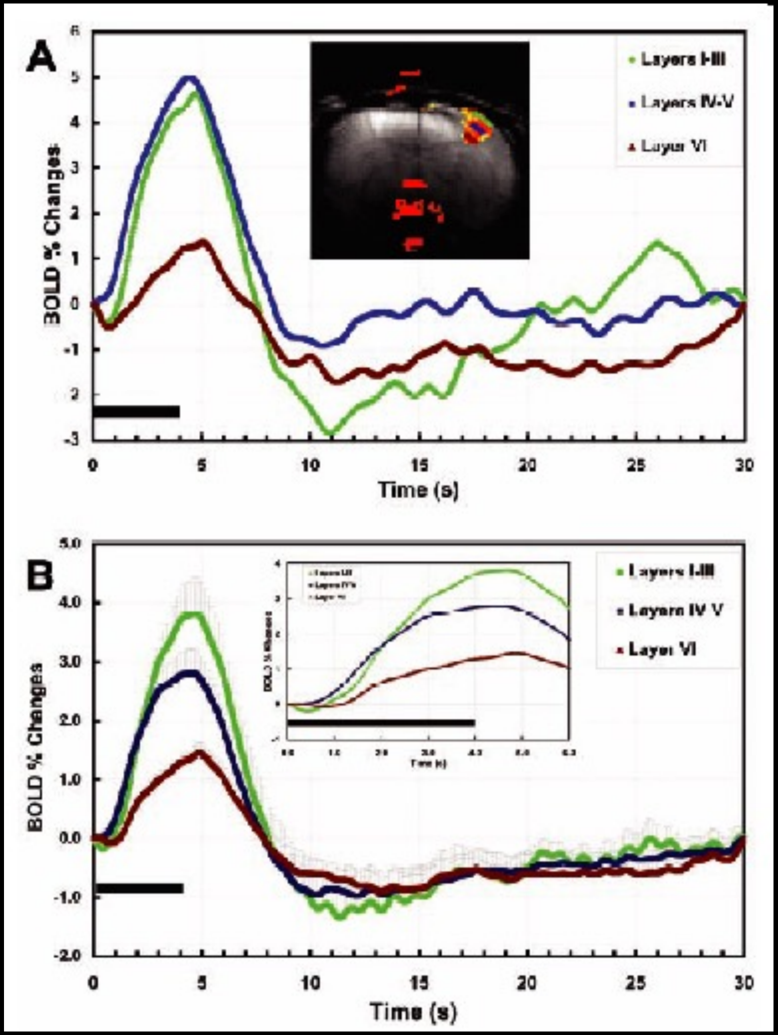

11.7 T

An approach to probe some neural systems interaction by functional MRI at neural time scale down to milliseconds

Seiji Ogawa[†‡], Tso-Ming Lee[†], Ray Stepnoski[†], Wei Chen[§], Xiao-Hong Zhu[§], and Kamil Ugurbil[§]

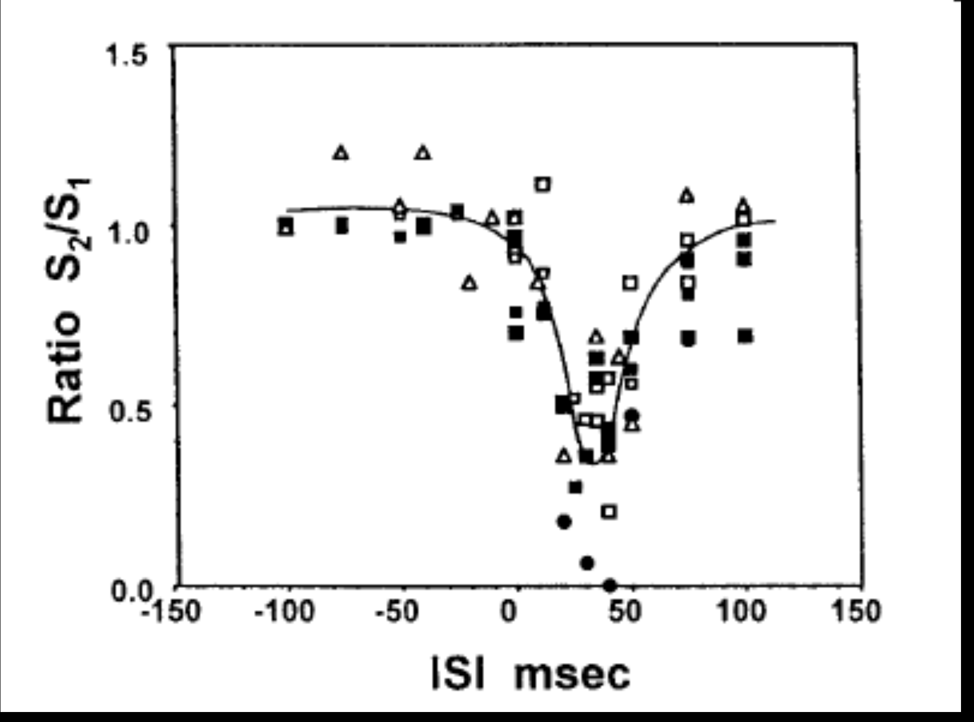

11026–11031 PNAS **September 26, 2000** vol. 97 no. 20

FMRI Basics and Beyond

- Information Content
- Sensitivity
- Resolution
- Image quality
- Paradigm Design and Processing

Maximizing Signal

- Higher Bo Field
  - Linear or greater increase in S/N
  - Tradeoff in susceptibility artifacts
- Radio frequency Coils
  - Smaller the coil the higher the S/N
  - Tradeoff in coverage
- Choice of repetition time (TR)
  - Faster is better (more data points to average)
  - Tradeoff in coverage (10 slices/sec)
    - *min TR = (time/slice) x number of slices in volume*
  - Diminishing returns because of noise correlation
- Voxel volume
  - Linear relationship between S/N and voxel volume
  - Larger voxels increase partial volume averaging -> reduction of functional signal
- Averaging
  - Increase in sensitivity by sqrt(N)
  - System and subject instabilities increase with longer

Temporal vs. Spatial SNR- 3T

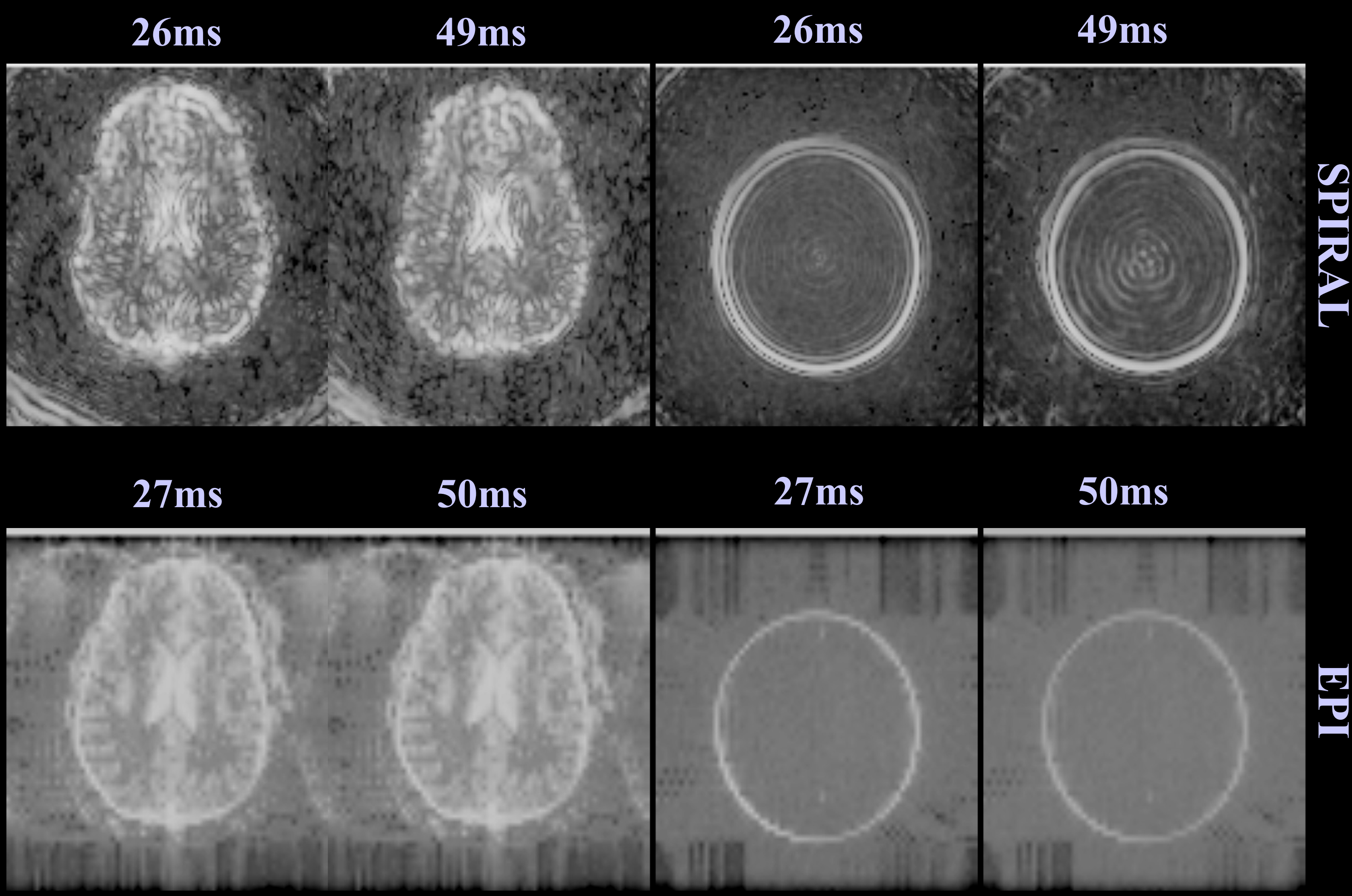

Physiologic Fluctuations

Cardiac	0.6 to 1.2 Hz
Respiratory	0.1 to 0.2 Hz
Low Frequency	0.0 to 0.1 Hz

0.25 Hz Breathing at 3T

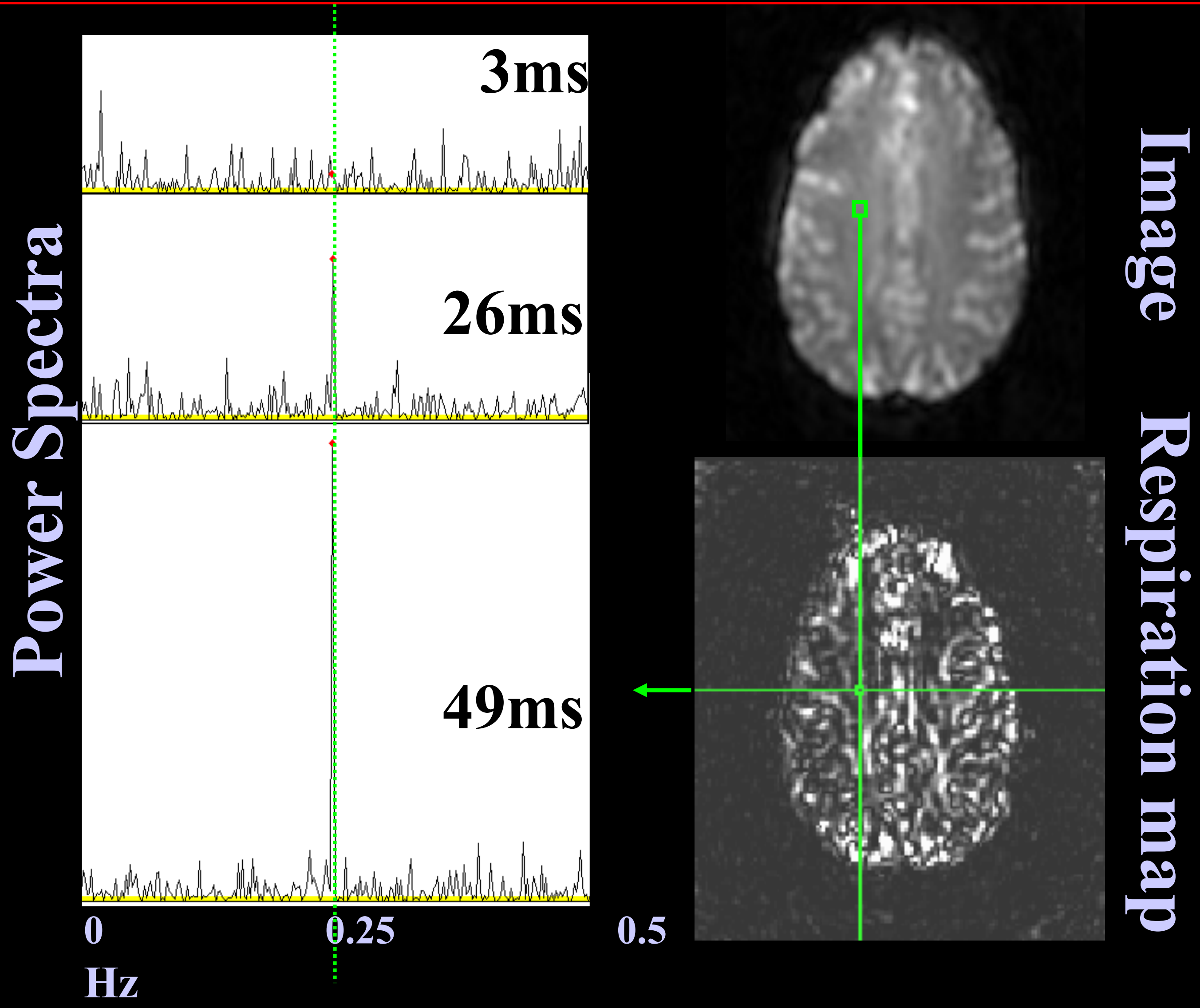

0.68 Hz Cardiac rate at 3T

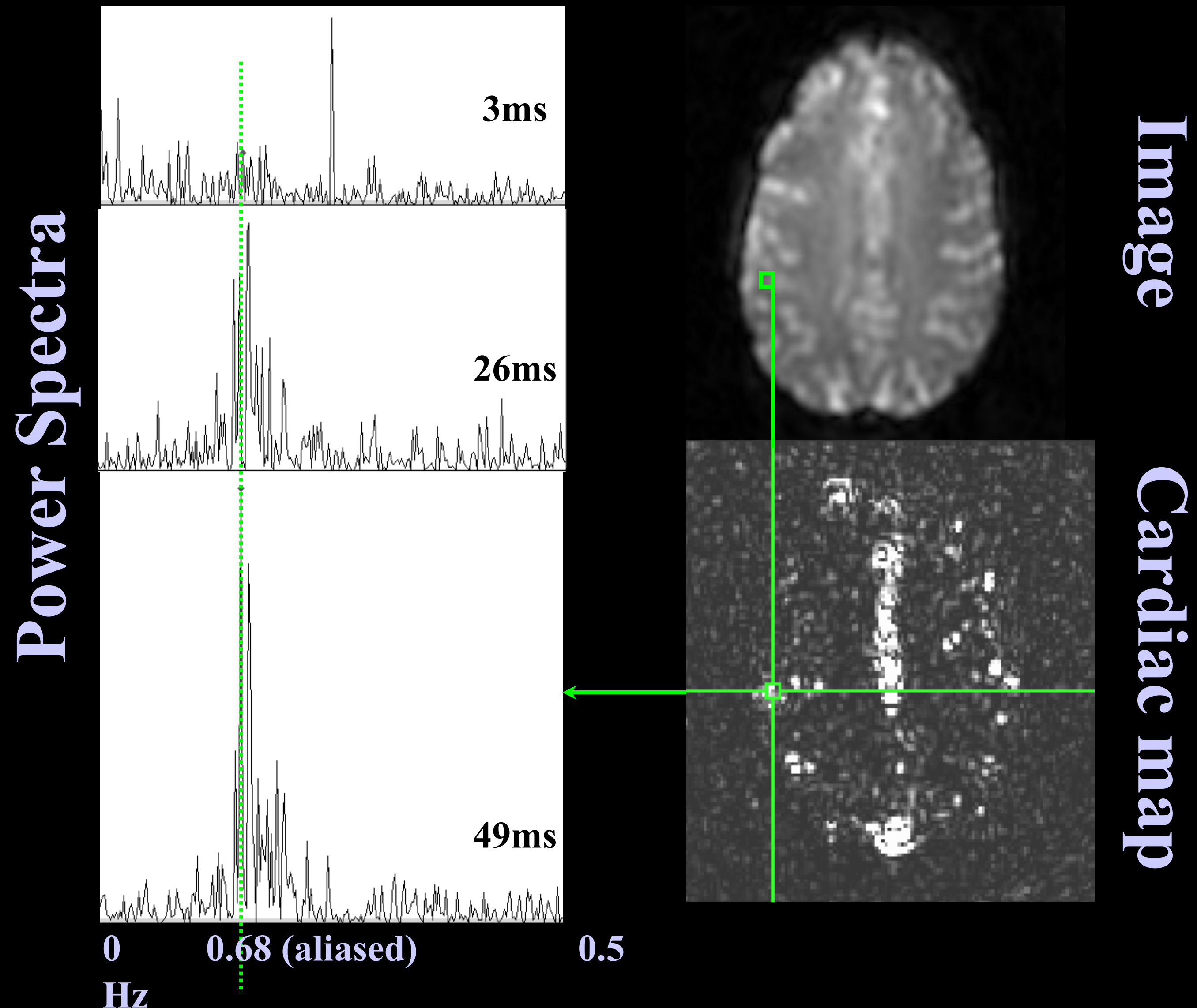

Magnetic Resonance in Medicine 45:595–604 (2001)

Neuroimaging at 1.5 T and 3.0 T: Comparison of Oxygenation-Sensitive Magnetic Resonance Imaging

Gunnar Krüger,* Andreas Kastrup, and Gary H. Glover

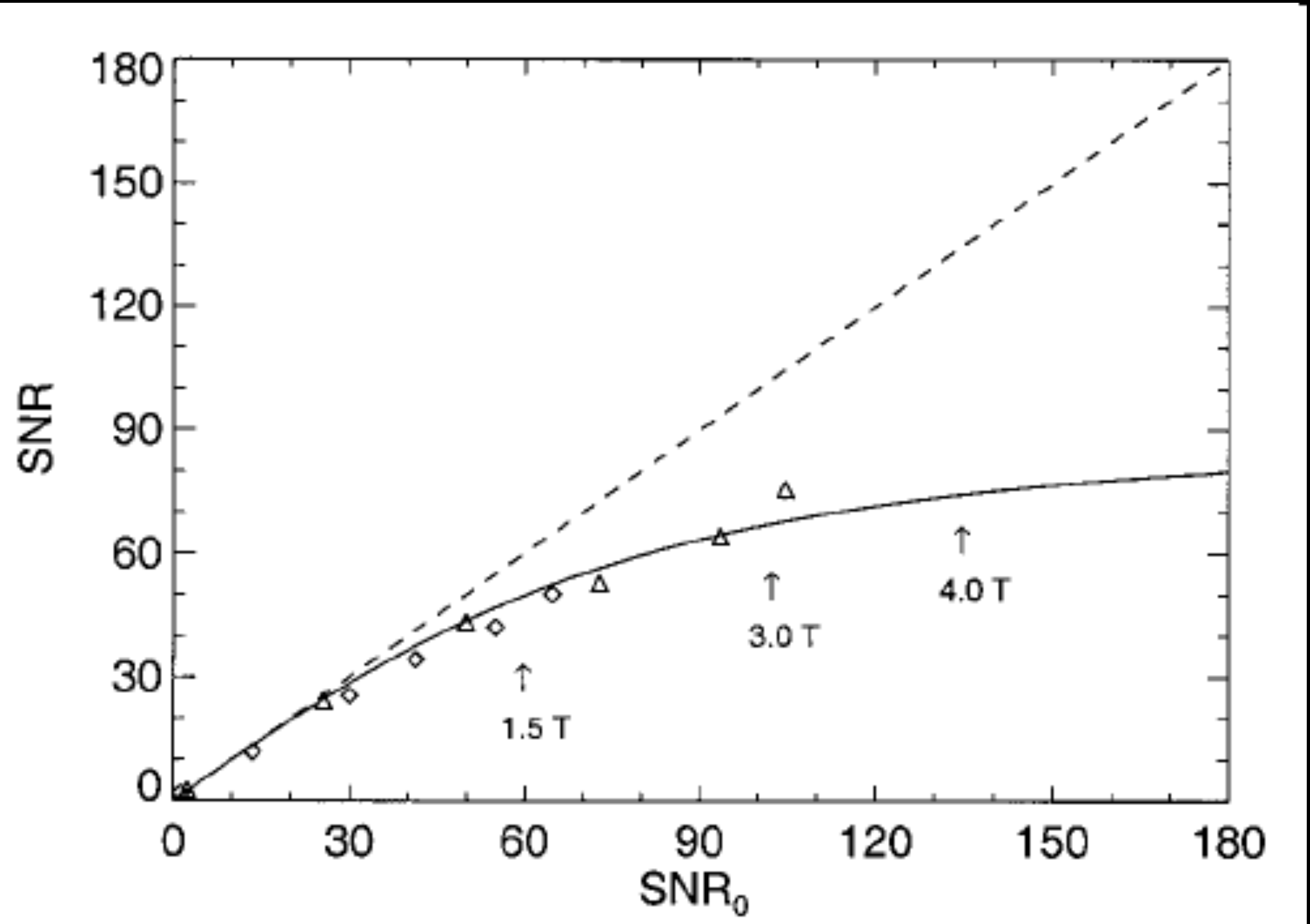

Temporal S/N vs. Image S/N

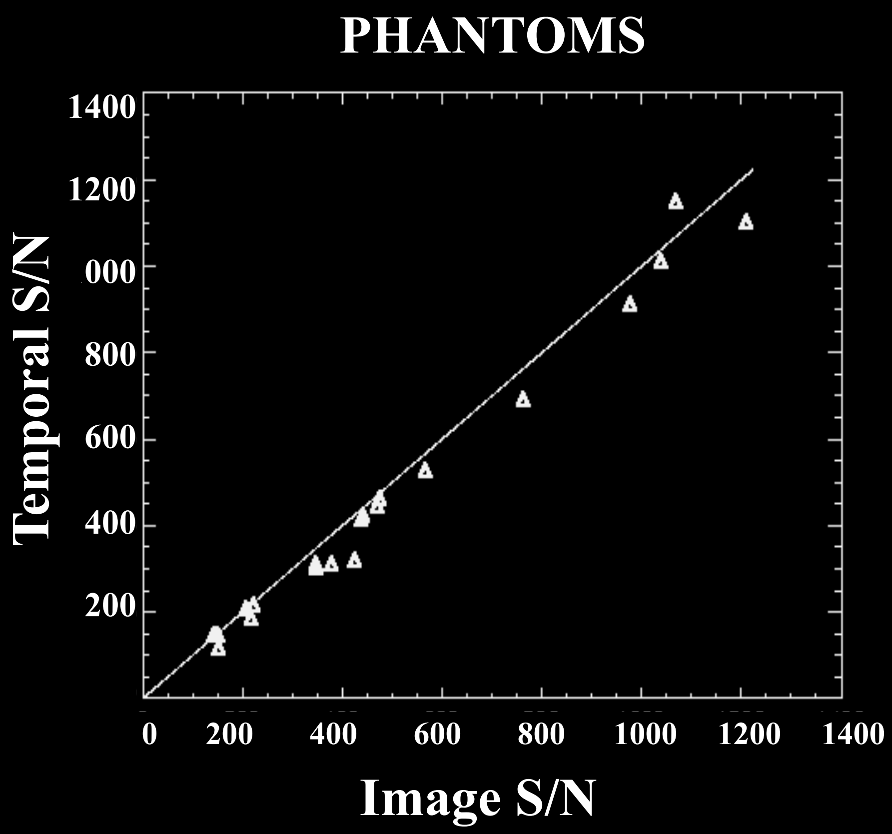

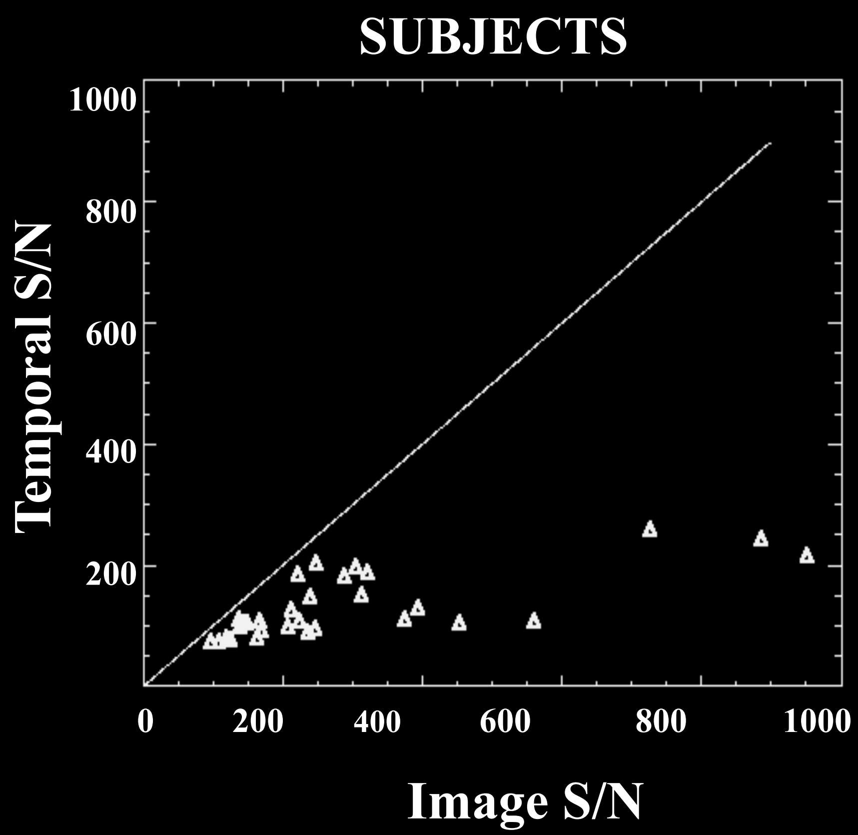

N. Petridou

Temporal vs. Image S/N
Optimal Resolution Study

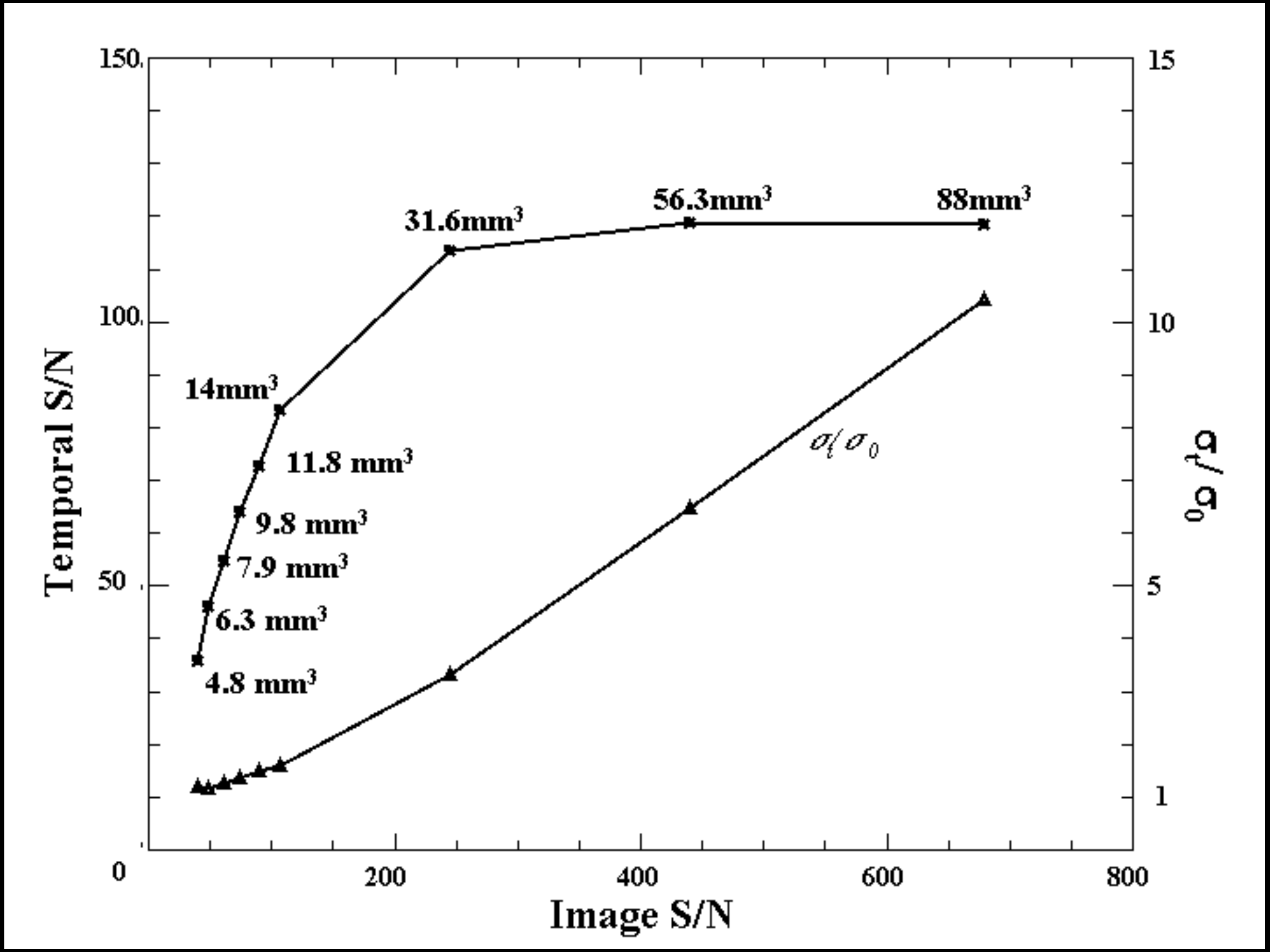

Human data

Petridou et al

Temporal vs. Image S/N Optimal Resolution Study

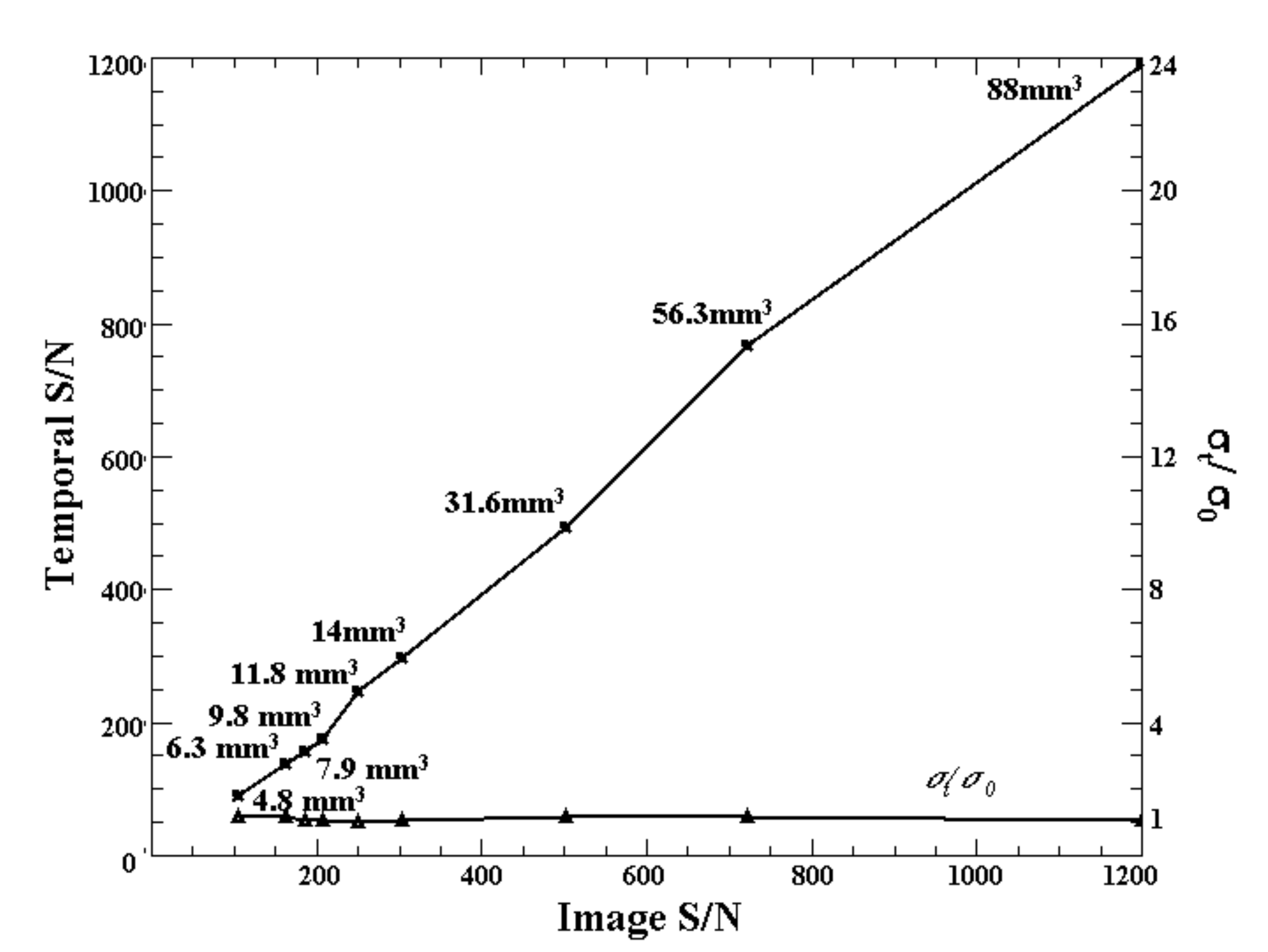

Phantom data

Petridou et al

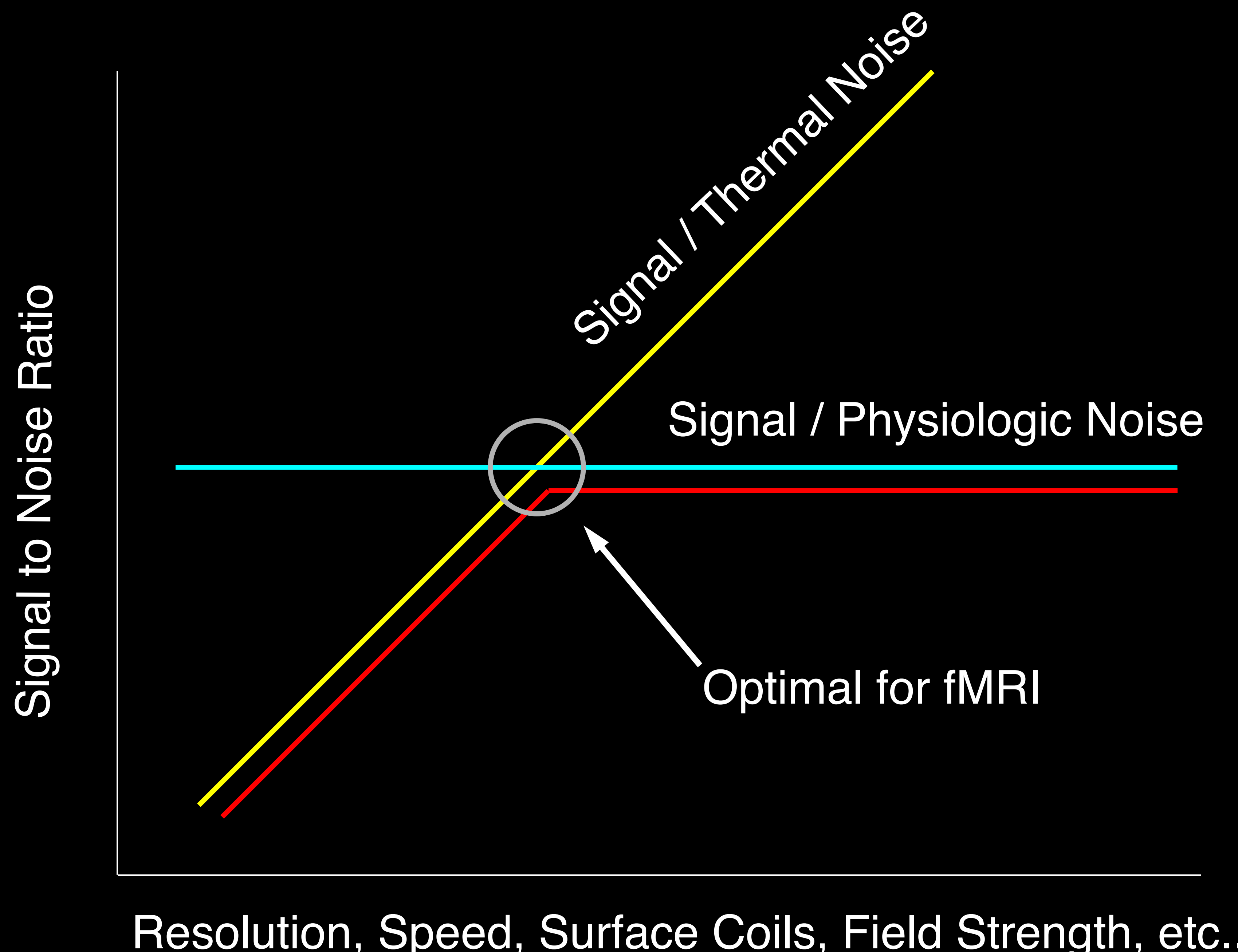
Signal / Thermal Noise
Signal / Physiologic Noise
Optimal for fMRI
Signal to Noise Ratio
Resolution, Speed, Surface Coils, Field Strength, etc..

Doubling Sensitivity with RF coils

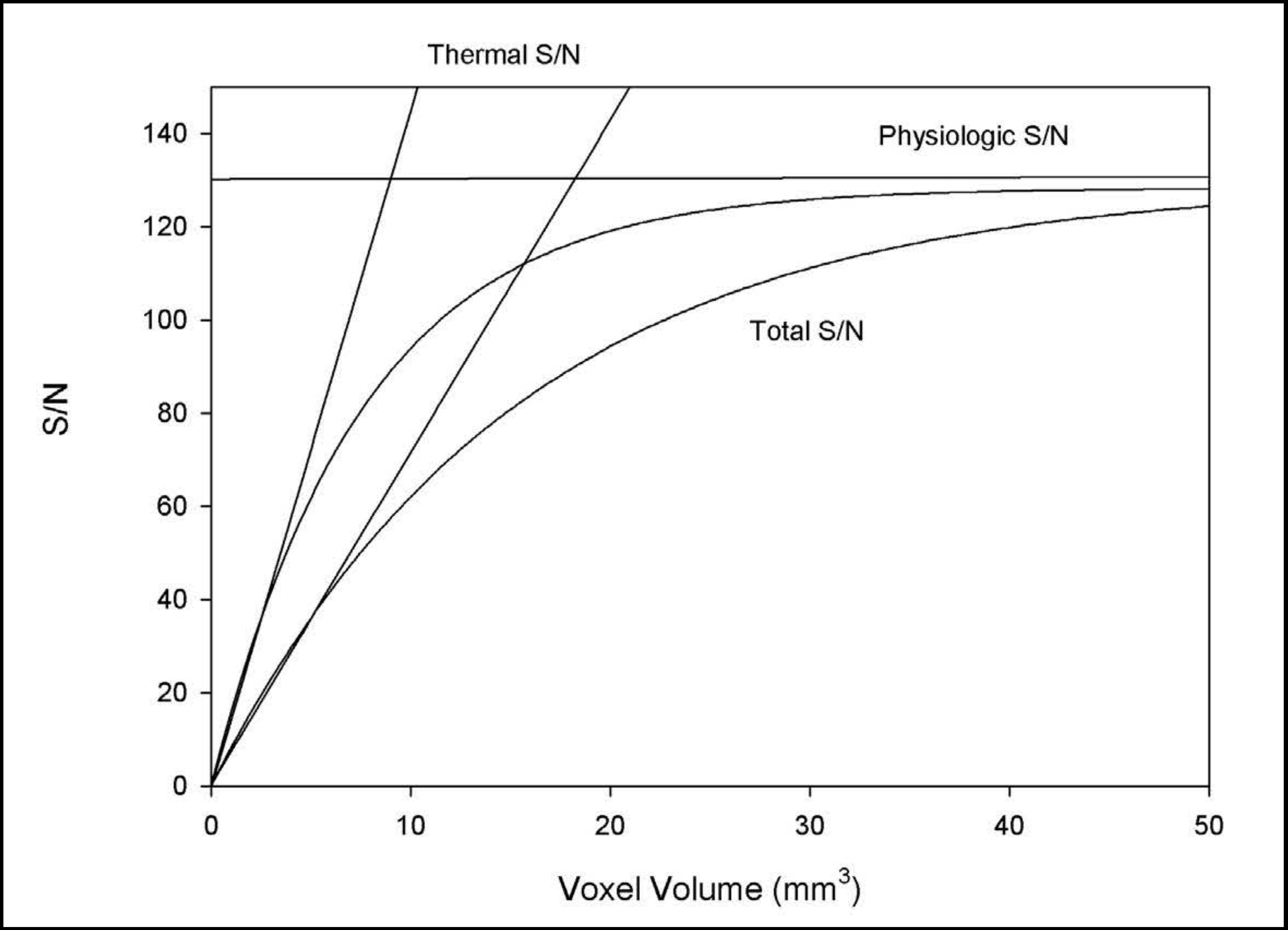

Single shot full k-space echo-planar-imaging with an eight-channel phase array coil at 3T.

Jerzy Bodurka[1], Peter van Gelderen[2], Patrick Ledden[3], Peter Bandettini[1], Jeff Duyn[2]
[1]Functional MRI Facility NIMH/NIH, [2]Advance MRI NINDS/NIH, [3]Nova Medical Inc.

Quadrature Head Coil | 8 Channel Array

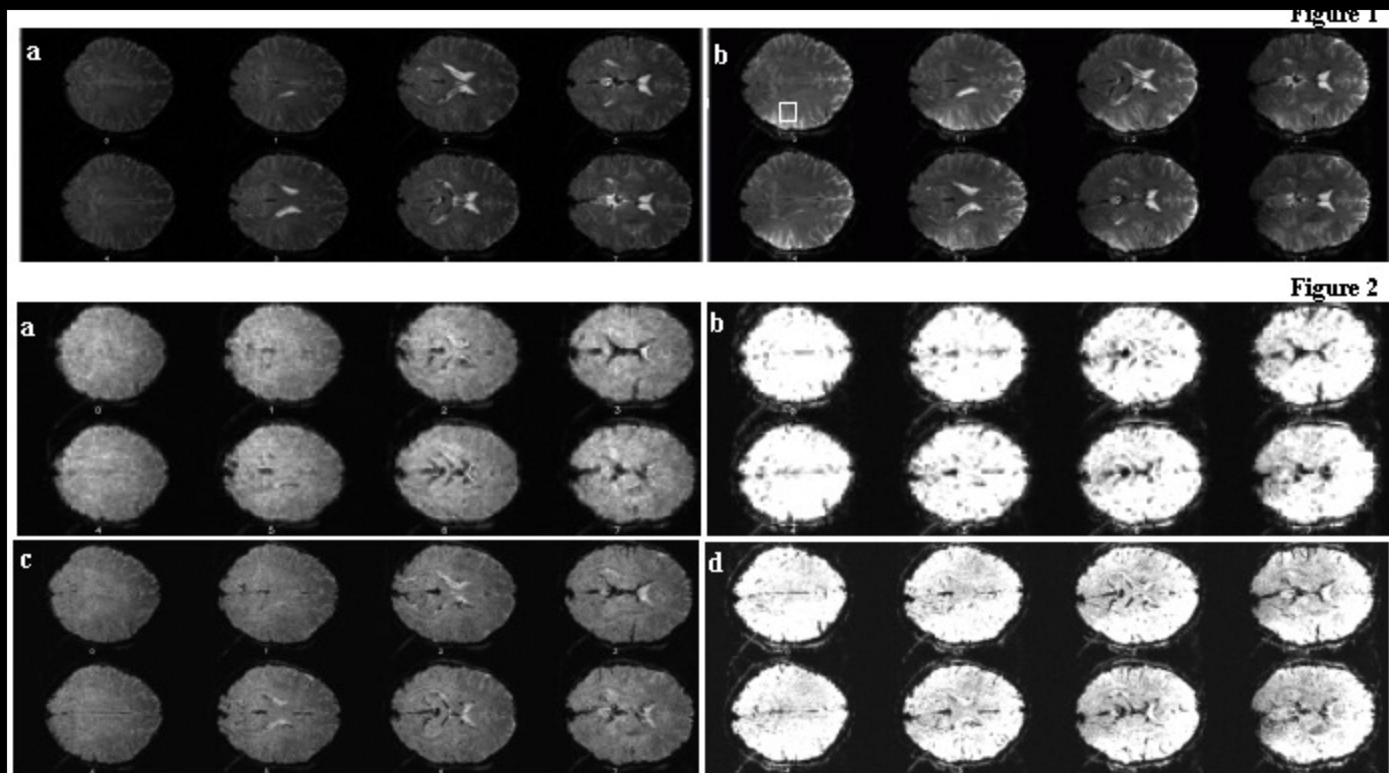

128 x 96 | SNR

64 x 48 | TSNR

128 x 96

Reducing Physiologic Fluctuations

- Filtering
- Pulse sequence
  - single vs. multishot
  - strategies for multishot
- Gating with correction for variable TR

Temporal Artifacts

- System instabilities
- Motion
  - Drift
  - Stimulus correlated
  - Stimulus uncorrelated

Minimizing Temporal Artifacts

Recognize?
- Edge effects
- Shorter signal change latencies
- Unusually high signal changes
- External measuring devices

Correct?
- Image registration algorithms
- Orthogonalize to motion-related function *(cardiac, respiration, movement)*
- Navigator echo for k-space alignment *(for multishot techniques)*
- Re-do scan

Bypass?
- Paradigm timing strategies..
- Gating (with T1-correction)

Suppress?
- Flatten image contrast
- Physical restraint
- Averaging, smoothing

FMRI Basics and Beyond

- Information Content
- Sensitivity
- Resolution
- Image quality
- Paradigm Design and Processing

Single Shot EPI

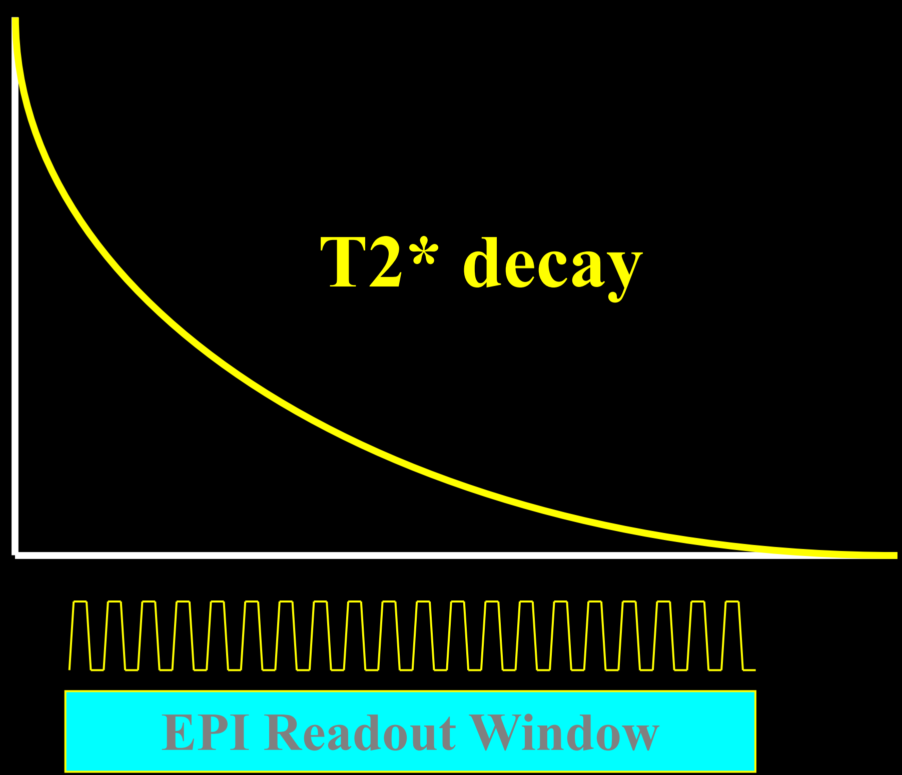

≈ 20 to 40 ms

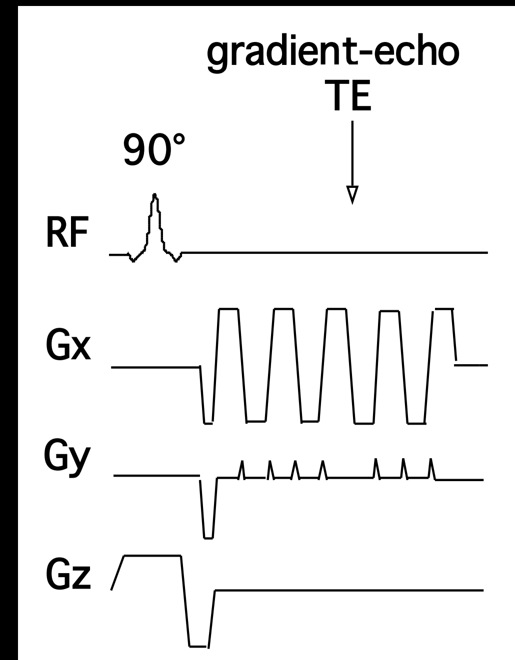

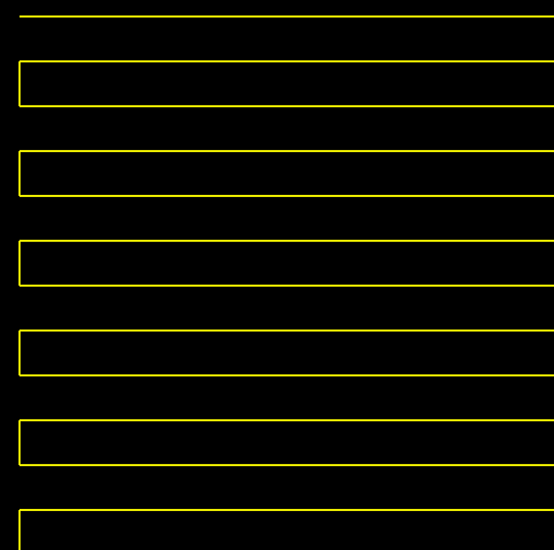

Imaging System Components

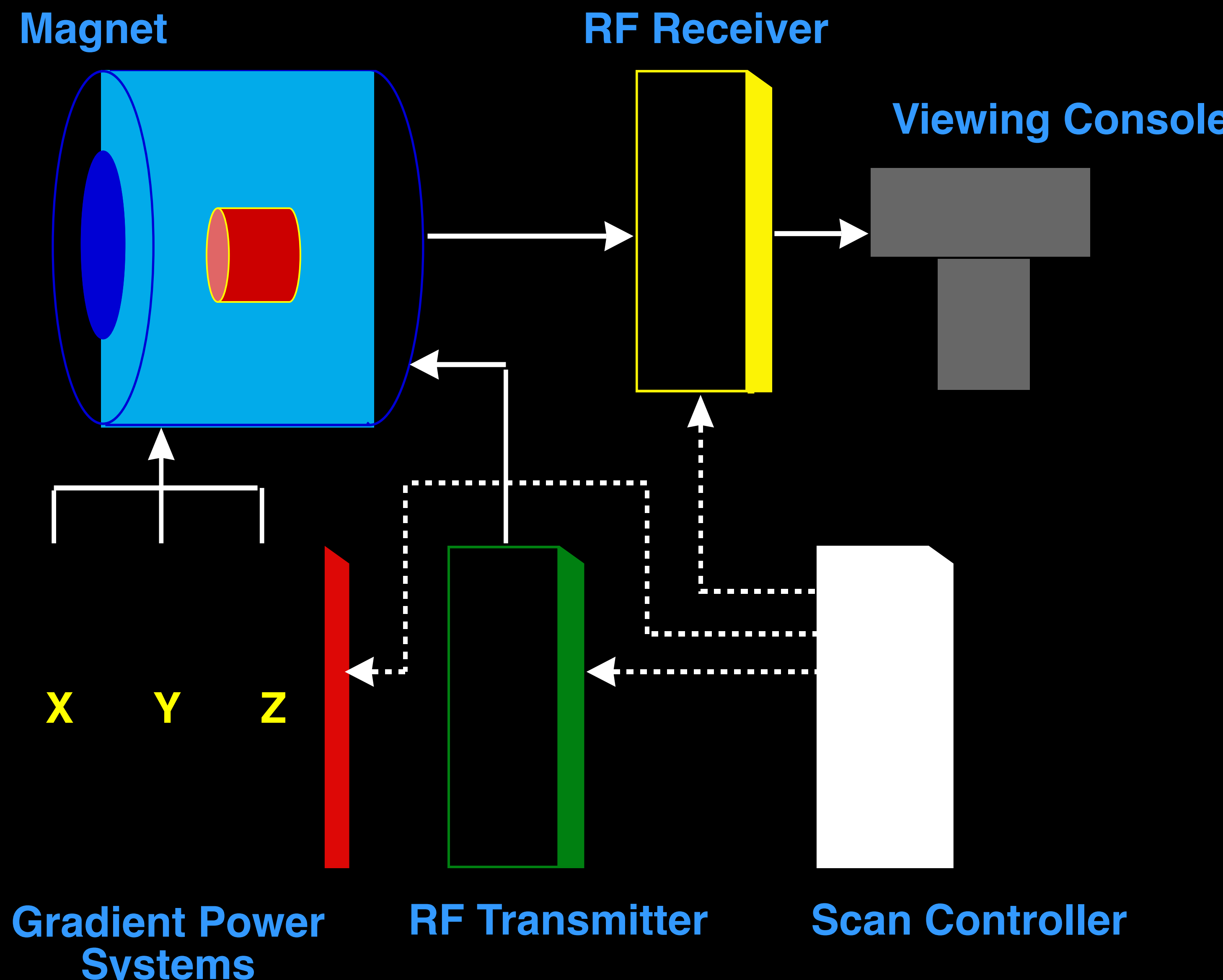

Echo Planar Imaging at the Medical College of Wisconsin

1991-1992

1992-1999

Imaging System Components

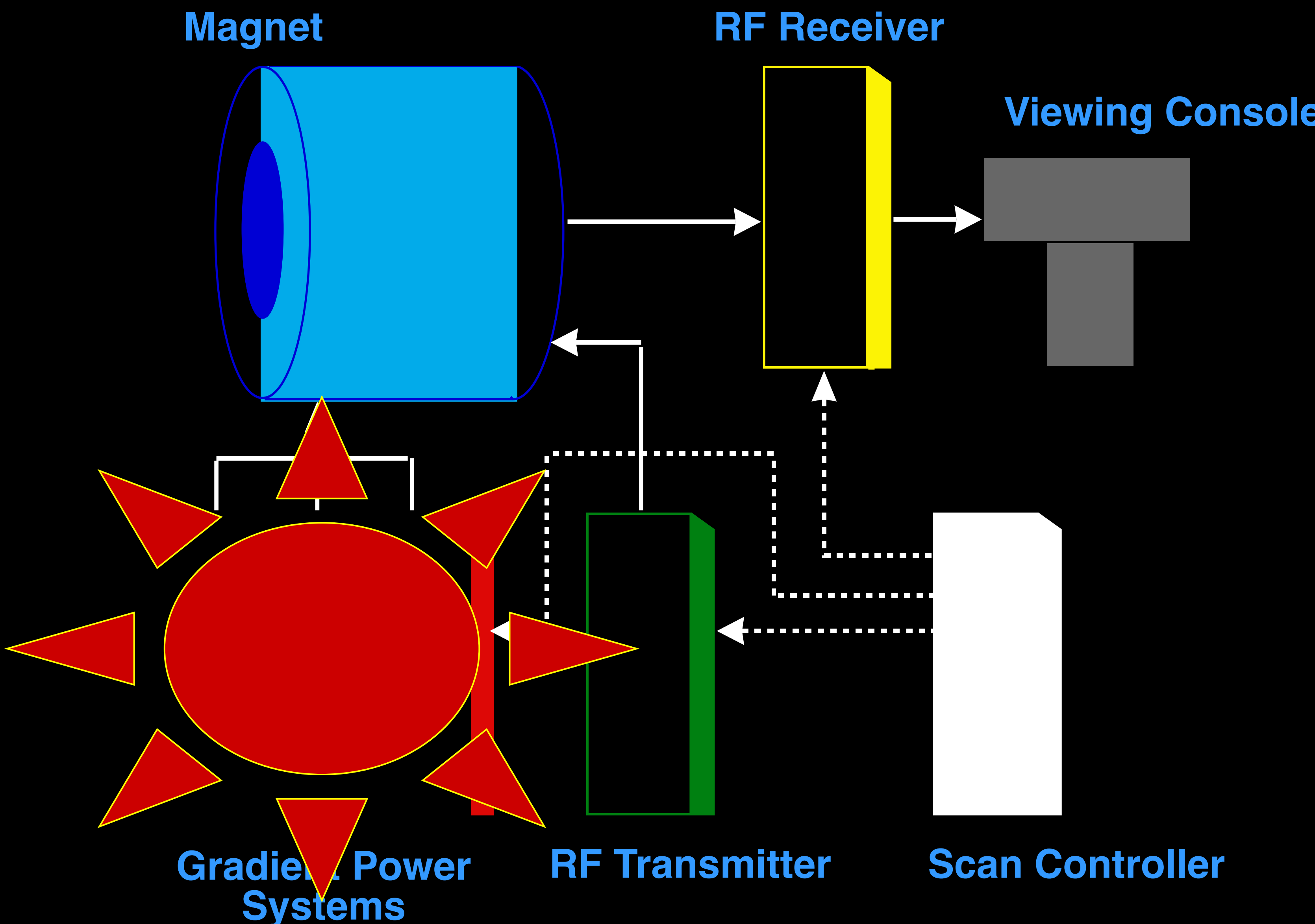

General Electric 3 Tesla Scanner

Multishot Imaging

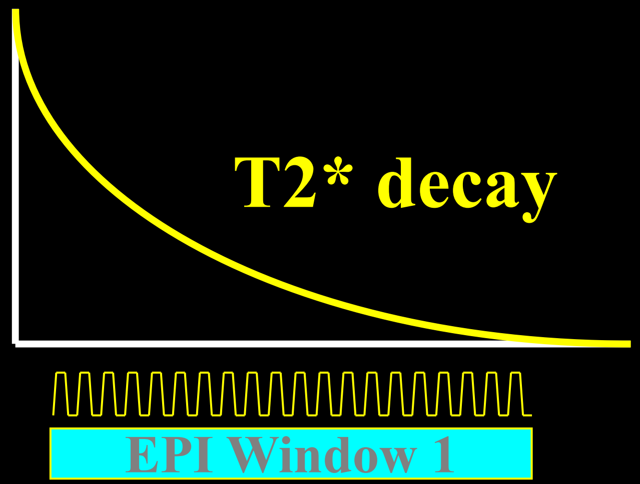

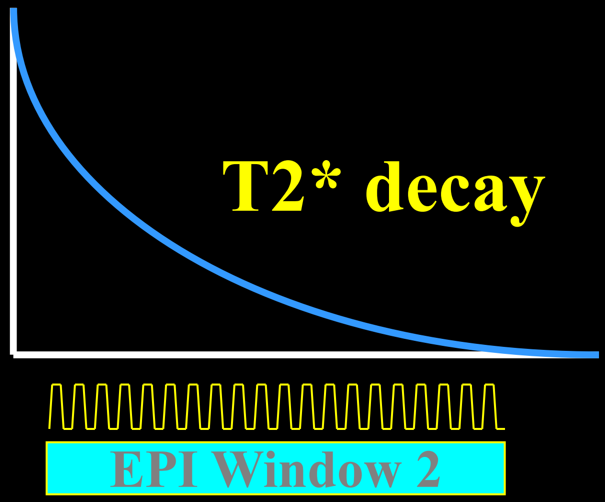

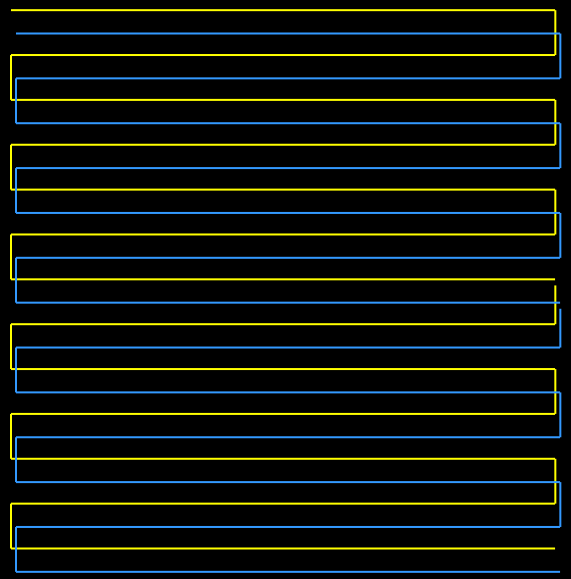

Multi Shot EPI

Excitations	1	2	4	8
Matrix Size	64 x 64	128 x 128	256 x 128	256 x 256

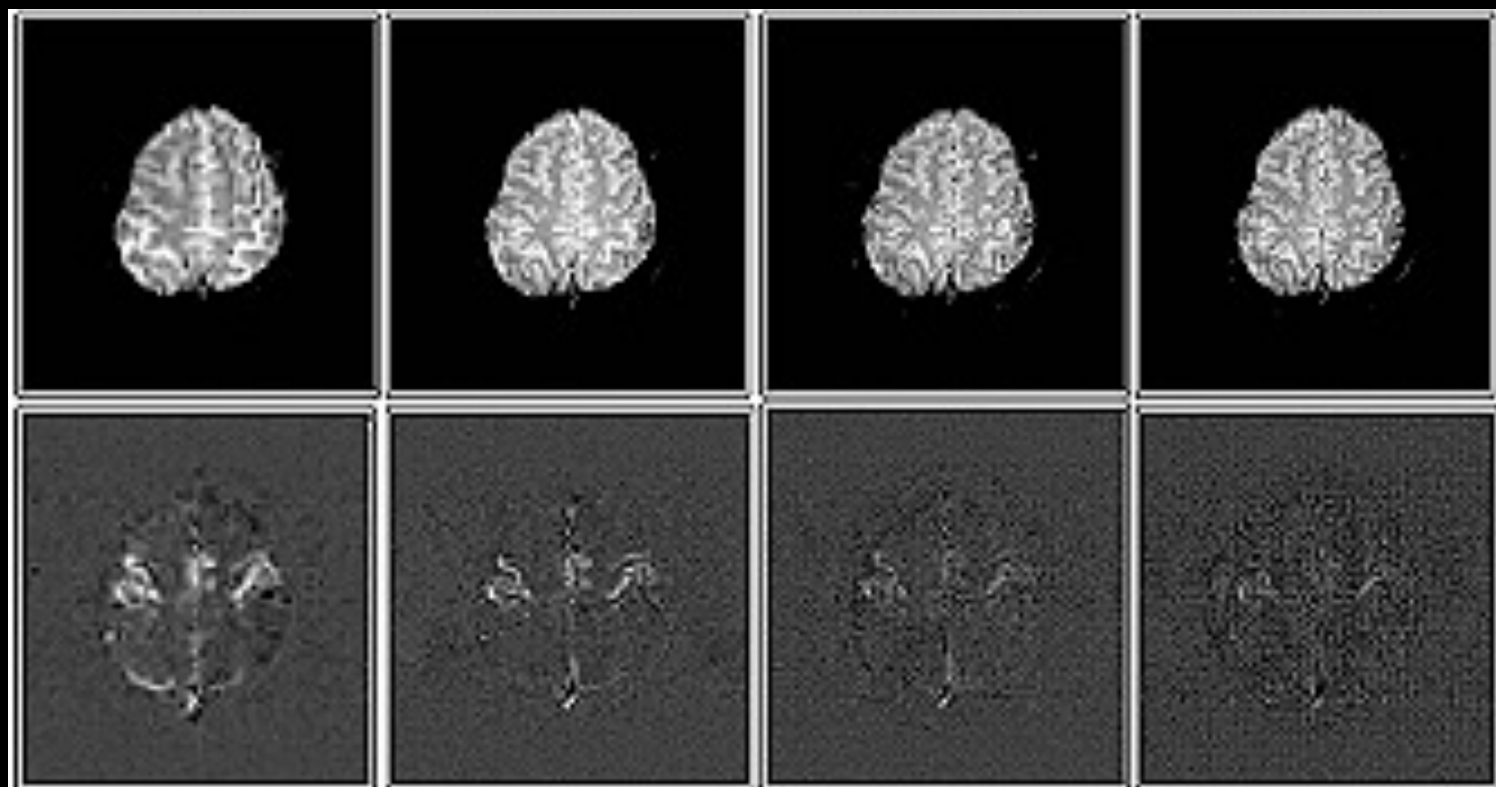

Partial k-space imaging

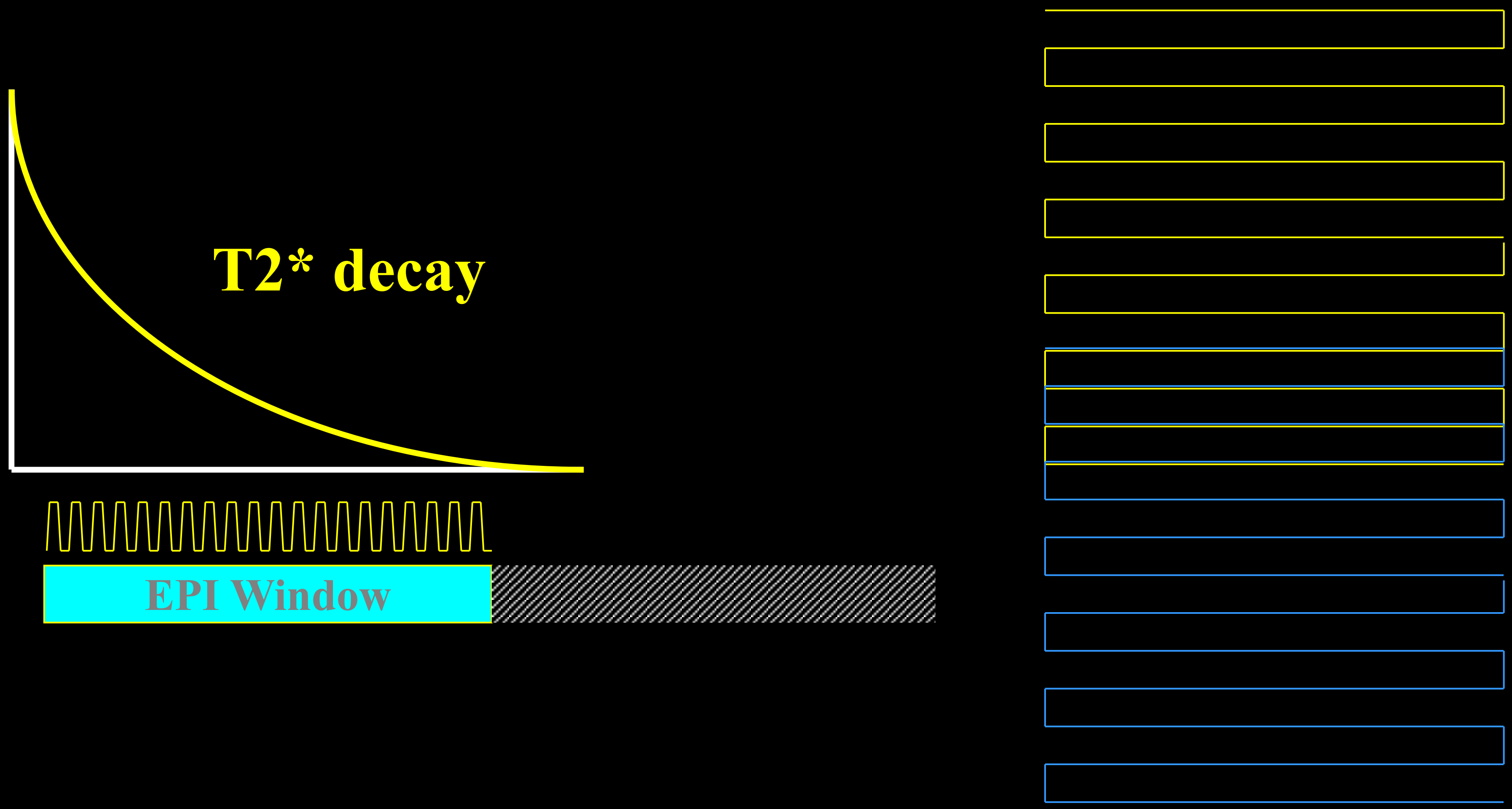

Single - Shot EPI at 3T:
Half NEX, 256 x 256, 16 cm FOV

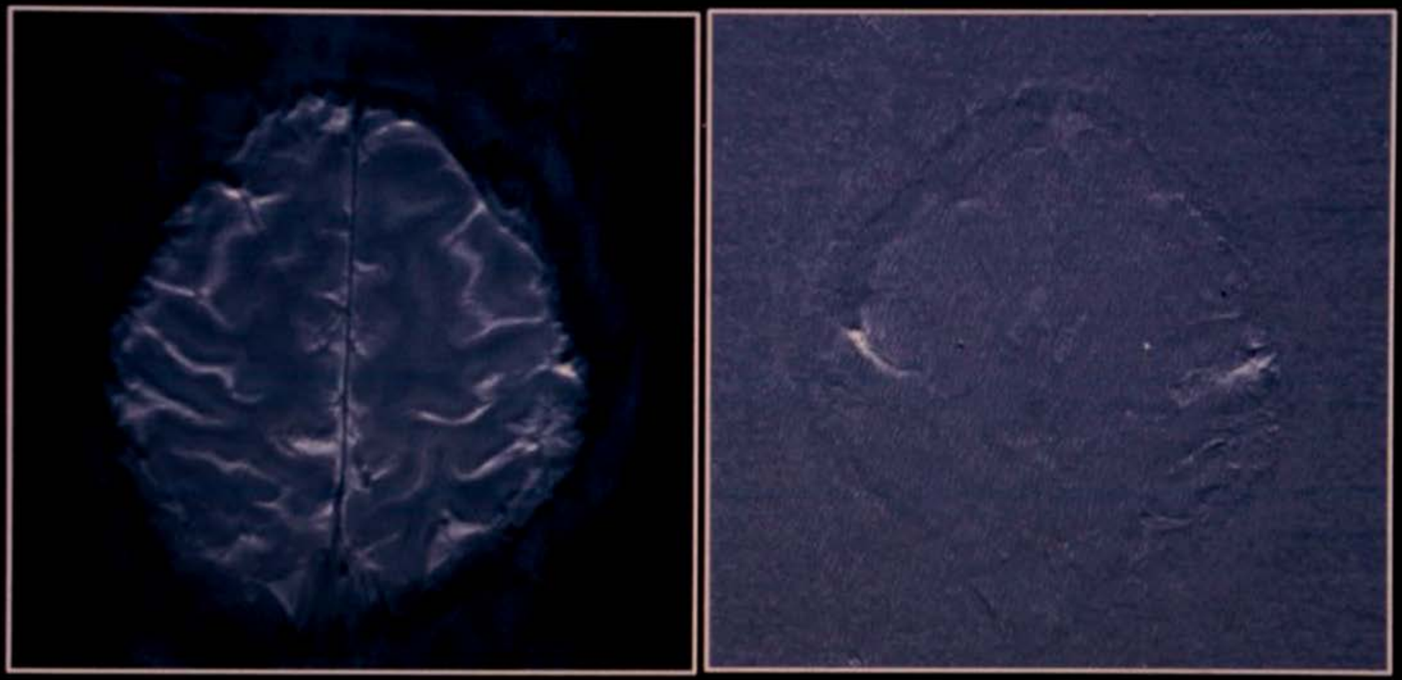

Single shot full k-space echo-planar-imaging with an eight-channel phase array coil at 3T.

Jerzy Bodurka[1], Peter van Gelderen[2], Patrick Ledden[3], Peter Bandettini[1], Jeff Duyn[2]
[1]Functional MRI Facility NIMH/NIH, [2]Advance MRI NINDS/NIH, [3]Nova Medical Inc.

Quadrature Head Coil | 8 Channel Array

128 x 96

64 x 48

128 x 96

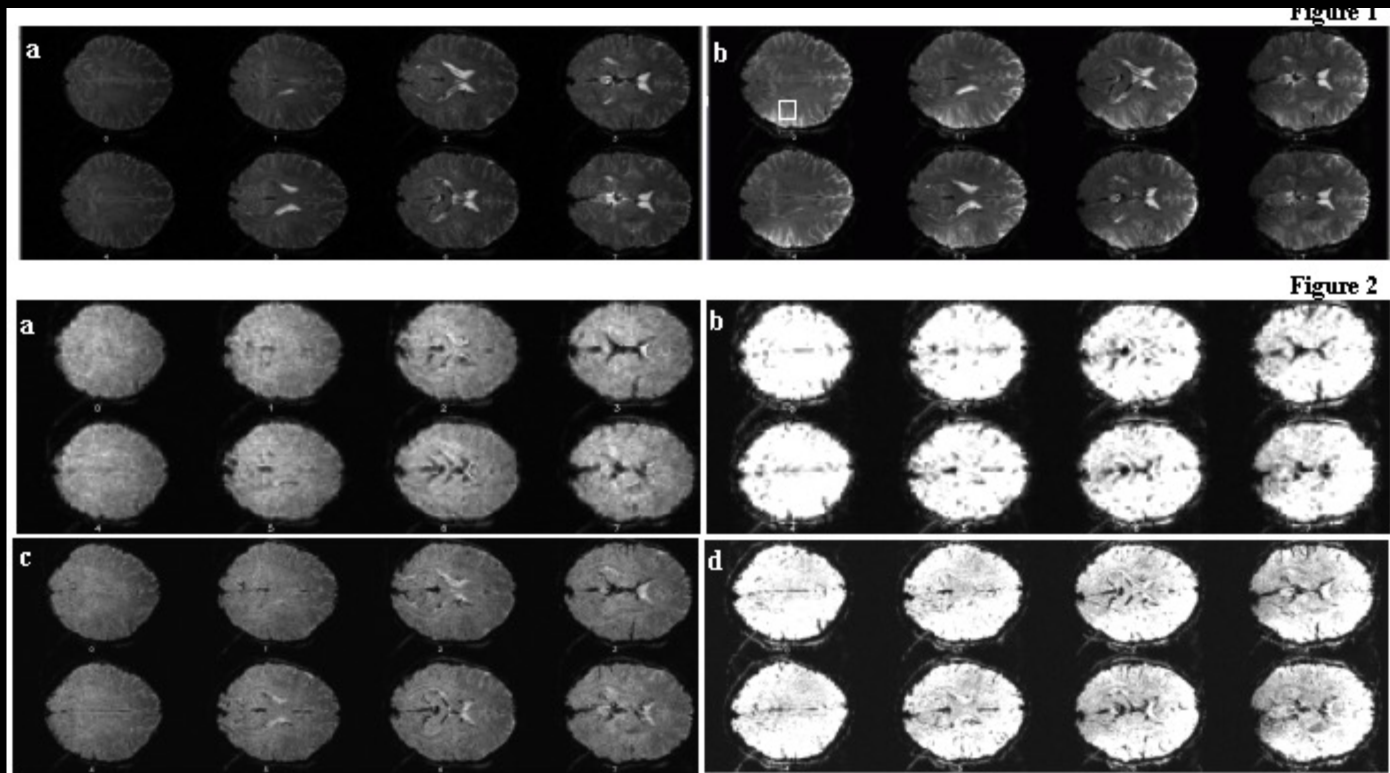

SNR

TSNR

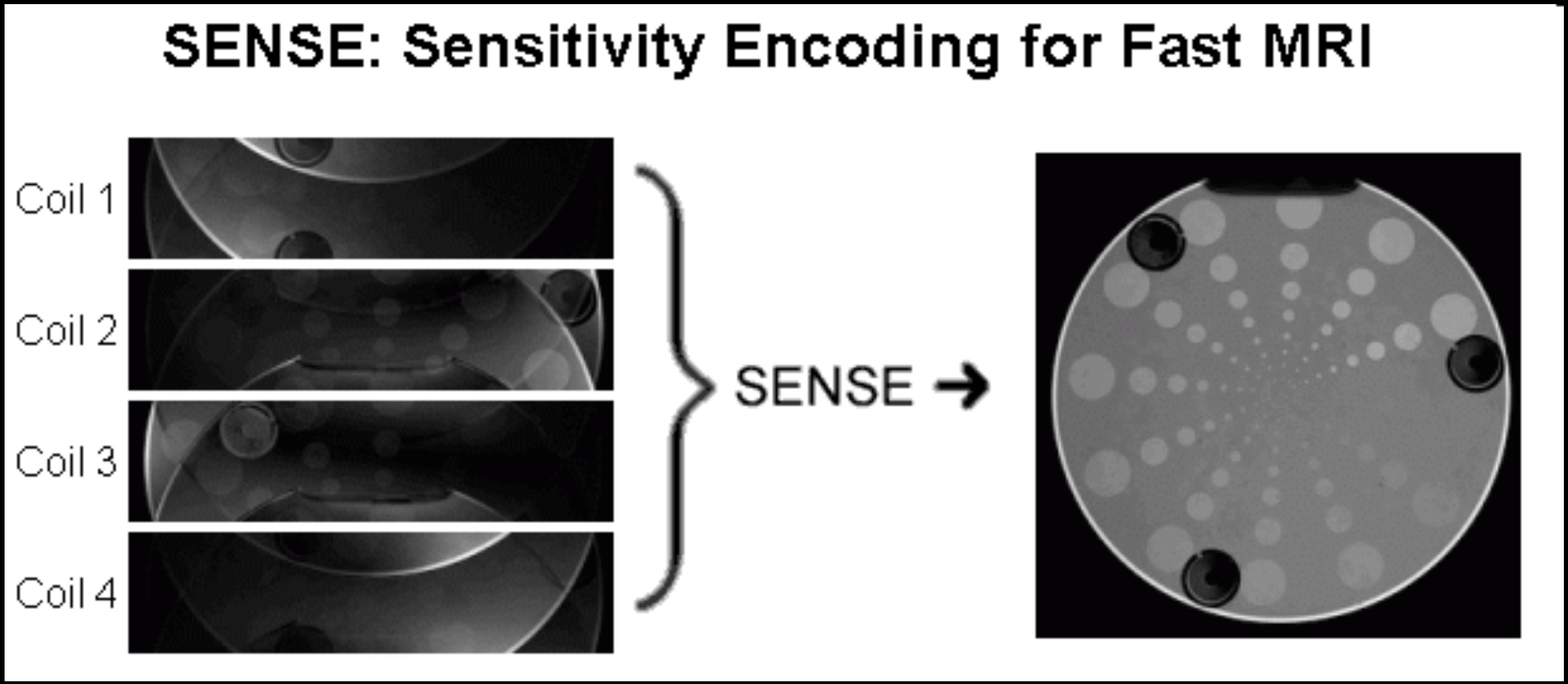

Pruessmann, et al.

SENSE Imaging

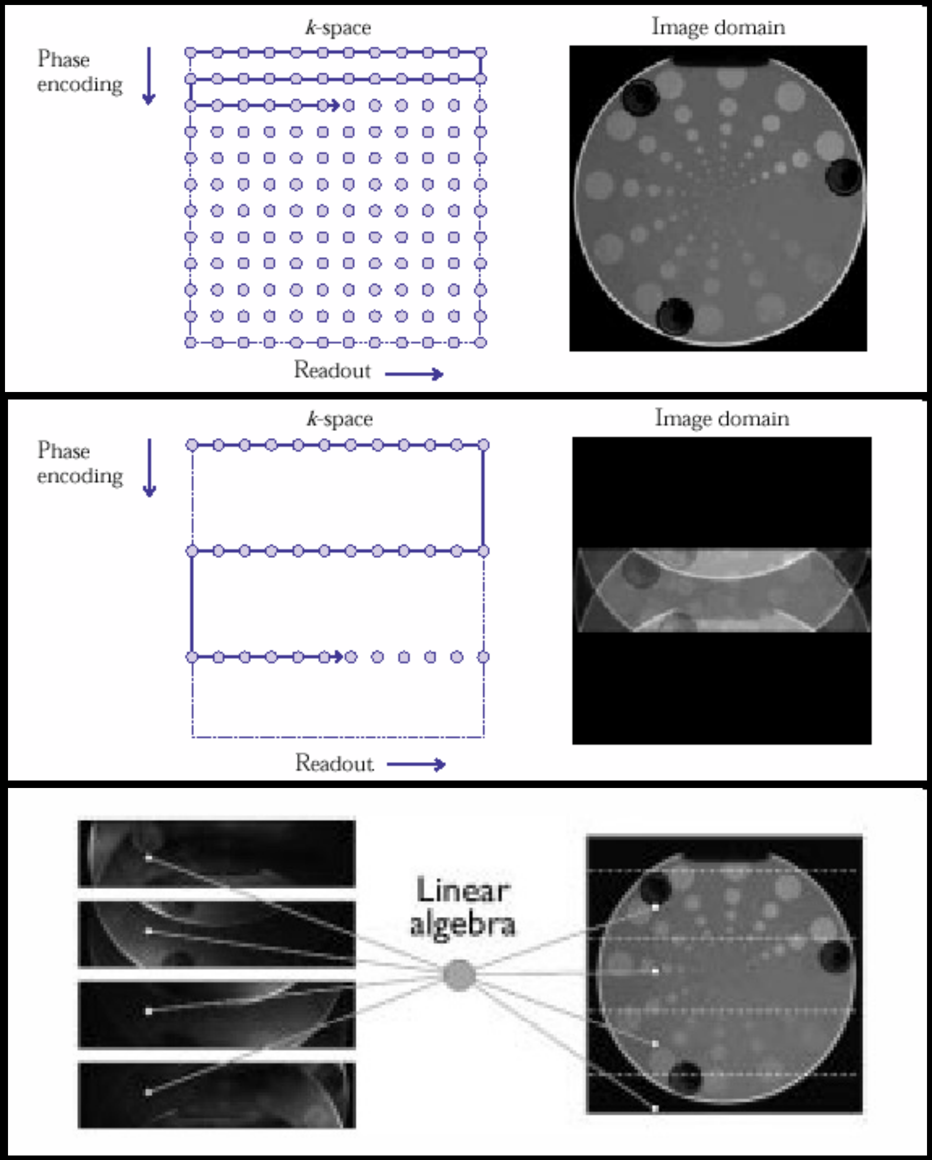

Pruessmann, et al.

Ocular Dominance Column Mapping using fMRI

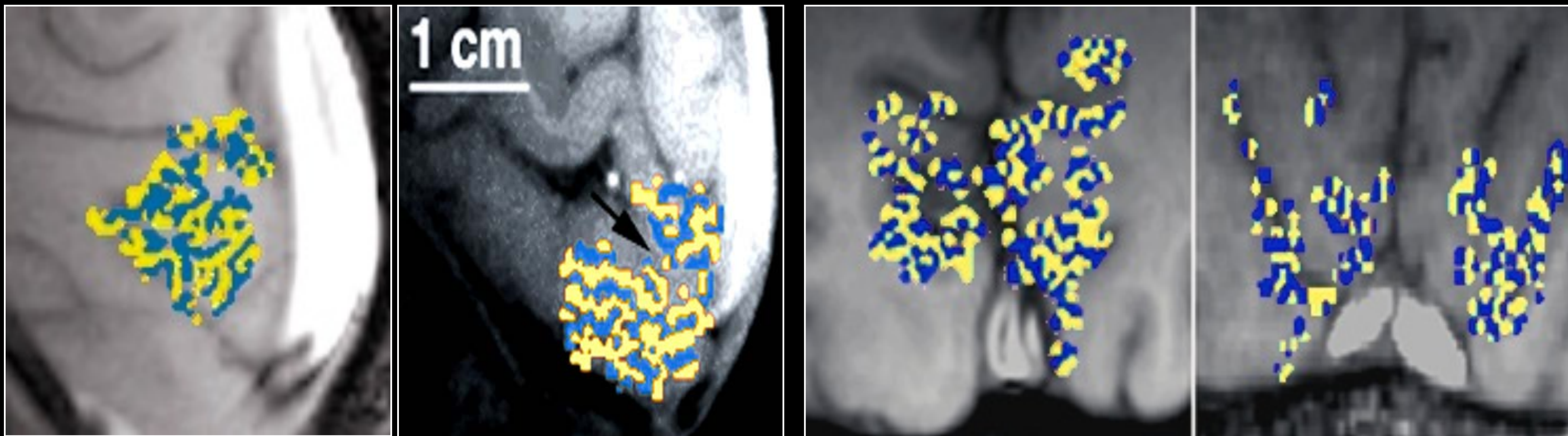

Menon, R. S., S. Ogawa, et al. (1997). “Ocular dominance in human V1 demonstrated by functional magnetic resonance imaging.” J Neurophysiol 77(5): 2780-7.

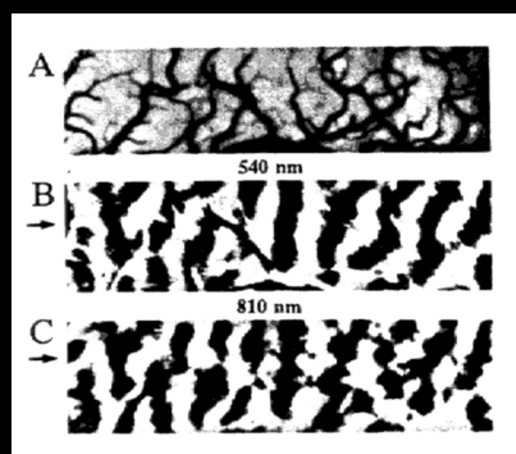

Optical Imaging

R. D. Frostig et. al, PNAS 87: 6082-6086, (1990).

FMRI Basics and Beyond

- Information Content
- Sensitivity
- Resolution
- Image quality
- Paradigm Design and Processing

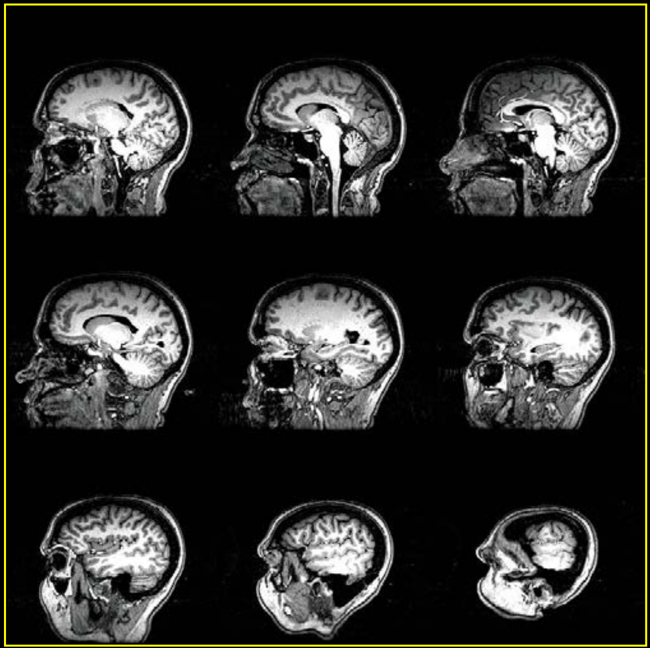
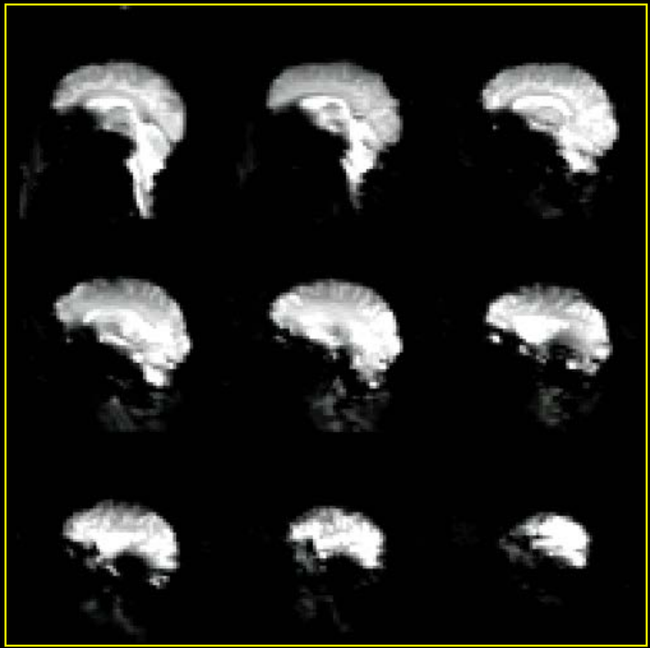
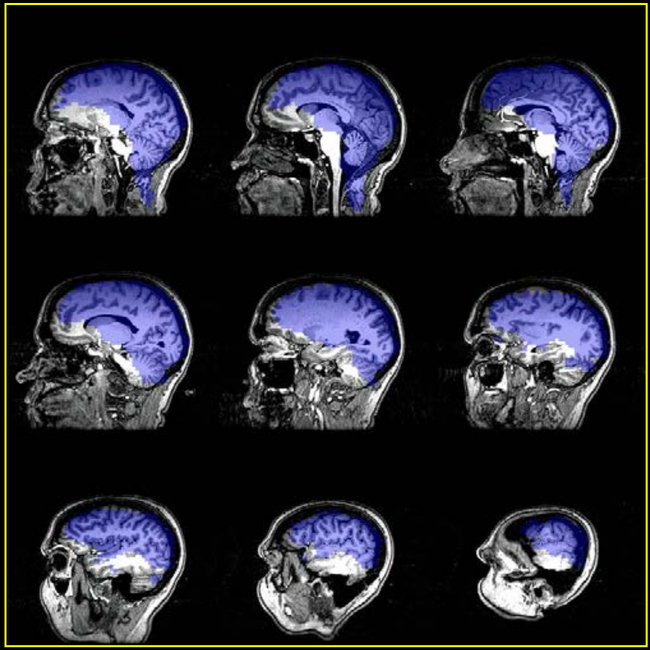

Magnetic Resonance in Medicine 42:290–299 (1999)

3D z-Shim Method for Reduction of Susceptibility Effects in BOLD fMRI

Gary H. Glover*

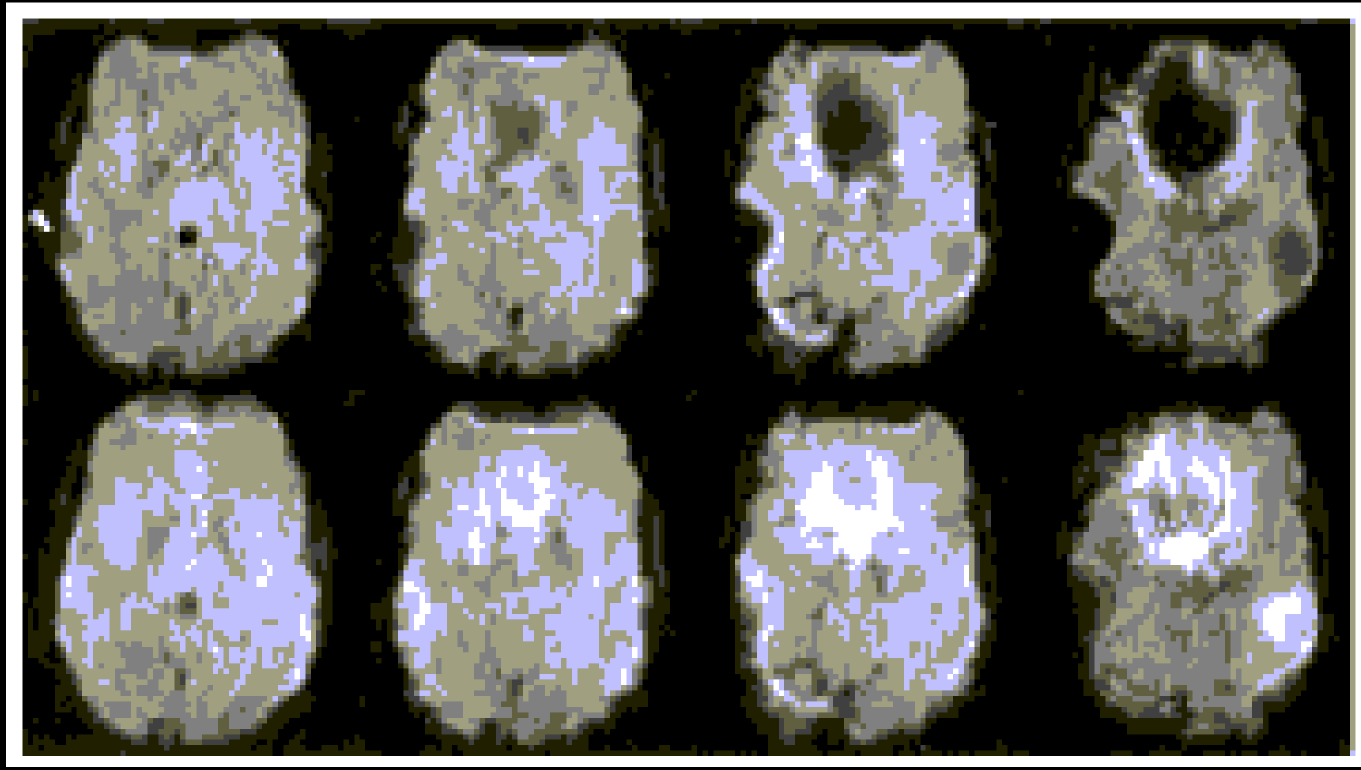

Magnetic Resonance in Medicine 48:906–914 (2002)

Optimization of Static Field Homogeneity in Human Brain Using Diamagnetic Passive Shims

James L. Wilson, Mark Jenkinson, and Peter Jezzard*

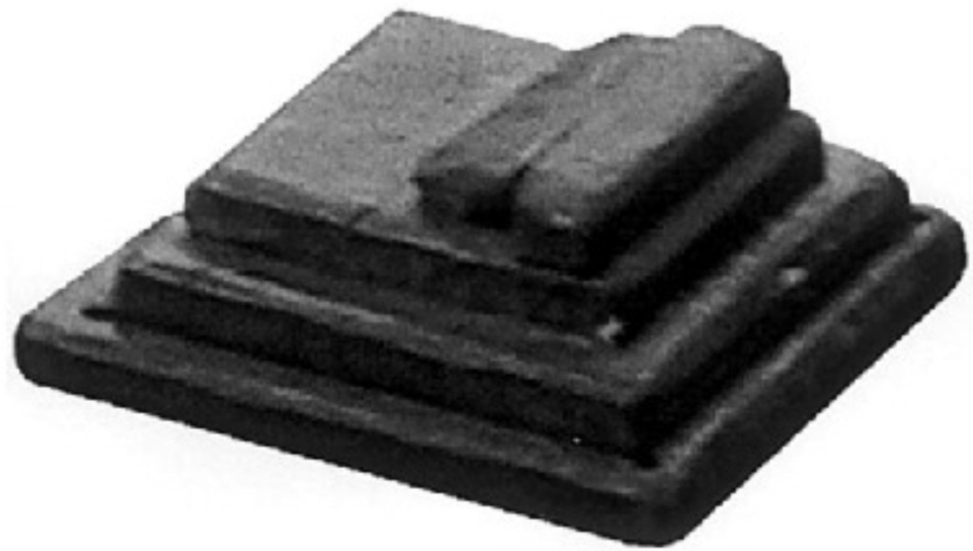

FIG. 1. Photograph of the mouth shim, comprising four plates of pyrolytic graphite, without the polymorph mold. The shallow end of the shim is placed near the front of the roof of the mouth. The shim is 33 mm in length and 26 mm in width, and each plate is 3 mm thick.

Magnetic Resonance in Medicine 48:906–914 (2002)

Optimization of Static Field Homogeneity in Human Brain Using Diamagnetic Passive Shims

James L. Wilson, Mark Jenkinson, and Peter Jezzard*

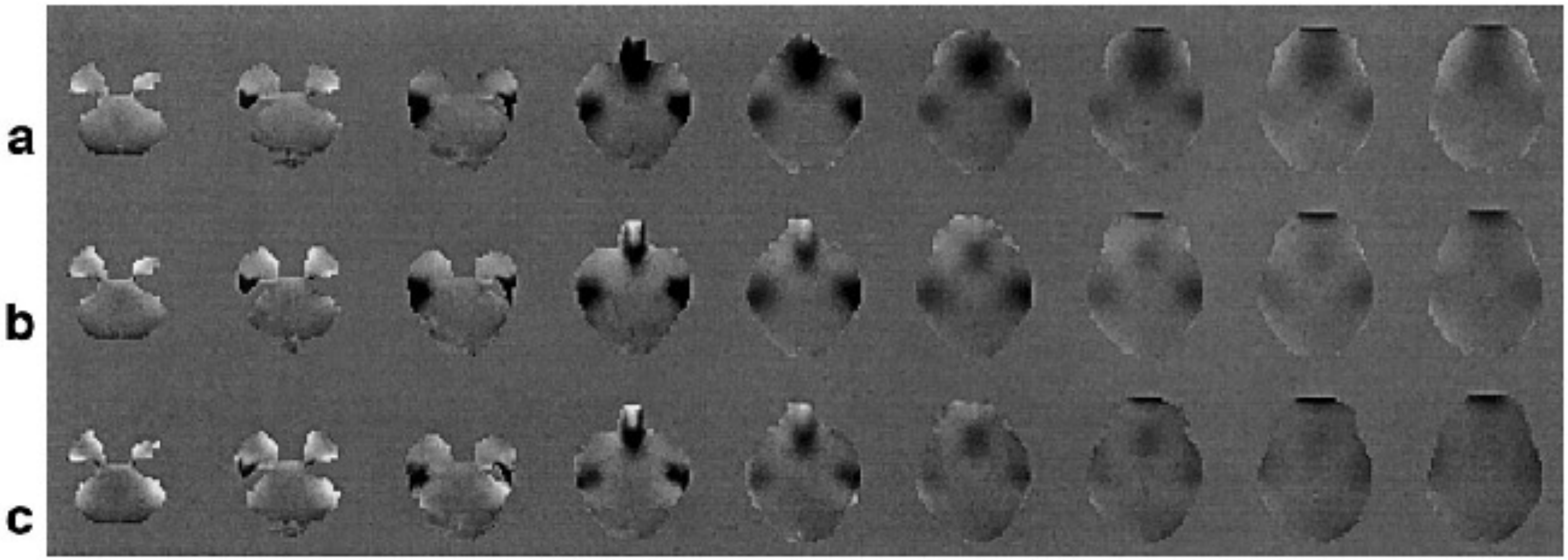

FIG. 3. Example of B_0 inhomogeneity reduction. Nine axial slices, from the bottom of the ITC to the top of the IFC, of manually brain masked B_0 maps of subject C are shown (**a**) without any passive shims, (**b**) with the mouth shim, and (**c**) with the mouth shim and ear shims. B_0 range is −1.2 ppm (white) to +1.2 ppm (black). Decreases in the IFC and ITC inhomogeneities are significant with placement of the mouth and ear shims, respectively, without compromising other brain regions.

Magnetic Resonance in Medicine 48:906–914 (2002)

Optimization of Static Field Homogeneity in Human Brain Using Diamagnetic Passive Shims

James L. Wilson, Mark Jenkinson, and Peter Jezzard*

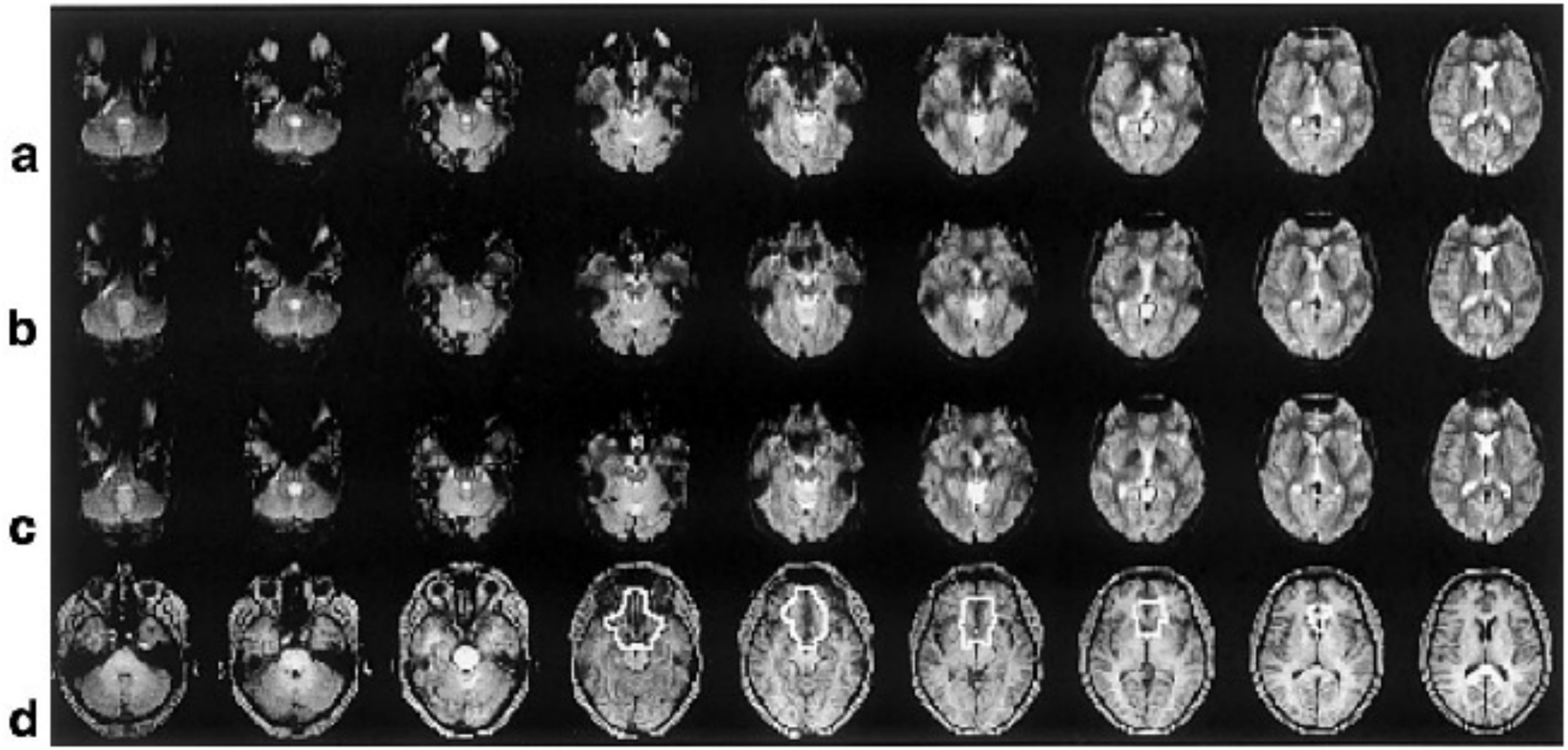

FIG. 4. Example of EPI susceptibility artifact reduction. Nine axial slices of subject C, corresponding to those shown in Fig. 3, are shown. A standard T_1-weighted structural image is provided in row **d** as a reference with an outline of the IFC mask of this subject superimposed. Unwarped gradient-echo EPI images are shown (**a**) without any passive shims, (**b**) with the mouth shim, and (**c**) with the mouth shim and ear shims. A considerable reduction in signal loss artifact in the IFC is evident with placement of the mouth shim. A smaller reduction in the ITCs is apparent with placement of the ear shims.

FMRI Basics and Beyond

- Information Content
- Sensitivity
- Resolution
- Image quality
- Paradigm Design and Processing

Neuronal Activation Input Strategies

1. Block Design
2. Frequency Encoding

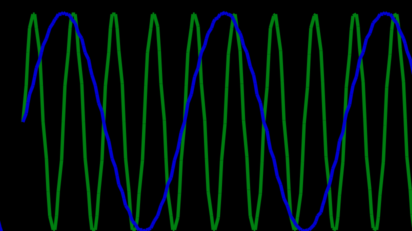

3. Phase Encoding

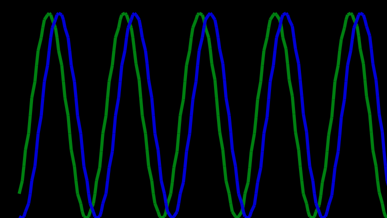

4. Event Related
5. Orthogonal Block Design

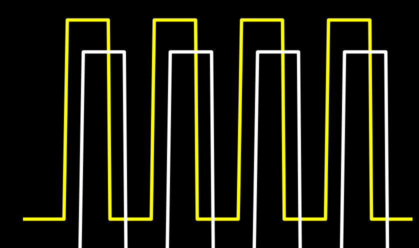

6. Free Behavior Design.

Neuronal Activation Input Strategies

1. Block Design
2. Frequency Encoding

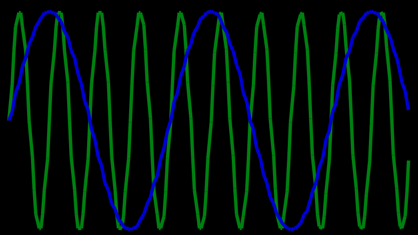

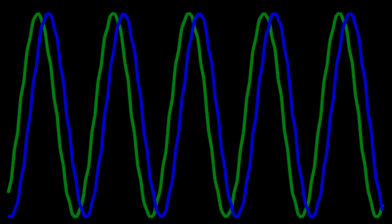

3. Phase Encoding
4. Event Related

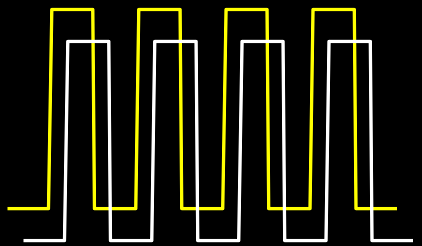

5. Orthogonal Block Design
6. Free Behavior Design.

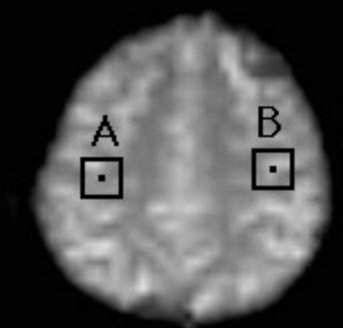

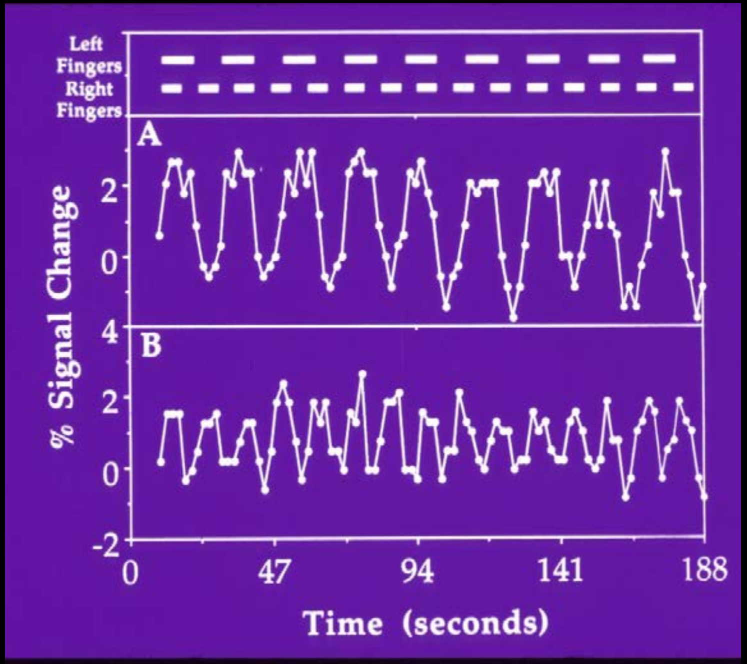

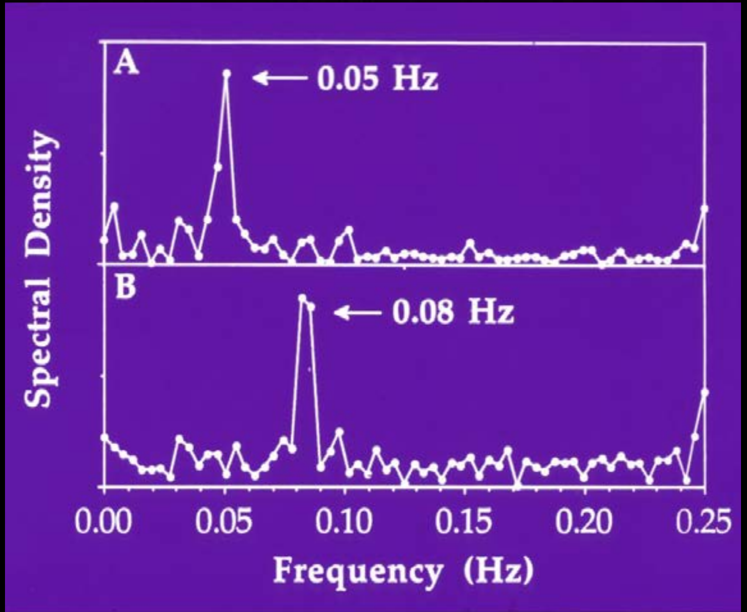

P. A. Bandettini, A. Jesmanowicz, E. C. Wong, J. S. Hyde, Processing strategies for time-course data sets in functional MRI of the human brain. *Magn. Reson. Med.* 30, 161-173 (1993).

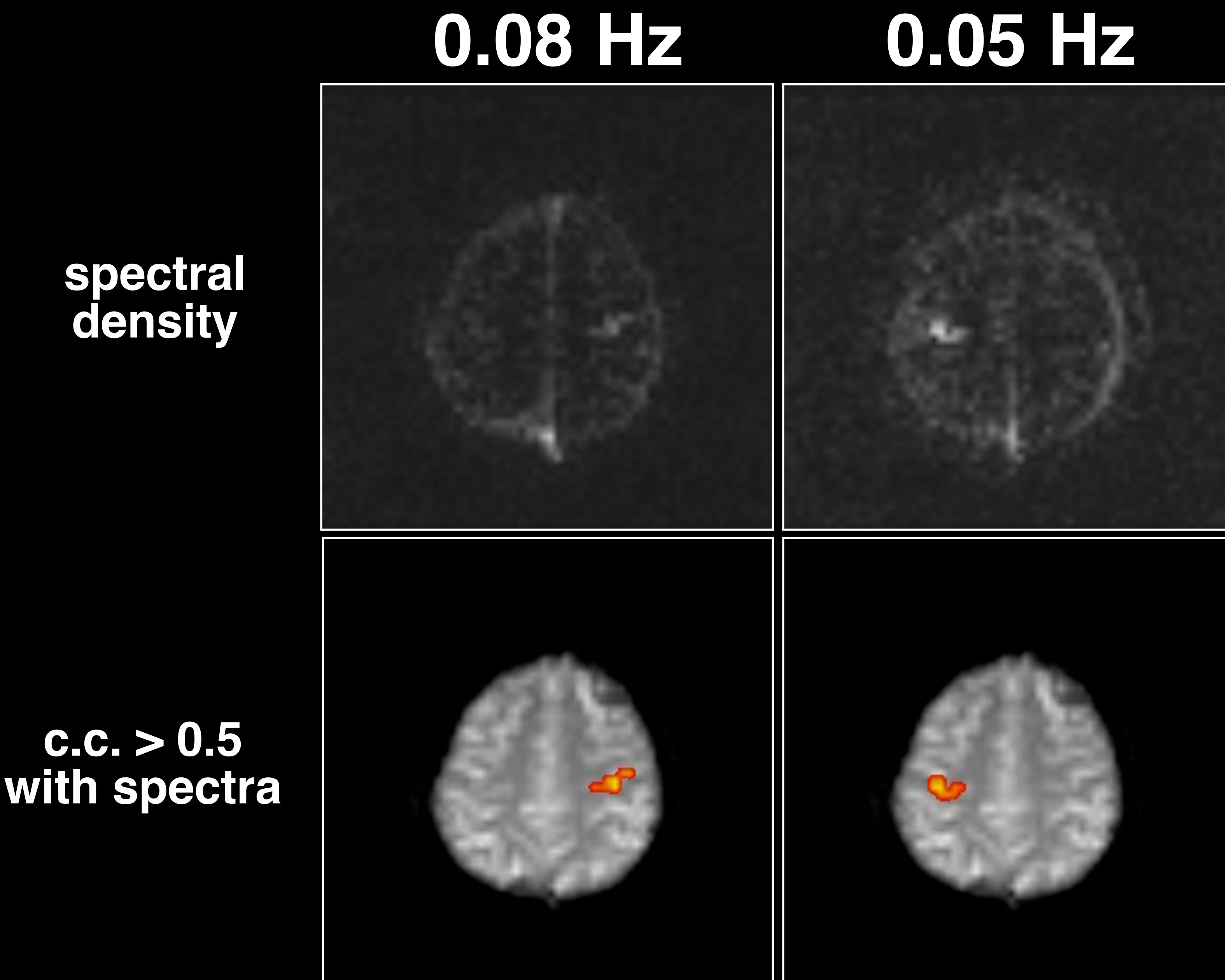

P. A. Bandettini, A. Jesmanowicz, E. C. Wong, J. S. Hyde, Processing strategies for time-course data sets in functional MRI of the human brain. *Magn. Reson. Med.* 30, 161-173 (1993).

Neuronal Activation Input Strategies

1. Block Design
2. Frequency Encoding

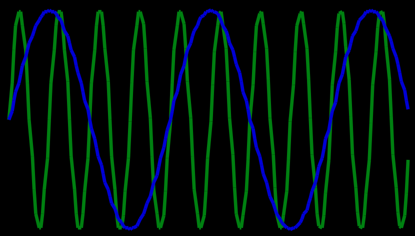

3. Phase Encoding

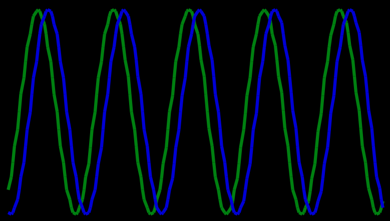

4. Event Related
5. Orthogonal Block Design

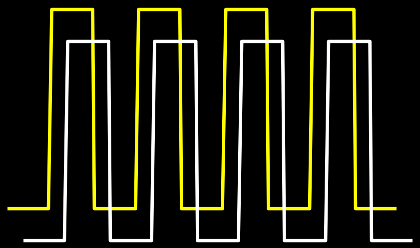

6. Free Behavior Design.

Proc. Natl. Acad. Sci. USA
Vol. 93, pp. 2382–2386, March 1996
Neurobiology

Mapping striate and extrastriate visual areas in human cerebral cortex

EDGAR A. DEYOE*, GEORGE J. CARMAN†, PETER BANDETTINI‡, SETH GLICKMAN*, JON WIESER*, ROBERT COX§, DAVID MILLER¶, AND JAY NEITZ*

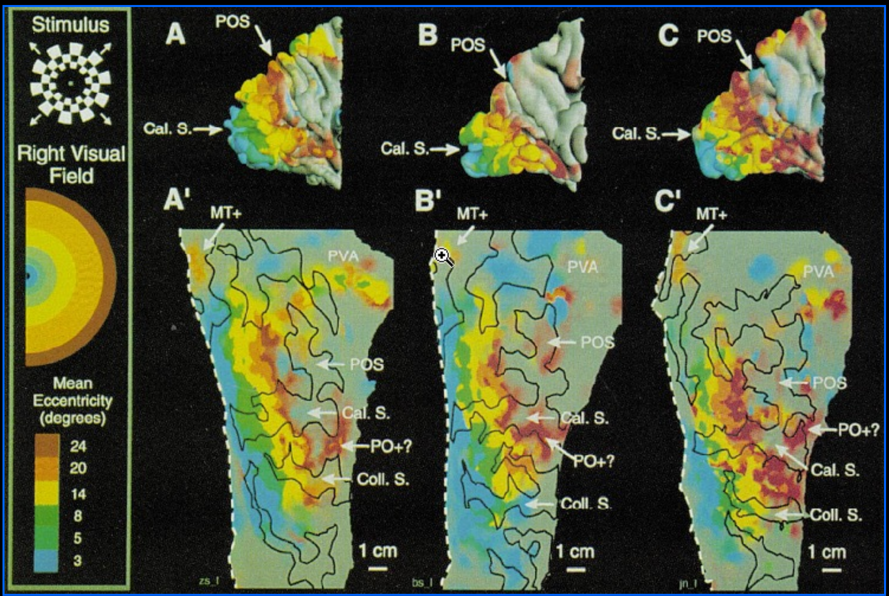

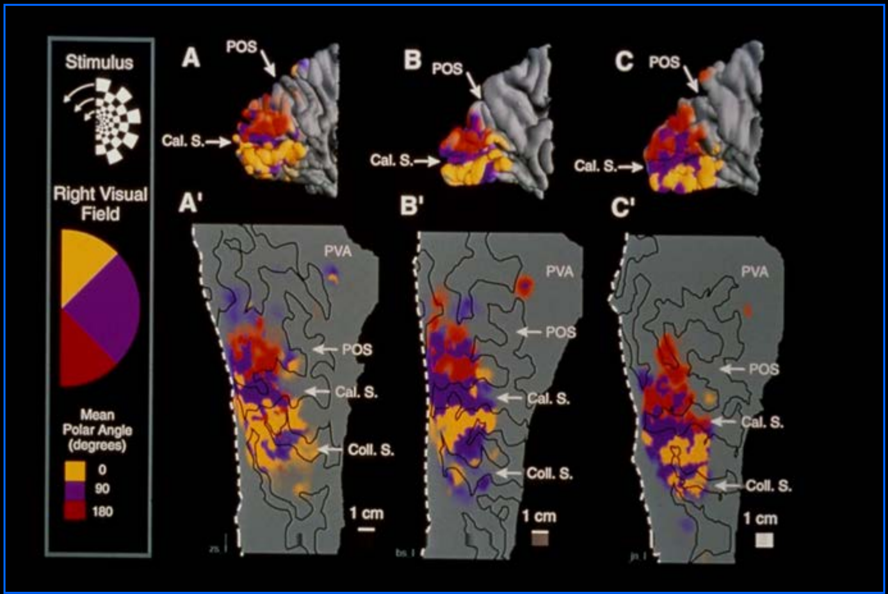

Neuronal Activation Input Strategies

1. Block Design

2. Frequency Encoding

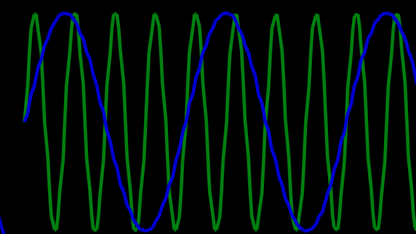

3. Phase Encoding

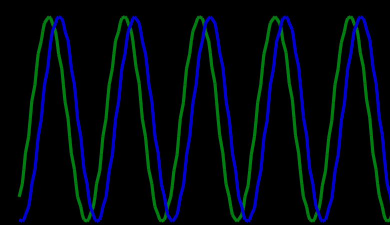

4. Event Related

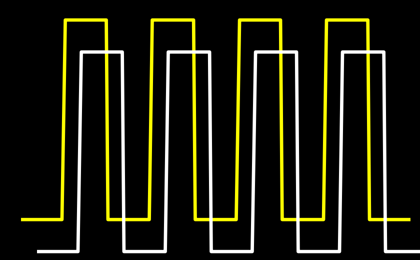

5. Orthogonal Block Design

6. Free Behavior Design.

First Event-related fMRI Results

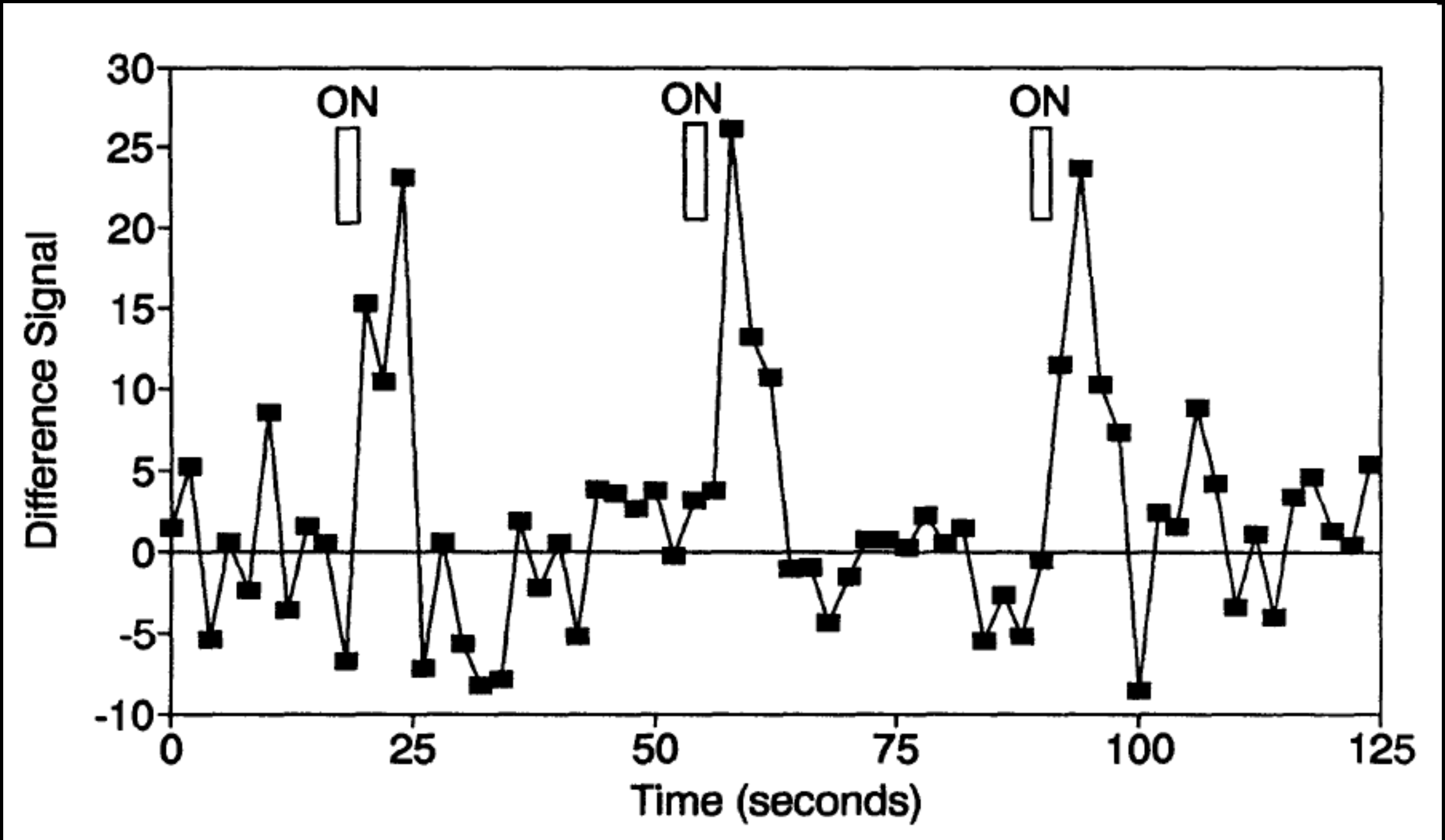

Blamire, A. M., et al. (1992). "Dynamic mapping of the human visual cortex by high-speed magnetic resonance imaging." Proc. Natl. Acad. Sci. USA 89: 11069-11073.

Event Related Advantages

- Task Randomization
- Post acquisition, Performance-based, data binning
- Natural presentation
- Reduction of habituation effects
- Overt responses
- Reduction of scanner noise effects
- More precise estimation of hemodynamic respons

Proc. Natl. Acad. Sci. USA
Vol. 93, pp. 14878–14883, December 1996
Neurobiology

Detection of cortical activation during averaged single trials of a cognitive task using functional magnetic resonance imaging

(neuroimaging/single trial/language/prefrontal)

Randy L. Buckner[†‡§¶], Peter A. Bandettini[†‡], Kathleen M. O'Craven[†‖], Robert L. Savoy[†‖],
Steven E. Petersen[**††], Marcus E. Raichle[§**††], and Bruce R. Rosen[†‡]

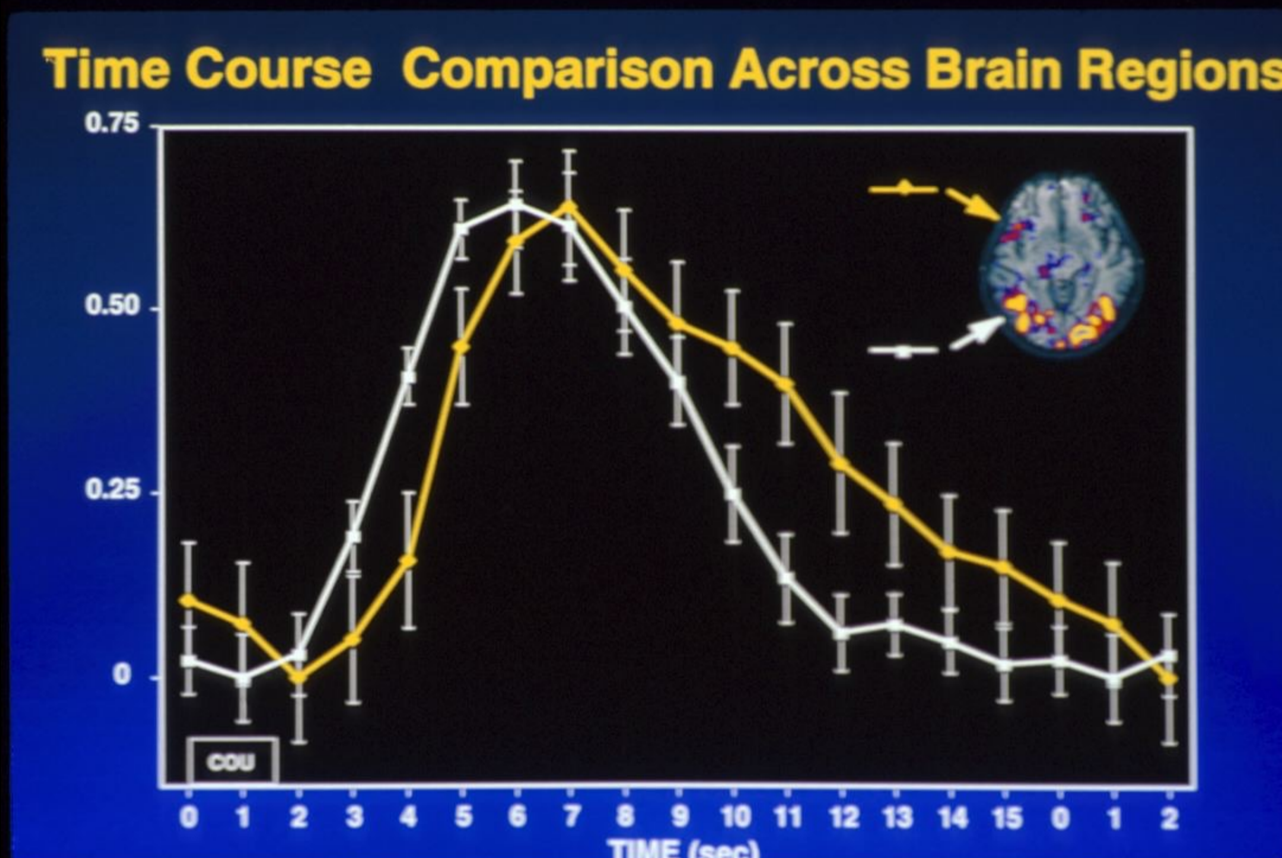

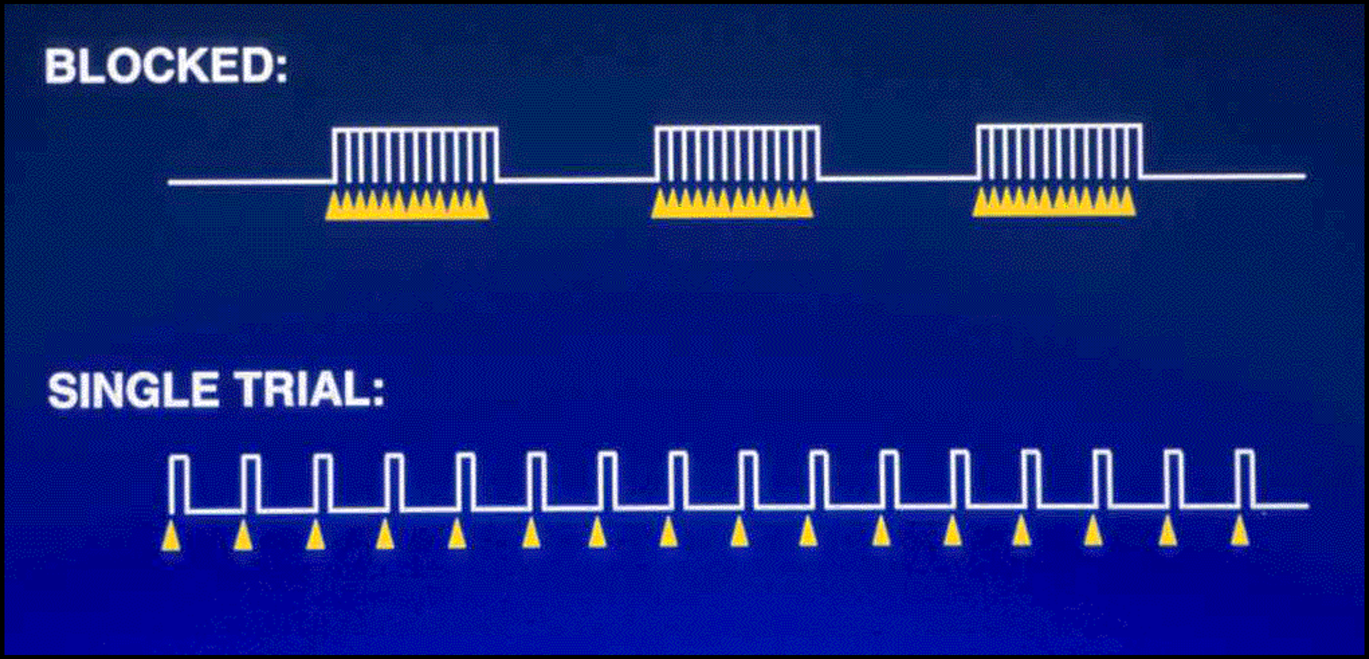
BLOCKED:
SINGLE TRIAL:

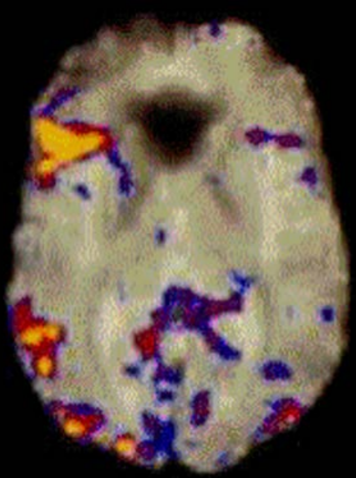

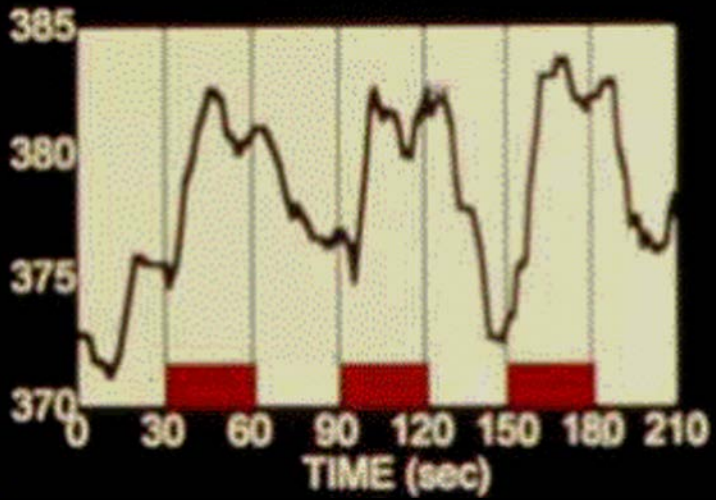
385
380
375
370
0
30
60
90
120
150
180
210
TIME (sec)

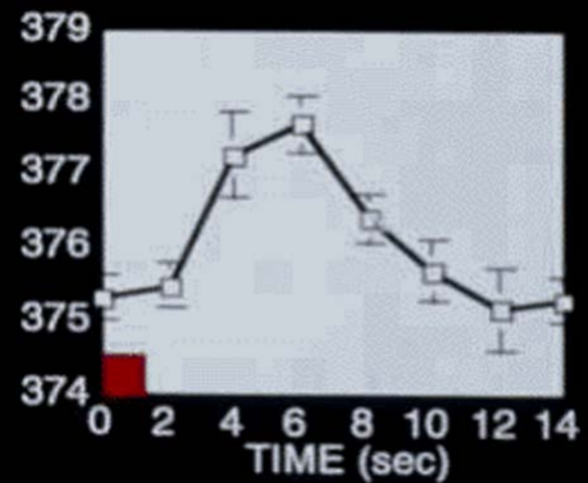
379
378
377
376
375
374
0
2
4
6
8
10
12
14
TIME (sec)

fMRI during tasks that involve brief motion

Blocked Design

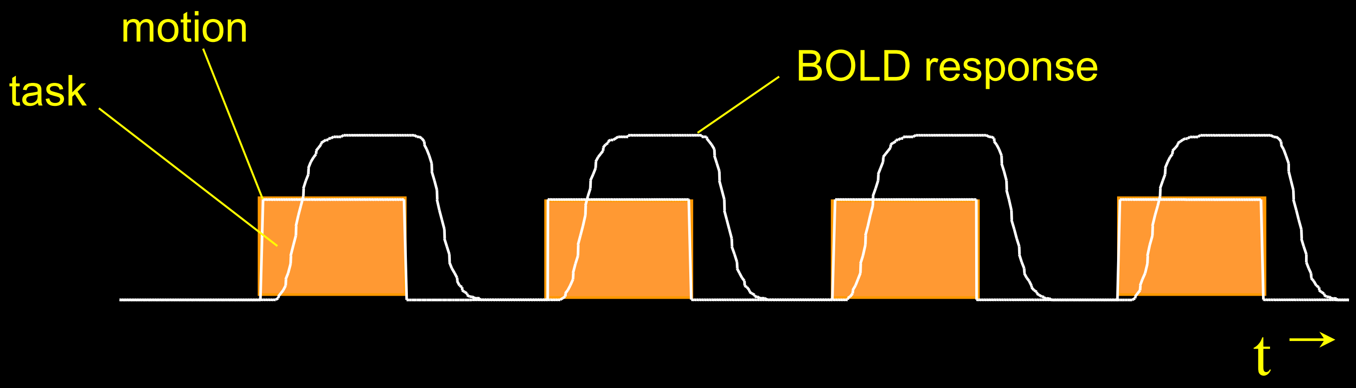

Event-Related Design

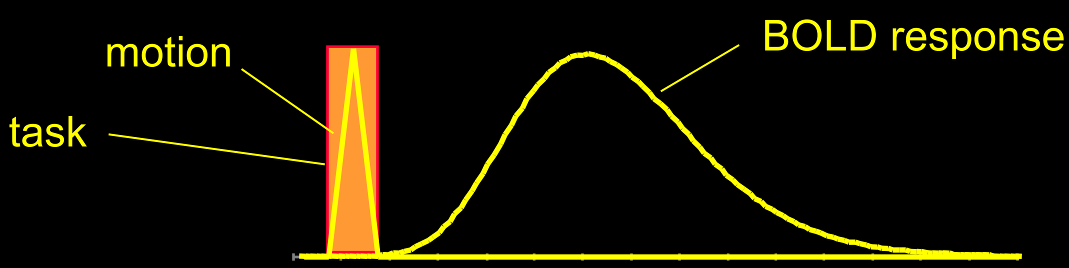

R. M. Birn, P. A. Bandettini, R. W. Cox, R. Shaker, Event - related fMRI of tasks involving brief motion. *Human Brain Mapping* 7: 106-114 (1999).

Overt Word Production

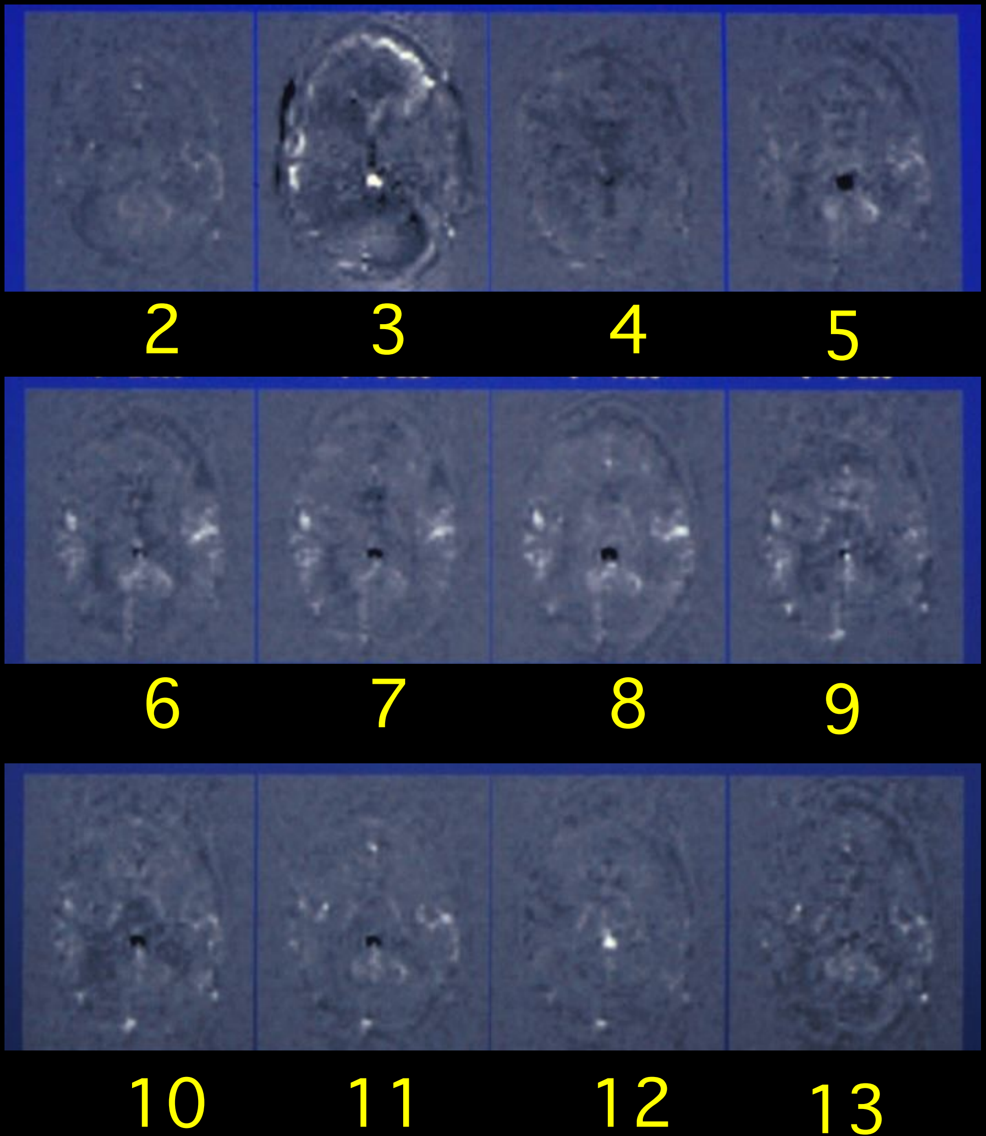

R. M. Birn, P. A. Bandettini, R. W. Cox, R. Shaker, Event - related fMRI of tasks involving brief motion. *Human Brain Mapping* 7: 106-114 (1999).

Speaking - Blocked Trial

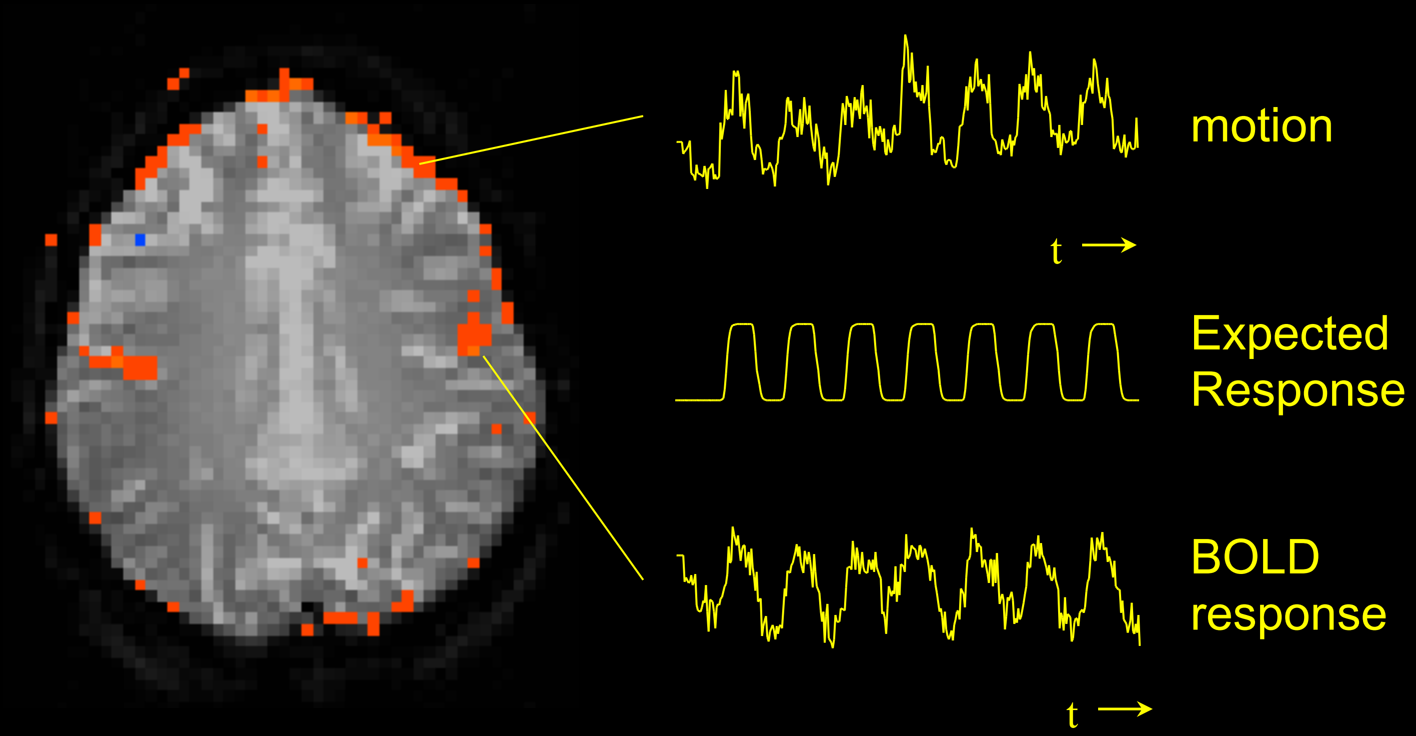

R. M. Birn, P. A. Bandettini, R. W. Cox, R. Shaker, Event - related fMRI of tasks involving brief motion. *Human Brain Mapping* 7: 106-114 (1999).

Speaking - ER-fMRI

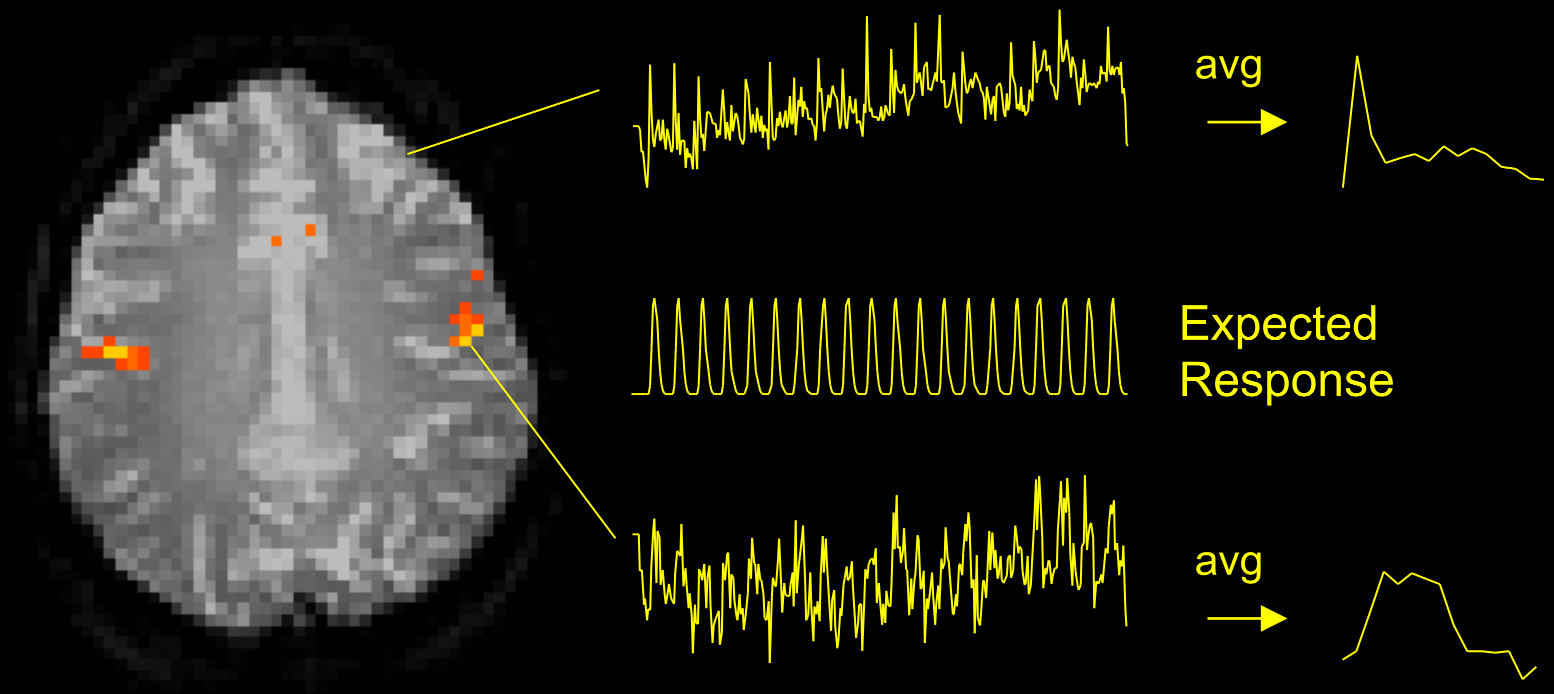

R. M. Birn, P. A. Bandettini, R. W. Cox, R. Shaker, Event - related fMRI of tasks involving brief motion. *Human Brain Mapping* 7: 106-114 (1999).

Motion-Decoupled fMRI:
Functional MRI during of overt word production

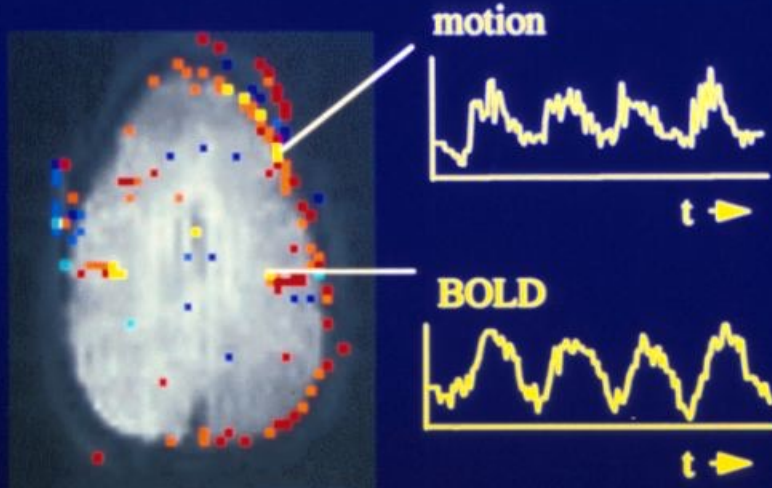

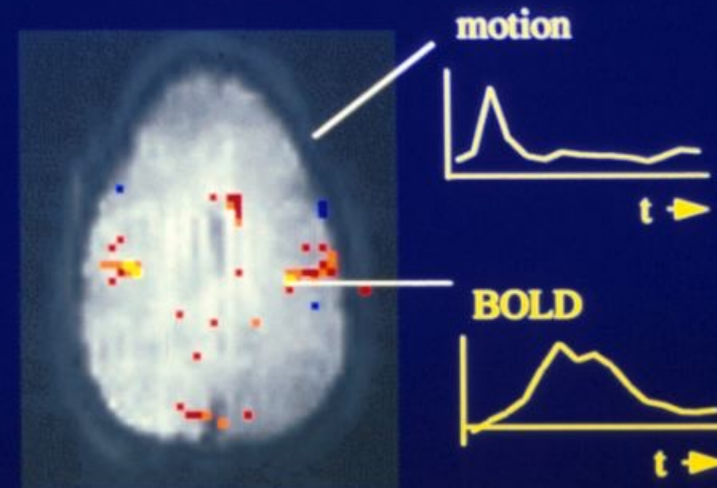

"block-trial" paradigm

Motion induced signal changes resemble functional (BOLD) signal changes

"single-trial" paradigm

Motion induced and BOLD signal changes are separated in time

R.M. Birn, et al.

Tongue Movement

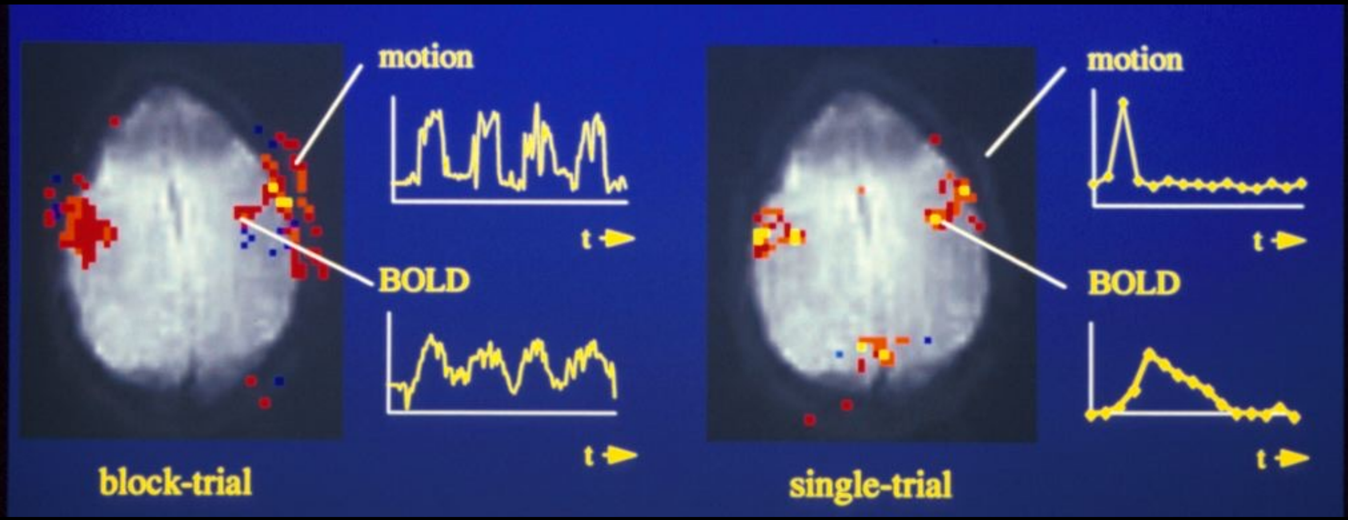

Jaw Clenching

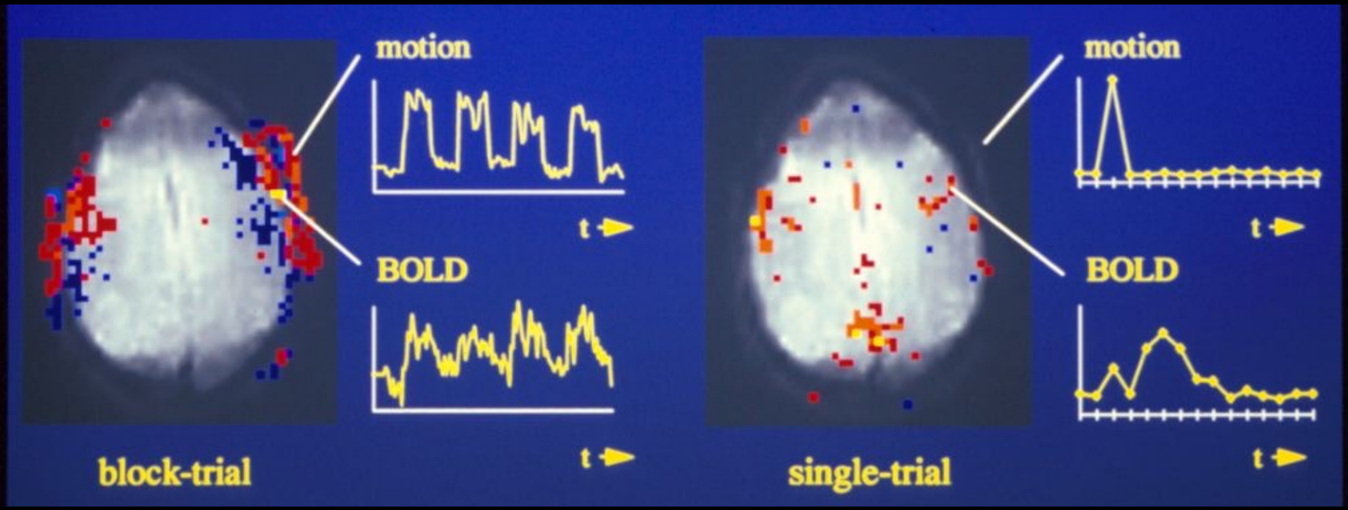

Swallowing - Event-Related

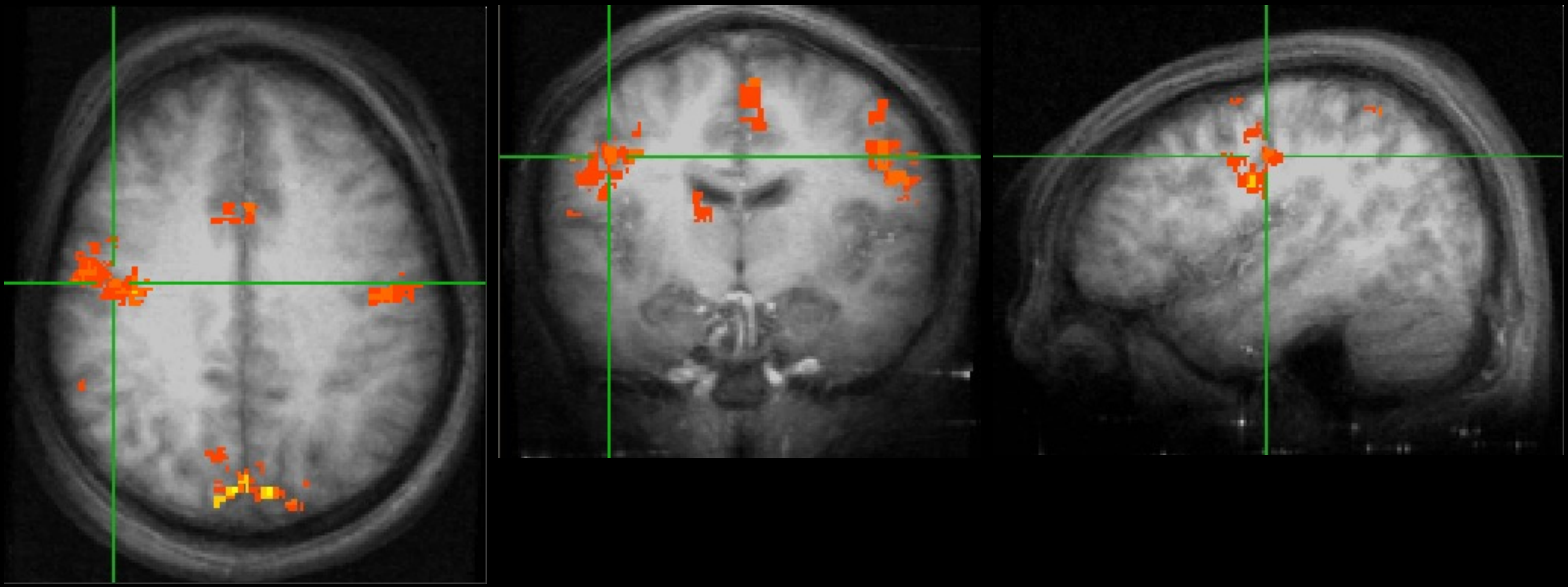

Detectability – constant ISI

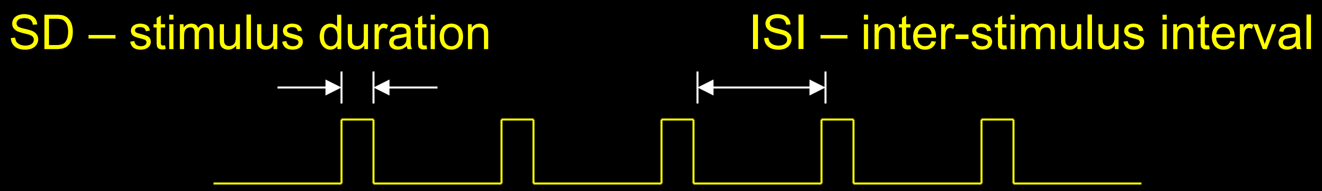

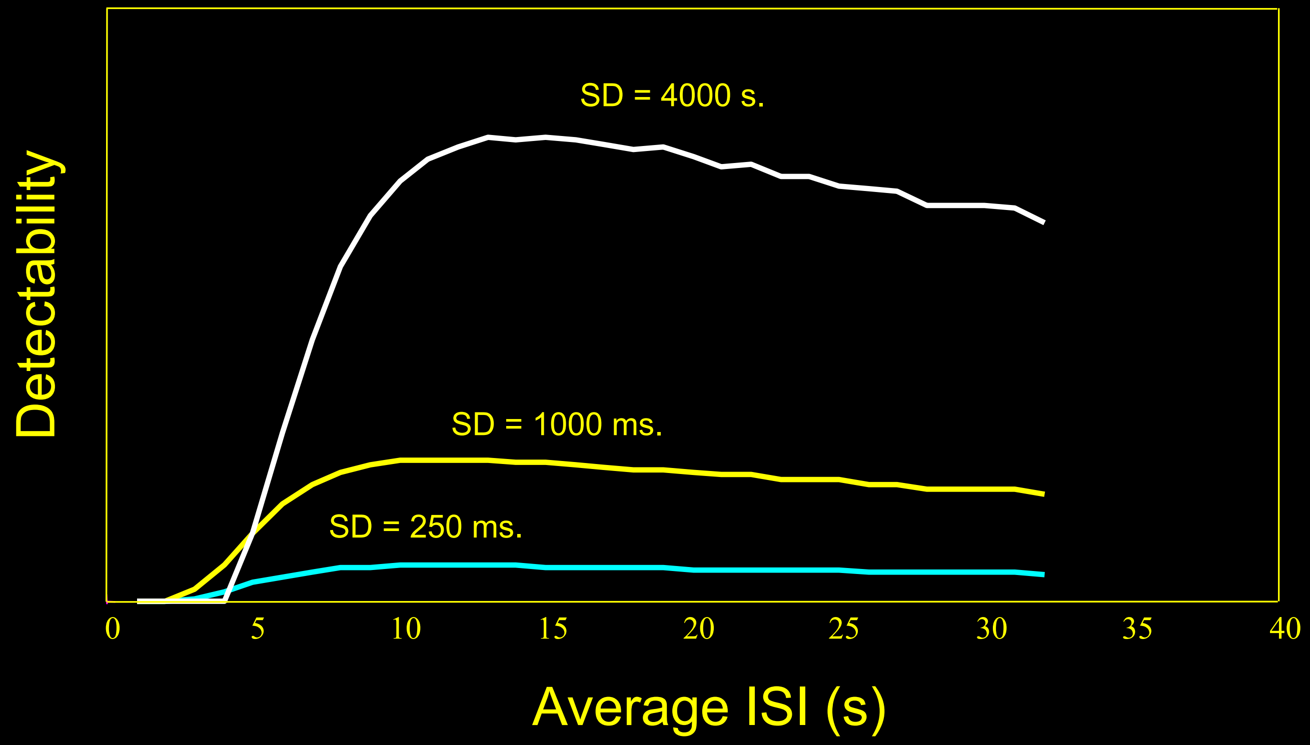

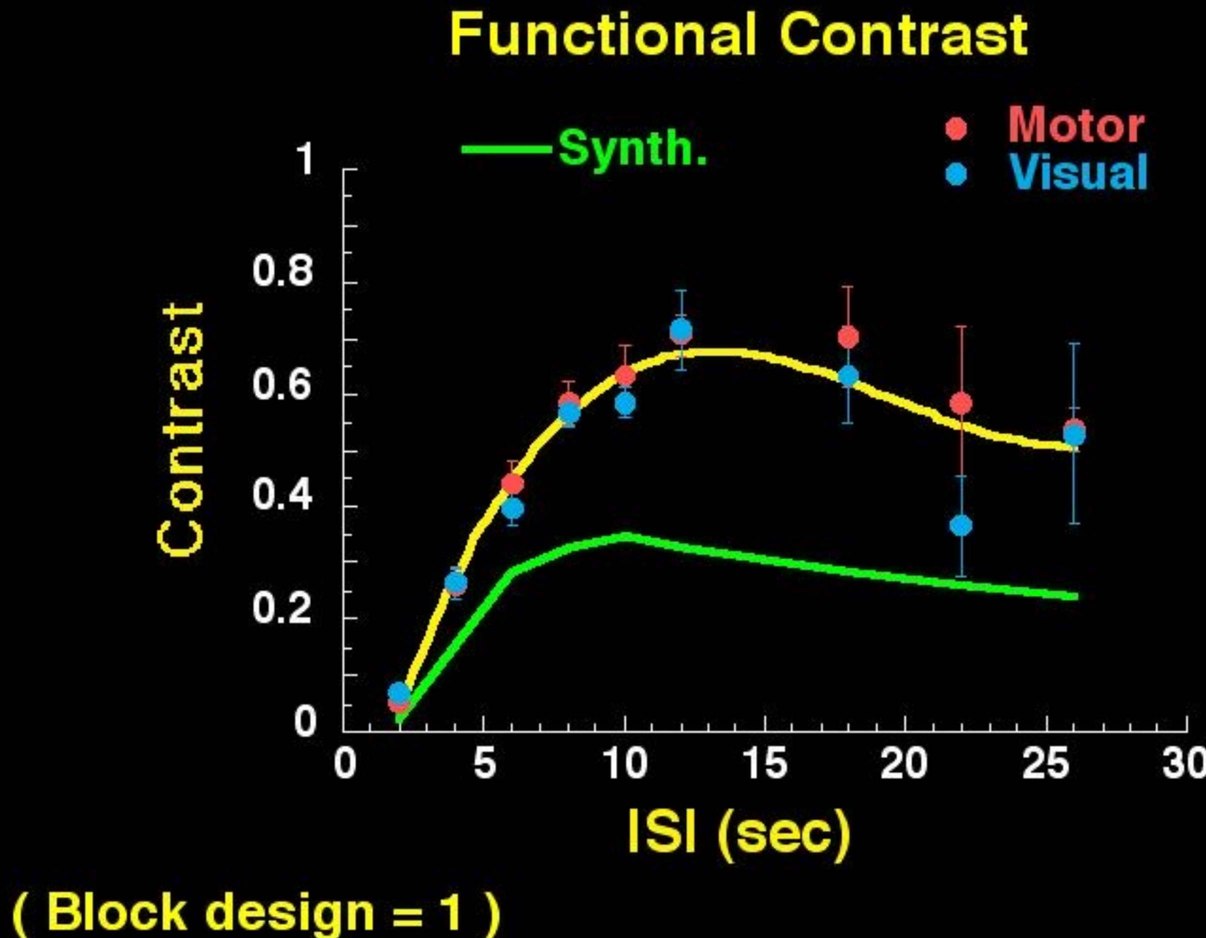

P. A. Bandettini, R. W. Cox. Functional contrast in constant interstimulus interval event - related fMRI: theory and experiment. *Magn. Reson. Med.* 43: 540-548 (2000).

Contrast to Noise Images

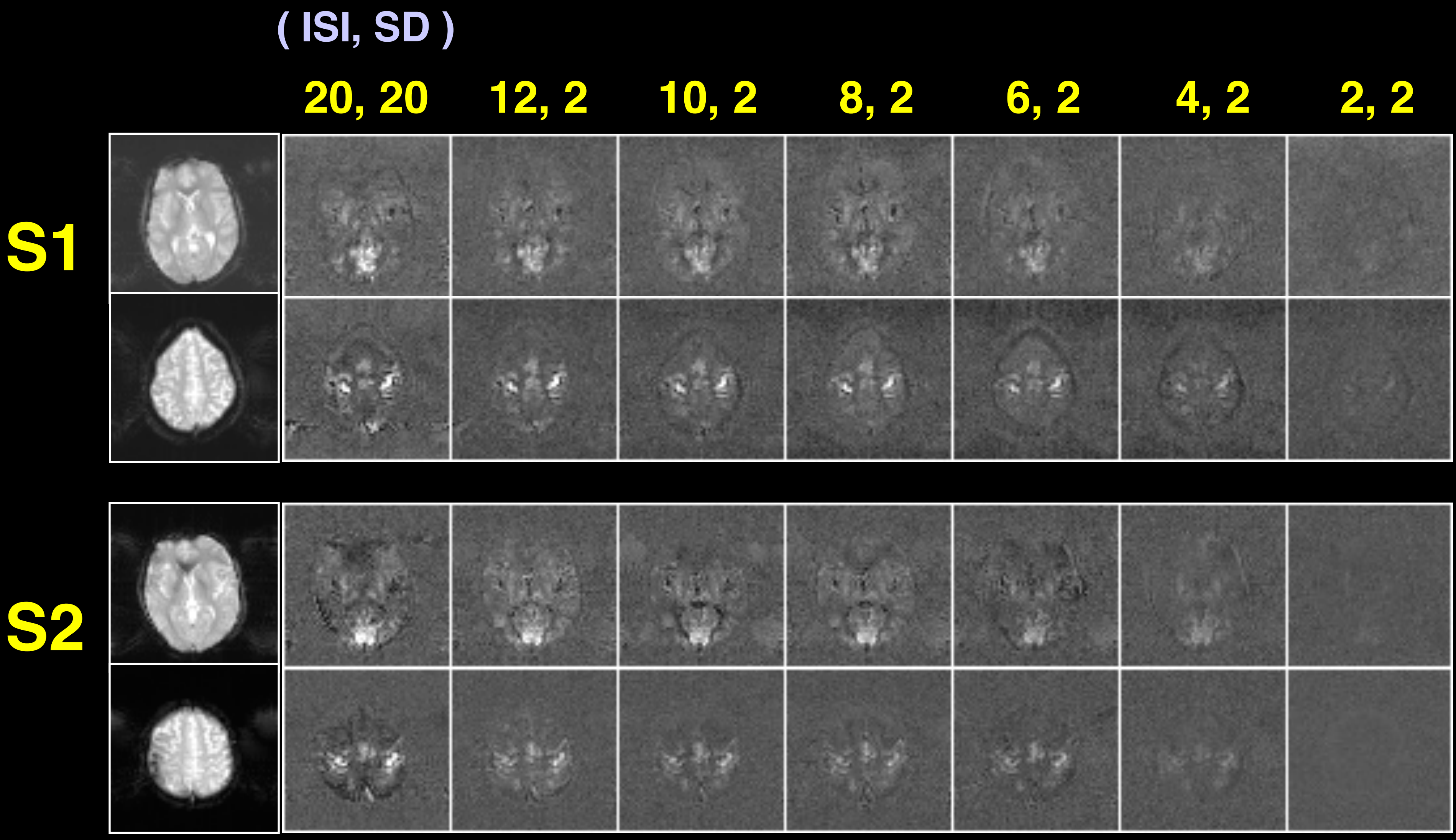

P. A. Bandettini, R. W. Cox. Functional contrast in constant interstimulus interval event - related fMRI: theory and experiment. *Magn. Reson. Med.* 43: 540-548 (2000).

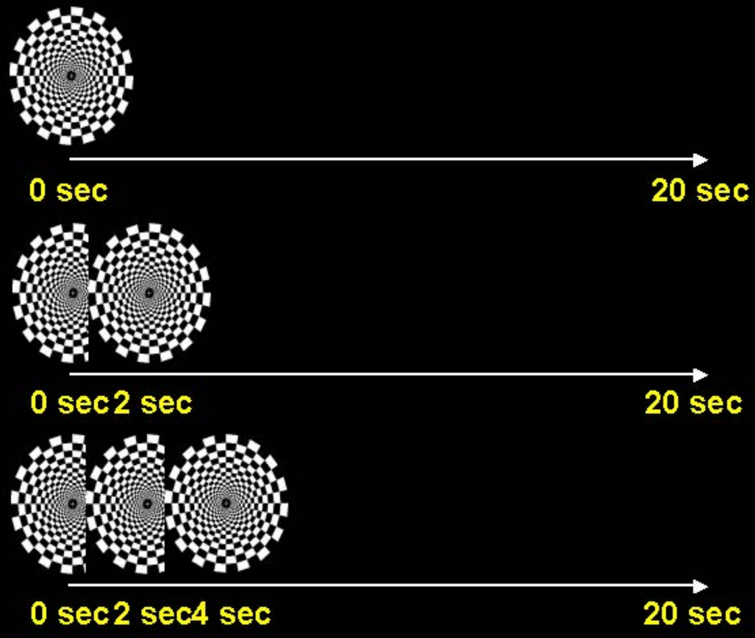

Human Brain Mapping 5:329–340(1997)

Selective Averaging of Rapidly Presented Individual Trials Using fMRI

Anders M. Dale* and Randy L. Buckner

RAW DATA

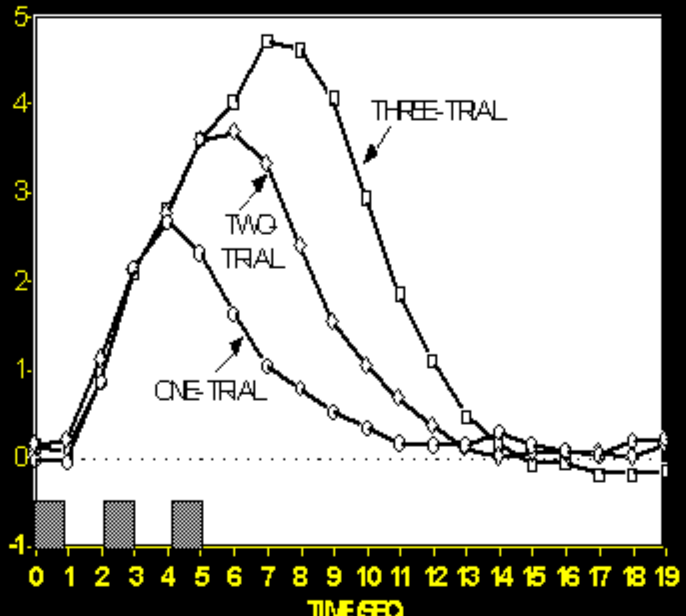

ESTIMATED RESPONSES

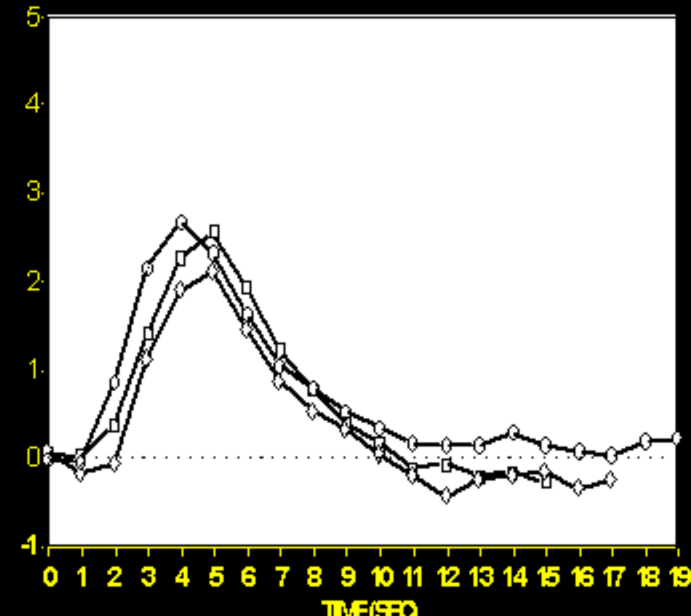

Detectability vs. Average ISI

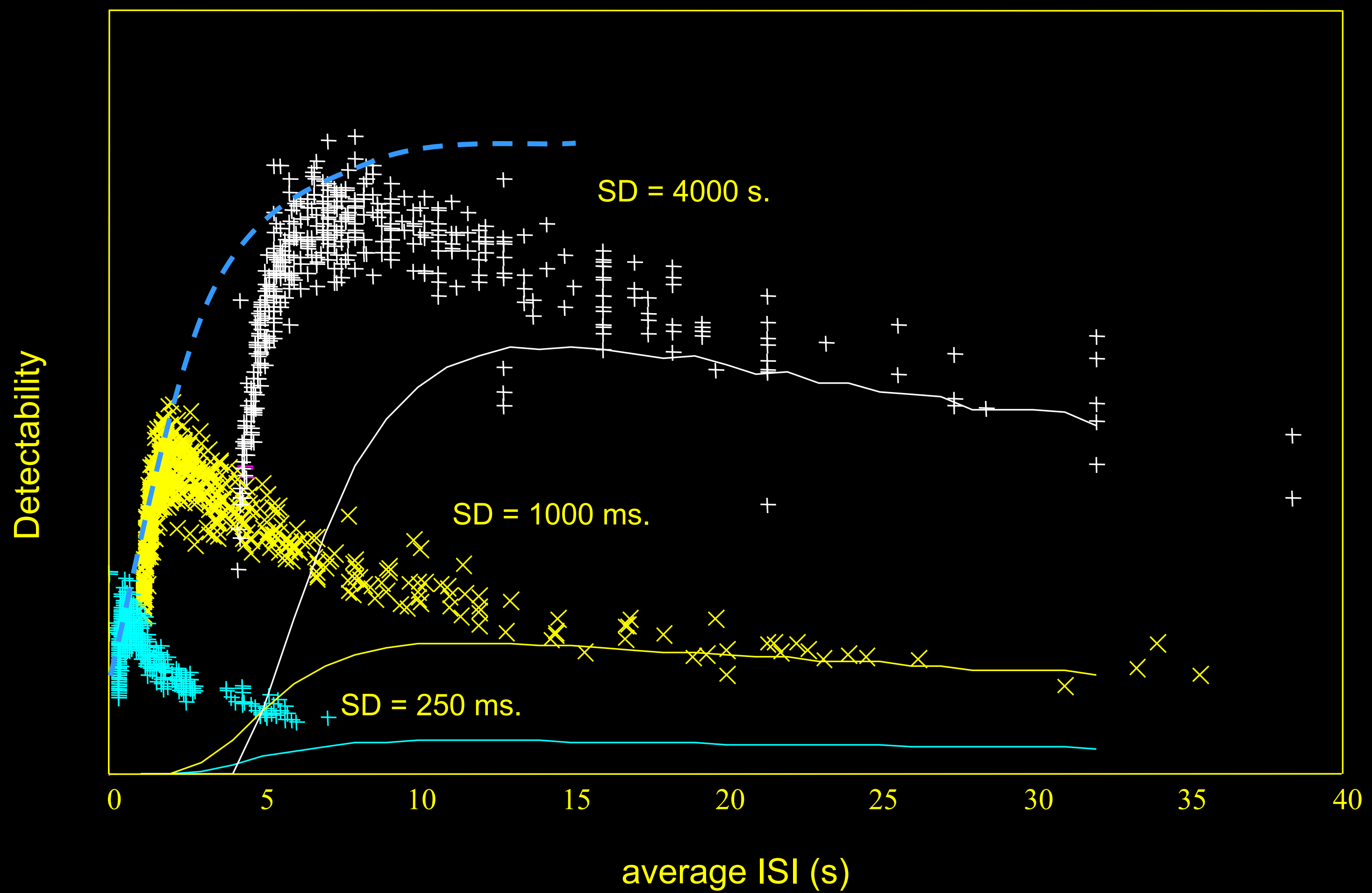

R. M. Birn, R. W. Cox, P. A. Bandettini, Detection versus estimation in Event-Related fMRI: choosing the optimal stimulus timing. *NeuroImage* 15: 262-264, (2002).

Estimation accuracy vs. average ISI

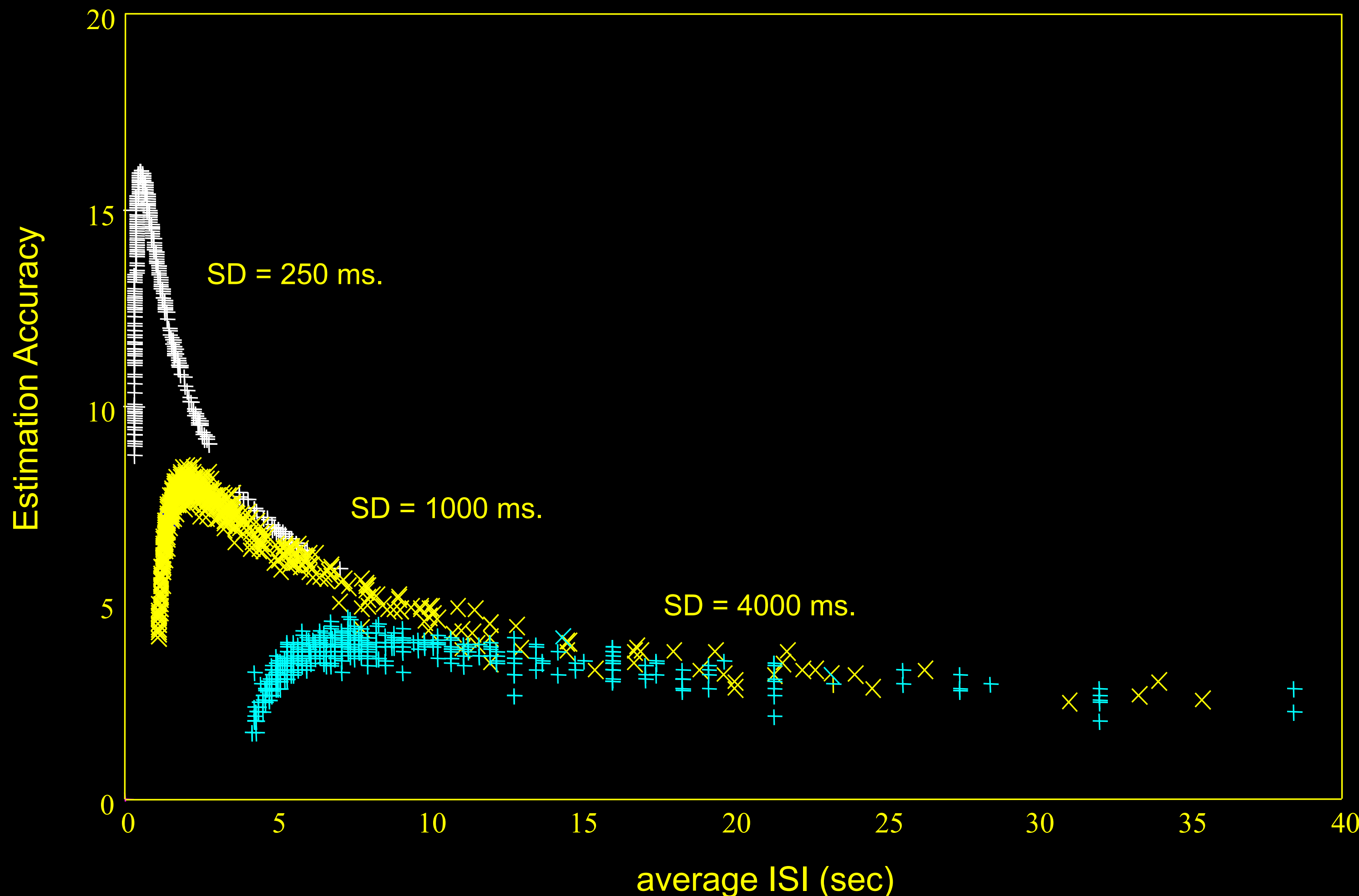

R. M. Birn, R. W. Cox, P. A. Bandettini, Detection versus estimation in Event-Related fMRI: choosing the optimal stimulus timing. *NeuroImage* 15: 262-264, (2002).

Varying "ON" and "OFF" periods

- *Rapid event-related design with varying ISI*

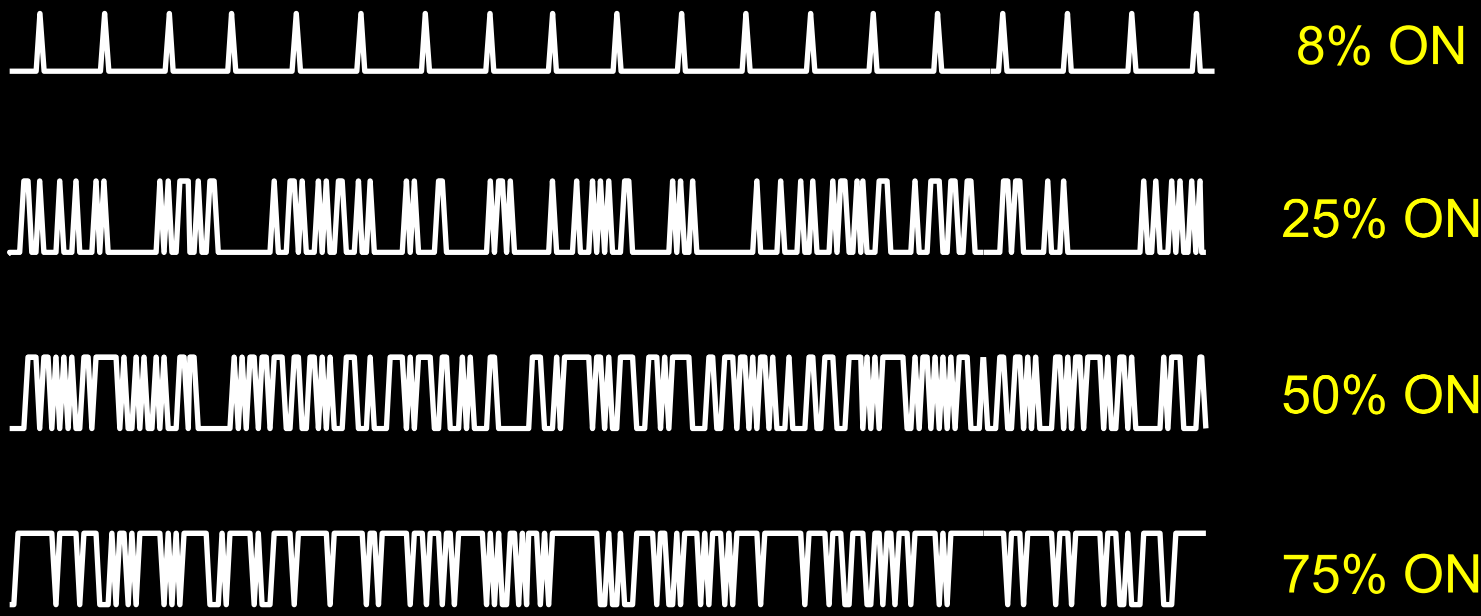

Varying "ON" and "OFF" periods

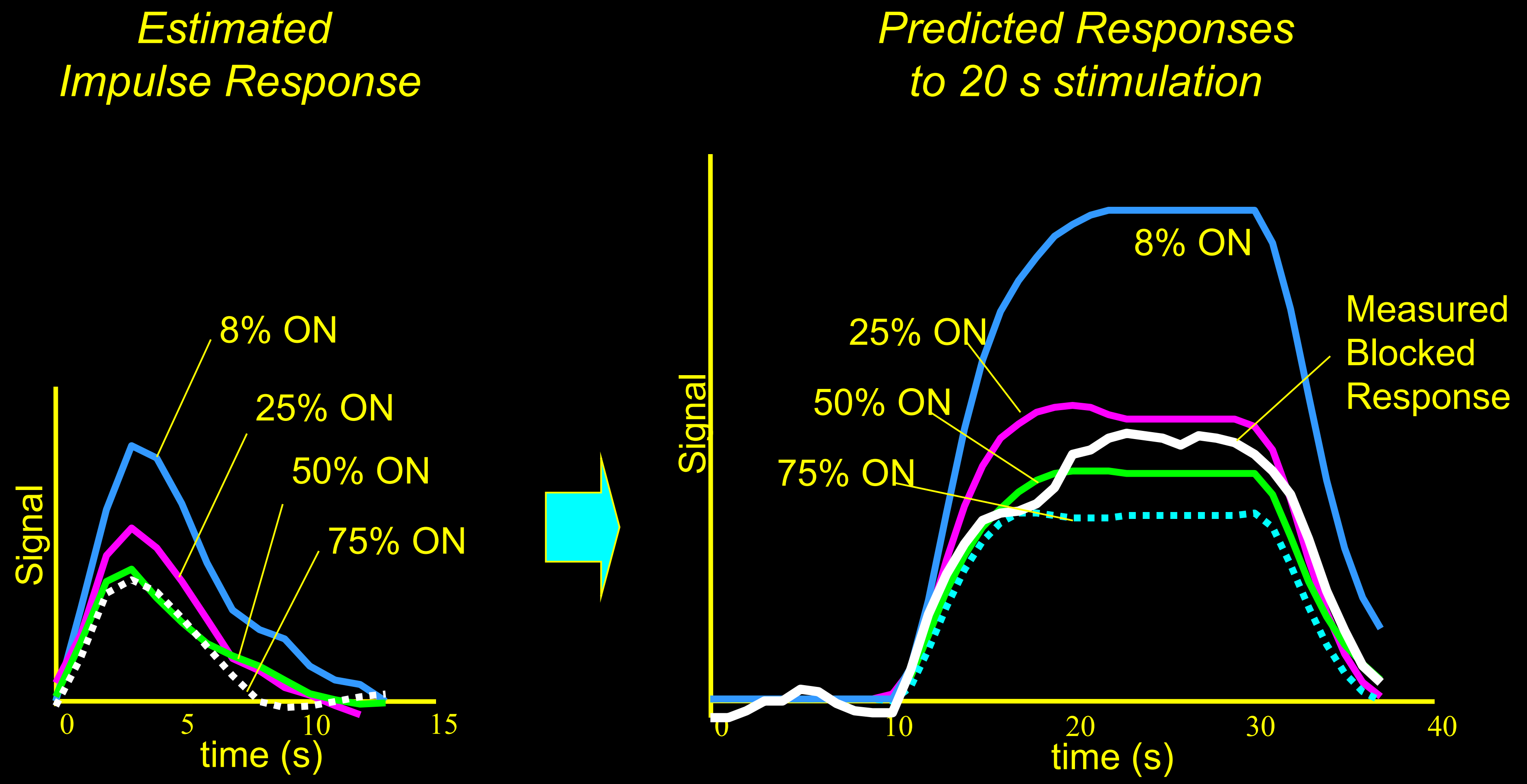

ODC Maps using fMRI

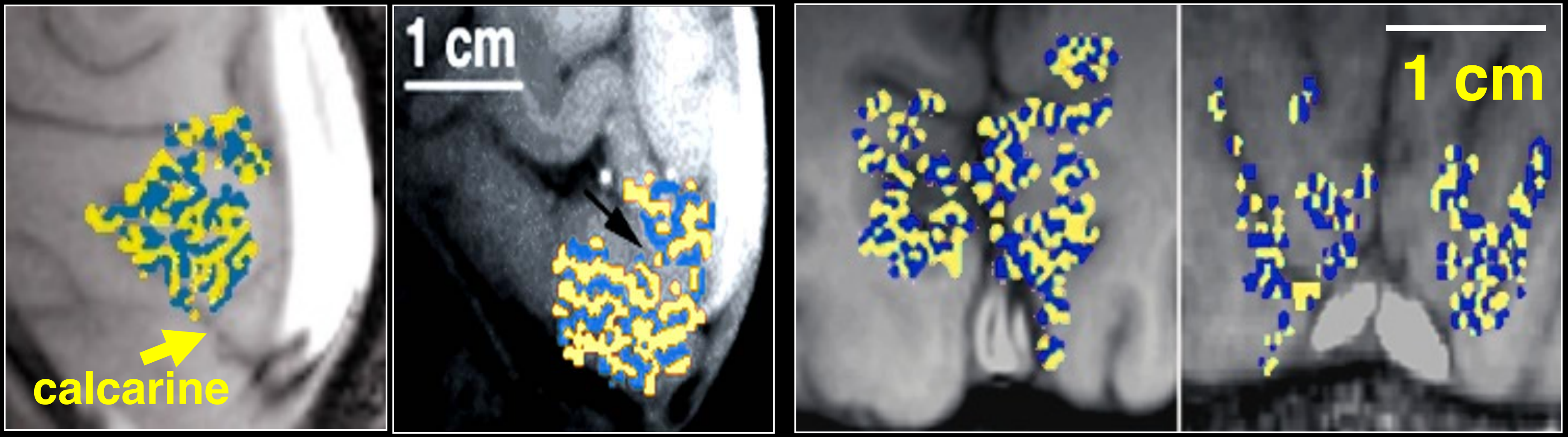

• Identical in size, orientation, and appearance to those obtained by optical imaging[1] and histology[3,4].

[1]Malonek D, Grinvald A. *Science* 272, 551-4 (1996).
[3]Horton JC, Hocking DR. *J Neurosci* 16, 7228-39 (1996).
[4]Horton JC, et al. *Arch Ophthalmol* 108, 1025-31 (1990).

Why short is better than long

The vascular response to
prolonged neural stimulation

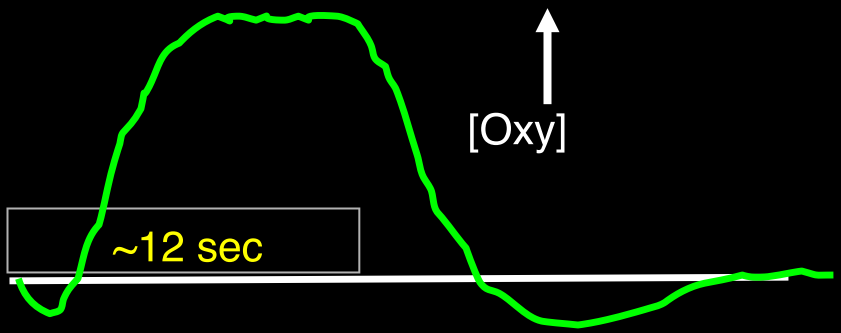

The vascular response to
brief neural stimulation

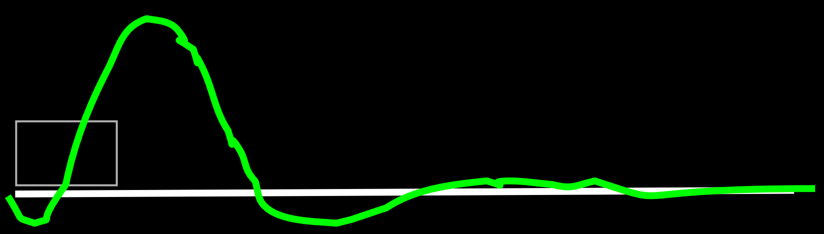

It is argued that fMRI cannot achieve submillimeter functional resolution because a saturated hyperoxic vascular response to neural activity spreads over many millimeters[1,2].

However, optical imaging has demonstrated that the hyperoxic response can yield well-localized maps when using short duration stimuli (<5 sec)[1].

[1]Malonek D, Grinvald A. Science 272, 551-4 (1996).
[2]Kim D-S, Duong T, Kim S-G. Nat Neurosci 3, 164-9 (2000).

Neuronal Activation Input Strategies

1. Block Design
2. Frequency Encoding

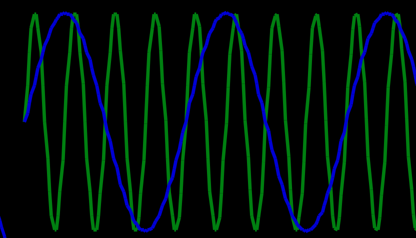

3. Phase Encoding

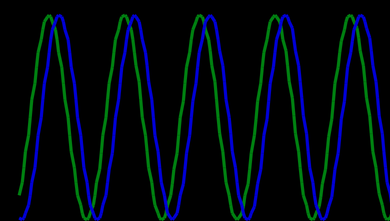

4. Event Related
5. Orthogonal Block Design

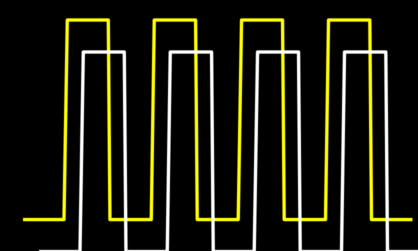

6. Free Behavior Design.

Example of a Set of Orthogonal Contrasts for Multiple Regression

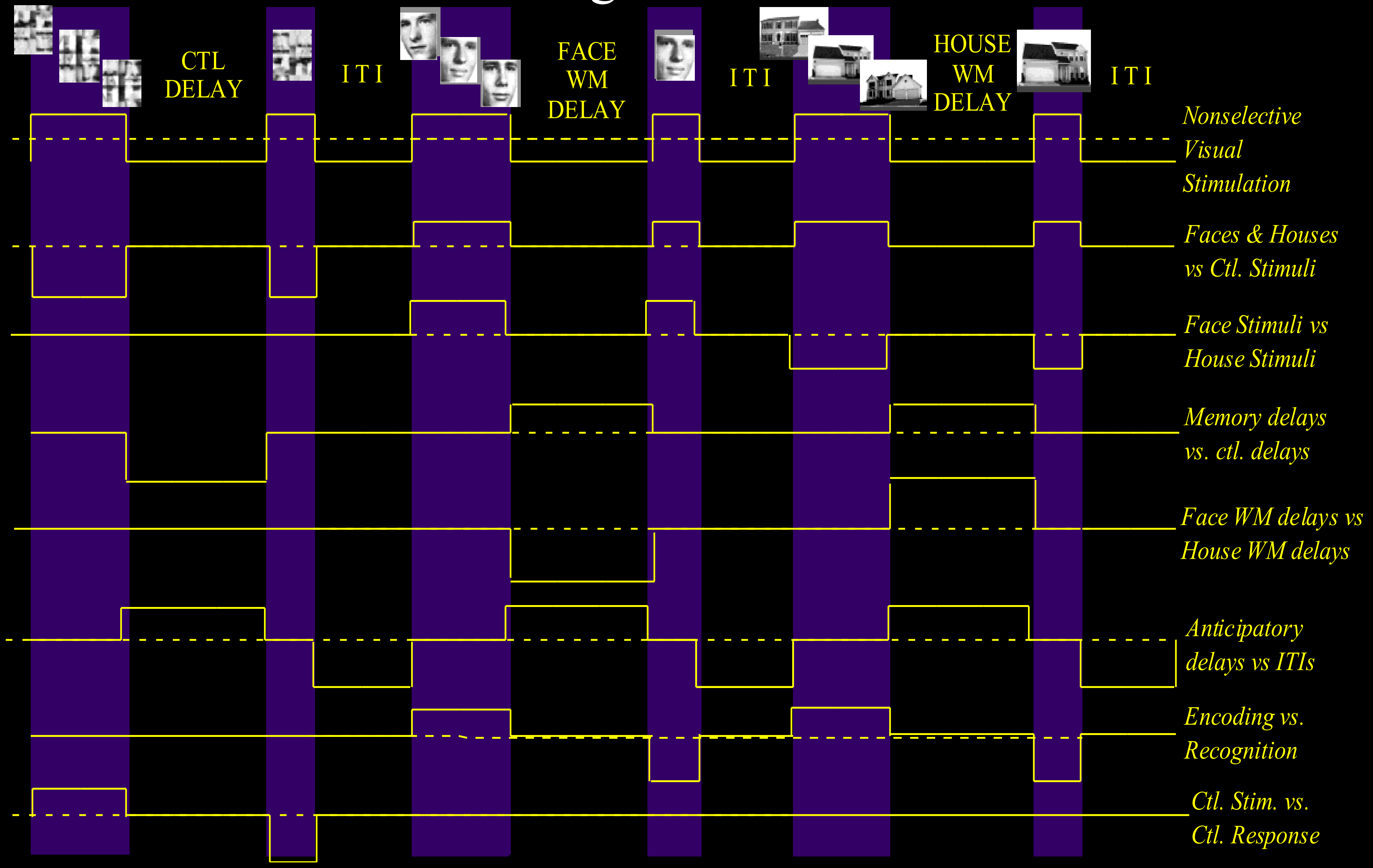

Neuronal Activation Input Strategies

1. Block Design

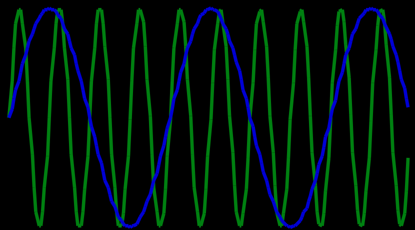

2. Frequency Encoding

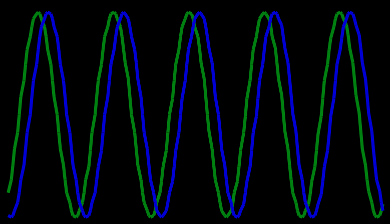

3. Phase Encoding

4. Single Event

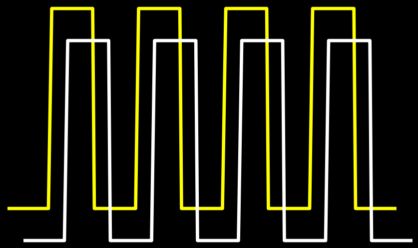

5. Orthogonal Block Design

6. Free Behavior Design.

Free Behavior Design

Use a continuous measure as a reference function:

- Task performance
- Skin Conductance
- Heart, respiration rate..
- Eye position
- EEG

Resting Hemodynamic Autocorrelations

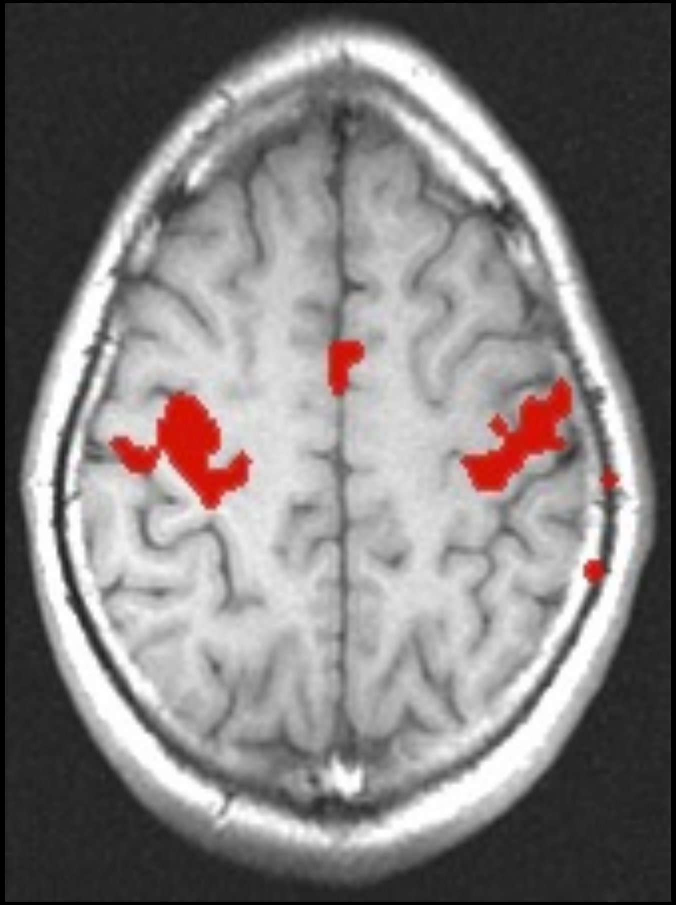

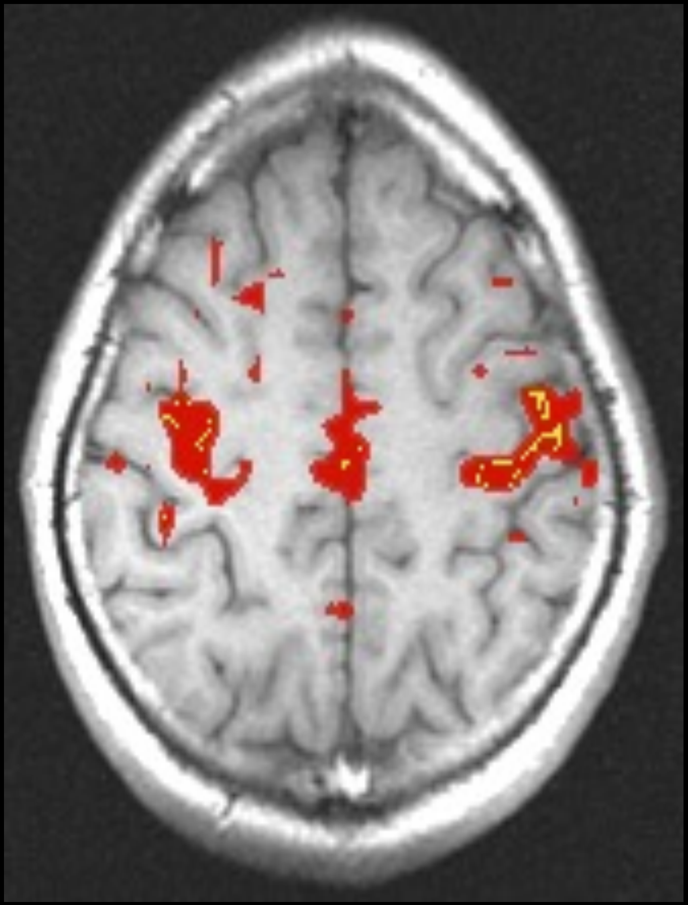

B. Biswal *et al*., MRM, 34:537 (1995)

The Skin Conductance Response (SCR)

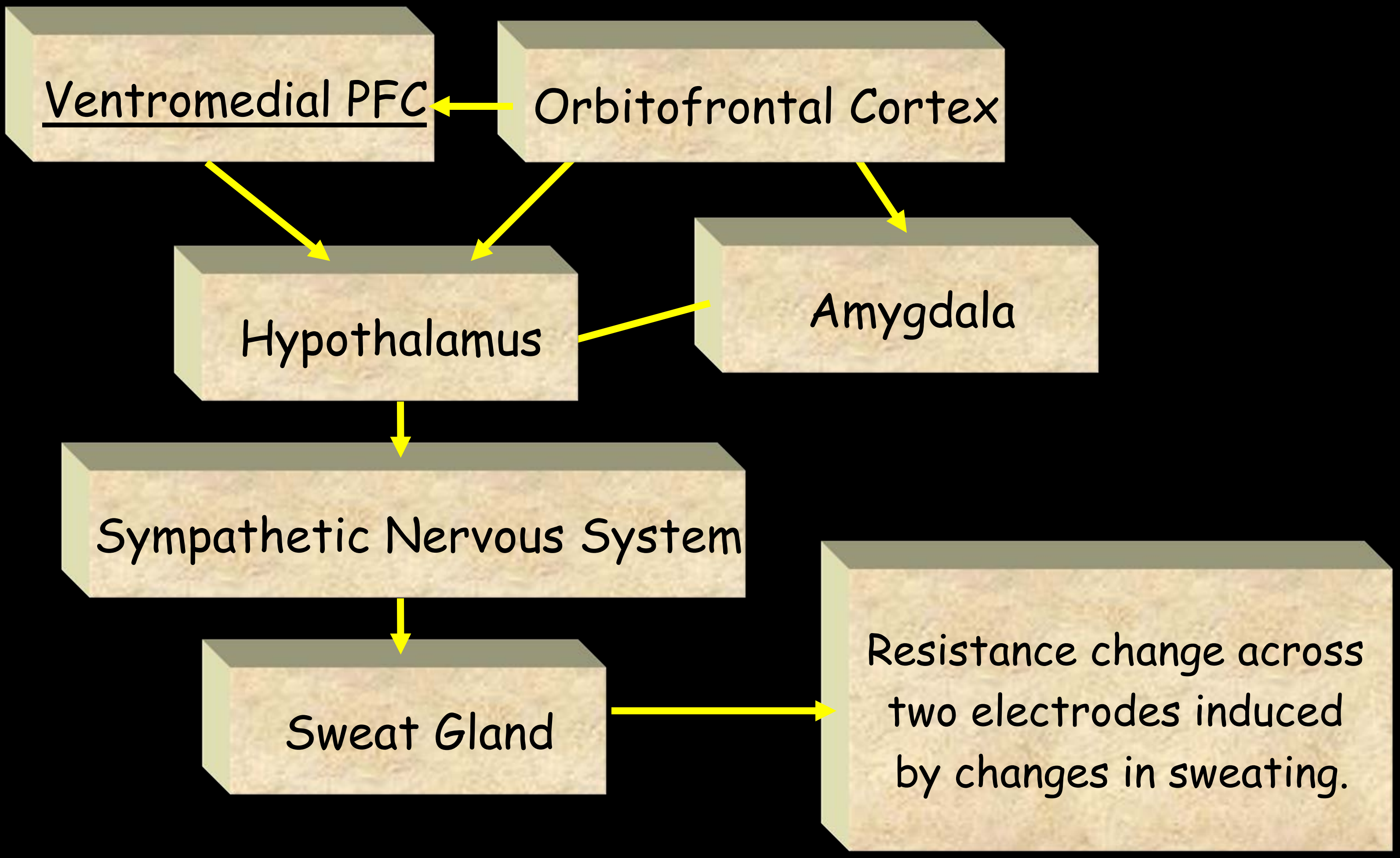

Skin Conductance Dynamics

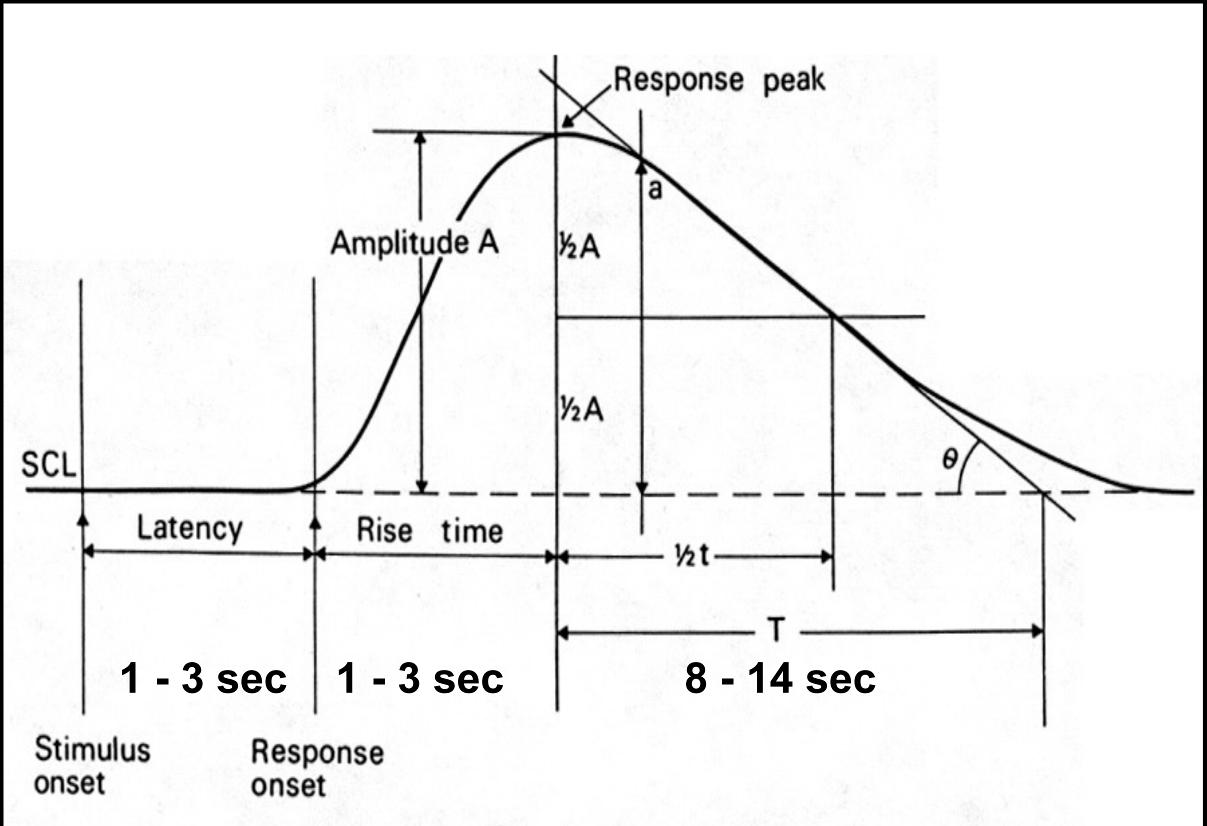

FIGURE 1. Diagrammatic skin conductance response.

- Boucsein, Wolfram (1992). Electrodermal Activity. Plenum Press, NY
- Venables, Peter, (1991). Autonomic Activity ANYAS 620:191-207.

Brain activity correlated with SCR during "Rest"

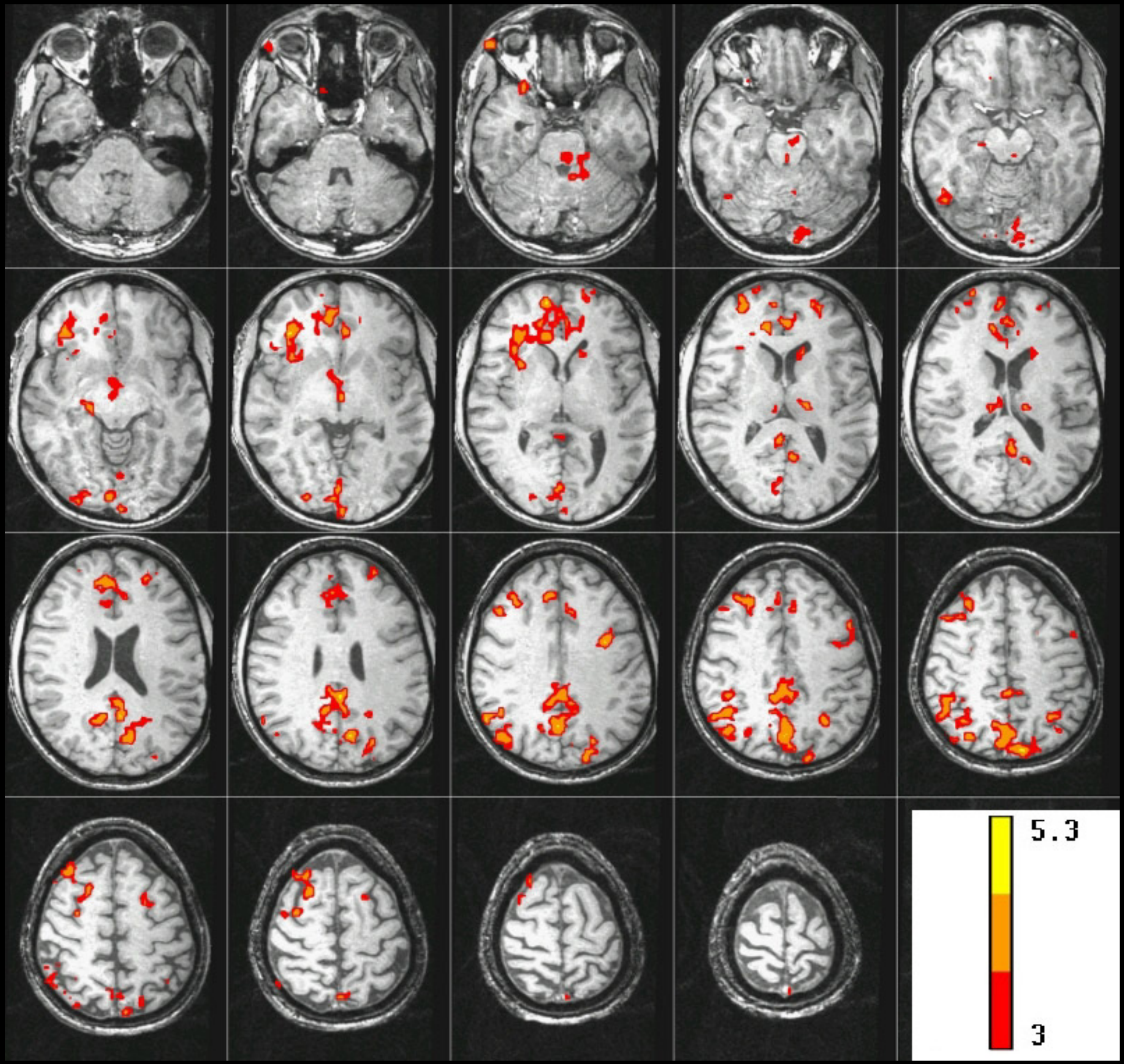

J. C. Patterson II, L. G. Ungerleider, and P. A Bandettini, Task - independent functional brain activity correlation with skin conductance changes: an fMRI study. *NeuroImage 17: 1787-1806, (2002).*

Brain activity correlated with SCR during "Rest"

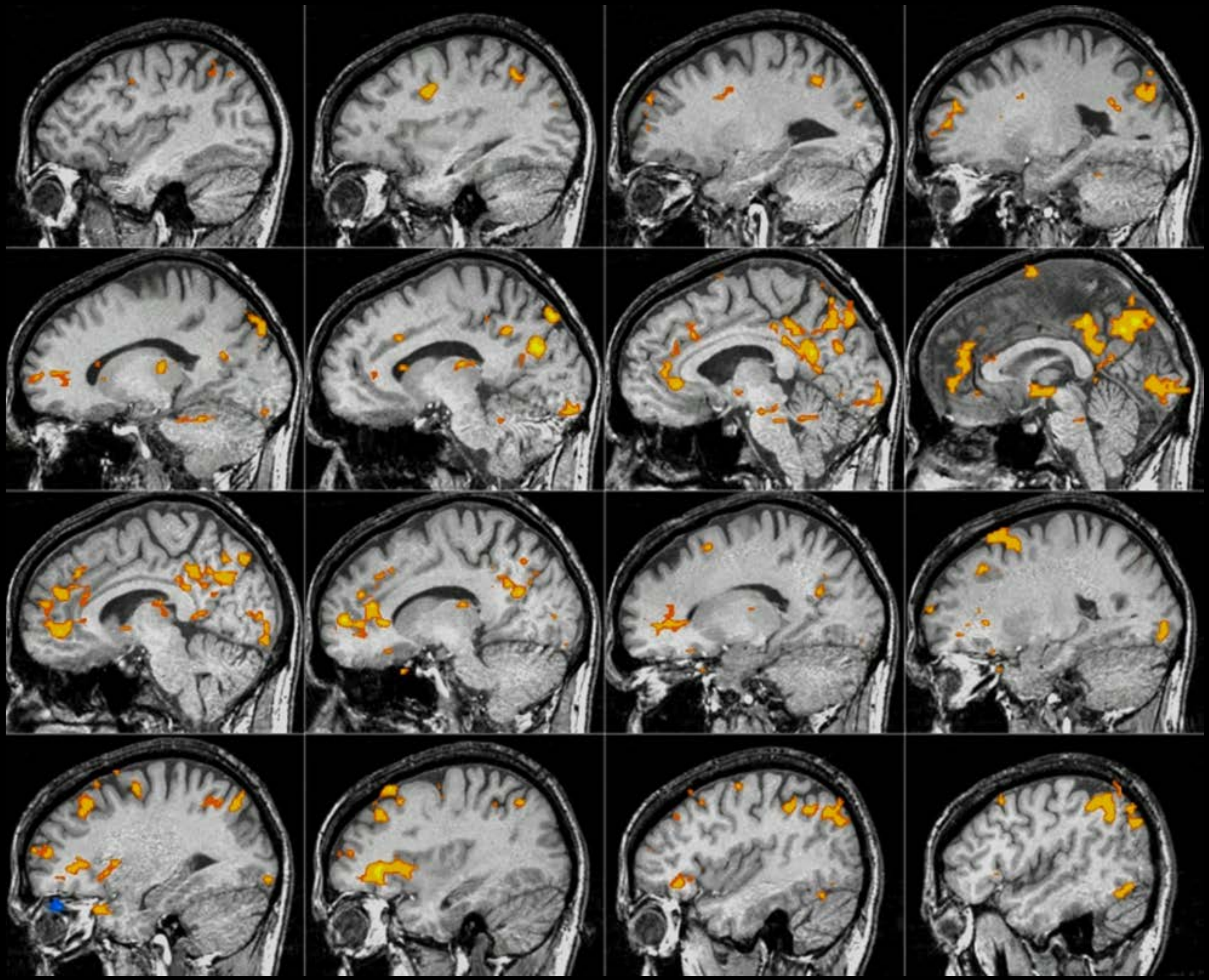

J. C. Patterson II, L. G. Ungerleider, and P. A Bandettini, Task - independent functional brain activity correlation with skin conductance changes: an fMRI study. *NeuroImage* ***17****: 1787-1806, (2002).*

Simultaneous EEG and fMRI of the alpha rhythm

Robin I. Goldman,[2,CA] John M. Stern,[1] Jerome Engel Jr[1] and Mark S. Cohen

Ahmanson-Lovelace Brain Mapping Center, UCLA, 660 Charles Young Drive South, Los Angeles, CA 90095; [1]Department of Neurology, UCLA School of Medicine, Los Angeles, CA; [2]Hatch Center for MR Research, Columbia University, HSD, 710 W. 168th St., NIB-1, Mailbox 48, NY, NY 10032, USA

[CA,2]Corresponding Author and Address: rg2146@columbia.edu

Received 28 October 2002; accepted 30 October 2002

DOI: 10.1097/01.wnr.0000047685.08940.d0

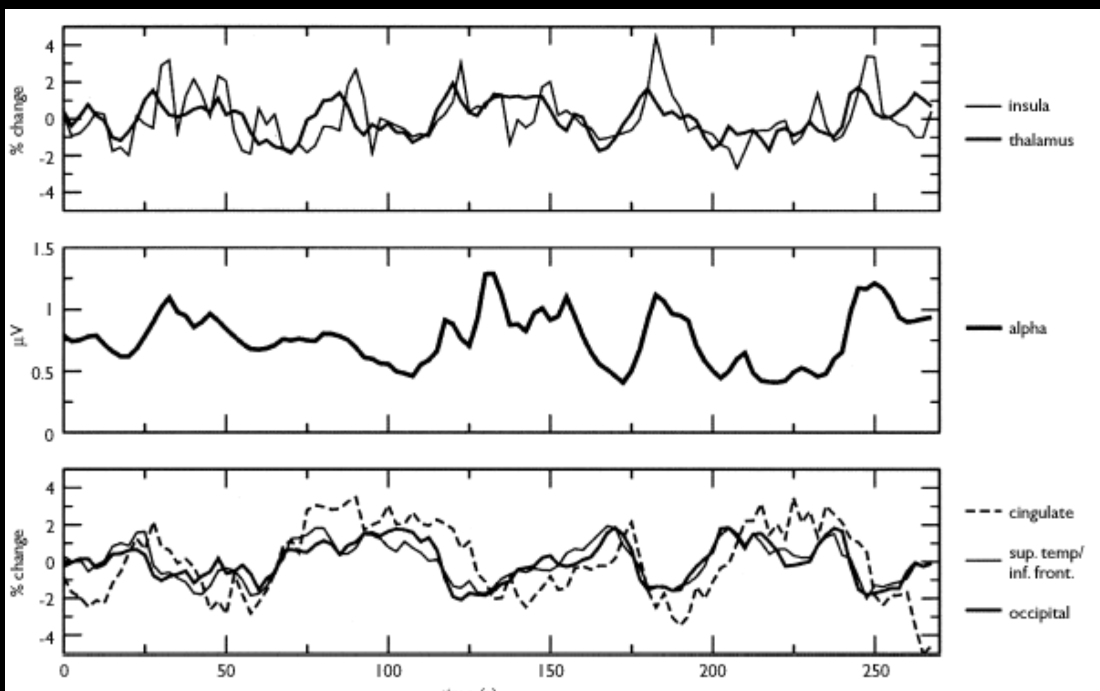

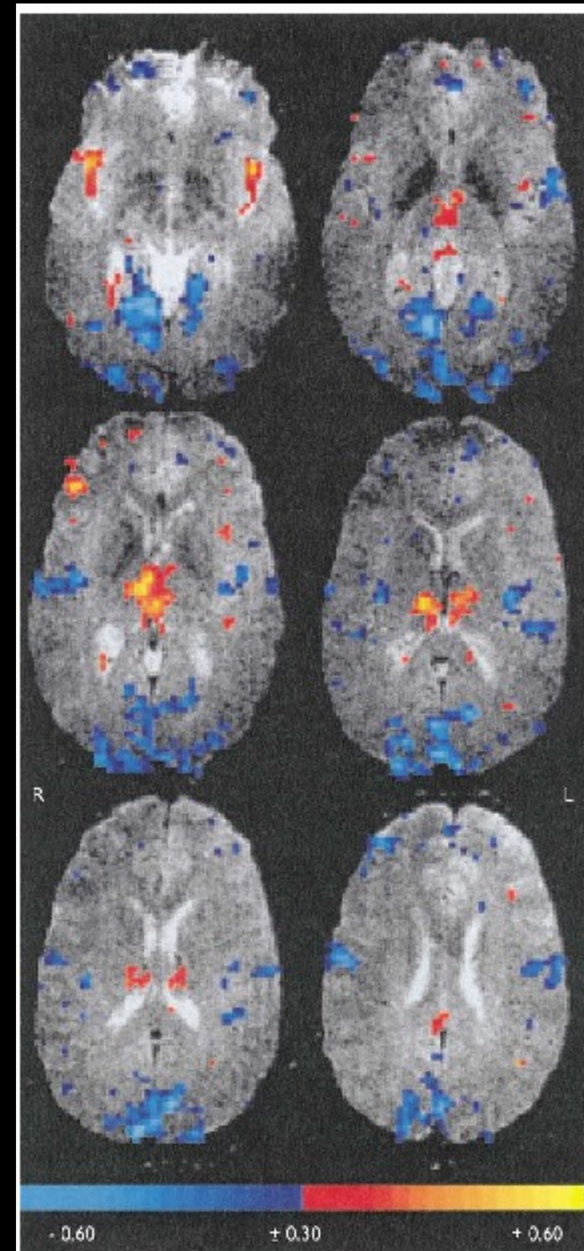

FMRI Basics and Beyond

- Information Content
- Sensitivity
- Resolution
- Image quality
- Paradigm Design and Processing

Technology

1.5T,3T, 4T
EPI
MRI
Local Human Head Gradient Coils
ASL
BOLD
EPI on Clin. Syst.
Spiral EPI
Multi-shot fMRI
Nav. pulses
Diff. tensor
Real time fMRI
Quant. ASL
Dynamic IV volume
Mg⁺
Z-shim
Simultaneous ASL and BOLD
Venography
7T
SENSE
Baseline Susceptibility
>8 channels
“vaso”
Current Imaging?

Methodology

Baseline Volume
IVIM
Correlation Analysis
Parametric Design
Linear Regression
Event-related
Phase Mapping
Surface Mapping
Motion Correction
Deconvolution
Multi-Modal Mapping
ICA
Mental Chronometry
Fuzzy Clustering
CO_2 Calibration
Free-behavior Designs
Latency and Width Mod
Multi-variate Mapping

Interpretation

Blood T2
Hemoglobin
BOLD models
B_o dep.
TE dep
SE vs. GE
Post-undershoot
NIRS Correlation
Veins
IV vs EV
Resolution Dep.
CO_2 effect
Inflow
Pre-undershoot
PET correlation
Fluctuations
ASL vs. BOLD
Extended Stim.
Linearity
Balloon Model
PSF of BOLD
Optical Im. Correlation
Metab. Correlation
Electrophys. correlation
Layer spec. latency
Excite and Inhibit

Applications

Volume - Stroke
∆ Volume-V1
BOLD -V1, M1, A1
V1, V2..mapping
Complex motor
Language
Motor learning
Presurgical
Plasticity
Imagery
Children
Attention
Priming/Learning
Face recognition
Memory
Tumor vasc.
Ocular Dominance
Clinical Populations
Emotion
Drug effects
Mirror neurons
Performance prediction

36 82 88 89 90 91 92 93 94 95 96 97 98 99 00 01 02 03

FIM Unit & FMRI Core Facility

Director:
Peter Bandettini

Staff Scientists:
Sean Marrett
Jerzy Bodurka
Frank Ye
Wen-Ming Luh

Computer Specialist:
Adam Thomas

Post Docs:
Rasmus Birn
Hauke Heekeren
David Knight
Anthony Boemio
Patrick Bellgowan
Ziad Saad

Graduate Student:
Natalia Petridou

Post-Back. IRTA Students:
Hanh Ngyun
Ilana Levy
Elisa Kapler
August Tuan
Dan Kelley

Visiting Fellows:
Sergio Casciaro
Marta Maieron
Guosheng Ding

Clinical Fellow:
James Patterson

Psychologist:
Julie Frost

Summer Students:
Allison Sanders
Julia Choi
Thomas Gallo
Jenna Gelfand
Hannah Chang
Courtney Kemps
Douglass Ruff
Carla Wettig
Kang-Xing Jin

Program Assistant:
Kay Kuhns

Scanning Technologists:
Karen Bove-Bettis
Paula Rowser
Alda Ottley